University of Southampton

Faculty of Engineering and Physical Sciences

Chemistry

Synthesis of Novel Cubane Scaffolds

By

Diego Edgard Collin

Thesis for the degree of Doctor of Philosophy

September 2021

University of Southampton

Abstract

Faculty of Engineering and Physical Sciences

Chemistry

Thesis for the degree of Doctor of Philosophy

Synthesis of Novel Cubane Scaffolds

by

Diego Edgard Collin

First synthesised in the 1960s and originally proposed as 3D benzene bioisostere in the 1990s, cubane scaffolds have gained real interest in medicinal chemistry the past decade. Substituting a phenyl ring by a cubyl unit could lead to improved physical and biological properties. Moreover, cubanes have find interest as non–aromatic rigid spacers in organic materials and polymers. However, the geometric requirements of cubane are far from ordinary, therefore, accessing cubane motifs is still hampered by non–trivial synthetic access.

With the growing awareness concerning hazardous chemicals and waste generated from synthetic chemistry, there has been a drive to re-evaluate the way organic chemistry is conducted. In some cases, processing chemical reactions in microreactors under a continuous–flow manner has shown to be particularly efficient. In addition, the use of light or electricity has been considered as sustainable methodology in order to replace potentially hazardous/toxic and costly chemical reagents.

This thesis aims to the development and optimisation of synthetic routes using flow photochemistry and electrochemistry in order to generate new cubane scaffolds.

Table of Contents

Table of Tables

Table of Figures

Table of Figures

Table of Schemes

Research Thesis: Declaration of Authorship

Print name: DIEGO EDGARD COLLIN

Title of thesis: Synthesis of Novel Cubane Scaffolds

I declare that this thesis and the work presented in it are my own and has been generated by me as the result of my own original research.

I confirm that:

1. This work was done wholly or mainly while in candidature for a research degree at this University;
2. Where any part of this thesis has previously been submitted for a degree or any other qualification at this University or any other institution, this has been clearly stated;
3. Where I have consulted the published work of others, this is always clearly attributed;
4. Where I have quoted from the work of others, the source is always given. With the exception of such quotations, this thesis is entirely my own work;
5. I have acknowledged all main sources of help;
6. Where the thesis is based on work done by myself jointly with others, I have made clear exactly what was done by others and what I have contributed myself;
7. Parts of this work have been published as:

Collin, D. E.; Kovacic, K.; Light, M. E.; Linclau, B. Synthesis of Ortho-Functionalized 1,4-Cubanedicarboxylate Derivatives through Photochemical Chlorocarbonylation. *Org. Lett.* **2021**, *23* (13), 5164–5169.

Collin, D. E.; Jackman, E. H.; Jouandon, N.; Sun, W.; Light, M. E.; Harrowven, D. C.; Linclau, B. Decagram Synthesis of Dimethyl 1,4-Cubanedicarboxylate Using Continuous-Flow Photochemistry. *Synthesis (Stuttg).* **2021**, *53* (07), 1307–1314.

Collin, D. E.; Folgueiras-Amador, A. A.; Pletcher, D.; Light, M. E.; Linclau, B.; Brown, R. C. D. Cubane Electrochemistry: Direct Conversion of Cubane Carboxylic Acids to Alkoxy Cubanes Using the Hofer–Moest Reaction under Flow Conditions. *Chem. – A Eur. J.* **2020**, *26* (2), 374–378.

Signature: Date:

Acknowledgements

First of all, I will never be enough grateful to Professor Bruno Linclau for the opportunity he offered me to carry out my PhD in his laboratory. I would like to thank him for the trust he placed in me and the autonomy I got continuously on this challenging project. It is exactly what I was looking for when I decided to cross the English Channel. I would like to thank him for his continued support and guidance and what he could taught me during these 3 years at Southampton. I would probably not be the same chemist and scientist without his supervision. I would also like to thank Professor David Harrowven and Professor Richard Brown for their advice and learningful discussions during the LabFact project and works published together.

I would like to thank all past and present members of the Linclau group over the past three years for their support and funny moments in and outside the lab. In no particular order: Simon, Hannah, Lawrence, Zhong, Gert-Jan, Lucas, Jean-Baptiste, David E., Rob, Kler, David W. I would like to thank specifically Mariana Manso who arrived at the same time in the group. Although, we could argue sometimes a lot, we often shared our frustrating days and supported each other over long discussions. She is definitely the best person to attentively listen and help during difficult time. I would also specifically thank Kristina for her precious help on the last chapter of this work. But also for the long chemistry–related discussions and the great tennis game on grass court we had together. Being able to play grass court in the UK is definitely something amazing!

I would also like to thank members of the Brown lab. I have also spent long hours working and chating with, Domenico, George and Sergio. More particularly, I am very grateful to Ana for her precious help and advice in electrochemistry. I have learn so much on her side and she is definitely the most brilliant electrochemist I know. Finally, I would like to thank the Harrowven group members for there help to settle in and outside the lab when I arrived in Southampton. In no particular order: Morgan, Ryan, Luke and I would like to thank Sun Wei for the enriching discussion and help in photochemistry.

I am very thankful to the University staff within the Chemistry department, Neil for the NMR services, Julie for mass spectrometry, Mark Light for providing my crystal structures and finally Mark and Keith for the running of stores and being a pleasure to talk with.

Finally, I must express my very profound gratitude to my parents, brother and sister for providing me support and continuous encouragement at any time throughout those three years of PhD.

Definitions and Abbreviations

ADMET	Adsorption, distribution, metabolism, excretion, toxicity
COSY	Correlation Spectroscopy
CV	Cyclic Voltammetry
DBU	1,8–Diazabicyclo[5.4.0]undec–7–ene
DCM	Dichloromethane
DMAc	Dimethylacetamide
DMAP	4–Dimethylaminopyridine
DMF	Dimethylformamide
DMP	Dess–Martin periodinane
ECF	Electrochemical fluorination
EDC	1–Ethyl–3–(3–dimethylaminopropyl)carbodiimide
Et_3N	Triethylamine
FDA	U.S. Food and Drug Administration
FEP	Fluorinated ethylene propylene
FTIR	Fourier–transform infrared spectroscopy
GC	Gas Chromatography
HFIP	Hexafluoroisopropanol
HMBC	Heteronuclear Multiple Bond Correlation
HOAt	*N*–hydroxy–7–azabenzotriazole
HOBt	*N*–hydroxybenzotriazole
HPLC	High–performance liquid chromatography
HRMS	High–resolution mass spectrometry
HSQC	Heteronuclear single quantum coherence spectroscopy
iPrOH	Isopropanol
IR	Infrared spectroscopy
LED	Light–emitting diode
LRMS	Low resolution mass spectrometry
MeCN	Acetonitrile
MeOH	Methanol
m.p.	Melting point
MS	Molecular sieves
MW	Molecular weight

NFSI	*N*–Fluorobenzenesulfonimide
NHPI	*N*–hydroxyphthalimide
NMR	Nuclear magnetic resonance
PhH	Benzene
PVDF	polyvinylidene fluoride
Pt	Platinum
RAE	Redox–active ester
R_f	Retention factor
RSM	Remaining Starting Material
RT	Room temperature
SS	Stainless steel
TFA	Trifluoroacetic acid
TFE	Trifluoroethanol
THF	Tetrahydrofuyran
TLC	Thin layer chromatography
UV	Ultraviolet

Chapter 1 Introduction

1.1 Escape from Flatland

Pharmaceutical and agrochemical industries are constantly looking for new molecular entities (NMEs).[1] While the 1990s are considered a golden era for those sectors, since the last decade the discovery of NMEs has declined. This global decline can be attributed to several factors such as safety regulations, healthcare costs, and clinical failures.[2] The latter can be due to pharmacokinetic (ADMET: adsorption, distribution, metabolism, excretion, toxicity) and pharmacodynamic properties, but the large fraction of quasi–planar candidate molecules has also be proposed as another contributing factor.[3] This observation was strengthened by a recent study reported by Brown and Boström, highlighting that most of the drug–like synthesised compounds were confined in space regions characteristic of rod or disc shapes molecules while very few were found in the space harbouring three–dimensional structures.[4]

In that regard, a recent survey[5] showed that drug–like molecules with substantial sp^3 fractions (Fsp^3) may improve their clinical success by influencing their pharmacokinetic properties. Therefore, by this growing awareness, pharmaceutical research is increasingly focused towards the exploration of different regions of chemical space in order to "*Escape from flatland*", leading to an increasing demand for new saturated building blocks (Figure 1).[5–8]

Since most of the FDA–approved drugs are benzene–containing molecules, the above–mentioned considerations have encouraged scientists to replace the benzene ring with 3D sp^3–rich benzene bioisosteres. In addition to modifying physico–chemical properties, phenyl replacement with saturated bioisosteres may also generate new intellectual property (IP) for drug candidates (Figure 1).[9]

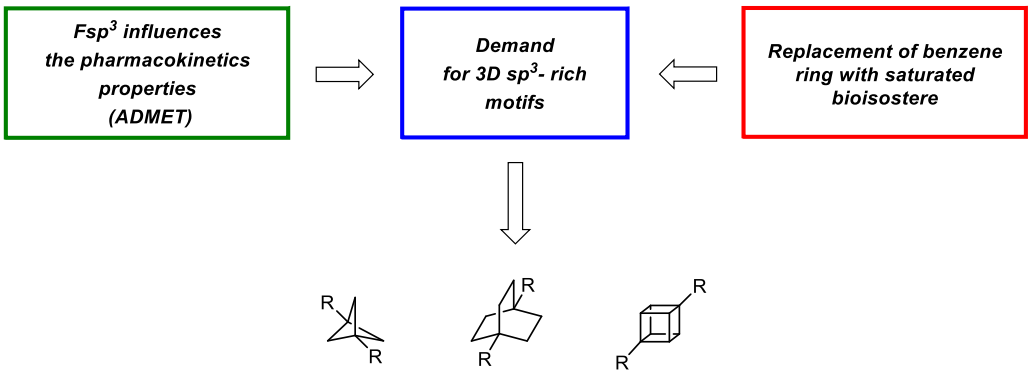

Figure 1. Diagram summarising the reasons for the demand of new saturated building blocks.

1.2 Isosterism

The concept of *isosterism* was originally contemplated by James Moir in 1909 but the term was only introduced by Irving Langmuir in 1919.[10] By regarding the electronic configuration of atoms, groups, and molecules, Langmuir compared the physical properties of various molecules such as N_2 and CO, N_2O and CO_2, and N_3^- and NCO^-, and found the number and arrangement of electrons to be similar in their valence shells in accordance to the octet rule.[11] The concept was further extended in 1925 with H. G. Grimm's hydride displacement law, stating that: "Atoms anywhere up to four places in the periodic system before an inert gas change their properties by uniting with one to four hydrogen atoms, in such a manner that the resulting combinations behave like pseudoatoms, which are similar to elements in the groups one to four places, respectively, to their right", meaning that the CH is isosteric to N and NH is isosteric to O and so on.

In 1932, Hans Erlenmeyer further broadened Grimm's classification and redefined isosteres as atoms, ions, and molecules that present the same number of electrons in their peripheral layers. He also included the proposition that elements in the same column of the periodic table are isosteres among themselves.

1.3 Bioisosterism

The emergence of *bioisosteres* as structurally distinct compounds recognised similarly by biological systems has found its origins in experiments conducted by Erlenmeyer and his colleagues, showing that antibodies were unable to discriminate between O, NH, CH_2 phenyl and thienyl rings in the context of artificial antigens (Figure 2).[12,13]

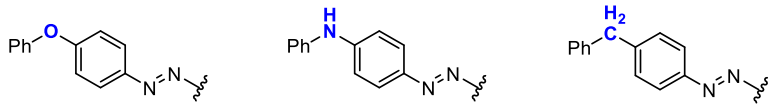

Figure 2. Grimm's hydride displacement law applied in the context of artificial antigens.[13]

The introduction of the *bioisosterism* concept is attributed to Harris Friedman who, in 1951, recognised the usefulness of the isosterism concept to design bioactive molecules, defining bioisosteres for isosteric compounds that demonstrate similar biological activities. However, according this definition, a compound may be *isosteric* but not necessarily *bioisosteric* meaning that this notion only depends on the context and not on physicochemical properties.[12] Therefore, an effective bioisostere for one specific biochemical application may not be translated to another one. In 1979, Thornber widened the definition of bioisosteres to subunits, groups, or molecules which possess physicochemical properties and produce similar biological effects.[14,15]

Bioisosteric replacement offers potential value in drug design and development since it enables the effect of steric size and shape; dipole and electronic properties; lipophilicity and polarity; or pKa on a biological response to be determined. Bioisosteres have been classified into classical and non–classical bioisosteres.

1.3.1 Classical Bioisosteres

Classical bioisosteres rely mainly on steric and electronic properties. They can be subdivided into five categories: monovalent, bivalent, trivalent, tetrasubstituted atoms, and ring equivalents. Mono–, di–, tri– and tetravalent bioisosteres are classified as groups of atoms that are involved in the interchange of single, two, three and four bond atoms respectively (Figure 3).[11] This strategy has been found to improve, in some cases, pharmacokinetic and toxicity properties by reducing the rate of metabolic modification. For instance, the use of a fluorine atom as a hydrogen isosteric replacement is one of the most used strategies and has found a wide range of applications in drug design. The incorporation of fluorine can productively modulate a range of properties such as metabolic stability, pKa, lipophilicity, and molecular conformation.[16–18] A well–known example consists of the introduction of two fluorine atoms into the cholesterol absorption inhibitor SCH48461, during the development of ezetimibe (marketed as Zetia™), to increase metabolic stability. Another example highlighting the use of divalent bioisosteres is the case of tolrestat (Figure 4). Initially developed for the control of certain diabetic complications, substituting C=S with C=O decreased the activity both *in vitro* and *in vivo* towards inhibition of aldose reductase.[11]

Ring equivalent bioisosteres consist of the interchange of one aromatic or heterocyclic moiety for another in a system. Benzene, pyridine, thiophene, and furan are the most common ring equivalent bioisosteres (Figure 3).[15] One successful use of this ring equivalent replacement resulted in the potent antihistamine mepyramine, which was derived from its analogue phenbenzamine by the replacement of the phenyl moiety with a pyridyl group (Figure 4).

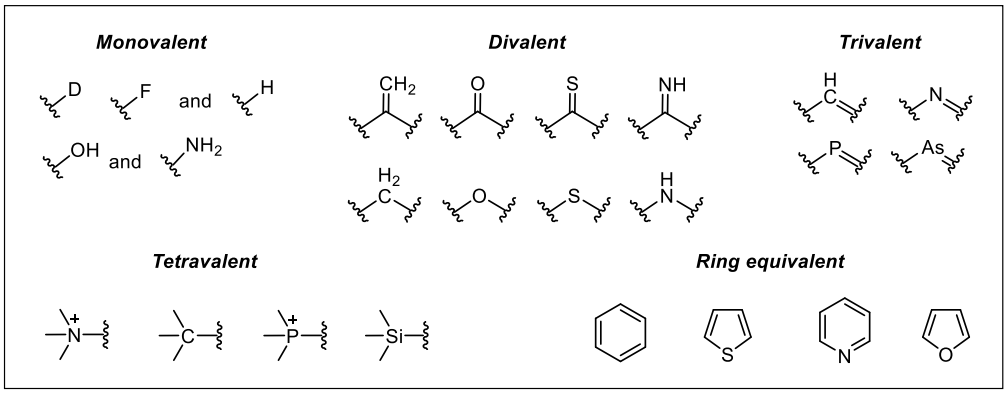

Figure 3. List of monovalent bioisosteres.[15]

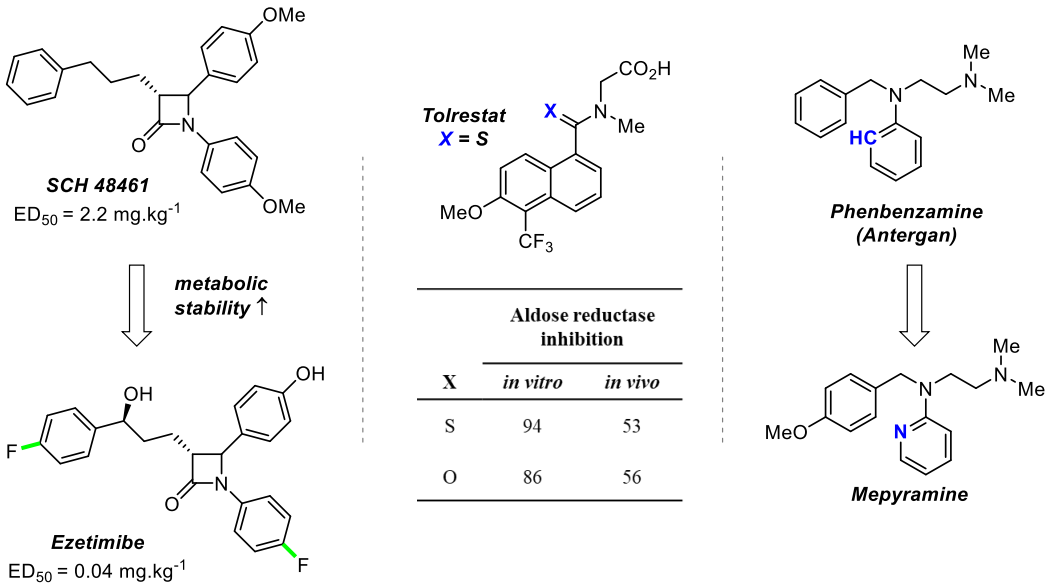

X	Aldose reductase inhibition *in vitro*	*in vivo*
S	94	53
O	86	56

Figure 4. Examples of reported applications of mono–, divalent and ring equivalent bioisostere respectively.[12,19]

1.3.2 Nonclassical Bioisosteres

Nonclassical bioisosteres do not strictly obey to the same rules as classical bioisosteres. Although these isosteres are capable of maintaining similar biological activity by mimicking the spatial arrangement, electronic or physicochemical properties, or functional group that is critical for the retention of biological activity, they are structurally distinct. They usually comprise different numbers of atoms and exhibit different steric and electronic properties.[19,20]

Nonclassical phenyl bioisosteres have received considerable attention in recent years due to the abundance of phenyl moieties present in medicinal chemistry. In some cases, phenyl ring derivatives may have low aqueous solubility due to, for example, π–π stacking interactions. While adding a polar group such as an alcohol or amine could address solubility issues, such modifications may also dramatically modify the potency. Therefore, replacing a phenyl ring by an alkyl group (linear, cyclic, or caged) can provide alternatives and may help to improve solubility and modify the physico–chemical properties that may not be accessible otherwise.

Property modulation of phenyl replacement with any saturated bioisosteres is usually difficult to predict. However, two main situations can be considered. First, the phenyl ring plays the role of a rigid linker holding two substituents together with a specific distance from each other, therefore, the phenyl replacement can enable this specific distance to be maintained whilst changing physico-chemical properties. In this case, the key factor is the length of the linker. For instance, if the distance between two pharmacophores is the defining element in the bioactivity, replacing the benzene ring with bicyclo[2.2.2]octane or cubane could be expected to give similar activity while replacement with bicyclo[1.1.1]pentane should reduce the activity due to the much shorter C–C bond respectively

(Figure 5). Second, the phenyl ring can also be involved in aryl–protein interactions. In this case, the replacement of a phenyl ring with a saturated linker is expected to decrease the activity.[21]

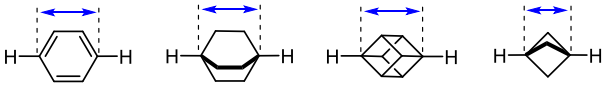

C-C (Å)	2.77	2.72	2.68	1.88

Figure 5. Carbon to carbon distances of several 3D benzene bioisostere compare to benzene. (From left to right) benzene, bicyclo[2.2.2]octane, cubane, bicyclo [1.1.1] pentane.[21,22]

Several examples have been reported. The cyclopropane moiety was investigated as a bioisostere of the phenyl ring in order to reduce the molecular weight and lipophilicity (Figure 6). Quantum mechanical calculations suggested that the phenylcyclopropane moiety is in a perpendicular instead of bisected conformation, which mimics the biologically active conformation of *ortho*–biphenyl groups (Figure 6).[23]

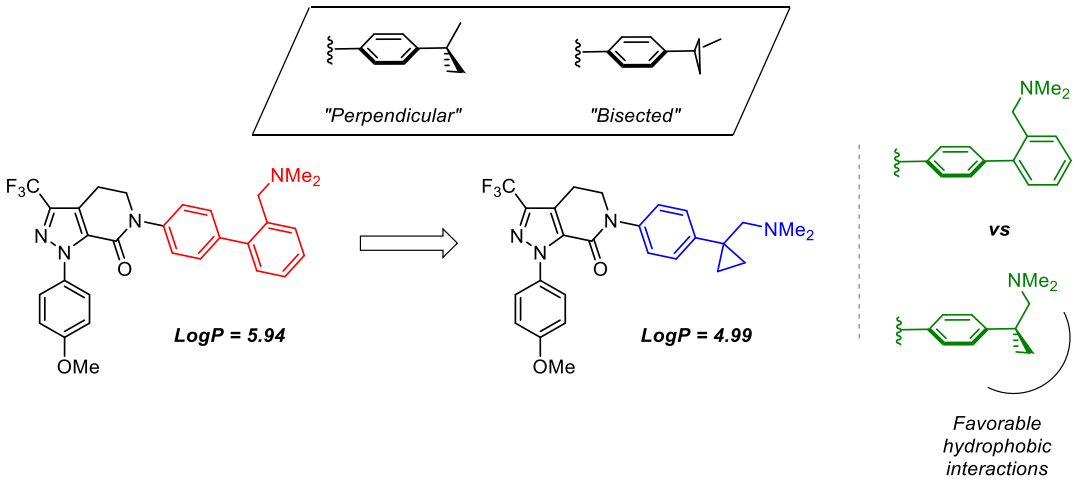

Figure 6. Cyclopropyl moiety as phenyl bioisostere.[23]

In 2012, a team at Pfizer led by Stepan reported the use of the bicyclo[1.1.1]pentane motif for the design of a potent and orally active γ–secretase inhibitor (Figure 7).[24] When compared with the analogue possessing an *ortho*–fluorophenyl ring, this inhibitor showed slightly better activity, metabolic stability, and substantially better permeability and aqueous solubility, which the authors attributed to the increase in three–dimensionality and concomitant disruption of planarity avoiding intermolecular π–stacking of the two aromatic rings as in initial compound. This work highlighted the physicochemical changes induced by the use of 3D nonclassical phenyl bioisosteres and showcases its potential use as a tactic to "*Escape from Flatland*" of multiple aryl systems in drug discovery.

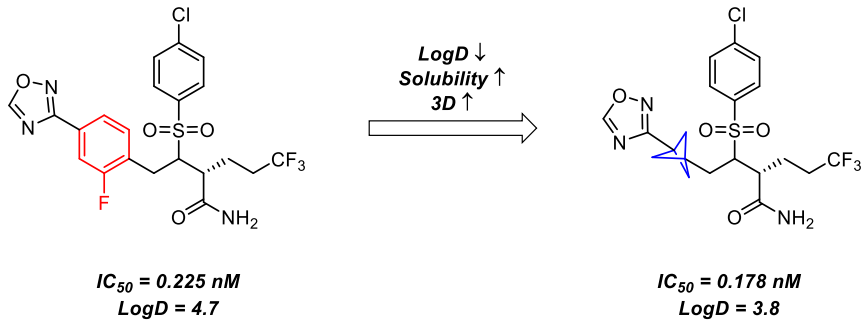

Figure 7. Bicyclo[1.1.1]pentane as a nonclassical phenyl ring bioiosostere.[24]

In 2017, the same strategy was applied in an extensive SAR (structure–activity relationship) study on Murine Double Minute 2 (MDM2) inhibitors for cancer treatment.[25] Starting with a cyclohexane-containing lead compound, the authors first investigated replacement of the cyclohexyl group with a rigid aryl group (Figure 8). However, the aryl derivative showed poor oral pharmacokinetic properties. Finally, replacing the aryl moiety with bicyclo[2.2.2]octane–1–carboxylic acid followed by further optimisation led to the discovery of a highly potent, chemically stable and efficacious MDM2 inhibitor, which has entered Phase I clinical trials.[25]

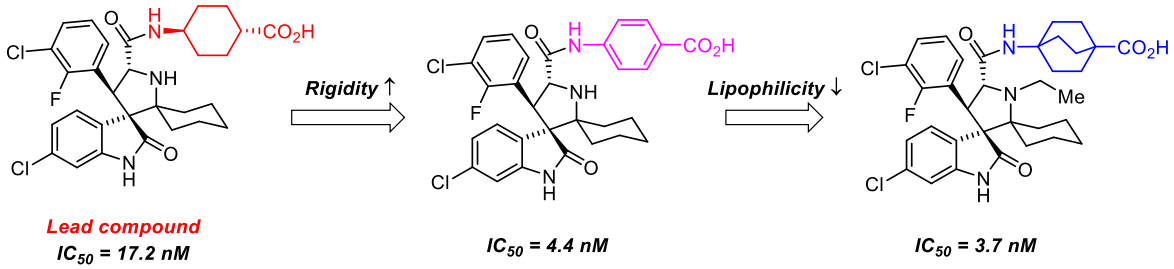

Figure 8. Bicyclo[2.2.2]octane–1–carboxylic as a 3D nonclassical phenyl bioisostere in MDM2 inhibitors for cancer treatment.[25]

1.3.3 Cubane as a Nonclassical Phenyl Bioisostere

1.3.3.1 Cubane as *mono*– and *para*–Substituted Phenyl Bioisostere

In 1992, Eaton suggested the potential of cubane as a phenyl bioisostere in pharmaceutical research.[26] The assumption was made based on the similar length of the diagonal of the cubane ring with that of benzene (Figure 9). In 2014, Wlochal and Davies reported the synthesis of medicinal chemistry–relevant cubane building blocks and their possible applications.[27] However, the recognition and validation of cubane as a nonclassical phenyl bioisostere has only been reported in 2016, by Tsanaktsidis, Savage, Williams *et al*.[28] In order to verify the assumption, the authors reported the study of cubane derivatives molecules used as drugs or agrochemicals (Figure 9).

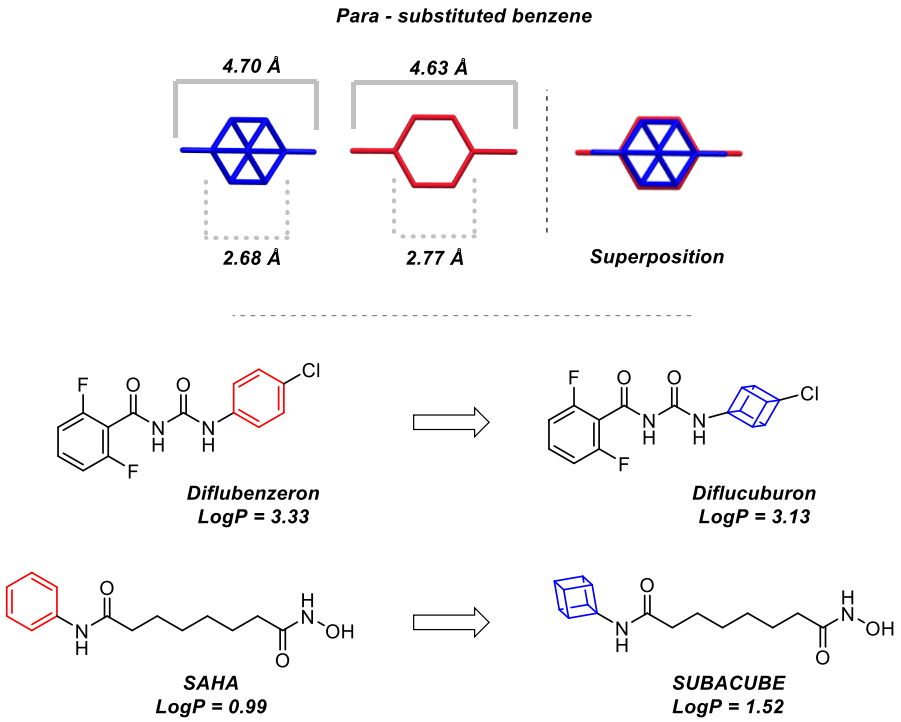

Figure 9. 2D diagonal view of 1,4–substituted cubane and benzene and Cubanes analogues of pharmaceuticals and agrochemicals molecules containing benzene ring.[28]

Among these, diflucuburon, a cubane analogue of diflubenzeron (insecticide) showed greater activity, whereas SUBACUBE performed identically compared to SAHA, a molecule approved by the FDA for the treatment of cutaneous T–cell lymphoma (CTCL) in 2006. The main attractions of cubane as a phenyl bioisostere for the development of bioactive molecules involve differences in solubility and metabolic stability compared to aromatic rings. Indeed, the inability of cubane to undergo π–stacking may lead to an increasing of its water solubility. Further, electron rich phenyl moieties such as phenol and aniline are easily *in vivo* oxidised by the cytochrome P–450, whereas cubane cannot or is only difficultly degraded according this metabolic pathway due to its poorly oxidisable C–H bonds.

Nicolaou *et al.*, in 2016, replaced the *para*–substituted benzene ring in imatinib with saturated cycloalkanes, including cubane (Figure 10).[29] While, the cubane derivative showed higher solubility in water with appropriate metabolic stability, it exhibited much lower potency than imatinib. The favourable aryl–alkyl interaction between imatinib and the enzyme seemed to be interrupted by the replacement of the aromatic ring with the aliphatic chains. However, compared to other saturated cycloalkyl derivatives, the imatinib cubane derivative showed the highest inhibitory activity against the desired target and the greatest cytotoxicity values against cancer cell lines.

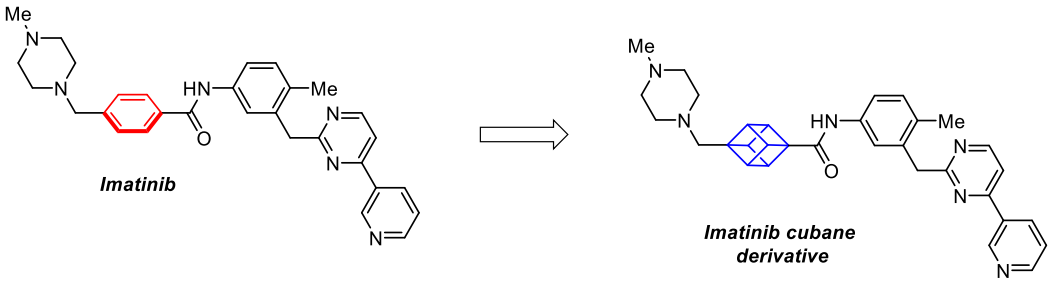

Figure 10. Replacement with cubane of *para*–substituted benzene ring in imatinib by Nicolaou *et al.*[29]

Polycyclic cage structures such as adamantane, trishomocubane, carborane, and cubane have found interest in the treatment of neurodegenerative diseases due to their hydrophobicity, which facilitates transport across the blood–brain barrier in the central nervous system. Kassiou et *al.* reported antidepressant activity of hydrocarbon–caged compounds, including cubane, in P2X7 antagonists (Figure 11).[30–32]

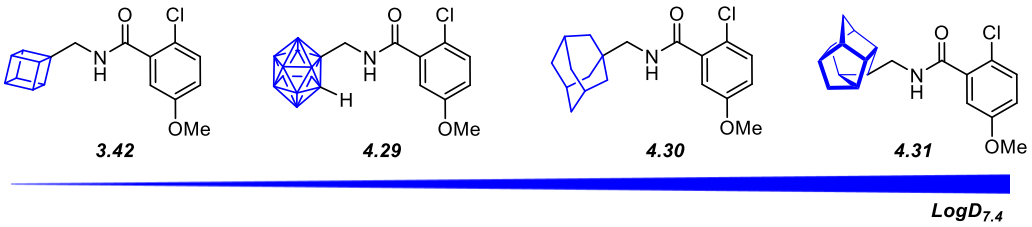

Figure 11. LogD$_{7.4}$ of hydrocarbon–caged P2X7 antagonists.

More recently, a team reported the identification of a cubane–modified aptamer (synthetic peptide molecule) against a malaria biomarker, the *Plasmodium vivax* lactate dehydrogenase (PvLDH) (Figure 12).[33] While the parasite *Plasmodium falciparum* causes the most severe disease with the highest mortality, *Plasmodium vivax* is more widely distributed and causes disease which is complex and recurring. The crystal structure of the cubamer–protein complex reveals an unprecedented binding mechanism involving the formation of a cubane pocket and an unusual C–H···O hydrogen bond with a leucine residue (Figure 12). This work shows that nucleic acids bearing exotic chemical functional groups enable remarkable binding interactions, and therefore open a myriad of possibilities for functional nucleic acids.

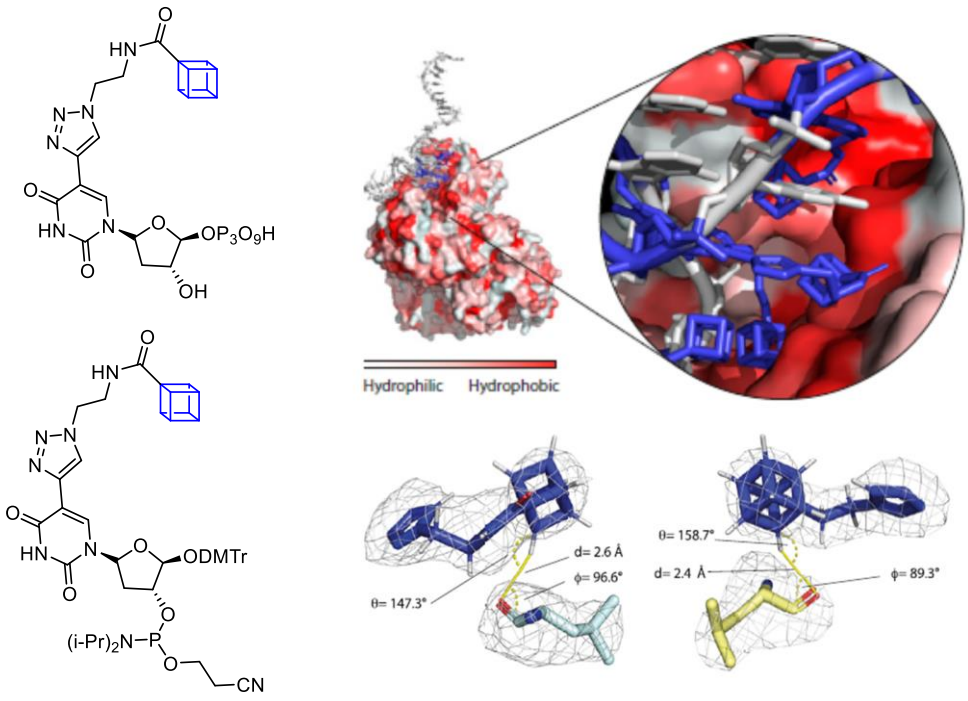

Figure 12. (*Left*) Cubane–modified deoxyuridine triphosphate and phosphoramidite for the synthesis of the nonnatural aptamer. (*Right*) Interactions of the cubamer with PvLDH by hydrophobic interactions and a unique hydrogen bond of the cubamer with PvLDH.[33]

1.3.3.2 Cubane as *ortho*– and *meta*–Substituted Phenyl Bioisostere

The interest of cubane derivatives as 3D benzene bioisosteres has only been demonstrated for p*ara*– and *mono*–substituted cubanes.[28] Nevertheless, cubane present also close similitude in size to *ortho*– and *meta*–substituted benzene (Figure 13), therefore, in that regards, there is a growing interest for 1,3– and 1,2–substituted cubane derivatives as *meta*– and *ortho*–substituted benzene bioisosteres.[34,35] However, the required non–trivial synthetic pathways hamper this type of application.[35]

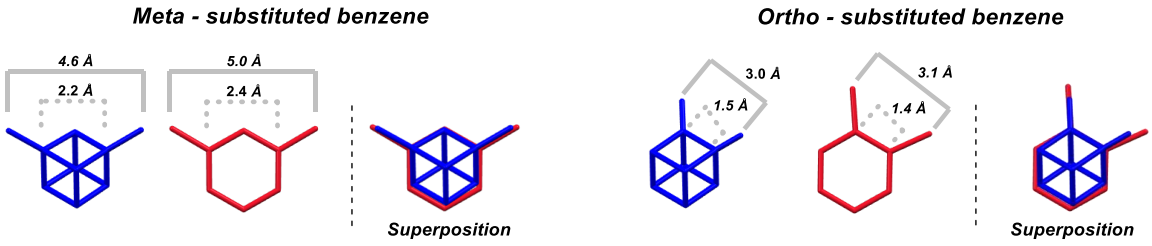

Figure 13. 2D diagonal view of 1,3– and 1,2–substituted cubane and benzene.

1.4 Cubane structure and functionalisations

1.4.1 General

The cube or hexahedron (6 faces) corresponds to one of the five regular convex polyhedrals known as the Platonic solids, alongside the tetrahedron (4 faces), octahedron (8 faces), dodecahedron (12 faces) and icosahedron (20 faces) (Figure 14). Historically, it was a topic of interest to synthesise the corresponding hydrocarbon analogues. Cubane, (IUPAC name: pentacyclo-[4.2.0.$0^{2,5}$.$0^{3,8}$.$0^{4,7}$]octane), was the first of these five solids to be successfully synthesised. Before its reported synthesis date, chemists believed that the synthesis of cubane could not be achieved due to the 90° C–C–C bonding angle of the sp^3 carbon atoms. The successful synthesis demonstrated the limitations of Pauling's hybrid–orbital theory. Whilst cubane is thermodynamically unstable (ΔH_f = + 144 kcal mol^{-1}) and very strained (≈ 161.5 kcal mol^{-1}), it is kinetically stable due to the formation of a highly unstable diradical intermediate during its decomposition pathway.[36]

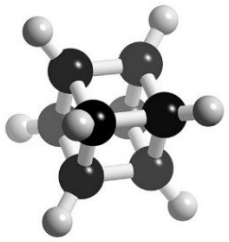

Figure 14. ball and stick model of cubane.

1.4.2 1,4–Cubanedicarboxylic acid: the primary cubane building block

Nowadays, the only practical large–scale synthesis of cubane leads to 1,4–cubanedicarboxylic acid **1.1** (Figure 15, see Chapter 2), and the synthesis of cubane derivatives relies heavily on interconversions of the carboxylic acid functional group or indirect decarboxylative functionalisation procedures.

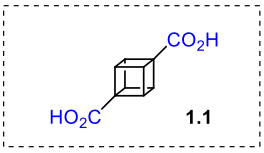

Figure 15. 1,4–cubanedicarboxylic acid (1.1).

1.4.3 Decarboxylative functionalisations of cubane

The first decarboxylative functionalisation was developed in the pioneering work of Eaton and Cole when they reported the isolation of cubane (**1.2**) in 1964.[37] A thermally induced homolytic cleavage of cubane *tert*–butyl perester **1.3** led to the formation of a cubyl radical intermediate which, by hydrogen abstraction from hydrogen donor such as cumene, led to **1.2** (Scheme 1). However, this pathway only afforded a maximum yield of 50% and was improved several years later by Della and Tsanaktsidis *via* a Barton decarboxylation (Scheme 1).[38] The radical chain decarboxylation was first

promoted using tributyltin hydride and later under visible light irradiation to give the corresponding *mono*–substituted cubane in 57% (**1.2**) and 82% (**1.6**) yields respectively.[38,39]

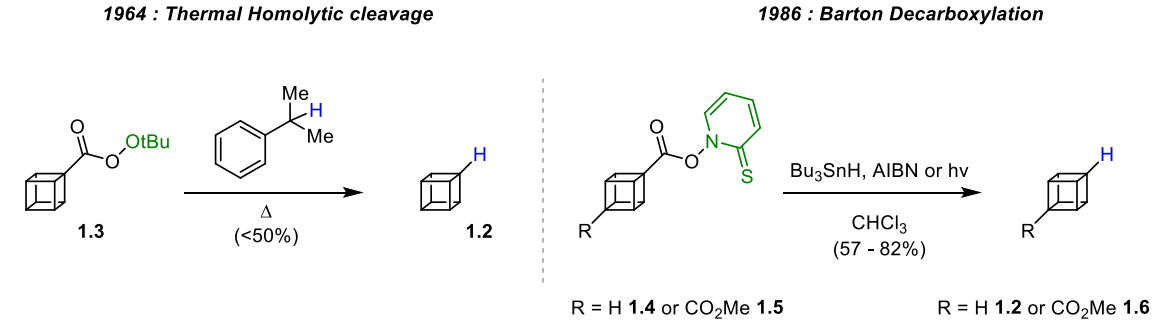

Scheme 1. Reported reductive decarboxylation for hydrogenolysis of cubane.[38,39]

In 1989, Moriarty and Khosrowshahi reported the first synthetic pathway for arylated cubane **1.8** from the carboxylic acid **1.7** (Scheme 2). Decarboxylation was achieved *via* a Kochi–type reaction consisting in the radical oxidative decarboxylation of a lead tetraacetate complex under visible light irradiation.[40,41] The corresponding arylated cubanecarboxylate **1.8** was obtained in a 66% yield (Scheme 2). In 2014, Baran *et al.* developed an "interrupted" Barton decarboxylation for the synthesis of sulfinate derivatives through the formation of a 2–pyridyl sulfone intermediate. Starting from the 4–methoxycarbonyl–1–cubanecarboxylic acid **1.7**, they obtained the cubane sulfone **1.9** in 42% isolated yield over three steps (Scheme 2).[42]

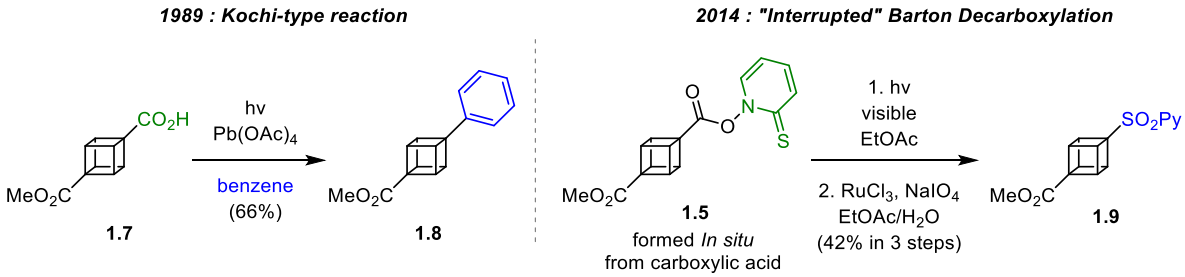

Scheme 2. Kochi–type arylation and "interrupted" Barton decarboxylation sulfonylation of cubane.[41,42]

Another decarboxylation synthetic pathway consists of the formation of a redox active ester (RAE) such as NHPI (*N*–hydroxyphthalimide) **1.10**, HOAt (*N*–hydroxy–7–azabenzotriazole) **1.11** or HOBt (*N*–hydroxybenzotriazole) **1.12**, which can undergo a radical chain decarboxylation *via* a single–electron–transfer (SET) mechanism (Scheme 3). In 2016, the Baran group were the first to report an Fe–catalysed radical aryl–alkyl (**1.8**, **1.13** and **1.14**) cross–coupling on cubane using a redox active–ester approach.[43,44] In the same year, they showed that a nickel catalyst could be used for SET reduction of RAEs, and applied this to a Barton decarboxylation and Giese reaction on cubane with 77% and 56% yields respectively (Scheme 3).[45] Recently, Senge *et al.* reported an improved pathway of Baran's procedure for which the coupling with electron–rich aryl moieties proceeded in yields up to 58%, although the use of electron–deficient moieties drastically decreased the yield.[46]

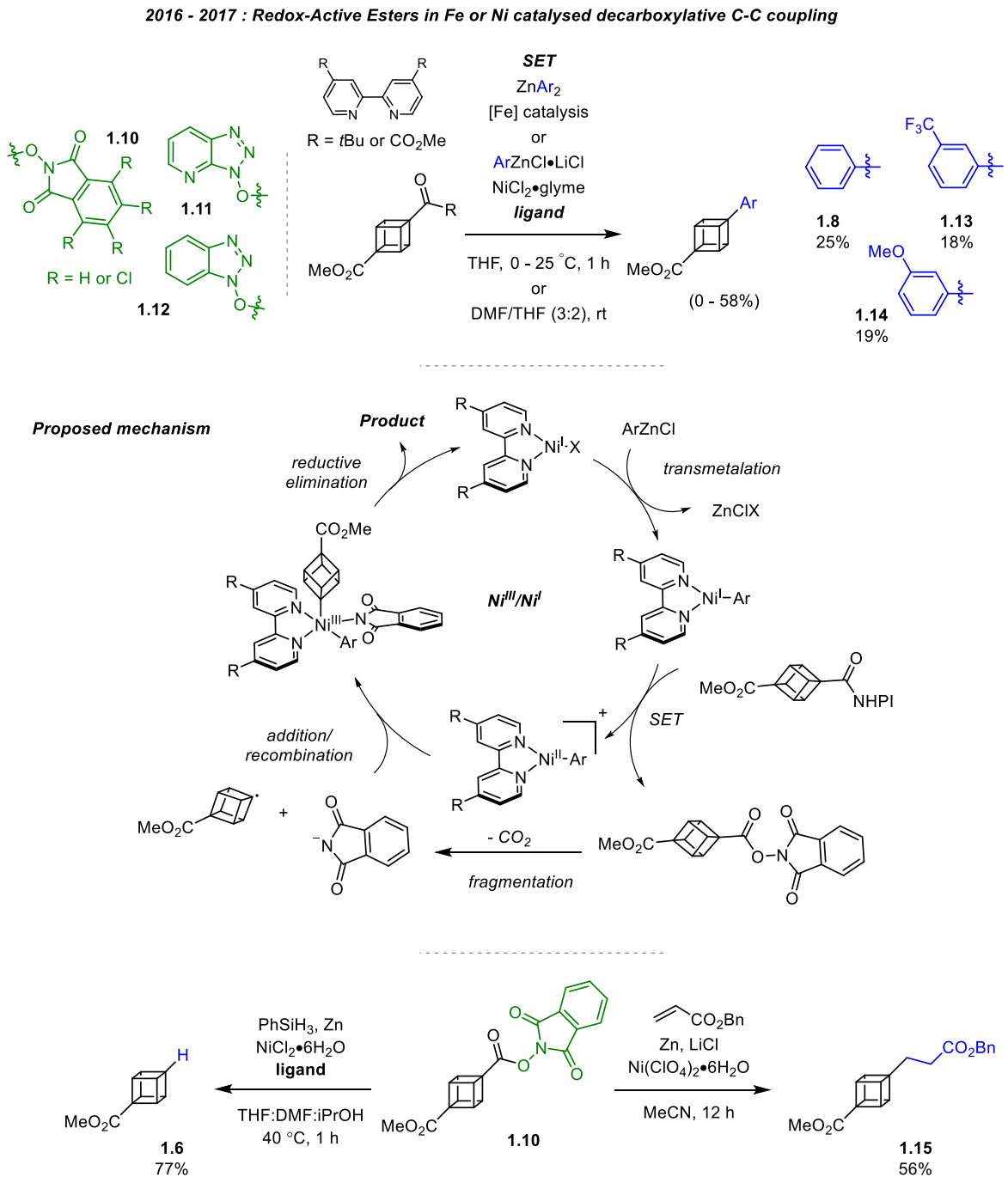

Scheme 3. Redox–Active Esters in Fe or Ni–catalysed decarboxylative C–C coupling.[43,44,46]

After exploring C(sp^2)–C(sp^3) and C(sp^3)–C(sp^3) bond formation on cubane, Baran and co–workers expanded their efforts and reported a developed nickel catalysed decarboxylative borylation (Scheme 4).[47] Their procedure enabled them to isolate borylated cubane **1.16** with a 45% yield. During the same period, with the emergence of photoredox–catalysis under visible light, Aggarwal *et al.* reported a redox–active–ester decarboxylative borylation under visible light irradiation in the presence of bis(catecholato)diboron in dimethylacetamide, which enabled them to obtain **1.16** in a 46% yield.[48]

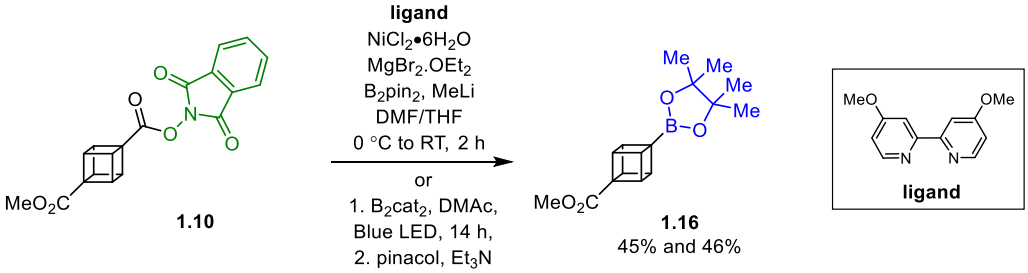

Scheme 4. Ni–catalysed and photoinduced decarboxylative borylation.[47,48]

1.4.4 Halogen–Exchange of Cubane

Halogen exchange on 1,4–iodocubane derivative **1.17** using *tert*–butylithium followed by addition of alkyl halides and various types of electrophiles was reported by Senge *et al.*.[49–52] However, the formed cubyllithium is not highly nucleophilic, and therefore has shown limitation in its use with some electrophiles, such as carbon–based ones. In order to increase the nucleophilicity, Matsubara *et al.* reported a protocol in 2019 for an iodine−metal exchange reaction on cubane using lithium organozincates (Scheme 5).[53] This methodology was further used to access chiral polysubstituted cubanes by the same group.[54]

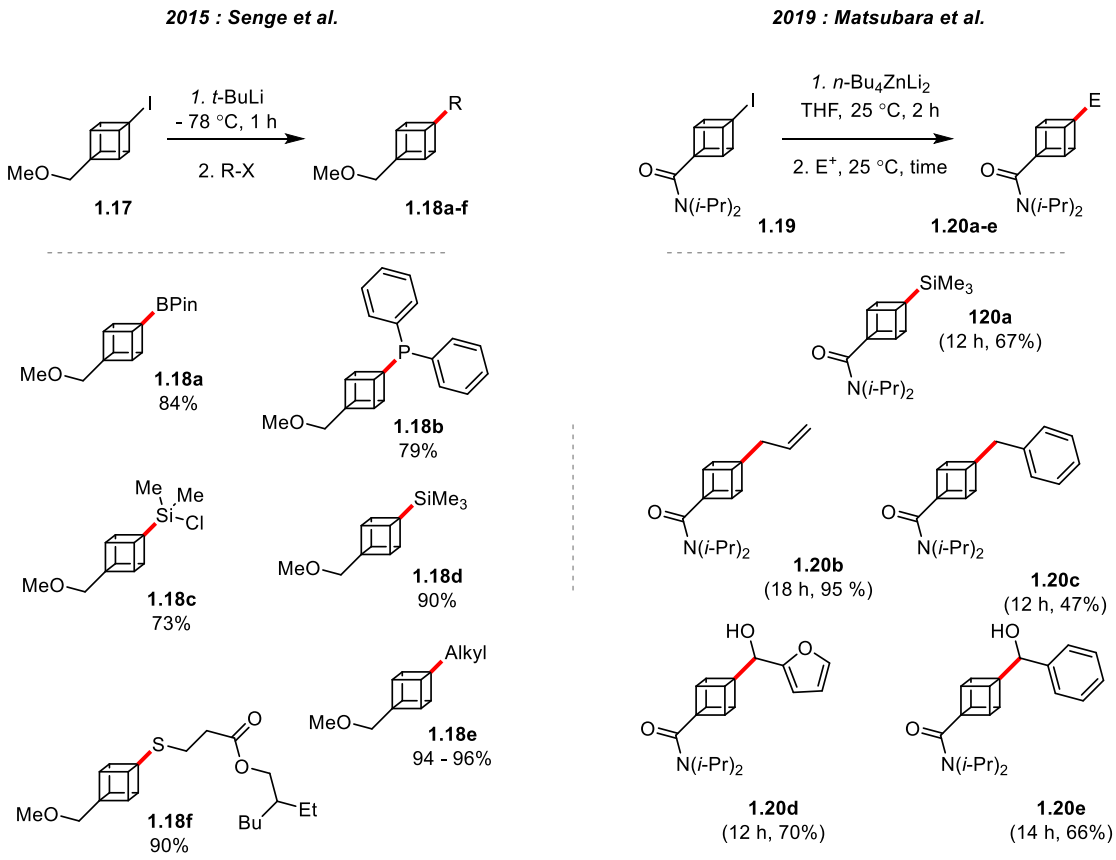

Scheme 5. Generation of cubyllithium anion via halogen–exchange for the synthesis of 1,4–cubane derivatives.[52,53]

1.4.5 *Ortho*–Metalation

A strategy to functionalise the cubane framework, developed by Eaton *et al.*, was to consider *ortho*–lithiation as reported on arenes.[55] They showed the similarity in the C–C–H angle and amount of *s* character (≈ 31%) in the C–H bond between the arene and cubane (Scheme 6). In 1995, Eaton and Castaldi reported *ortho*–lithiation of cubane diisopropylamide **1.21** using lithium 2,2,6,6–tetramethylpiperidide as the base, followed by transmetallation with mercuric chloride.[56] In order to avoid the use of the toxic mercury salt, Bashir–Hashemi improved the transmetallation with the use of magnesium bromide diethyl etherate.[57] The obtained transmetallated species were subsequently trapped using iodine, carbon dioxide, or bromobenzene to give the corresponding 1,2,4–trisubstituted cubanes **1.24**, **1.25** and **1.26**.[56–60] Toyeda, Ueda *et al.* reported the use of piperidine as an *ortho*–directing group for the synthesis of 1,2–cubanecarboxylic acid derivative **1.25** in a low yield.[61] Since then, various polysubstituted cubane derivatives have been synthesised according this method, enabling access to different positions of the cube.[62]

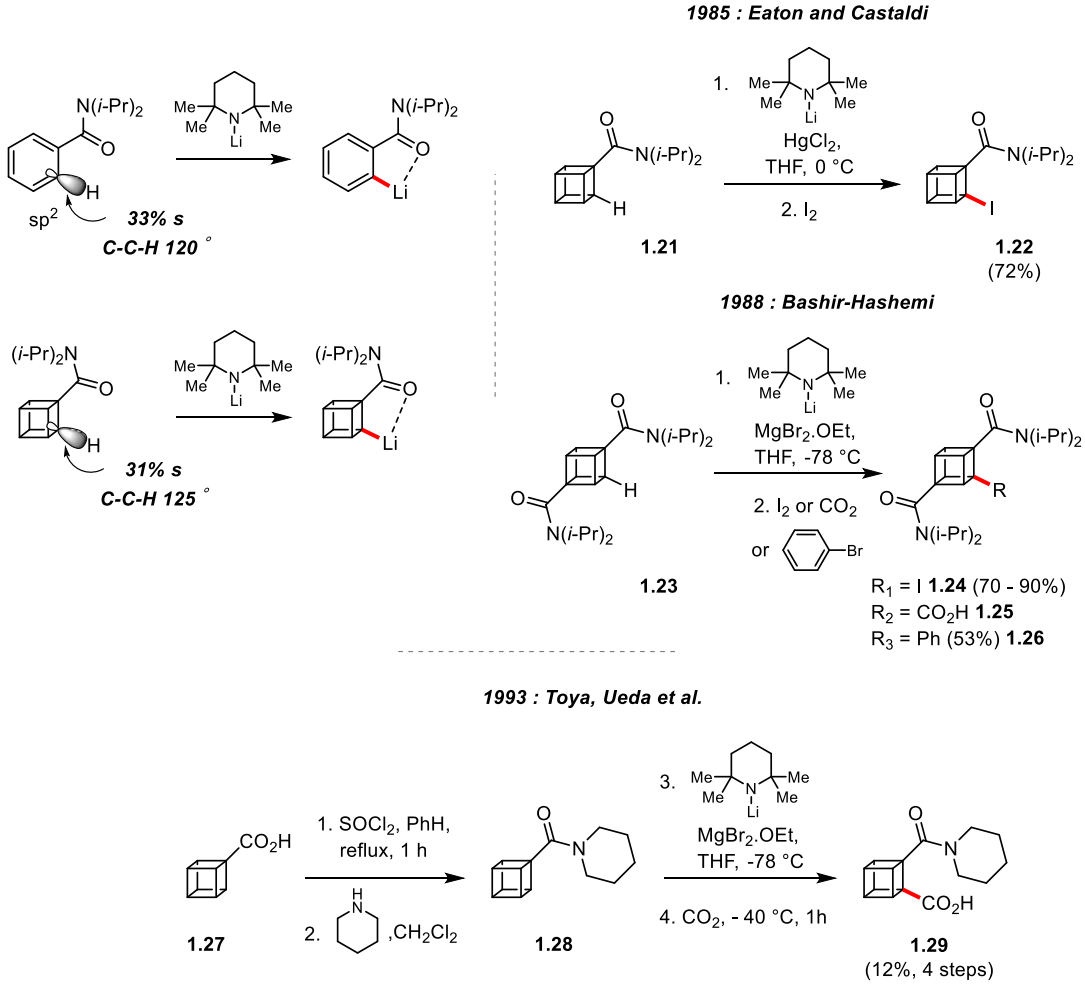

Scheme 6. Comparison between *ortho*–lithiation of benzamide and cubanamide.[55–58,61]

In the quest to synthesise cubene (**1.32**), starting from **1.21**, Eaton and Maggini reported *ortho*–metalation followed by lithium–halogen exchange reaction on 1,2–diiodocubane **1.31** using *tert*–butyl lithium (Scheme 7).[49,50]

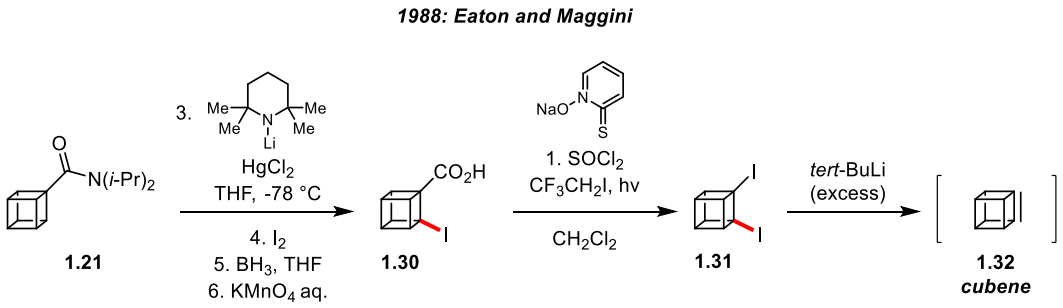

Scheme 7. Accessing 1,2–cubene structure via ortho–metalation and halogen–exchange.[49,50]

1.4.6 Photochemical Chlorocarbonylation of Cubane

Another method for the synthesis of polysubstituted cubanes consists of the photochemical reaction of cubane in oxalyl chloride to give cubane carbonylchloride derivatives.[63,64] Originally reported by Kharasch and Brown in 1940 on cyclohexane, the method was applied to cubane by Bashir–Hashemi in 1993 (Scheme 8).[63,65] Direct irradiation of cubane carboxylic acid **1.27** in oxalyl chloride afforded a mixture of diacid chlorides in 1:1:3 ratio between 1,2– (**1.36**), 1,4– (**1.37**), and 1,3–disubstitution (**1.38**) (Scheme 8).[64]

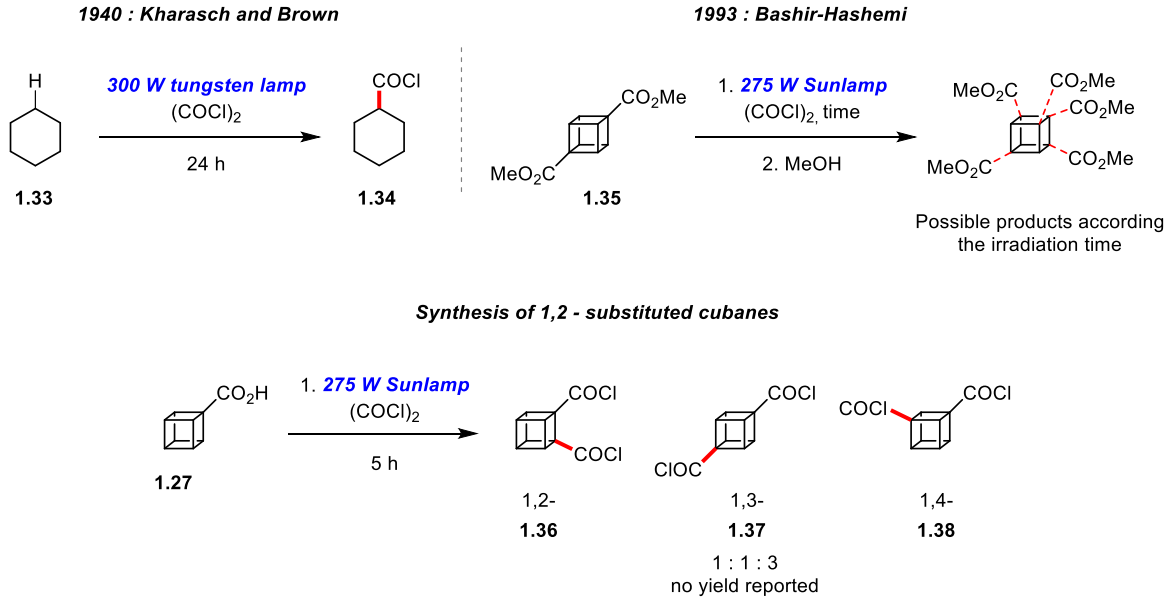

Scheme 8. Photochemical carboxylation originally reported by Kharasch and Brown applied by Bashir–Hashemi on cubane.[64]

When the reaction was performed on dimethyl 1,4–cubanedicarboxylate **1.35**, followed by esterification with methanol, trimethyl 1,2,4–cubanedicarboxylate **1.44** was obtained after 6 h irradiation in a 72% yield. Longer irradiation led to a mixture of tetracarbomethoxycubanes **1.45** and **1.46** in a 55% yield.[63] Bashir–Hashemi observed a high degree of regioselectivity according to the irradiation time, which could be explained by statistical factors and a polar effect. As depicted in Figure 16, **1.6** has three *alpha* (or *ortho*), three *beta* (or *meta*) and one *gamma* (or *para*) positions, and in the presence of an electron–deficient group the chlorine radical preferentially abstracts a hydrogen from the least electron–deficient carbon atom, which is the most distant from the electron–withdrawing group.[63]

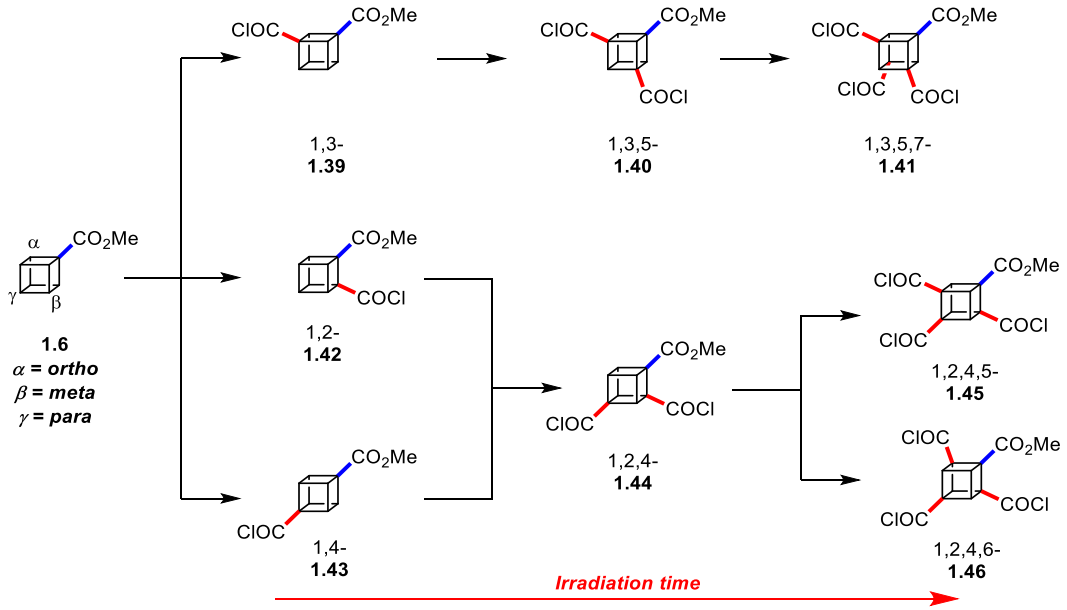

Figure 16. Degree of substitution according irradiation time in oxalyl chloride.[63,64]

1.4.7 Intermediate pre–functionalisation in the synthesis of 1,4–cubanedicarboxylic acid

In 1994, Lowe *et al*, in contrast to direct cubane functionalisation, considered to work on the monoprotected cycloadduct **1.42** prior to the [2+2] photocycloaddition in the developed synthesis of dimethyl 1,4–cubanedicarboxylate **1.35** (see Chapter 2).[66] They reported the synthesis of *ortho*–methylated dimethyl 1,4–cubanedicarboxylate **1.53** *via* 1,4–organocuprate addition on **1.47**. Reaction of **1.47** with methyl magnesium chloride and catalytic amount of copper iodide followed by addition of dry *N*–bromosuccinimide furnished the *gem*–dibromide **1.49** in 60–65% yield after recrystallisation. Afterwards, the dibrominated intermediate **1.49** was subjected to elimination with pyridine under reflux and the corresponding dienone **1.50** was isolated in 65–70% yield. The diketone **1.51** was obtained *via* deketalisation in sulfuric acid. Finally, [2+2] photocycloaddition in methanol followed by a double Favorskii rearrangement, acidic workup and esterification led to *ortho*–methylated dimethyl 1,4–cubanedicarboxylate **1.53** in 14% overall yield starting from **1.47**.

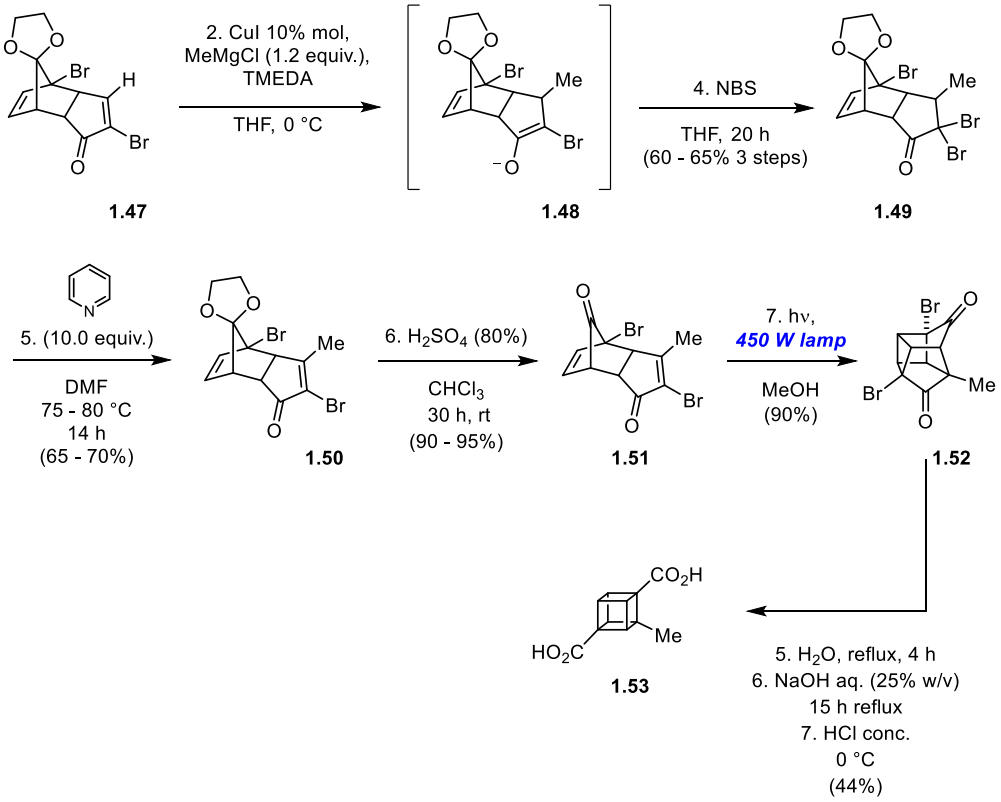

Scheme 9. Synthetic pathway for the synthesis of *ortho*–methylated dimethyl 1,4–cubanedicarboxylate 1.53.

1.5 Continuous–Flow

1.5.1 General

Up to a few years ago, chemical reactions were mostly carried out using macroscopic batch flasks or reactors (Figure 17). The assets of these for chemical synthesis are well known. Batch reactors are cost–efficient and easily adaptable for most types of chemistry. However, batch chemistry suffers from technical limitations hampering upscaling and/or working with toxic or explosive chemicals due to poor mixing and low heat transfer efficiency.[67]

Continuous–flow processing consists of conducting chemical reactions in micro– and/or mesofluidic reactors, which are typically characterised by channels with internal dimensions smaller than 1 mm (Figure 17). This enables chemical reactions to progress under strictly controlled conditions offering a wide range of advantages such as fast mixing, efficient heat transfer, and homogeneity of the reaction medium. Moreover, one of the advantages of using continuous–flow is the possibility of working at high temperatures and pressures, which can improve and enable new conditions for chemical synthetic routes. Finally, recent studies have demonstrated that telescoping batch reactions into continuous–flow processes reduces solvent waste, saves energy, decreases waste generation, and improves product quality.[67–69]

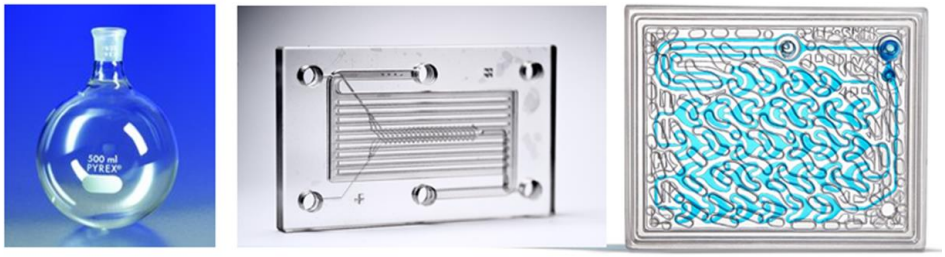

Figure 17. (*Left*) Batch reactor (*Middle*) Microfluidic reactor (*Right*) Corning® Mesofluidic reactor.

Under continuous–flow conditions only a fraction of the total reaction volume is reacting at a time "t". The time the solution will spend inside the microreactor corresponds to the *residence time*, which can be directly controlled by the flow–rate and reactor volume. From these parameters the *residence time* (t_R) can be calculated according the relationship illustrated on Figure 18, using the *internal volume* of the reactor (V_i) and the *flow rate* (Ø) at which the solution is injected inside the microreactor. A considerable advantage of continuous–flow microreactors is that the scale–up does not depend only of the volume of the reactor but can also be achieved by increasing the number of reactors, making it easier to upscale from milligram to multigram scale.[70]

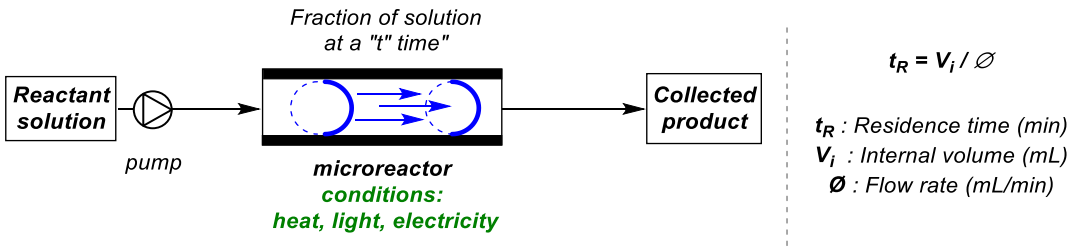

Figure 18. Illustration and Equation connecting residence time, internal volume and flow rate.

1.5.2 Flow photochemistry

Since the last decade, driven by a growing awareness concerning hazardous chemicals and waste, the use of light to carry out chemical reactions has seen a resurgence. Photons are considered to be a traceless and green reagent, hence rendering the photochemical process environmentally friendly and sustainable. However, before the use of continuous–flow microreactors for photochemical reactions, the typical setup consisted of an immersion–well photoreactor in conjunction with mercury–vapour discharge lamps, known as a batch photoreactor. This setup suffers from several drawbacks such as over–irradiation, scalability, safety and, more problematically, the decrease in photon absorption with increasing distance from the lamp (Beer–Lambert Law).[70,71]

Batch photoreactors are usually suitable for milligram–scale synthesis up to few grams. However, in a laboratory fumehood, it becomes very difficult to scale up to multigram–scale. This could be explained by the linear relationship between the absorption of light by the medium and the path length (l), the molar extinction coefficient (ε) of the species and the concentration (C) of the solution (Figure 19). Therefore, if a large amount of compound has to be produced at a relatively low concentration, large volume batch reactors will be necessary, which consequently increases the path length and *vice–versa*. Moreover, batch photoreactors require high power medium pressure lamps, ranging from 125 to 400 W for lab scale to 60 kW for industrial scale, which operate optimally around 600 °C. Therefore, recirculating chiller cooling systems are required for lab experiments and probably stronger systems for industrial scale.[71–74]

$$A = -\log I/I_0 = \varepsilon C l$$

A : absorption of the light by a solution
ε : Molar extinction coefficient (M^{-1} cm^{-1})
C : Concentration of the absorbing species (M)
l : path length (cm)

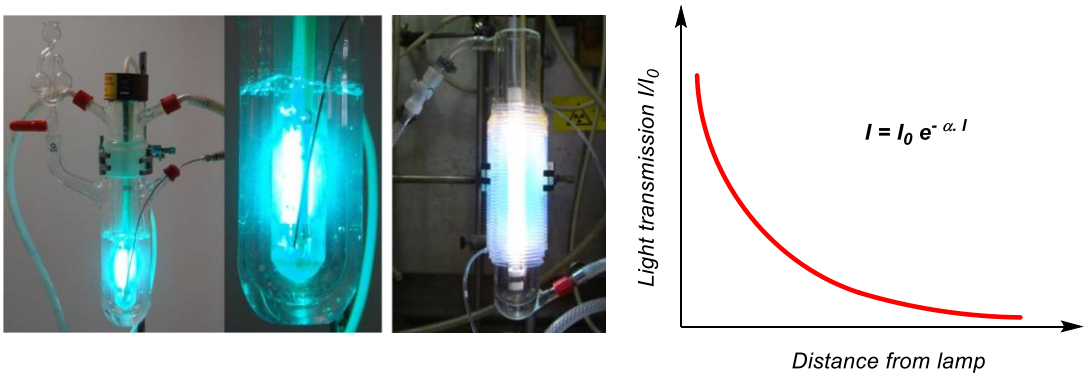

Figure 19. (*Top*) Beer–Lambert Law. (*Left*) Immersion–well photoreactor in conjunction with mercury–vapour discharge lamps (batch photomicroreactor) *(Middle*) Illustration of FEP tubing wrapped around halogen light source (photomicroreactor) (*Right*) Illustration of the Beer–Lambert Law.[72]

The use of microreactors in flow photochemistry can potentially overcome all the issues encountered with batch photochemical processes. The intrinsic property of microreactors, defined by a high surface–to–volume ratio (S/V), enables better mixing and faster heat transfer. Moreover, the small size of the microreactor drastically reduces the attenuation of light intensity as a function of the path length, and consequently enables working at higher concentrations.[71,73]

Obviously, the selection of an adequate light source remains pivotal for photochemical applications and mainly depends on the overlap between the emission spectrum of the light source and the absorption wavelength(s) of the photoactive species. The cost, energy efficiency, lifetime, as well as the physical dimension of the light source and photoreactor are also important criteria when considering a photochemical process. Mercury–based and compact fluorescent lamps (CFL) have been commonly used for UV and visible–light applications respectively. However, these lamps emit a broad band of wavelengths which can interfere in some cases with the substrate or the product themselves, potentially leading to side–reactions or decomposition.[73] Moreover, the wavelengths that are not useful for the chemical transformations represent a loss of energy, and consequently, a lack of process efficiency. In that regard, the use of lamps irradiating a narrower range of wavelengths are expected to be more efficient even at lower power. Another solution consists of using optical filters. In the last few years, due to the progress made in that field, a number of photochemical continuous–flow applications with Light Emitting Diodes (LEDs) have been reported. LED technology enables very narrow emission bands, and the emitted wavelengths can be tailored and

matched more adequately with the photochemical application. Furthermore, LEDs consumed less energy and their temperature can be controlled with cheaper and lower–energy cooling systems.[73]

1.5.3 Flow Electrochemistry

In electrochemistry, the products are generated by the addition or removal of electrons. The simplest general electrochemical setup consists of a power supply connected to two electrodes where the electron(s) transfer occurs to generate a reactive intermediate from either the substrate to one of the electrodes for the *oxidation*, or from the electrode to the substrate for the *reduction*. The electrode where the *oxidation* reaction occurs is called the *anode*, whereas *reduction* occurs at the *cathode*. In both cases, depending on where reaction with the substrate takes place, either the anode or cathode is defined as the *working electrode* (Figure 20). The other electrode, known as the *counter electrode*, is used to close the electric circuit. The electrical current, measured in amperes, passes through the solution from the cathode to the anode to complete the circuit. Depending on the type of reaction, the generated reactive intermediate can be prematurely reduced or oxidised before the desired reaction occurs. In order to avoid this, a semi–permeable membrane or a salt–bridge can be added to separate the anodic and cathodic chambers (*divided cell*, Figure 20).[75]

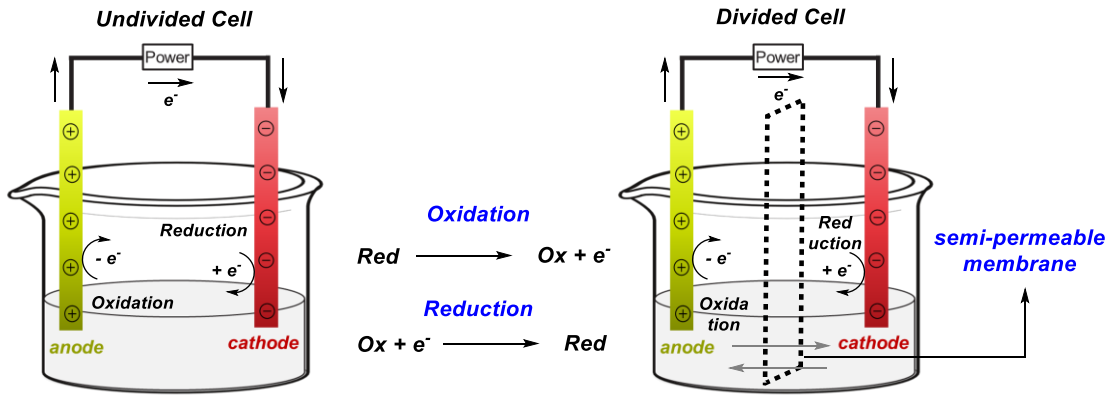

Figure 20. (*Left*) Undivided and (*Right*) divided electrolysis cell.

Since the development of organic electrosynthesis until today, reactions have been (and are still mainly) carried out in glass cells such as beaker cells. However, while such cells are easily assembled from laboratory glassware, they usually produce slow chemical transformations with long reaction times, and sometimes poorly reproducible conditions. The recent increase in high temperature chemistry, cryogenic reactions, and photochemistry under flow conditions has led to the implementation of flow processes in electrochemistry, and therefore the development of flow electrochemical cells.[76,77] Flow cells consist of bed electrodes with a narrow interelectrode gap in which the solution is pumped through (Figure 21). As described for divided batch cells, a semi–permeable membrane is added between both electrodes (Figure 21). Flow cells can be operated either with recycling of the reactant through the cell or in a single pass mode. Compared with conventional

batch electrochemistry, the use of flow cells present numerous advantages. Due to the small electrode gap between the two electrodes, the high surface–area–to–volume ratio facilitates electron transfer between electrodes, providing high scalability and cleaner transformations than comparative batch processes. Several studies and designs of flow cells have been reported through the years.[77]

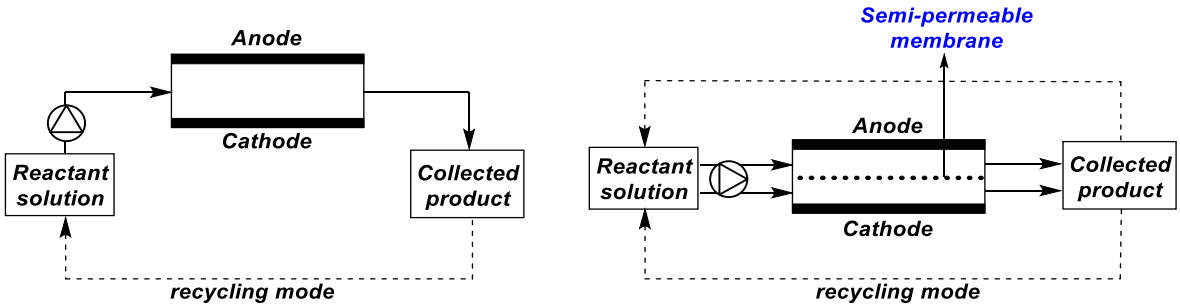

Figure 21. Flow electrochemical cell representation. (*Left*) undivided cell (*Right*) divided cell.

1.6 Aim of the project

Although numerous functionalised cubanes have been synthesised in the past 60 years, its use in agrochemicals, medicinal chemistry and drug development remains somewhat underexplored. Most of the reported transformations consist of 1,4–carboxylic acid group interconversion. Although carboxylic acid groups enable broad and straightforward diversification in synthetic chemistry, functionalisation of carboxylic acids into more complex functional groups through decarboxylative procedures remain challenging.[78] Moreover, polysubstituted cubane derivatives are difficult to access due to limited and impractical reported pathways. Nowadays, the commercially available cubane building block, dimethyl 1,4–cubanedicarboxylate, remains expensive to purchase and its synthesis is still hampered by technical challenges to routine multigram synthesis in a laboratory fumehood.

In the past decade, industry and the organic chemistry community have turned toward the use of reagentless techniques such as photochemistry and electrochemistry for the implementation of sustainable process and the discovery of new synthetic pathways. Initially developed in conventional batch chemistry, the implementation of these techniques in flow chemistry has brought advantages such as efficiency and safety.

This work aims to develop efficient protocols for the functionalisation of cubane. In order to reach this goal, the photocycloaddition step required for the synthesis of dimethyl 1,4–cubanedicarboxylate will be implemented in continuous–flow in order to access multigram quantities whilst avoiding the use of a batch photoreactor. This is described in chapter 2. Next, based on the potential of decarboxylative functionalisations of dimethyl 1,4–cubanedicarboxylate, this work aims to develop an oxidative decarboxylative process under flow electrochemical conditions to achieve a Hofer–Moest reaction and potentially access a wide range of new alkoxy cubane derivatives. This is described in chapter 3. Finally, C–H abstraction of the cubane core will be investigated to access polysubsituted cubane scaffolds and described in chapter 4.

Chapter 2 Synthesis of Dimethyl Cubane Dicarboxylate

2.1 Reported Synthetic Routes towards Dimethyl Cubane Dicarboxylate

2.1.1 Eaton and Cole's synthesis

In 1953, William Weltner Jr. concluded at the end of his paper on "acetylenic strained hydrocarbons" that tricyclooctane (cubane) might or might not be synthesised, precipitating the quest for its synthesis.[79] Ten years later, despite some erroneous claims by Freedman[80], Throndsen and Zeiss[81], Philip Eaton and Thomas Cole were the first to report this feat in 1964.[36,37,82] They reported two communications describing first the isolation of the dimethyl 1,4–cubanedicarboxylate **1.35** (Scheme 10) and secondly cubane itself (Scheme 12).[37,82] The cubane system **1.35** was obtained from 2–cyclopentenone **2.1** in eight steps as illustrated in Scheme 10 and relies on three main synthetic elements: the highly *endo*–selective [4+2] Diels–Alder reaction (**2.4→2.5**), a [2+2] photocycloaddition (**2.5→2.6**) and finally a double Favorskii rearrangement (**2.6→1.35**).

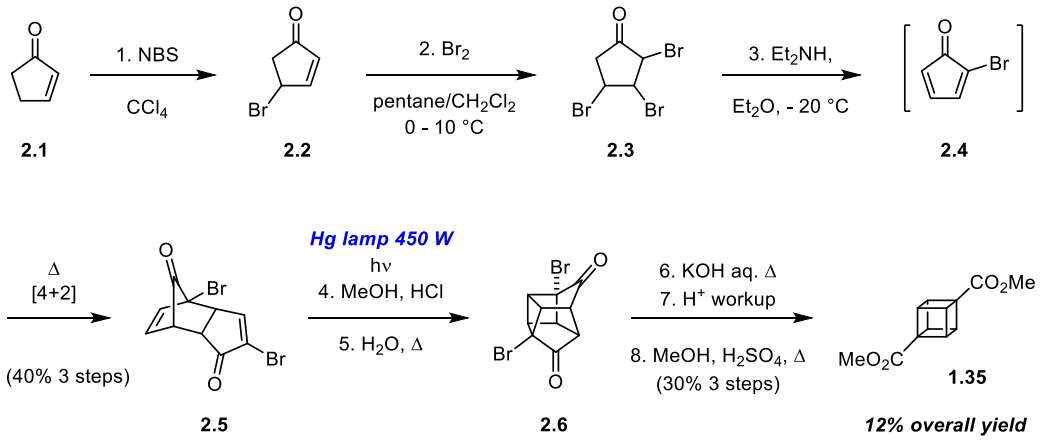

Scheme 10. Eaton and Cole's synthesis of the dimethyl 1,4–cubanedicarboxylate.[82] Reprinted with permission from ref [83]. Copyright 2021 Georg Thieme Verlag KG.

Eaton and Cole reported two bromination steps from the cyclopentenone **2.1** by using *N*–bromosuccinimide and molecular bromine respectively. The tribromocyclopentanone **2.3** was subjected to a double dehydrobromination to give 2–bromocyclopentadienone **2.4** that spontaneously dimerised to give **2.5**. The [4+2] Diels–Alder cycloaddition occurs with complete regio– and stereo–selectivity to give the corresponding *endo* product **2.5**. Eaton proposed the structure of **2.5** postulating that the dimerisation occurs via an *endo*–transition–state analogous to cyclopentadione, and that the dienophilic reactivity of **2.4** would be lowest at the halogen–substituted double bond in analogy to what is observed for chlorobenzoquinone. Furthermore, the reaction proceeds *via* a transition state **1** (Figure 22) by which the unfavourable interaction of like dipoles is minimised, unlike in the

alternative *endo*–transition state **2**, consequently leading to **2.5** instead of **2.7**. Moreover, in the *exo*–Diels–Alder product, the two alkenes are not correctly positioned to allow the [2+2] cycloaddition in the next step (**2.5→2.6**). Finally, the last steps give the 1,4–disubstituted cubane which can only be obtained when the bromine atoms are arranged as in the cycloadduct **2.5** and not **2.7**.

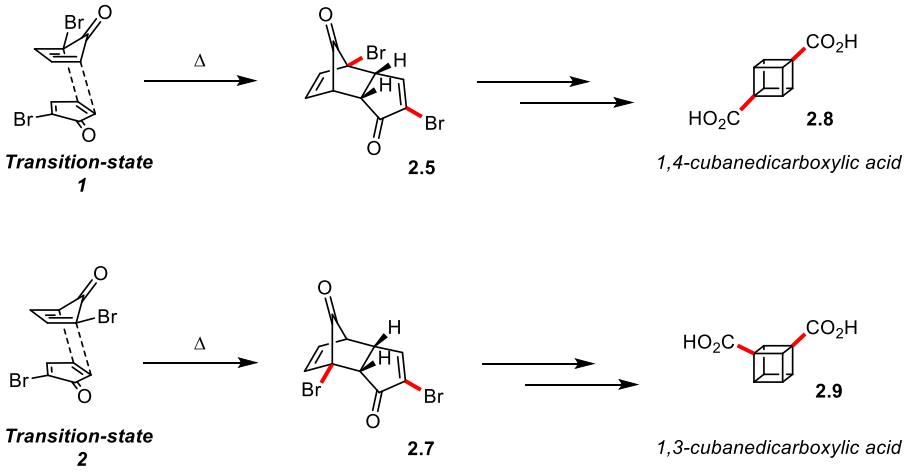

Figure 22. Transition–state leading to 1,4–substituted cubane.[82]

Irradiation of **2.5** in acidic methanol using a mercury lamp (450 W) lead to the formation of the caged intermediate, obtained presumably as the bishemiketal form of **2.6**. Afterwards, the diketone **2.6** was obtained *via* deketalisation in refluxing acidic water followed by dessication. Finally, double Favorskii rearrangement, acidic workup followed by esterification led to dimethyl 1,4–cubanedicarboxylate **1.35** in 12% overall yield starting from 2–cyclopentenone **2.1**. The Favorskii rearrangement can be formulated as a semi benzylic acid–type rearrangement. The scale was not reported by Eaton and Cole in those communications.

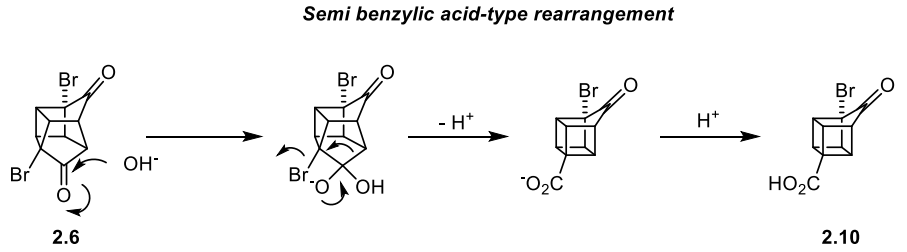

Scheme 11. Benzylic acid–type rearrangement for the Favorskii rearrangement of 2.6.[82]

The isolation of cubane itself reported by Eaton and Cole the same year involved a slightly different synthetic pathway (Scheme 12).[37] Bisethylene ketal cycloadduct **2.11** was prepared by protection of the dione **2.5** with ethylene glycol and subsequently hydrolysed to the mono–protected cycloadduct **1.47**. In contrast to their first communication, the photochemical step was now carried out in benzene instead of methanol to give the desired photocycloadduct **2.12**. A first Favorskii rearrangement, followed by a reductive decarboxylation through a thermal–induced homolytic cleavage of *tert*–butyl perester in cumene, led to the homocubyl ketal intermediate **2.15**. Finally, after acetal deprotection

in acidic medium, cubane **1.2** was obtained from **2.16** through a similar sequence: ring contraction *via* Favorskii rearrangement and reductive decarboxylation *via* the perester **1.3**.

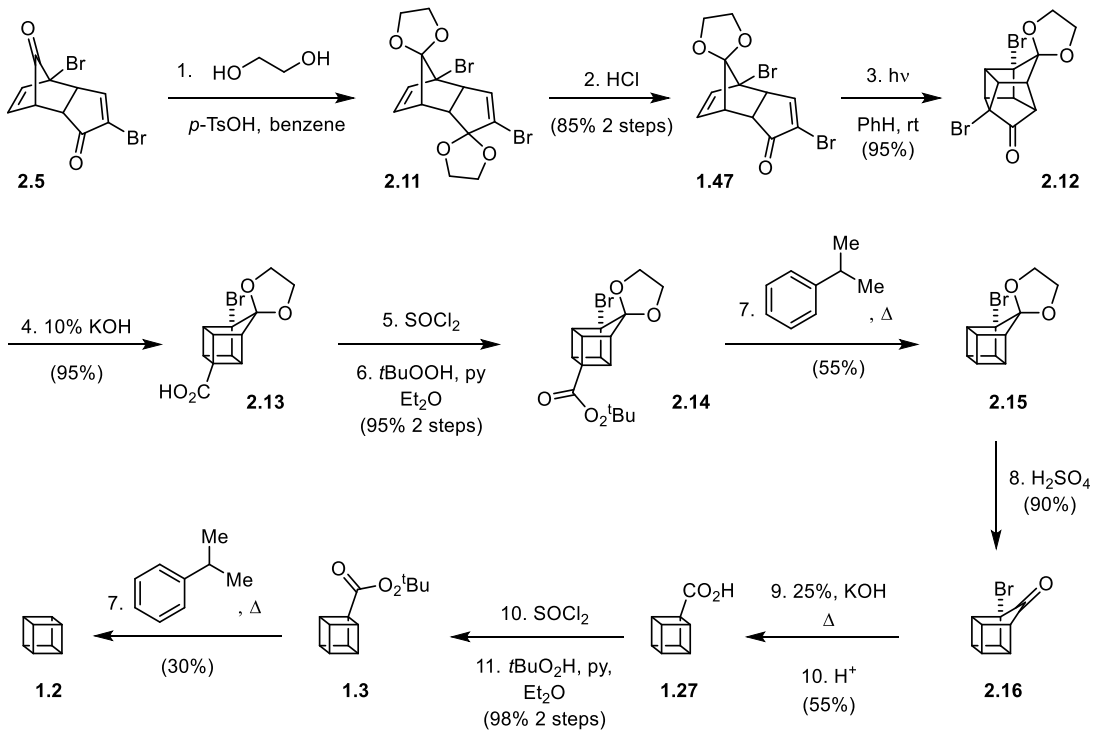

Scheme 12. Eaton and Cole's cubane synthesis.[37]

2.1.2 Chapman's Synthesis

Several years later, in 1970,[84] Chapman and co–workers reported several modifications from the original work. It builds in part upon the work of both Eaton and DePuy on cyclopentadienone ketals, leading to the replacement of cyclopentenone **2.1** used originally by Eaton with cyclopentanone ethylene ketal **2.17** as starting material.[85] The Chapman synthesis provided a necessary step forwards in regards to the synthesis of cubane, eliminating the need for the highly toxic carbon tetrachloride. Also, the required 1–bromo–1,4–diene moiety was now obtained in one operation, as opposed to Eaton's two successive brominations. In addition, the use of ethylene ketal protection of 2–bromocyclopentadienone (**2.19** compared to **2.4**) increased the reactivity of the Diels–Alder dimerisation, and the corresponding cycloadduct **2.11** was obtained with 76% yield. After selective enone deprotection, irradiation of the **1.47** in benzene with 450 W Hanovia medium–pressure mercury lamp for 24 h on 17–gram scale afforded the caged ketal **2.12**. The [2+2] photocycloaddition was also carried out in benzene. Subsequently the hydrolysis of the ketal in sulfuric acid conditions led to the hydrates of **2.6**, and was followed by dessication/recrystallisation to give caged dione **2.6** in 43% yield over three steps. Finally, the double Favorskii rearrangement followed by esterification with diazomethane delivered the desired dimethyl 1,4–cubanedicarboxylate **1.35**. However, they reported a low, approximate 3% overall yield which was attributed to problems encountered with the double Favorskii rearrangement.[84]

Chapman *et al.* could not reproduce the results obtained for the double ring contraction by Eaton *et al.* and obtained approximately 10% yield despite exploring a range of reaction conditions. However, two years later, Luh and Stock reported the use of the original approach without difficulty in addition to the improvement of this step to 75% by using 25% (w/v) aqueous potassium hydroxide under 2 h reflux.[86]

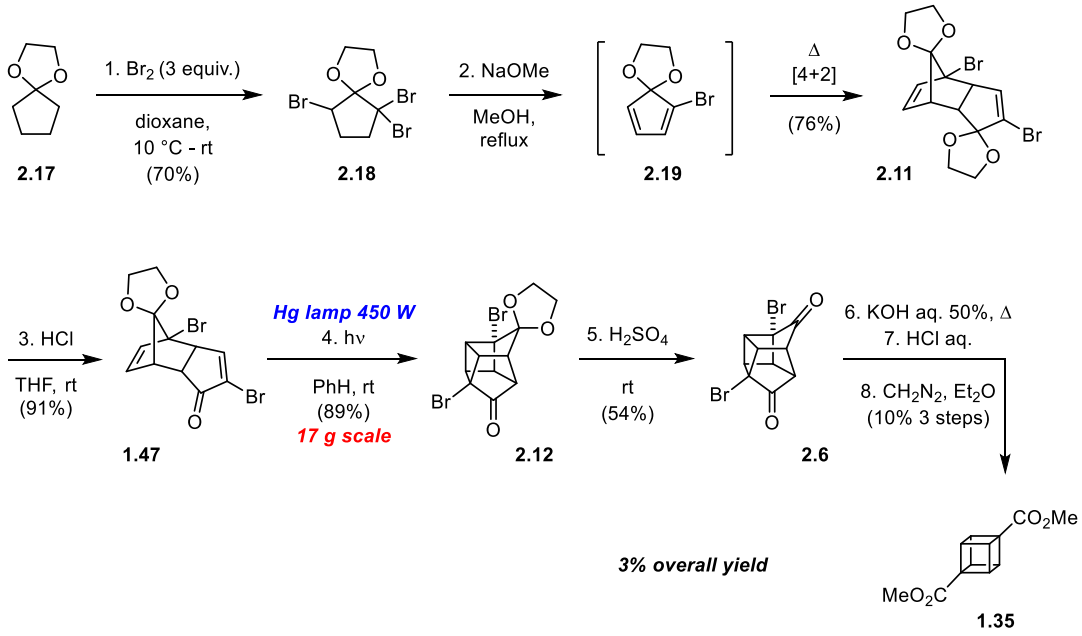

Scheme 13. Chapman's synthesis of dimethyl 1,4–cubanedicarboxylate.[84] Reprinted with permission from ref [83]. Copyright 2021 Georg Thieme Verlag KG.

2.1.3 Tsanaktsidis's *et al.* Synthesis

In 1997, Tsanaktsidis and co–workers reported an optimised practical laboratory synthesis of dimethyl 1,4–cubanedicarboxylate **1.35** on decagram–scale.[87] Built on key elements from Eaton's and Chapman's approaches, they started from cyclopentanone ethyl ketal **2.17**, but later deprotected the bisethylene ketal cycloadduct **2.11** to the dione **2.5**, prior to the photochemical step, rather than using the mono–protected cycloadduct **1.47**. The photochemical step was carried out on 50 g scale with a 450 W Hanovia medium mercury lamp in a water–cooled Pyrex immersion well apparatus. However, no irradiation time was reported. According their procedure, the photocycloaddition was carried out in acidic methanol leading presumably to a mixture of hemiketals and ketals of **2.6**. Tsanaktsidis *et al.* confirmed and improved the Luh and Stock protocol for the double ring contraction with the use of 25% (w/v) aqueous sodium hydroxide solution. Finally, the use of acidic Dowex® resin in anhydrous methanol for the esterification of the 1,4–cubanedicarboxylic acid **1.1** and subsequent purification step by sublimation under reduced pressure, followed by recrystallisation in methanol/acetonitrile enabled them to isolate dimethyl 1,4–cubanedicarboxylate **1.35** with an overall yield of 23%.

In 2013, the same group reported a pilot–scale synthesis for the production of half a kilogram of **1.35**.[88] In order to process kilogram scale of **2.5**, the [2+2] photocycloaddition step was implemented in a semi–batch continuous–flow photoreactor in which the solution was pumped continuously for 7 days (173 h). The structure of the photoreactor consists of a fixed volume cell of 6.4 L (Pyrex glass) with a 2 kW medium pressure Hg lamp (Scheme 14).

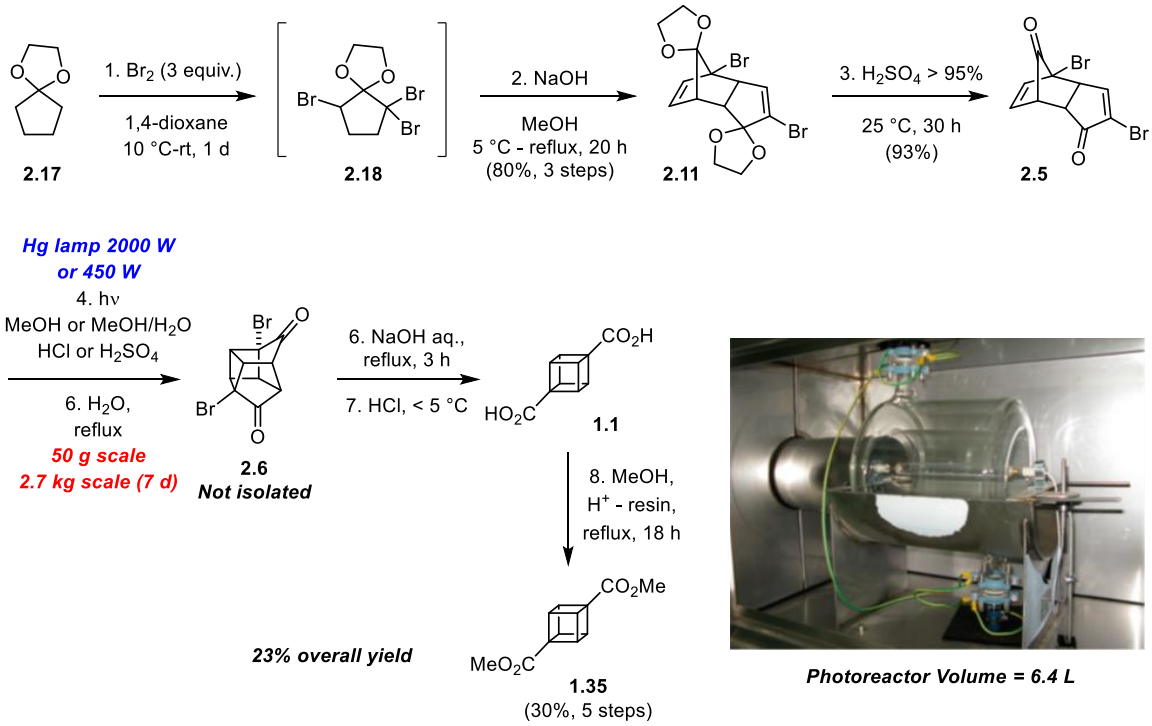

Scheme 14. Tsanaktsidis and co–workers improved synthesis of 1.35.[87,88] Reprinted with permission from ref [83]. Copyright 2021 Georg Thieme Verlag KG.

2.2 Reported Synthetic Routes towards 1,3–Cubanedicarboxylic acid

In 1966, Barborak, Watts, and Pettit reported the synthesis of 1,3–cubanedicarboxylic acid *via* an elegant 3–step synthesis in 51% overall yield.[89] The authors exploited the reactivity of cyclobutadiene–iron tricarbonyl which undergoes Diels–Alder reaction *via* oxidative decomposition using cerium ammonium nitrate in the presence of 2,5–dibromo 1,4–benzoquinone **2.21**. Irradiation of **2.22** enables a [2+2] photocycloaddition, followed by a double Favorskii rearrangement leading to 1,3–cubanedicarboxylic acid.

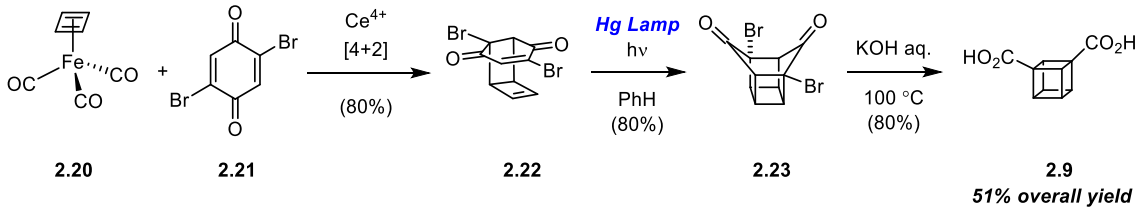

Scheme 15. Petitt *et al.* synthesis of 1,3–cubanedicarboxylic acid (2.9).[89]

Another approach consists of the [2+2] photocycloaddition of octasubstituted tricyclo[4.2.0.0^{2,5}]octa–3,7–diene derivatives **2.24** to synthesise octasubstituted cubanes **2.25**–**2.28** such as depicted in Scheme 16.[90–93]

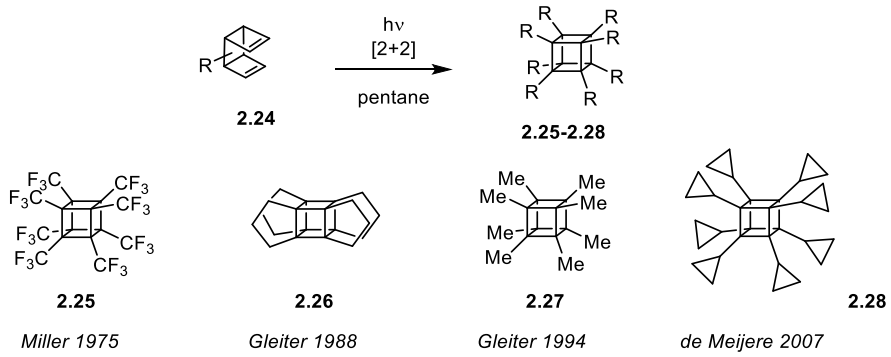

Scheme 16. General reported synthetic pathway for the synthesis of octasubstituted cubanes.[90–93]

2.3 Results and Discussion

2.3.1 Outline of the synthesis

Dimethyl 1,4–cubanedicarboxylate **1.35** is an expensive starting material, it was therefore decided to develop a large–scale in–house synthesis starting from cyclopentanone, with a custom build flow–photoreactor to enable the [2+2] photochemical step. This section describes the optimisation of this synthesis, which features elements of the different syntheses available in the literature.

Although the synthesis on decagram and kilogram–scale has been reported by Tsanaktsidis *et al.*, the apparatus used is not available.[88] Typically, the [2+2] photocycloaddition step has been achieved *via* immersion well glassware with a pressurised mercury lamp. These lamps emit from 200 to 450 nm in the UV–spectrum and operate optimally at high temperature which requires water–cooled immersion–well apparatus. The fixed size of such glassware limits scalability, with the need to always adopt larger–sized reactors or to use it as a recycling photochemical cell as in Tsanaktsidis' procedure. This last operation procedure needs, even for decagram synthesis of cubane, several days of irradiation. Despite the development of commercially available flow photochemical reactors in the last years, they remain expensive to purchase and are usually limited in reactor size, leading us

to develop a custom–built photoreactor. In contrast to optimisation in batch, the identification of the photocycloadduct intermediates is required for optimisation of the different flow parameters. Therefore, as part of the optimisation process in the flow reactor, additional efforts were devoted to the characterisation of the photocycloadduct **2.6**.

2.3.2 Synthesis of the photocycloaddition intermediate

Our synthetic endeavour began with the synthesis of the cycloadduct **2.5**. Following the protocol of Tsanaktsidis *et al.*, the protected cyclopentanone **2.17** was tribrominated using molecular bromine in dioxane, followed by a double elimination reaction in the presence of a sodium hydroxide solution in methanol, to generate the highly reactive 2–bromocyclopentadienone ethylene ketal **2.19**. As reported previously by Tsanaktsidis *et al.*, while the first elimination proceeds rapidly, the second dehydrobromination requires a higher temperature. Indeed, we observed by ^{1}H NMR analysis that the desired cycloadduct **2.11** could not be obtained without sufficient heating. Finally, compound **2.11** was obtained as a beige solid in 89% yield without any chromatographic purification. The fourth step consists of the hydrolysis of both acetals in concentrated sulfuric acid. The crude *endo*–2,4–dibromodicyclopentadiene–1,8–dione **2.5** could be obtained in 86% yield by precipitation in ice–water. This 4–step sequence has been upscaled to 50 g of **2.17**. For safety reasons, further upscaling was not attempted given the large volume of molecular bromine required (up to 70 mL) for the conversion of **2.17** to **2.18**.

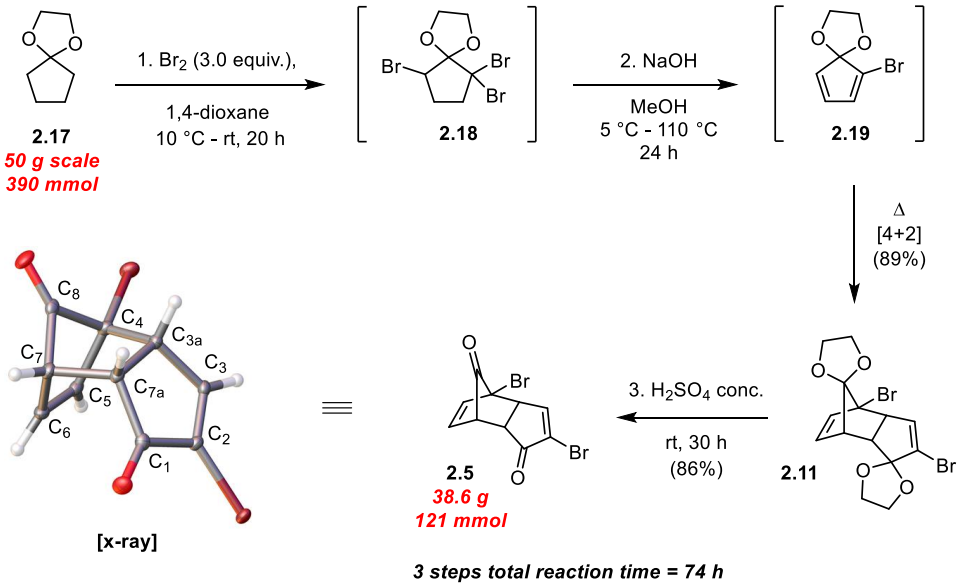

Scheme 17. Synthesis of the cycloadduct 2.5 prior to the [2+2] photochemical step. Reprinted with permission from ref [83]. Copyright 2021 Georg Thieme Verlag KG.

Dissolution of **2.5** in methanol lead to a dark solution, consistent with reported procedures (Figure 23, left). In order to prevent fouling or clogging of the microreactor with impurities, **2.5** was subjected to further purification by recrystallisation in hexane/ethyl acetate (2:1) to afford colourless crystals,

which produced a colorless solution upon dissolving in methanol (Figure 23, right). Tsanaktsidis *et al.* mentioned the need for recrystallisation to furnish a pure analytical sample, however, the crude cycloadduct **2.5** was used without additional purification in their process. According to the crystal structure, not previously reported, the distances between $C_6 – C_2$ and $C_5 – C_3$ are 3.475 Å and 2.992 Å respectively.

Figure 23. (*Left*) Solution of 2.5 without recrystallisation in methanol. (*Right*) Solution with obtained crystals.

2.3.3 [2+2] photocycloaddition using Flow Photochemistry

2.3.3.1 Construction of the flow apparatus

With the desire to develop a low–cost process, accessible to any research laboratory, the photoreactor was constructed according the method reported by Harrowven *et al*.[94] Even though the setup is inspired from the pioneering work of Booker–Milburn, the one used is far less expensive and only requires commercially available light bulbs.[72] Low–energy 9 W and 36 W lamps were used instead of 450 or 2000 W medium–pressure mercury lamps previously reported by Eaton, Chapman and Tsanaktsidis. The lamps were fitted in a quartz tube wrapped with one layer of FEP tubing (0.8 mm ID x 1.6 mm OD), and protected from eyesight with aluminium foil. For the large–scale reactor, tubing was additionally wrapped on the outside of the aluminium foil to allow water cooling. A syringe pump for preliminary and small–scale experiments, and a peristaltic pump for large–scale experiments, were used. The use of quartz glassware enables access to a broad spectrum of UV light, simply by changing the lamp.[94]

2.3.3.2 Selection of the irradiation source

According the work of Eaton, Chapman and Tsanaktsidis, pyrex glassware has always been reported. The latter is known to filter radiation below 300 nm. The UV–absorption spectrum of **2.5** shows two main peaks. A strong UV absorbance at 247 nm due to $\pi \rightarrow \pi^*$ transition and a weaker, difficultly observable band between 300 and 350 nm corresponding to the $n \rightarrow \pi^*$ transition, previously mentioned by Tsanaktsidis *et al.* to be responsible for the desired transformations.[88] It was decided

to investigate the use of UV–C (λ = 254 nm), UV–B broadband spectrum (λ = 280 – 370 nm) and narrowband spectrum (λ = 280 – 315 nm).

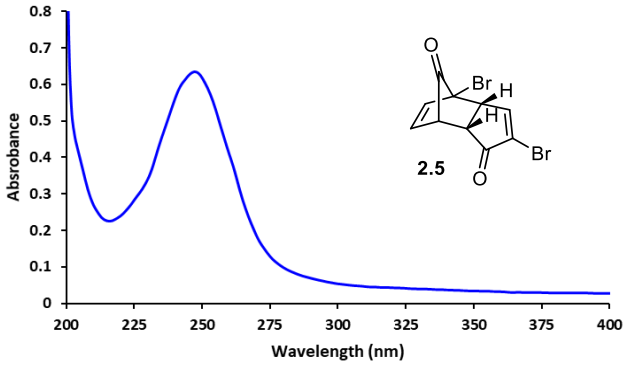

Figure 24. UV–spectrum of dione 2.5.

2.3.3.3 Structure of the photocycloaddition product

The optimisation of the [2+2] photocycloaddition step using continuous flow required full characterisation of the reaction mixture components. While Eaton and Chapman reported ^{1}H NMR data of the dione **2.6**, in our hands, the spectra obtained from evaporating flow reactor output aliquots proved to be much more complex as depicted on (Figure 25).

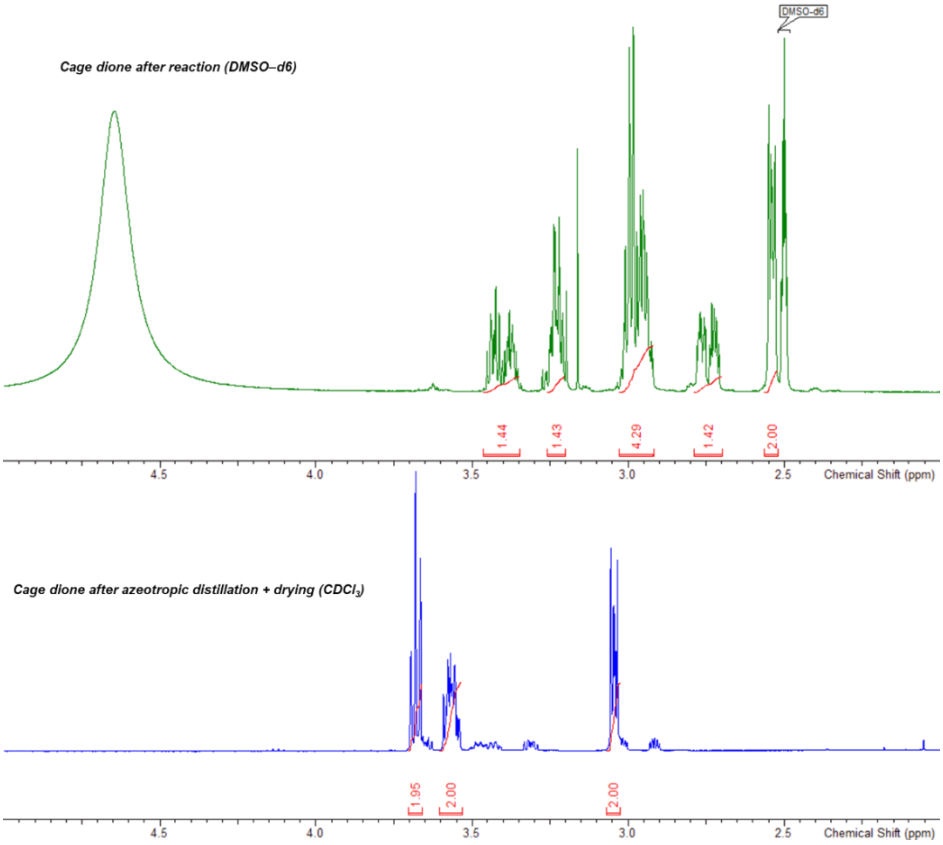

Figure 25. (*Green*) Crude Photocycloadduct obtained after reaction (*Blue*) Cage dione 2.6 after azeotropic distillation and drying.

Because the photochemical step was carried out in acidic methanol/water, the dione **2.6** is presumably accompanied by its hydrates **2.6a** and **2.6b** after removal of solvent (Figure 26). While this has been noted by Eaton, Chapman, and Tsanaktsidis, no characterisation of these species was available. In addition, **2.6** has only been characterised by ^{1}H NMR (at 100 MHz), in which the overlapping individual proton environments could not be assigned (Figure 25). In order to achieve full mixture analysis of the collected crude samples at the outlet of the reactor, a full characterisation of **2.6** and its hydrate derivatives was undertaken.

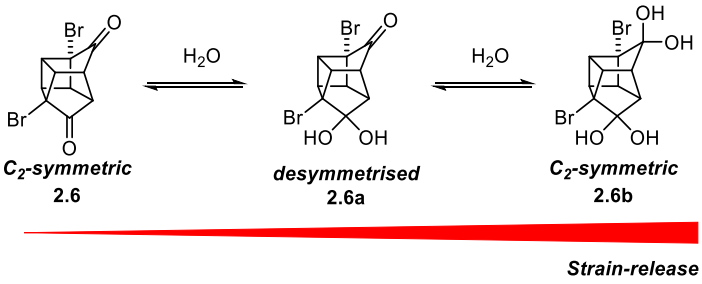

Figure 26. The dione 2.6 and its hydrate(s) 2.6a and 2.6b.

In contrast to previously reported[82], we found that the dione **2.6** could be isolated *via* repeated azeotropic distillation using toluene. Unlike the hydrate forms **2.6a** and **2.6b**, the dione **2.6** was soluble in chloroform. Upon standing, however, the ketone **2.6** slowly rehydrates if it was not stored over P_2O_5 in a desiccator.

As depicted in Figure 27, **2.6** possesses a C_2–rotational axis going through the middle of two bonds (indicated in yellow, Figure 27). Therefore, only three chemically distinct proton environments are expected by ^{1}H NMR analysis, with H–3 and H–1 as doublets and H–2 as a doublet of doublets, which, at higher field (400 MHz), could be observed in the ^{1}H NMR spectrum. In addition, the five environments observed for **2.6** in the ^{13}C NMR spectrum clearly indicated two–fold molecular symmetry, with the resonance at 203.2 ppm showing the presence of the carbonyl groups (see Appendix A.1 Figure 54 for details).

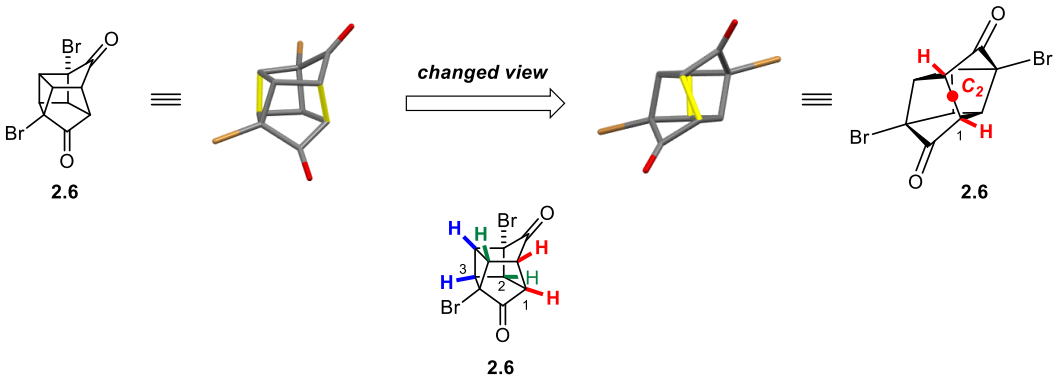

Figure 27. Presence of a C_2–axis in 2.6. Reprinted with permission from ref [83]. Copyright 2021 Georg Thieme Verlag KG.

Table 1. ^{1}H NMR characterisation data of 2.6 reported by Eaton and Chapman in $CDCl_3$ (100 and 400 MHz).

Authors	^{1}H NMR τ (ppm) (originally reported)	^{1}H NMR δ (ppm)	^{13}C NMR δ (ppm)
Eaton *et al.*	6.37 (m, 4H), 6.95 (m, 2H)	3.63 (m, 4H) 3.05 (m, 2H)	-
Chapman *et al.*	6.28 – 6.44 (m, 4H) 6.86 – 7.02 (m, 2H)	3.56 – 3.72 (m, 4H) 2.98 – 3.14 (m, 2H)	-
This work	-	3.04 (dd, J = 5.1, 3.2 Hz, 2H_1)	41.0 (CH_1)
		3.53 – 3.60 (m, 2H_2)	43.6 (CH_2)
		3.66 – 3.70 (m, 2H_3)	45.1 (CH_3)
		-	53.1 (C–Br)
		-	203.2 (CO)

The complete assignment of **2.6** spectra (Figure 25) was achieved enabling a correction of the previously reported data (Table 1).[95] The assignment of the proton pair H–2 could be easily given by ^{1}H COSY NMR as they correlate with H–3 and H–1. However, the HMBC NMR did not reveal the correlations needed to enable the unambiguous assignment of H–1 and H–3. Nevertheless, work on similar caged molecules (Figure 28) by Dunn *et al.*[96], and Stedman and Davis[97] have shown that protons α–to the carbonyl are located in its shielding zone, and therefore, our assignments of H–1 and H–3 was based on these observations.[96,97]

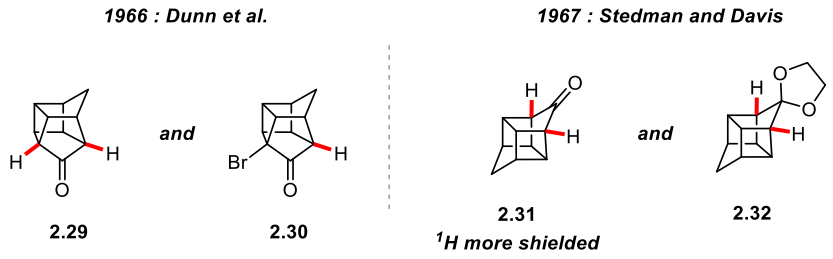

Figure 28. Studied structures by Dunn *et al.*, and Stedman and Davis to determine the shielding of α–protons.[96,97]

Next, we decided to assign the NMR spectra of the hydrates **2.6a** and **2.6b**. Based on the C_2–symmetry of **2.6** and the equilibrium occurring between the hydrates and the corresponding dione

2.6, we reasoned that the dihydrate (**2.6b**) was also C_2–symmetric whereas the formation of the monohydrate (**2.6a**) will lead to desymmetrisation, and therefore, will increase the number of proton environments explaining the more complex spectrum observed. The observation of only one carbonyl peak (205.9 ppm) in the ^{13}C NMR spectrum together with two hydrate carbon peaks (106.1 ppm) and nine C–H (3 + 6) peaks, confirmed the presence of both the mono– and dihydrates (See Appendix A.1 Figure 57). The ^{1}H COSY NMR analysis allowed assignment of the resonances of the dihydrate and of the monohydrate (See Appendix A.1 Figure 55).

Pleasingly, despite the spectral complexity, those results revealed that only the desired carbocycle was formed during irradiation. Moreover, the conversion towards **2.6** according to residence time in continuous–flow could be now easily calculated (see Appendix A.2 for details).

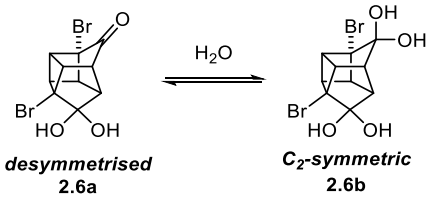

Table 2. ^{1}H and ^{13}C NMR chemical shifts of 2.6a and 2.6b. **Reprinted with permission from ref [83]. Copyright 2021 Georg Thieme Verlag KG.**

Compounds	^{1}H (ppm)	^{13}C (ppm)
2.6a	3.41 – 3.46 (m, 1H), 3.35 – 3.40 (m, 1H), 3.20 – 3.26 (m, 2H), 2.77 (m, 1H), 2.72 (m, 1H)	205.9 (CO), 107.5 ($C(OH)_2$), 66.5 (C–Br), 56.1 (C–Br), 48.4 (CH), 48.0 (CH), 47.4 (CH), 46.9 (CH), 43.8 (CH), 39.9 (CH)
2.6b	2.93 – 3.03 (m, 4H), 2.52 – 2.57 (m, 2H)	106.1 (2 x $C(OH)_2$), 67.4 (2 x C–Br), 50.9 (CH), 49.2 (CH), 44.0 (CH)

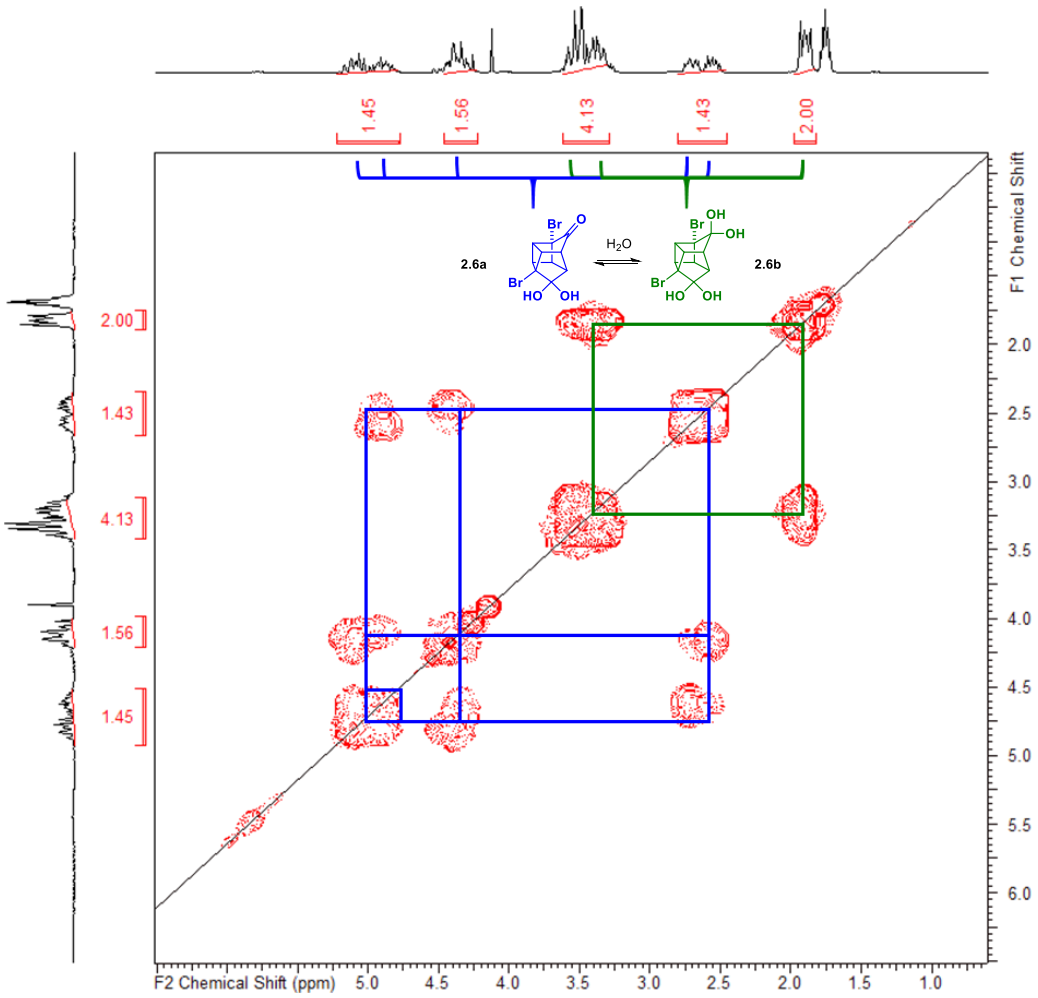

Figure 29. ^{1}H COSY NMR spectrum of the mixture of hydrates 2.6a and 2.6b (DMSO–d_6, 400 MHz). (*Blue line*) Desymmetrisation of the monohydrate 2.6a (*Green line*) Symmetrisation of the dihydrate 2.6b. Reprinted with permission from ref [83]. Copyright 2021 Georg Thieme Verlag KG.

2.3.3.4 Intramolecular [2+2] Photocycloaddition under Continuous–Flow

Our initial efforts started with the irradiation of *endo*–2,4–dibromocyclopentadiene–1,8–dione **2.5** using a 9 W UV–C lamp (λ = 254 nm). However, after 1 hour, fouling of the tubing was observed, resulting in the presence of a yellow coating on the inside wall of the tubing. While the use of high–intensity light sources might be a reason for fouling, this is very unlikely with a 9 W lamp, and it was assumed that it might be due to side reactions. Nevertheless, 1,4–cubanedicarboxylic acid (**1.1**) could be isolated after 8 h irradiation after three further steps (377 mg scale). The fouling of the microreactor could be avoided by changing the UV–C lamp for 9 W UV–B broadband lamp (λ = 280 – 370 nm). Using this lamp, complete conversion of dione **2.5** was reached after 45 minutes under photoirradiation (entries 1–4, Table 3). In order to improve the throughput, we decided to double the concentration (entries 6 and 7, Table 3), however, no gain in productivity was obtained as the residence time had to be increased accordingly to achieve the same conversion (entry 7, Table 3).

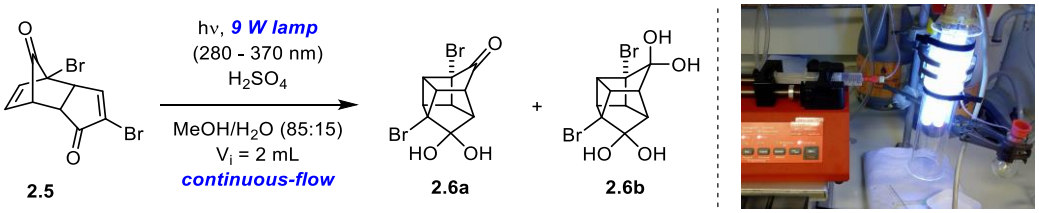

Table 3. Residence time screening for conversion of dione 2.6a and 2.6b under 9 W UV–B broadband irradiation. Reprinted with permission from ref [83]. Copyright 2021 Georg Thieme Verlag KG.

Entry	Concentration [M]	Flow rate [mL.min^{-1}]	Residence time [min]	Conversion [%]
1	0.1	0.400	5	44
2	0.1	0.133	15	77
3	0.1	0.066	30	94
4	**0.1**	**0.044**	**45**	**>99**
5	0.1	0.033	60	>99
6	0.2	0.044	45	66
7	**0.2**	**0.011**	**90**	**>99**

The above continuous–flow setup enabled us to synthesise **2.6** on milligram–scale with a theoretical productivity (P_{theo}) of ≈ 83 mg/h. However, with the desire to easily access cubane on multigram–scale we decided to pursue our efforts towards the upscaling of the process. In regards to the small–scale reactor, we envisaged that increasing the power of the lamp should increase the reaction rate and consequently the productivity. In our type of setup, the use of a stronger lamp required an increase in the reactor volume. However, one main advantage with continuous–flow in microreactors is scalability and therefore, a new reactor was constructed in a similar manner as the small one. The

9 W UV–B lamp was switched for 36 W UV–B narrowband and broadband lamps, which are widely available from their widespread use in the phototherapeutic treatment of dermatological pathologies. The UV–B narrowband lamp emits from 280 to 315 nm with one major peak at 311 nm whereas the UV–B broadband emits from 280 to 370 nm with a major peak at 302 nm (see Appendix A.3 for details). As observed in Table 4, these lamps performed equally well with little difference in residence time required to achieve full conversion (entries 3–4 and 7–8, Table 4) despite the broadband spectrum showing a better overlap with the UV–spectrum of **2.5**. For both lamps quantitative conversion was reached after 30 minutes of passing through the reactor (entries 3 and 7, Table 4).

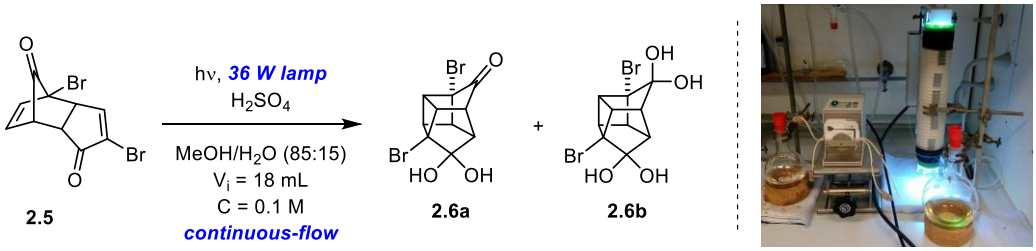

Table 4. Residence time screening for conversion of dione 2.6a and 2.6b under 36 W UV–B broadband and narrowband respectively. Reprinted with permission from ref [83]. Copyright 2021 Georg Thieme Verlag KG.

Lamp	Entry	Flow rate [mL.min^{-1}]	Residence time [min]	Conversion [%]
UV–B broadband (36 W)	1	3.6	5	14
	2	1.2	15	46
	3	**0.6**	**30**	**>99**
	4	0.4	45	>99
UV–B narrowband (36 W)	5	3.6	5	20
	6	1.2	15	50
	7	**0.6**	**30**	**>99**
	8	0.4	45	>99

The increase in internal volume of the reactor 9–fold, and of the power of the lamp, enabled us to increase the theoretical productivity of **2.6** from 83 mg/h to 1.14 g/h. The loss of half of the mass during the Favorskii rearrangement coupled with the desire to produce a large amount of dimethyl 1,4–cubanecarboxylate **1.35** in the shortest time interval possible, convinced us to increase the throughput of the process. Another main advantage of continuous–flow in microreactors is that the upscaling can also be easily achieved by a "numbering–up" strategy. Two additional similar microreactors were integrated in sequence to increase the internal volume from 18 mL to 54 mL

enabling to increase the flow rate while keeping the same residence time as well as the same tube diameter. For commercial availability reasons the UV–B narrowband lamp was preferred over the broadband one.

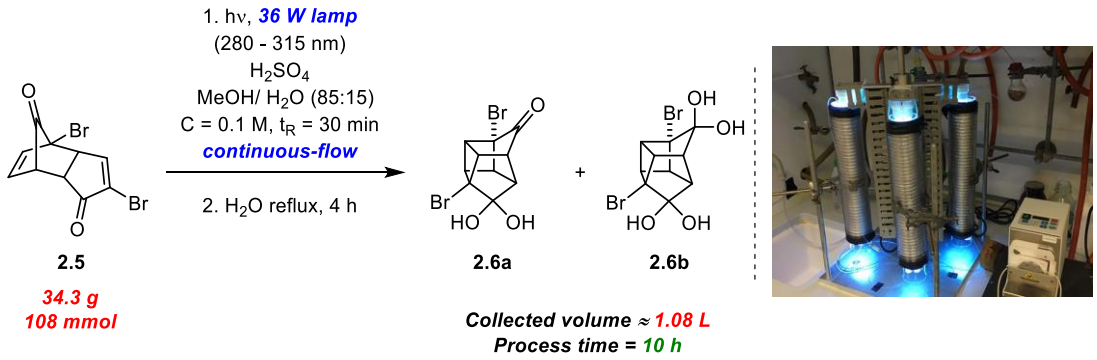

Scheme 18. Upscaling of the [2+2] photochemical step with three reactors in series. Reprinted with permission from ref [83]. Copyright 2021 Georg Thieme Verlag KG.

Finally, with this 3–coil reactor setup and the optimised conditions, 34.3 g of dione **2.5** were transformed into **2.6** after 10 h with quantitative conversion. Unlike previous reported procedures, the single passage through the reactor prevents over–irradiation, and thus degradation. Moreover, it enables us to process large volume of solution safely, where the use of batch photoreactors would be impractical.

2.3.4 Final steps of the synthesis

After passing through the photomicroreactor, the collected solution was concentrated under vacuum and the crude cage dione **2.6** was refluxed in water to ensure hydrolysis of any formed dimethyl ketals. The double ring contraction was then effected using Tsanaktsidis' conditions, followed by acidification with cold concentrated hydrochloric acid giving crude cubane dicarboxylic acid. After several attempts to use the crude 1,4–cubanedicarboxylic acid directly, we quickly realised that impurities present were difficult to remove even after further chemical transformations. Therefore, esterification of the carboxylic acids **1.1** was carried for further purification as originally reported.[88] As observed in Table 5, no significant differences between the acidic conditions used could be observed with yields ranging between 51–56%. Steglich esterification and methylation with iodomethane in the presence of potassium carbonate were unsuccessful.

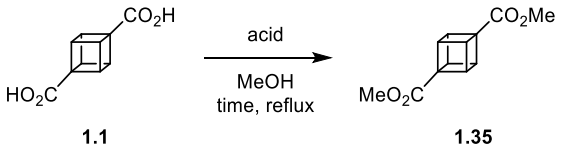

Table 5. Optimisation of the esterification step from 1.1

(Experiments conducted by Edward Jackman.)

Entry	Acid	Time reflux	Yield [%]
1	HCl	17 h	51
2	H_2SO_4	17 h	56
3	Dowex 50WX8 - 100	17 h	53
4	Me_2SO_4 / $LiOH.H_2O$	3 h	15
5	SO_2Cl	18 h	52

The obtained low yield was explained by the presence of impurities and residual amount of water in 1,4–cubanedicarboxylic acid **1.1**. Tsanaktsidis *et al.* reported the use of acidic Dowex® resin for the esterification and a purification step by sublimation under extremely reduced pressure (100 – 120 °C/0.01 mmHg or 1.33*10^{-5} bar), followed by recrystallisation in methanol/acetonitrile.[87,88] However, purification of >10 g by sublimation seemed to be impractical and arduous to carry out. We found that the use of concentrated hydrochloric acid for esterification on decagram–scale gave better results than acidic Dowex® resin despite the need of water/organic phase extraction versus simple filtration. Purification was achieved by column chromatography enabling the isolation of dimethyl 1,4–cubanedicarboxylate **1.35** without the need of sublimation and recrystallisation as previously reported.[87] From 34.3 g of **2.6**. the following 4 steps sequence, hydrolysis, double Favorskii rearrangement, acidification, and esterification enabled us to isolate 12.8 g of pure dimethyl 1,4–cubanedicarboxylate **1.35** in 54% yield (Scheme 19).

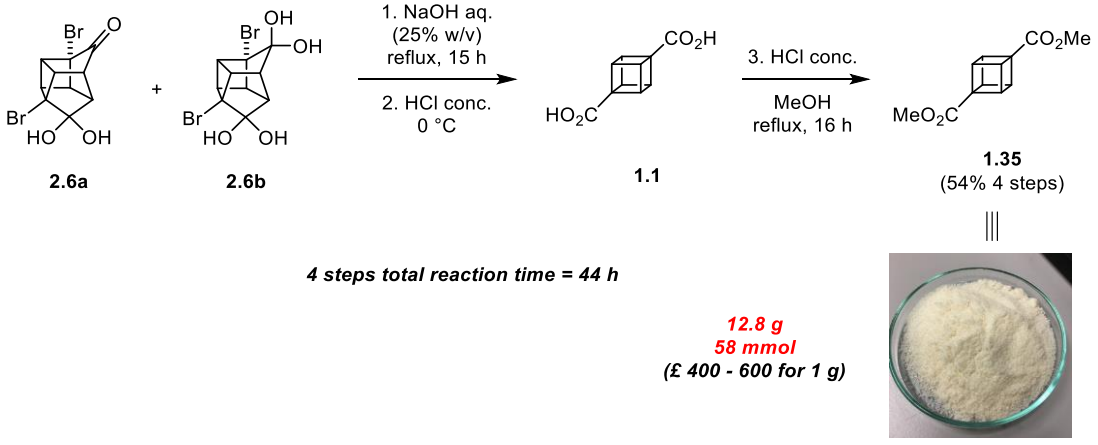

Scheme 19. Synthesis of dimethyl 1,4–cubanedicarboxylate 1.35. Reprinted with permission from ref [83]. Copyright 2021 Georg Thieme Verlag KG.

2.4 Conclusion

In the quest to synthesise new functionalised cubane derivatives, we envisioned that a practical large–scale synthesis of dimethyl 1,4–cubanedicarboxylate (**1.35**) would greatly facilitate access to these desired motifs.

In conclusion, this main goal was achieved by carrrying out a 8–step synthesis, building on the work of Tsanaktsidis *et al.*[87,88] The synthesis of dimethyl 1,4–cubanedicarboxylate **1.35** was performed and optimised on 50 g scale of cyclopentanone ethylene ketal **2.17**. The synthesis started with bromination with molecular bromine in dioxane of **2.17**, followed by double dehydrobromination under basic conditions leading to the highly *endo*–selective [4+2] Diels–Alder cycloaddition. The desired *endo*–cycloadduct **2.11** was isolated in 89% yield (Scheme 20). Afterwards, the hydrolysis of both ketals in concentrated sulfuric acid followed by recrystallisation afforded **2.5** in 86% yield.

Unlike the previously reported syntheses, the [2+2] photochemical step has been implemented under a continuous–flow process. The photoreactor has been developed according to a 'Do–It–Yourself' (DIY) approach with inexpensive commercially available equipment enabling a drastic reduction in the process time while removing the need for expensive batch photoreactors. The developed photoreactor enabled us to deliver multigram–scale of the caged intermediate **2.6** in a short space of time with a productivity of 3.42 g/h. Moreover, unlike the batch photoreactors used previously, the number of reactors used can be adjusted according the processed scale. Careful analysis of the reaction mixture after irradiation allowed full characterisation of the photocycloadduct **2.6** and its hydrates. Dimethyl 1,4–cubanedicarboxylate (**1.35**) was obtained in decagram–scale quantities in overall yields between 33–40%.

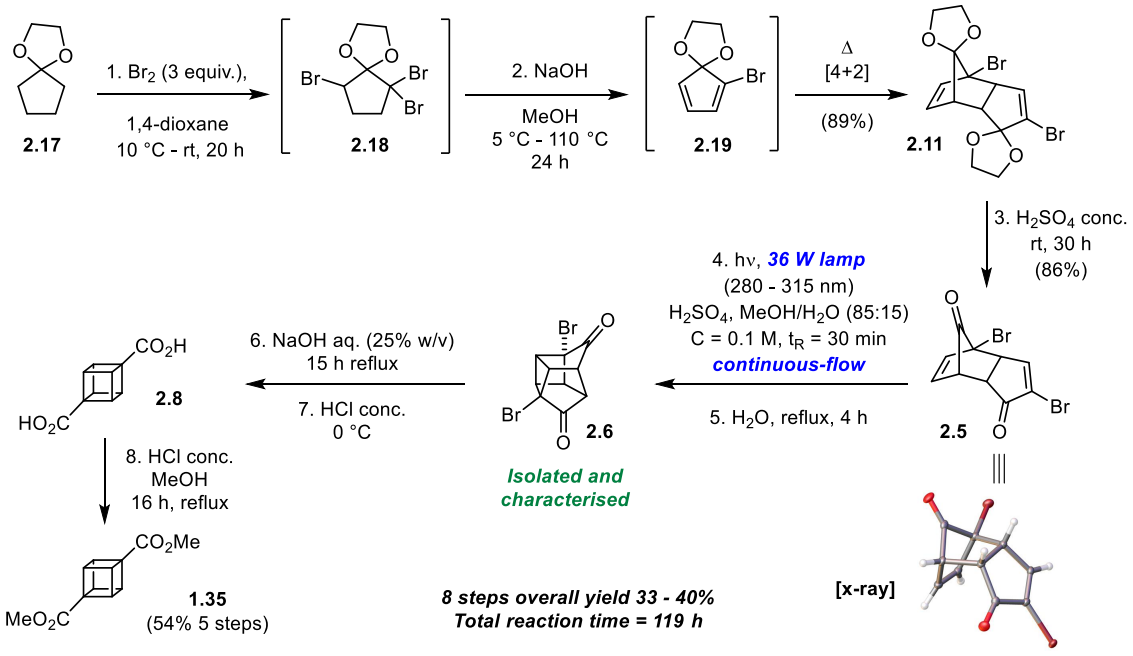

Scheme 20. 8–steps synthesis of dimethyl 1,4–cubanedicarboxylate 1.35. Reprinted with permission from ref [83]. Copyright 2021 Georg Thieme Verlag KG.

Chapter 3 Cubane Electrochemistry

3.1 Introduction

3.1.1 Context

The emergence of "sustainability" in chemistry has prompted synthetic chemists to look for traceless and green reagents leading to the re-discovery of old technologies such as electrochemistry, mechanochemistry and photochemistry. Despite electrochemistry has historically been one of the first techniques used for transforming organic molecules, the use of electricity for organic reactions has comparatively received little attention from the organic chemistry community until the last few years.[75,77] Most of the electrochemical reactions have usually been carried out in specialised laboratories or were more a subject of interest in physical and analytical chemistry. The lack of suitable equipment, combined with the fact that many organic chemists may have been intimidated by this unfamiliar territory, can be regarded as the main reasons why electrochemistry has remained a niche area in organic synthesis for a long time.[98]

3.1.2 History and Classics in Organic Electrochemistry

Electrochemistry started when Alessandro Volta invented the first electrical battery, the "Volta Pile" in 1800.[99] However, it is only three decades later that the first nonspontaneous electrochemical organic transformation was described, with the electrolysis of acetate by Faraday.[100] Inspired by that, Kolbe reported, in 1849, the anodic oxidation of carboxylic acids such as fatty acids **3.1** with loss of carbon dioxide to generate an alkyl radical which can combine to form symmetrical dimers and/or unsymmetrical coupling products, or can be added to double bonds (Scheme 21).[101102] In contrast to oxidation, the first electrochemical cathodic reduction seems to be the dehalogenation of trichloromethanesulfonic acid using a zinc electrode.[75] In 1907, Tafel reported the rearrangement for the reduction of *β*–ketoesters **3.3** into the corresponding hydrocarbon **3.4** (Scheme 21).[103]

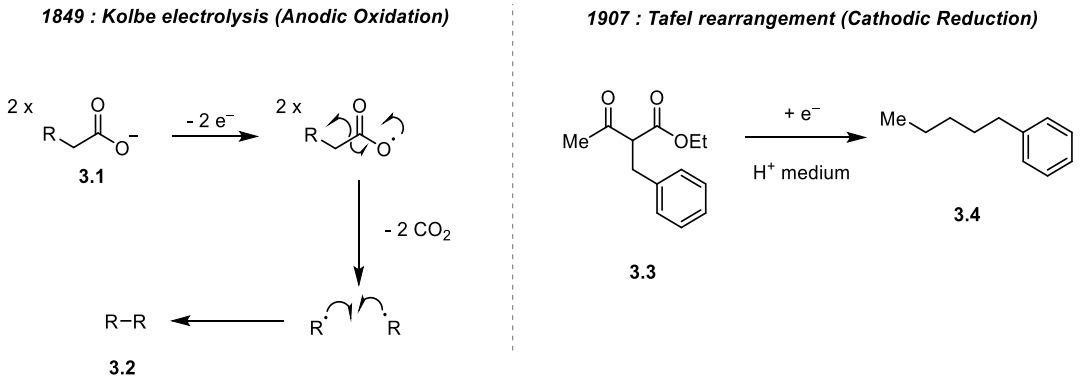

Scheme 21. Kolbe electrolysis and Tafel rearrangement.[102,103]

In 1889, Haber was the first to demonstrate the importance of the applied potential at the working electrode, illustrated by the stepwise reduction of nitrobenzene (**3.5**) into nitrosobenzene (**3.7**), phenylhydroxylamine (**3.8**) and aniline (**3.9**) (Scheme 22).[104] During the 19th and 20th century, electrochemical reactions were exclusively carried out under constant current conditions (*galvanostatic*) with the potential increasing over time, until the invention of the *potentiostat* in 1942. During *potentiastic* conditions, a fixed constant potential is applied and the current is decreasing over time.[75] The development of appropriate setups coupled with the progressing knowledge in the field enable the use of electrochemistry on industrial scale such as the Simons fluorination process, discovered in the 1930s, and the Monsanto adiponitrile process, discovered by Baizer in 1960 (Scheme 22).[105] In electrochemical fluorination (ECF) organic molecules are dissolved in anhydrous hydrogen fluoride and oxidised at the anode, while the Monsanto process consists of the hydrodimerisation of acrylonitrile to form adiponitrile *via* cathodic reduction (Scheme 22).[104]

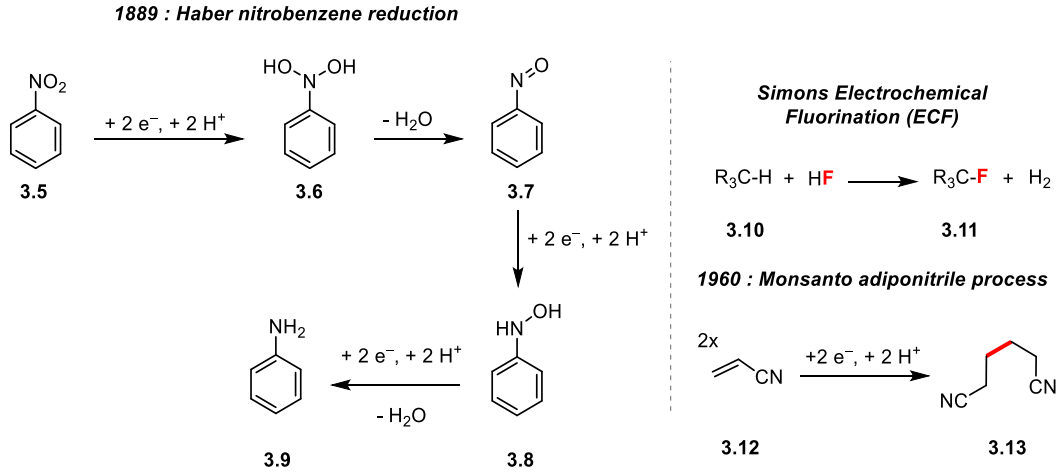

Scheme 22. (*Left*) Haber nitrobenzene reduction (*Right*) Industrial scale: Simons electrochemical fluorination and Monsanto adiponitrile synthesis.[104]

In 1975, Tatsuya Shono reported the anodic oxidation of carbamates in methanol which leads to α–methoxylation of alkyl amines.[106] This reaction, known as the Shono–type oxidation is probably one of the most studied electrochemical transformations. In these conditions, the weakest α–C–H bond of an alkyl amine is oxidised to generate an iminium cation which is directly trapped with methanol.[107] In 2011, Brown *et al.* studied the methoxylation of *N*–formylpyrrolidine **3.14** (Scheme 23A) in a microfluidic electrolysis cell for routine laboratory synthesis.[108] An application has been reported in 2015 with the late–stage Shono oxidation of bicyclic lactam **3.16** by Moeller and Aube *et al.* enabling to access a variety of complex substrates such as **3.17** (Scheme 23B).[109] The original Shono oxidation is limited to the use of methanol, as it plays both the role of nucleophile and of solvent. Carbon–centered nucleophiles are difficult to use due to their low oxidation potential competing with the substrate. In order to circumvent this issue, Yoshida *et al.* invented the "cation pool" method consisting of the accumulation of an acyl iminium ion at cryogenic temperature (Scheme 23C). These highly reactive intermediates can subsequently be quenched with various

nucleophiles. The original batch process was later converted to a flow process, with the use of a divided electrochemical flow cell to improve temperature and carbocation control.[110–112]

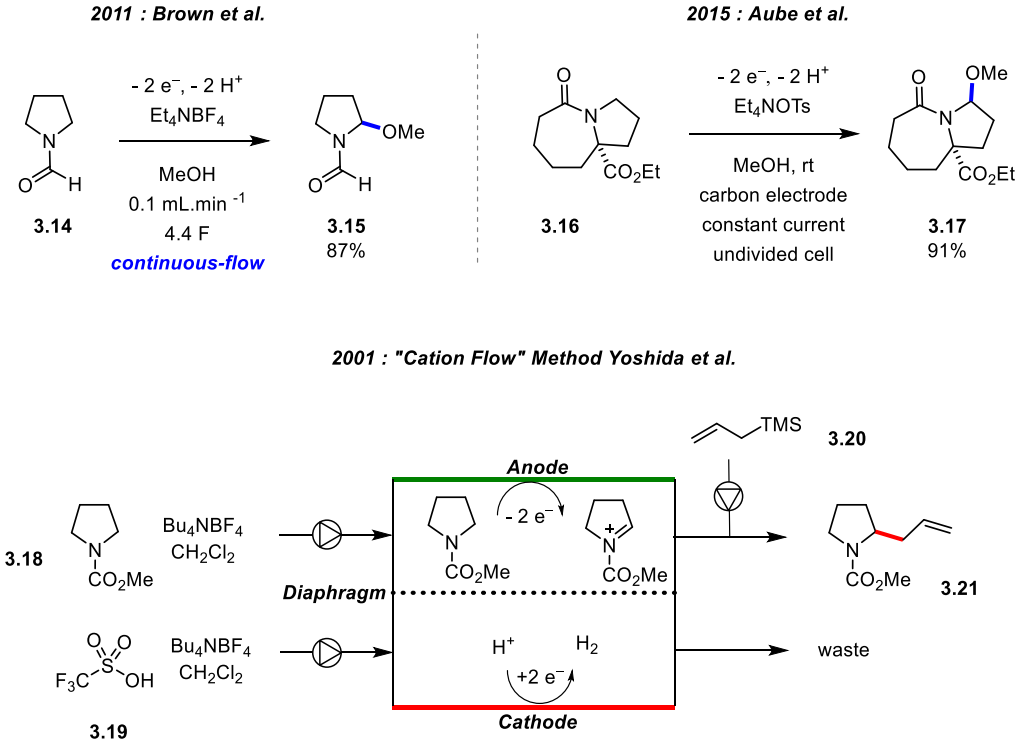

Scheme 23. (*A*) Continuous–flow Shono oxidation of *N*–formylpyrrolidine (*B*) Shono oxidation on bicyclic lactam derivative (*C*) Yoshida *et al.* "cation flow" method for Shono–type oxidation.[108–110]

In 2016, Brown *et al.* reported the design of a microflow electrolysis cell, the Ammonite 8, consisting of an undivided cell under constant current conditions (Scheme 24).[76] This flow reactor was used for the electrochemical deprotection of *p*–methoxybenzyl ethers (PMB) of alcohols,[113] and the methodology was applied to a wide variety of substrates. The use of continuous–flow conditions enabled access to several grams of product in a matter of hours.

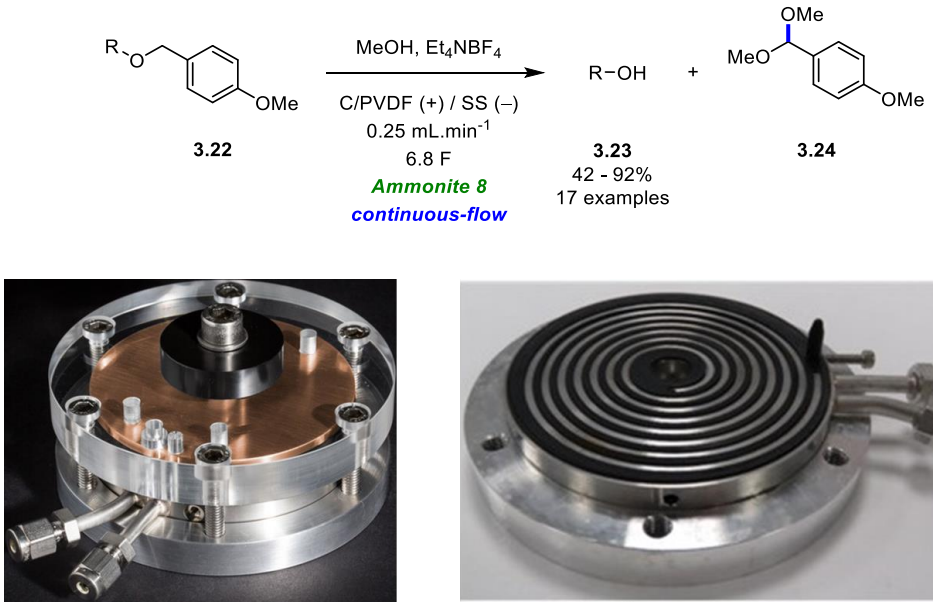

Scheme 24. Electrochemical deprotection of *para*–methoxybenzyl ethers and pictures of the *Ammonite 8* electrolysis cell.[77,113]

In 2015, in contrast to an oxidation process, Waldvogel *et al.* developed a divided flow cell for the scaled–up of the electrochemical reductive dehalogenation of a spirocyclopropane–proline derivative **3.25**, an important building block of Ledipasvir, an NS5A inhibitor (Scheme 25).[114]

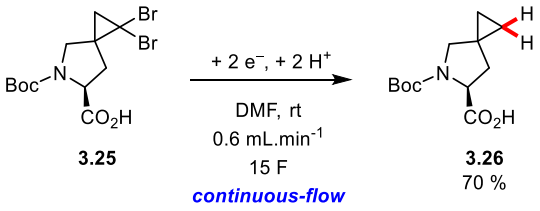

Scheme 25. Reduction of spirocyclopropane–proline (3.25) derivative by Waldvogel *et al.*[114]

3.1.3 The Hofer–Moest Reaction

The Hofer–Moest reaction, reported in 1902, is a variant of the Kolbe electrolysis. Several experimental factors such as pH, additives, solvent, electrodes and temperature influence the outcome of the Kolbe dimerisation.[102] Moreover, the conditions usually require high current densities and high concentrations in order to increase the concentration of radicals at the electrode to favour the dimer formation (Scheme 26). However, depending on the conditions, the formed radical can sometimes be further oxidised to a carbocation, and subsequently quenched by nucleophiles such as alcohols, water and/or nitriles. Moreover, further elimination or rearrangements of the formed carbocation can lead to different products.

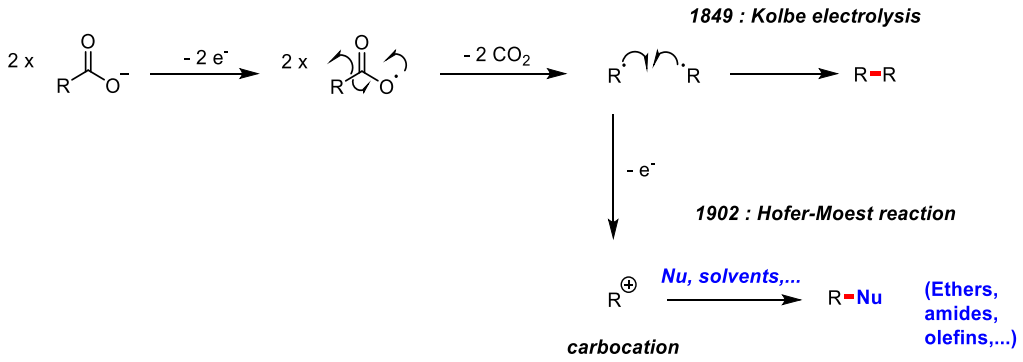

Scheme 26. Mechanistic relation between the Hofer–Moest and the Kolbe.[102]

Several examples of Hofer–Moest reactions have been reported through the years and applied on a broad scope of substrates (Scheme 27). In 1963, James A. Waters reported the anodic decarboxylation of 3–*β*–acetoxybisnorallocholanic acid (**3.27**) in methanol and ethanol.[115] The electrolysis was carried out using platinum electrodes in the corresponding alcohol in presence of metallic sodium. The methoxy– and ethoxy–products were obtained in 42% and 27% yield, respectively. Moreover, the authors also reported the formation of the corresponding alkene and hydrogenolysis products. Another example using sodium methoxide in methanol with platinum electrodes was reported by Gassman and Fox with the Hofer–Moest reaction of quinuclidine–2–carboxylic acid (**3.29**) leading to the methoxy–product **3.30** obtained in 43% yield (Scheme 27).[116] The Hofer–Moest has also found application in sugar chemistry with the decarboxylation of D–glucuronic acid in methanol reported by Kitagawa *et al.* in 1981.[117] In that case, diethylamine and glassy carbon were used as base and electrode respectively.[117,118] In accordance with the previously discussed Shono–type oxidation, anodic decarboxylation of proline derivatives was achieved under Hofer–Moest conditions due to the formation of stable acyl iminium. Renaud and Seebach reported the anodic decarboxylation of (2*S*,4*R*)–4–hydroxy–proline **3.33** using triethylamine and platinum electrode. 2–methoxy–4–hydroxyl–pyrrolidine **3.34** was obtained as a mixture of diastereoisomers in 97 % yield.[119] Five years later, Tamm *et al.* reported the synthesis of aminocyclopropanol in two steps starting from 1–aminocyclopropanecarboxylic acid **3.35**. The first step consisted of the anodic decarboxylation in ethanol with the presence of sodium ethoxide leading to the corresponding ethoxy–1–aminocyclopropane **3.36** obtained in 79% yield.[120]

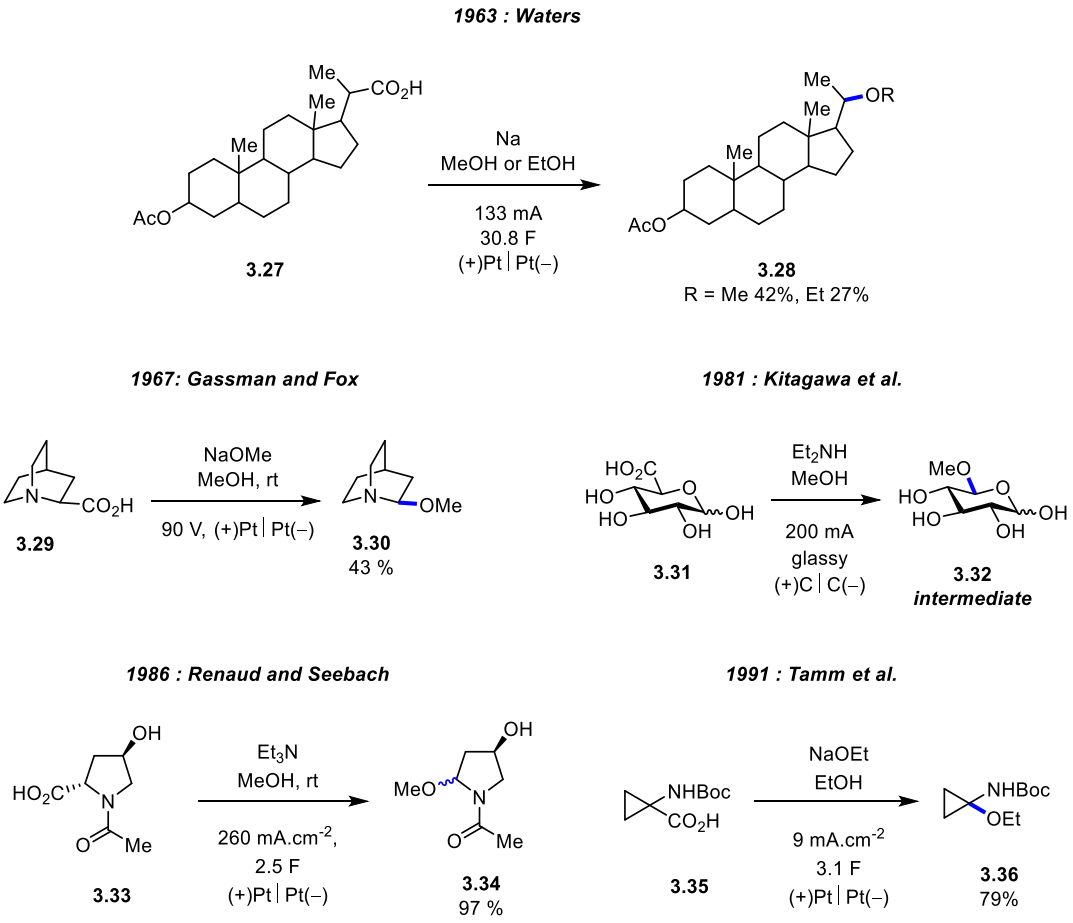

Scheme 27. Examples of reported Hofer–Moest reactions in the literature.[115–117,119,120]

During the non–Kolbe electrolysis, rearrangement of the formed carbocation can occur by alkyl, phenyl or oxygen migration (Scheme 28).[102] E.J Corey *et al.* reported the anodic decarboxylation of *exo*– and *endo*–norbornane 2–carboxylic acid **3.36** producing in both cases only the *exo*–norbornyl methyl ether **3.37** in 35–40% yield. Moreover, the electrolysis of *exo*– and *endo*–5–norbornene–2–carboxylic acid **3.39** gave 3–methoxynotricyclene (**3.40**) in 56% yield.[121] Another carbocation rearrangement has been exploited for the synthesis of muscone, used in perfurmery, by Shono *et al.*.[122] They applied electrochemical decarboxylation of *β*–hydroxycarboxylic acid **3.41** to obtain the ketone **3.42** and **3.43** with the migration of the *β*–alkyl group in the formed carbocation leading to ring expansion.

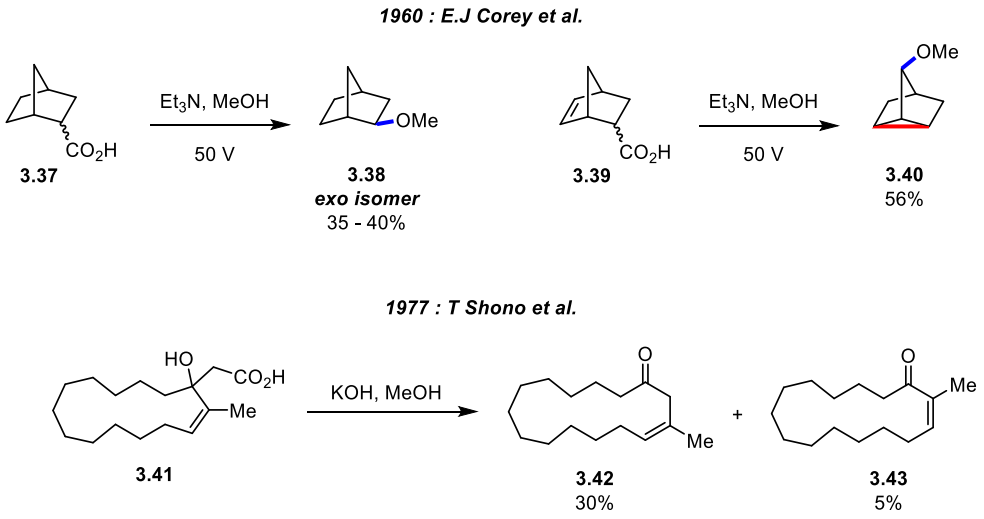

Scheme 28. Examples of generated carbocation *via* anodic decarboxylation.[121,122]

The disadvantage of the Hofer–Moest reaction is that solvent–quantities of the alcoholic nucleophiles are required to permit the current to pass, limiting the scope of alcoholic nucleophiles. At the same time of our work, in 2019, Baran and Blackmond *et al.* reported the synthesis of hindered ethers in non–alcoholic solvents (Scheme 29).[123] They circumvented the limitation of the Hofer–Moest conditions by performing the electrochemical decarboxylation in a non–nucleophilic solvent enabling the use of more complex alcoholic substrates (in excess), and other nucleophiles such as potassium fluoride and water (**3.47** and **3.49** respectively). They found that the use of dichloromethane in presence of molecular sieves suppressed the formation of by–products obtained *via* elimination, rearrangement, hydrogenolysis or hydration. Moreover, they showed that depending on the substrates, addition of silver additives as sacrificial oxidant improved the yield. The developed methodology enabled the authors to drastically reduce the number of synthetic steps for the synthesis of 12 complex scaffolds such as **3.44** obtained in two steps in 51% yield compare to 4% yield in three steps reported previously (Scheme 29). However, despite a large number of substrates (>80), unlike the original Hofer–Moest reaction, these conditions consist of a heterogeneous medium which might therefore be scale–dependent. They mentioned that primary and secondary carboxylic acids without any stabilising effect such as oxygen, nitrogen heteroatoms or phenyl groups are usually not well tolerated for electrochemical decarboxylation. Moreover, a low yield was obtained for the coupling of tertiary carboxylic acids with tertiary alcohols. Despite the impressive reported array of ether products, cubane carboxylic acid was reported to be a challenging substrate, which did not give the Hofer–Moest product under their conditions.

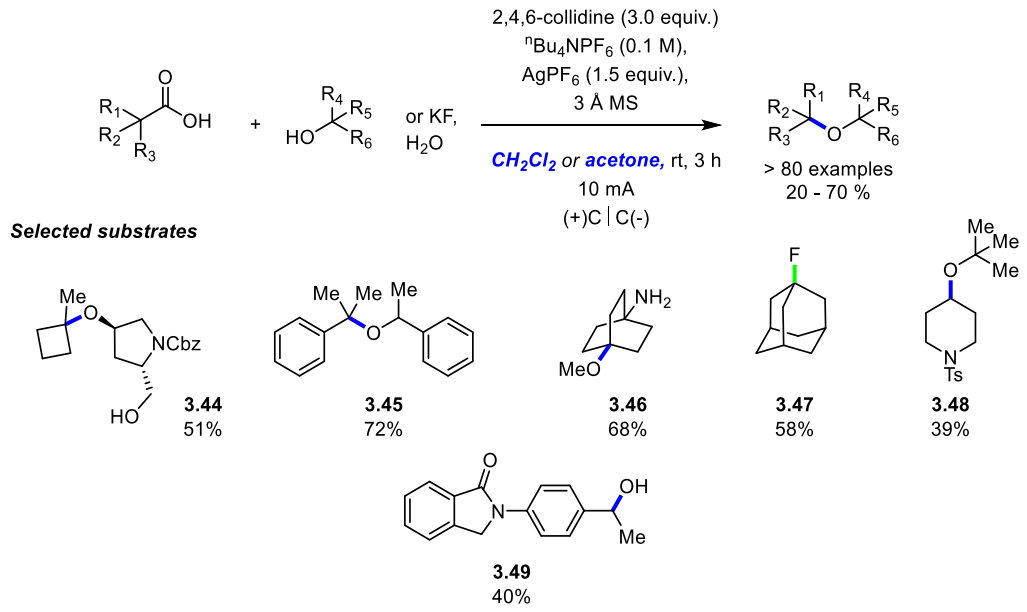

Scheme 29. Baran, Blackmond *et al*. Hindered dialkyl ether synthesis by Hofer–Moest type electrochemical decarboxylation.[123]

3.1.4 Methoxycubanes

3.1.4.1 Methoxycubane as Anisole Bioisostere

With the recent validation that cubane could act as a phenyl bioisostere, direct oxidative decarboxylation transformation at the bridgehead position of cubane could lead to new *para*–substituted benzene–replacement motifs. An sp^3 aniline bioisostere has been reported by Baran *et al.* with amine–substituted [1.1.1]bicyclopentane *via* strain–release amination procedure and more recently, Stephenson *et al.* reported the synthesis of 1–aminonorbornanes under photoredox catalysis.[124,125]

The anisole moiety, accounting for a large fraction of alkoxy aryl ethers in drugs, is an important substructure found in many commercialised drugs such as Diltiazem **3.50**, a calcium channel blocker, used to treat high blood pressure and to control chest pain; Venlafaxine **3.51**, an antidepressant; or Anisindione **3.52**, a synthetic anticoagulant.[126] Recently, rocaglate derivatives **3.53** isolated from the plant *Aglaia foveolata* have been shown to exhibit cytotoxic activity comparable to taxol (Scheme 30).[127] Moreover, concerning the isosteric replacement of anilines with saturated carbocycles, we inferred that alkoxy–cubanes could act as alkoxy aryl ethers bioisostere and might be of interest for metabolic stability modification.[128] An example of this concerns the metabolic pathway of MaxiPost™ (Scheme 30), a drug used to prevent strokes, going through the formation of quinone methide **3.56** generated by loss of fluoride following demethylation to the phenol.[129]

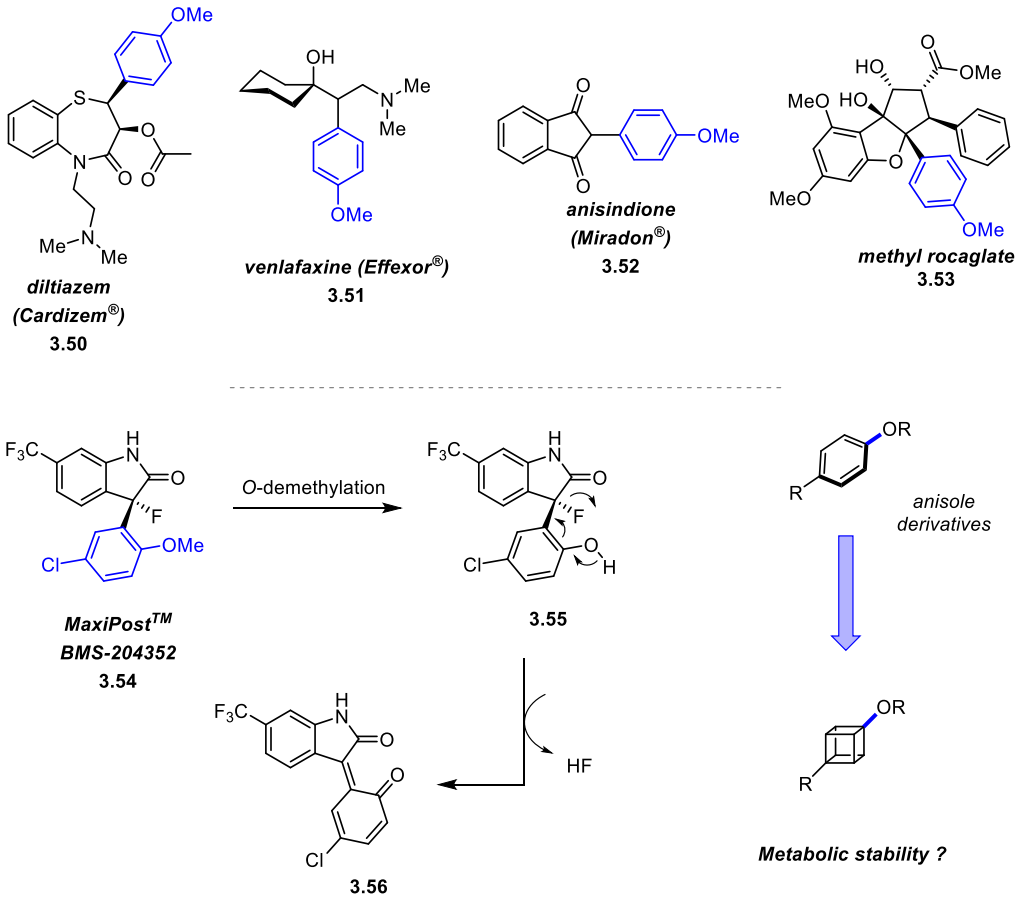

Scheme 30. Example of pharmaceutical drugs/natural products containing anisole motifs and MaxiPost™ metabolic pathway.[129]

3.1.5 Previous Syntheses of Methoxycubane

In 1988, Eaton reported that photolysis of a dilute (0.03 M) solution of 1,4–diiodocubane in methanol afforded 1–iodo–4–methoxycubane in 10% yield (Scheme 31).[130] Later, the synthesis of methyl 4–methoxy–1–cubanecarboxylate **1.7** was achieved in 31% yield by Irngartinger *et al.* through photolysis of methyl 4–iodo–1–cubanecarboxylate (**3.57**), accessed from the carboxylic acid derivative **1.7** or their pyridyl esters.[131,132] This was subsequently improved up to 58% by Williams *et al.*[132] The photolysis was carried out in methanol under inert atmosphere for 22 h irradiation.[131] However, the high dilution required makes the process unsuitable for gram–scale synthesis. Another synthetic route to access **3.59** consists of the solvolysis of methyl 4–triflate–1–cubanecarboxylate **3.58**, which was obtained by oxidative deiodination from the corresponding iodo–cubane **3.57** under reflux for three days.[133] However, while the solvolysis of cubyl triflate is reported to be fast, the presence of electron–withdrawing groups at C–4 position drastically retards or prevents the solvolysis.[133] The exact reaction time and the yield was not reported in the literature. With regard to the eight reaction steps required to synthesise the cubane starting building block, avoiding pre–functionalisation such as iodo, triflate, thiohydroxamic acid and/or redox–active esters intermediates would be greatly beneficial for cubane functionalisation enabling to reduce the number of steps

required to reach the target, and the direct conversion of **1.7** to alkoxy cubanes **3.59** is described in the section below.

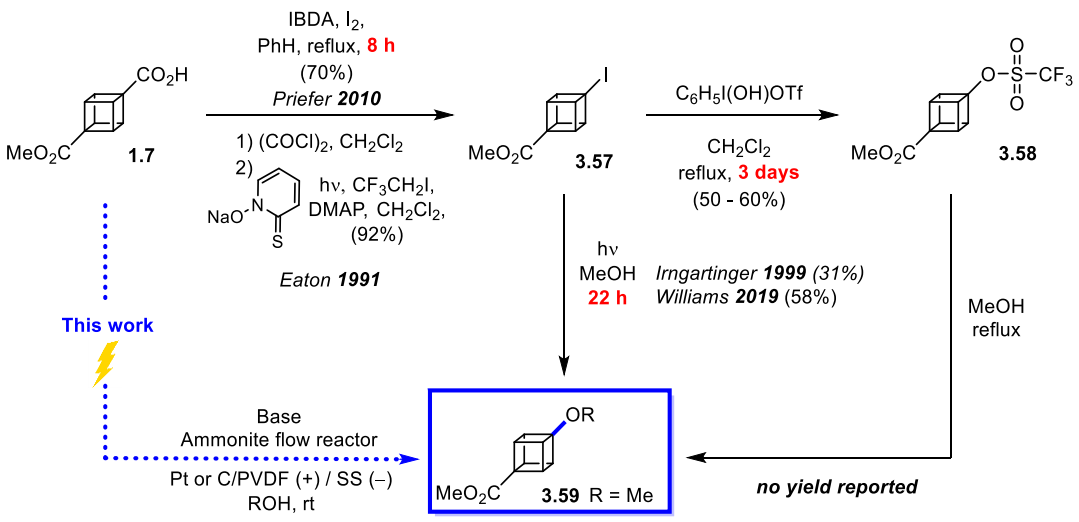

Scheme 31. Previous reported reactions for the synthesis of methyl 4–methoxy–1–cubanecarboxylate (3.59).

3.2 Results and Discussion

3.2.1 Optimised Conditions for Electrochemical Decarboxylation of Cubane

3.2.1.1 Pt anode

From accessing dimethyl 1,4–cubanedicarboxylate on gram–scale according the reported synthesis in Chapter 2, 4–methoxycarbonyl–1–cubanecarboxylic acid **1.7** was saponified according a previously reported procedure.[134] Our initial experiments towards cubane reactivity under electrochemical conditions started with typical Kolbe–type electrolysis continuous–flow conditions in an undivided cell as previously reported by Brown *et al.*[76] Partial deprotonation using a half equivalent of potassium hydroxide as base and excess current (6.2 F), calculated according Faraday's law (see Chapter 5 for details), was applied in MeOH, using Pt as anode material. Without supporting electrolyte, preliminary experiments established that 0.5 equivalent of base was required to reach the desired cell current and methyl 4–methoxy–1–cubanecarboxylate (**3.59**) was obtained in 14% yield as the major product (Table 6, Entry 1). In addition, small amount of hydrogenolysis product **1.6** (<5%) was observed and 50% of the starting material **1.7** was recovered. In regard to Kolbe dimerisation, the formation of a cubyl dimer was not observed, presumably due to the dilute conditions used compared to what is usually required for such reactions (> 0.5 M).[76,102] However, **1.7** was found not to be soluble at such concentration in methanol. Moreover, the large amount of starting material required to use of continuous–flow (≈ 500 mg per experiment) at such a concentration would not be tenable with regard to the supply of starting material. Nevertheless, this promising initial result

showed that the cubane ring itself was clearly compatible with anodic oxidation, and that processes proceeding through cubyl radical and carbocation formation are viable.

Optimisation efforts using a Pt anode were pursued in order to increase the conversion of 4–methoxycarbonyl–1–cubanecarboxylic acid (**3.59**). It was found that one equivalent of acetic acid was required to reach complete conversion, and a significantly improved yield of 40% was obtained (Table 6, Entry 2). The use of typical supporting electrolytes such as Et_4NBF_4 (Table 6, Entry 4) and perchlorate salts (from $NaClO_4$, $LiClO_4$) (Table 6, Entry 5–7) were found to supress decarboxylation of cubane, with only traces of desired product **3.59** observed. The cross–Kolbe product **3.60** and acetoxycubane **3.61** and were observed as minor by–products in the crude reaction mixtures and 1–cubanecarboxylate **1.6** and methyl 1–methyl–4–methylcubanecarboxylate **3.60** could not be separated by chromatography column. While acetic acid was initially added to investigate the formation of a cross–Kolbe product, it was assumed that, in this case, the presence of acetic acid could play the role of supporting electrolyte to increase the conductivity in the medium, and the addition of an excess of acetic acid was found to not to lead to a significant increase the formation of **3.60** and **3.61**.

The formation of an unidentified slight deposit on the Pt electrode was observed upon usage, which could be due to electrode passivation. It was observed that the amount of deposit was correlated with an increase of the voltage in the cell. With the desire to upscale the process for gram–scale synthesis, preventing deposit build–up was deemed important. Thinking that the deposit could be explained by the accumulation of decomposed material because of a slow flow rate (0.2 $mL.min^{-1}$), the latter was doubled while maintaining the same amount of charge (0.4 mL min^{-1}, 400 mA (6.2 F)), which led to the isolation of methyl 4–methoxy–1–cubanecarboxylate **3.59** in 36% yield in a gram–scale reaction, along with the formation of the reported byproducts (Table 6, Entry 8). In those conditions, electrode passivation was reduced and enabled upscaling on gram–scale.

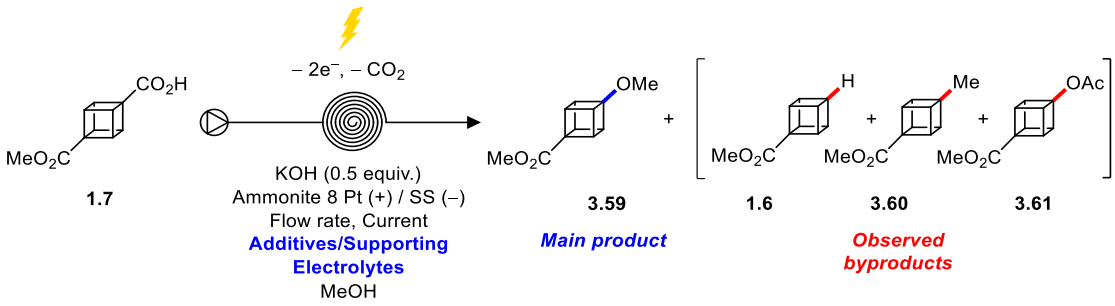

Table 6. Additives and/or electrolytes screening for electrochemical decarboxylation of 1.7 using Pt anode.

Entry	Additives/Supporting Electrolytes	Flow rate [mL.min^{-1}]	Current (Charge)	RSM [%][a]	Yield [%]
1	None	0.2	200 mA (6.2 F)	50	14[a]
2[c]	**AcOH**	**0.2**	**200 mA (6.2 F)**	**None**	**40[a], 36[b]**
3[c]	$(CH_3)_3CCO_2H$	0.2	200 mA (6.2 F)	nd	22[b]
4[d]	Et_4NBF_4	0.2	200 mA (6.2 F)	nd	traces
5[d]	$NaClO_4$	0.2	200 mA (6.2 F)	nd	traces
6[d]	$LiClO_4$	0.2	200 mA (6.2 F)	nd	traces
7[e]	TFA	0.2	200 mA (6.2 F)	nd	traces
8[c]	AcOH	0.4	400 mA (6.2 F)	None	36[b]

General conditions: 0.25 mmol of **1.7**, MeOH (2.5 mL), *c* = 0.1 M. [a] Yield of **3.59** determined using calibrated GC; [b] Isolated yield; nd = not determined. [c] 1.0 equiv. of the corresponding acid. [d] 5 mM of supporting electrolyte. [e] 5.0 equiv. of trifluoroacetic acid. RSM = Remaining starting material. Nd = not determined.

With this procedure in hand, we decided to turn towards the synthesis of different cubane–ethers by performing the reaction in different alcohol solvents. Although, methoxy–cubane is probably the most interesting scaffold for anisole group replacement in a medicinal chemistry context, the synthesis of different alkoxy–cubanes leads to new molecular entities. However, attempts to use other alcohols as nucleophiles were hampered by poor solubility of the inorganic base, potassium hydroxide, limiting further development of these conditions. Changing the base for potassium carbonate showed similar results (Scheme 32). While Baran, Blackmond *et al.* reported the use of heterogeneous solutions in a batch electrochemical setup, such approach is not desirable in a flow system.[123] Qualitative solubility studies were carried out in order to determine if the use of co–solvents would be suitable to assure complete solubility. However, solubility issues persisted with most of alcoholic organic solvents and therefore, we turned towards the use of organic bases.

Solvent \ Base	KOH	Et_3N
methanol	Soluble	Soluble
ethanol	Soluble	Soluble
isopropanol	Insoluble	Soluble
n-propanol	Insoluble	Soluble
CF_3CH_2OH	Soluble	Soluble
HFIP	Soluble	Soluble

Scheme 32. (*Left*) Precipitation in isopropanol with KOH (0.5 equiv.) as base. (*Right*) Precipitation in isopropanol with K_2CO_3 (5 mol %) as base. In both cases, a very viscous gel formed. (*Table*) Qualitative analysis of the solubility of 1.7 in different solvents. Concentration of 1.7, c = 0.1 M and 0.5 equivalent of base. HFIP = 1,1,1,3,3,3–hexafluoropropan–2–ol.

Similar yields were obtained using 2,6–lutidine, DBU and triethylamine (Table 7, entries 1, 2 and 3), however, the required current was not achieved under the applied limited potential (12 V) using 2,6–lutidine, and electrode passivation was more significant with DBU than with triethylamine. As depicted in Scheme 32, the use of triethylamine leads to complete solubility in alcoholic solvents unlike potassium hydroxide. In accordance with the use of potassium hydroxide, while **3.59** was obtained in 44% yield in presence of acetic acid, omitting the latter led to reduced conversion and only 8% of the desired product was obtained (Table 7, entry 4).

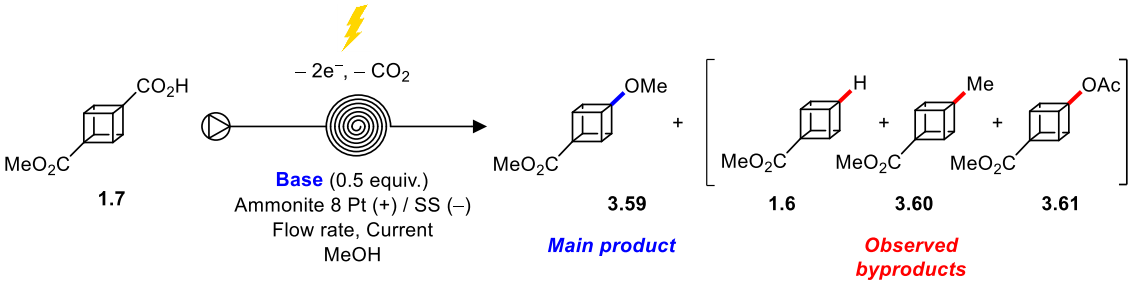

Table 7. Organic bases screening for electrochemical decarboxylation of 1.7 using Pt anode.

Entry	Conditions	Flow rate [mL.min^{-1}]	Current (charge)	Yield[a] [%][a]
1[c]	Et_3N, AcOH	0.2	200 mA (6.2 F)	44
2[c]	2,6–lutidine, AcOH	0.2	200 mA (6.2 F)	46[b]
3[c]	DBU, AcOH	0.2	200 mA (6.2 F)	44
4	Et_3N	0.2	200 mA (6.2 F)	8[d]

[a]Calculated using calibrated GC; [b] Required current was not achieved under the applied limited potential (12 V); [c] AcOH (1.0 equiv.) [d] no AcOH added, 82% remaining starting material.

3.2.1.2 Carbon anode

In order to improve the carbocation formation and avoid cross–Kolbe product, the efforts turned towards the use of carbon anodes under basic conditions with added perchlorate salts as supporting electrolyte.[102] In the current work, exchanging the Pt anode for a carbon material (C/PVDF, carbon polyvinylidene fluoride composite) under the previously optimised conditions, resulted in a reduced yield of **3.59** (12%, Table 8 Entry 1) alongside with decomposition products (^{1}H NMR analysis). However, after several experiments, it was found that decreasing the applied charge from 6.2 F to 2.5 F gave an elevated yield of 44% (Table 8, Entry 2) of the methyl ether **3.59**. Furthermore, omission of AcOH as supporting electrolyte led to a further improvement to 52% (, Entry 3), avoiding formation of methyl– and acetoxy–cubane (**3.60** and **3.61**) byproducts. However, decreasing the flow rate, while maintaining the same cell current (double amount of charge, 5.0 F), also gave a decreased yield of 24% (Table 8, Entry 4), highlighting the potential for overoxidation of the methoxylated product **3.59**. This could be confirmed by resubmitting the reaction mixture containing **3.59** to the electrolysis conditions, resulting in a decreased yield of 30% (from 52% with one pass through the reactor). Increasing or decreasing the number of equivalents of base led to lower yields and incomplete conversion (, 5 and 6). Different bases and supporting electrolytes were explored (Table 8, Entries 7 to 10), but the yield could not be improved further, and similar as when a Pt anode was used, the presence of $NaClO_4$ or Et_4NBF_4, retarded decarboxylation (Table 8, Entries 7 and 8). However, interestingly, the use of Et_4NBF_4 as supporting electrolyte enabled us to isolate fluorinated cubane **3.62** as additional byproduct (Scheme 33). This could be explained by the cubyl cation being traped by fluoride atom during the electrolysis.[123] While the use of 2,6–lutidine as base (Table 8, Entry 10) has shown similar results, faster increase of voltage in the cell was observed compare to trimethylamine over time. Significantly, anodic oxidation using the C/PVDF anode, 200 mA (2.5 F) and 0.5 mL min^{-1} allowed for the formation of **3.59** with increased productivity and substantially improved current efficiency (42% compared to 14% at Pt).

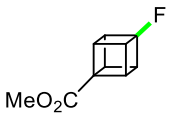

3.62
< 5 mg
isolated

Scheme 33. Fluorinated cubane obtained as byproduct.

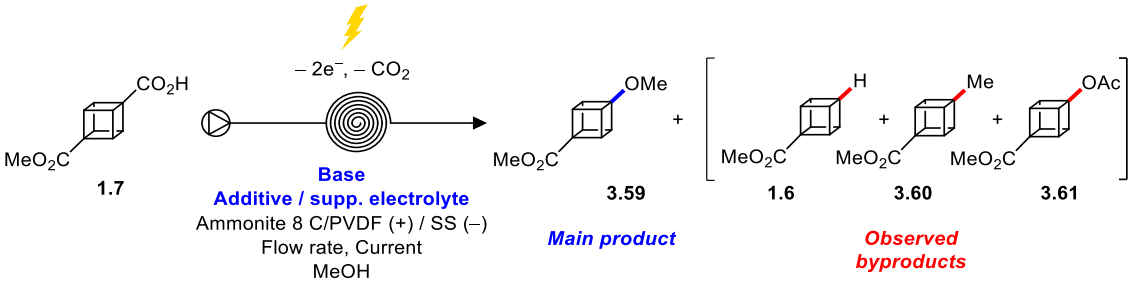

Table 8. Optimisation conditions for electrochemical decarboxylation of 1.7 using C/PVDF anode.

Entry	Conditions	Equiv. of base	Flow rate [mL.min^{-1}]	Current (charge)	RSM [%][b]	Yield [%][a]
1[c]	Et_3N, AcOH	0.5	0.2	200 mA (6.2 F)	None	12
2[c]	Et_3N, AcOH	0.5	0.5	200 mA (2.5 F)	None	44
3	**Et_3N**	**0.5**	**0.5**	**200 mA (2.5 F)**	**None**	**52**
4	Et_3N	0.5	0.25	200 mA (5.0 F)	None	24
5	Et_3N	0.75	0.5	200 mA (5.0 F)	22	36
6	Et_3N	0.25	0.5	200 mA (2.5 F)	None	28
7[d]	Et_3N, $NaClO_4$	0.5	0.5	200 mA (2.5 F)	32	4
8[d]	Et_3N, Et_4NBF_4	0.5	0.5	200 mA (2.5 F)	20	12
9	DBU	0.5	0.5	200 mA (2.5 F)	None	34
10	2,6–Lutidine	0.5	0.5	200 mA (2.5 F)	None	52

General conditions: 0.25 mmol of **1.7**, MeOH (5 mL), *c* = 0.1 M. [a] Yield of **3.59** determined using calibrated GC; [b] Determined using calibrated GC; [c] AcOH (1.0 equiv.); [d] 5 mM of supporting electrolyte.

3.2.2 Alcohol and Substrate Scope

With optimised conditions in hand, we explored different alcohols as nucleophiles (Scheme 34). A range of alkoxylated products from the corresponding alcohols with different steric hindrance were successfully synthesised (**3.59**–**3.67**). This included deuterated ethers, illustrated by the synthesis of methyl 4–methoxy(d_3)–1–cubanecarboxylate (**3.63**) in 40% yield. Selectively deuterated substrates are of interest for medicinal chemistry studies, where the use of deuteration has shown, in some cases, to improve the pharmacokinetic properties.[135] Furthermore, fluorinated cubane ethers (**3.66** and **3.67**) were obtained in moderate to good yields from TFE (2,2,2–trifluoroethanol) and HFIP (1,1,1,3,3,3–hexafluoroisopropanol), respectively. The application of fluorinated alcohols was not viable using

the C/PVDF anode, which swells in fluorinated solvents, but was possible using a Pt anode. Other sources of carbon that could be used with fluorinated solvents, such as glassy carbon, showed inferior results for this particular reaction.[136]

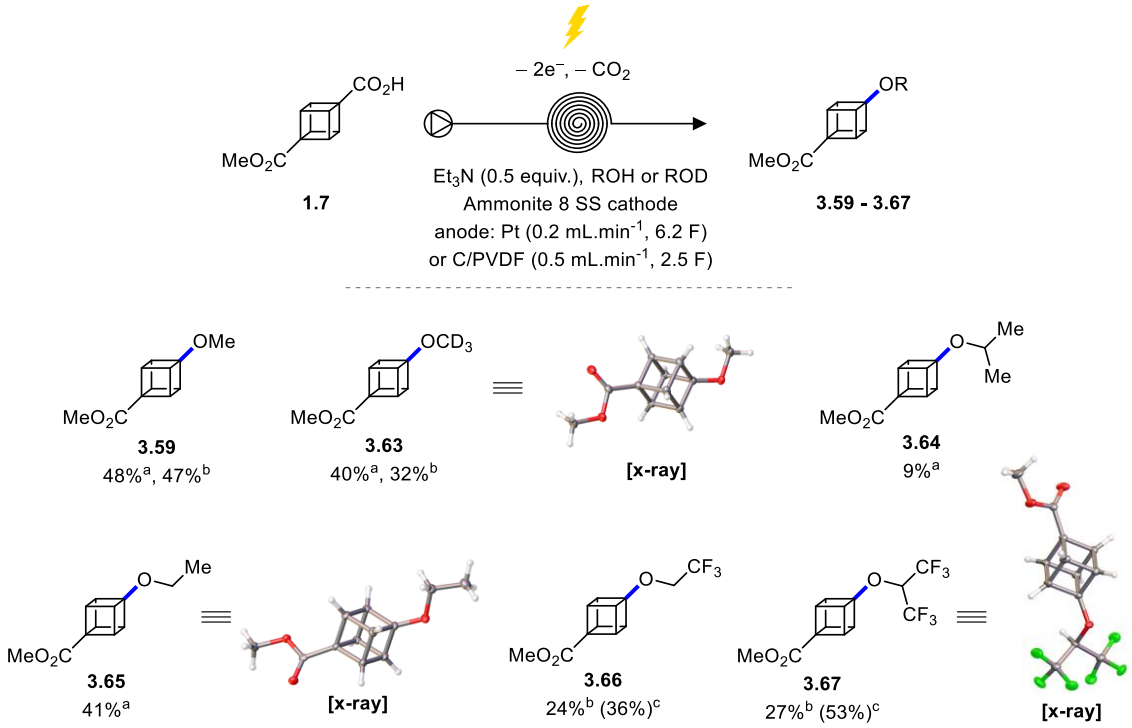

Scheme 34. Alcohols scope. [a] Isolated yield with C/PVDF, Cubanecarboxylic (0.1 M) [b] Isolated yield with Pt anode, 1.0 equiv. AcOH added. [c] ^{19}F NMR yield with *α,α,α*–trifluorotoluene as internal standard.

The substrate scope was further explored using different cubane functionalisation, with attention to potential chemoselectivity issues including oxidation of weak C–H bonds adjacent to amide nitrogens, which can easily be subjected to Shono oxidation as reported by Steve Ley *et al*. under continuous–flow electrochemistry conditions (Scheme 35).[137] Pleasingly, oxidation of the carboxylate occurred in preference, leading to compounds **3.68**–**3.75** in good yields (48–60%). Piperidine (**3.68**) and morpholine rings (**3.71**) remained unchanged, offering interesting scaffolds for application in drug discovery. Benzyl ethers, which are susceptible to anodic oxidation, were also tolerated albeit with the desired decarboxylative coupling product **3.72** obtained in a reduced 20% yield. Gratifyingly, the presence of a free alcohol in the molecule did not disturb the electrochemical transformation and compound **3.73** was obtained in 46% yield as the main product. However, while a *t*–butyl ester is compatible with the reaction conditions (**3.74**, 41%), a Boc–protected amine with or without the use of base did not lead to the desired electrolysis product **3.75**, and starting material was recovered.

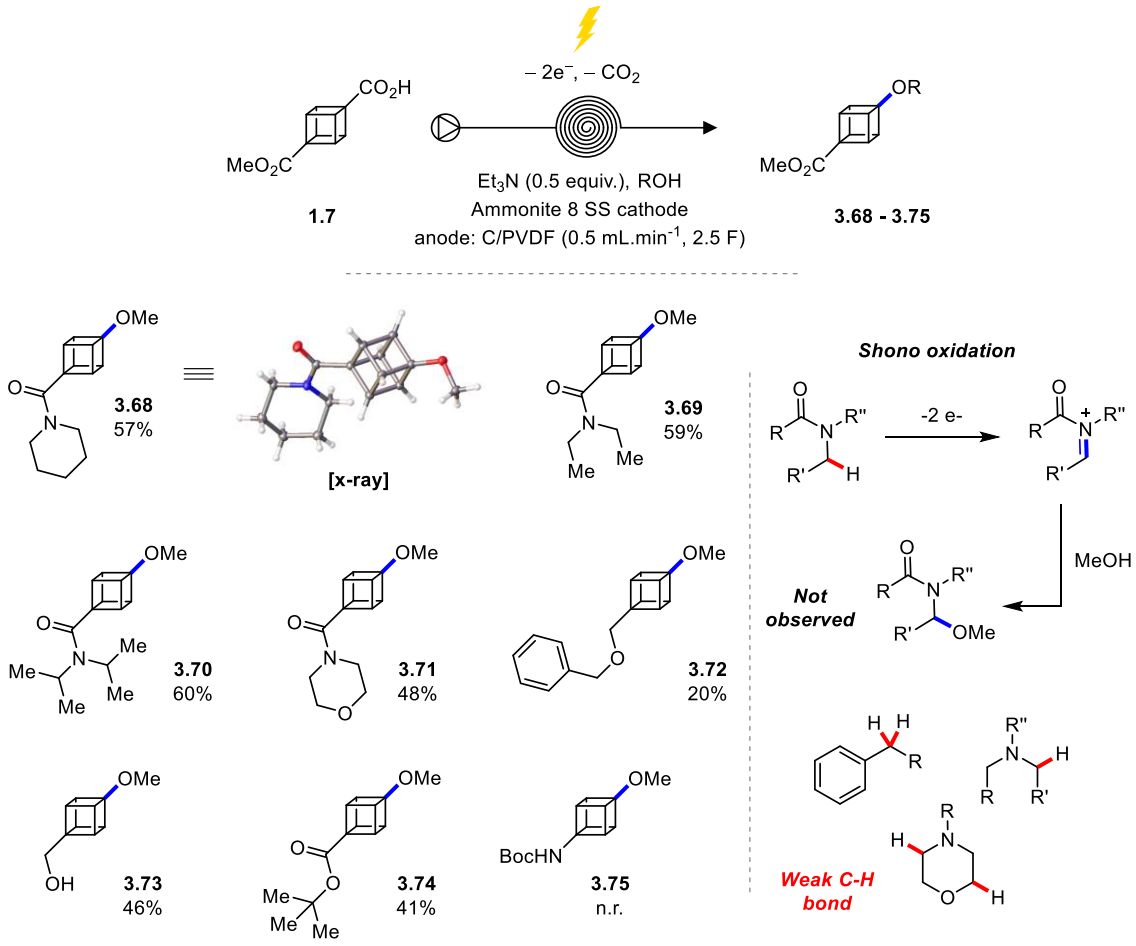

Scheme 35. Substrate scope for decarboxylation–methoxylation.

3.2.3 Upscaling

New transformations on cubane are usually merely reported on milligram–scale, however, in order to become of interest for medicinal chemistry purposes involving multistep syntheses, gram–scale access is highly desirable. Therefore, to demonstrate the ease of laboratory scale–up using the flow electrolysis approach, 12.5 mmol of starting material was successfully oxidised using the same reactor, giving 1 gram of pure methoxy–cubane **3.59** in only 4 h (Scheme 36). While, on small scale, the formation of methyl 1–cubanecarboxylate (**1.6**) as hydrogenolysis byproduct is insignificant, on gram–scale ~150 mg of **1.6** was isolated, which in itself is a useful derivative.

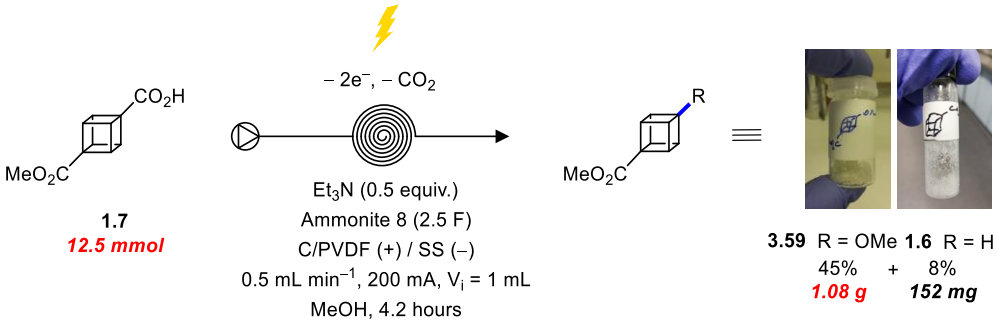

Scheme 36. Gram–scale decarboxylative functionalisation of cubane.

3.2.4 Comparison with the corresponding batch process

Although electrochemistry has gained attraction by the organic synthetic community, most of reported procedure under electrochemical conditions still rely on the use of batch electrochemical cells which has been further influenced by the development of the Electrasyn® by Baran and IKA in order to reduce reproducibility issues with the "home–made" electrochemical setups.[138] Therefore, it was decided to observe whether or not our conditions obtained in the Ammonite 8 were reproducible in a batch electrochemical cell making the process easily accessible. Moreover, we were interested to show the benefits of flow electrochemistry compare to batch. A Stainless steel and a C/PVDF electrode were built (Figure 30) to suit in a vial and the current to apply for the reaction was translated according the current density obtained under the flow conditions (See Chapter 5 section 5.4.2 and 5.4.3 for details). However, three hours of electrolysis time was required instead of 10 minutes in flow for the same scale (0.5 mmol), and a considerably increased amount of charge (4.0 F) was applied to achieve full conversion. Methoxy–cubane **3.59** was obtained in similar yield (50% yield by GC, Figure 30). An important parameter in the characterisation of an electrochemical process consists of the measure of the *Faradaic efficiency*, also known as the *Current* or *Coulomb efficiency*, which represents the efficiency with which a charge is transferred to the system facilitating the electrochemical reaction. The use of continuous–flow improved, in this case, the current efficiency to 42% from 25% in batch, a consequence of the high ratio of electrode area to electrolyte volume (A/V) and mass transfer regime (i.e., how fast reactant travels to the electrode) obtained with flow electrochemical cells (in this case, Ammonite 8).[77]

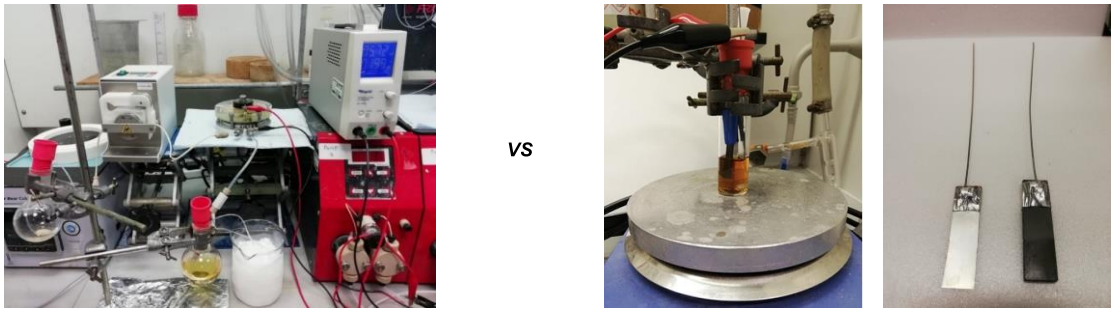

Figure 30. Current efficiency of electrochemical flow cell (Ammonites 8) *vs* batch cell (work done with Ana A. Folgueiras–Amador).

3.2.5 Synthesis of a new bioisostere

The demonstration of a one–step Hofer–Moest process in flow making **3.61** accessible on gram–scale, opens up possible applications of **3.61** as secondary building block for the synthesis of methoxylated phenyl bioisosteres. Cubanisidine **3.77** was identified as a bioisostere of the highly electron rich and genotoxic *para*–anisidine **3.78**, and its synthesis was undertaken (Scheme 37).[138] Saponification of ester **3.59** gave 4–methoxycubane carboxylic acid (**3.76**) in 94% yield, which was followed by Yamada–Curtius rearrangement to give the corresponding Boc–amine **3.75** in 69% yield. Cleavage of the carbamate protecting group delivered 4–methoxy–1–cubanamine as its hydrochloride salt **3.77**.

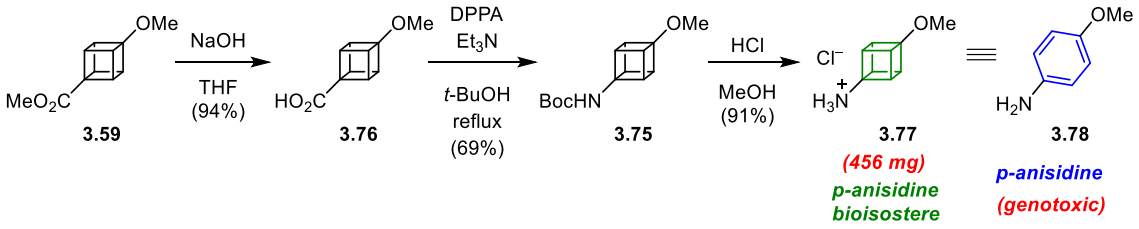

Scheme 37. Synthesis of cubanisidine as *para*–anisidine bioisosteres.

3.2.6 Synthesis of Methoxycubane drug derivative

Moreover, in order to highlight the use of 4–methoxy–1–cubanecarboxylate (**3.59**) in a drug–discovery context as anisole bioisostere, the cubane derivative of the synthetic drug anisindione **3.80** was investigated. Anisindione, known under the brand name Miradon®, is used as anticoagulant. 4–Methoxy–1–cubanecarboxylic acid (**3.576**) was reduced to 4–methoxy–1–cubanemethanol (**3.73**) in 82% yield, and subsequent oxidation to the corresponding aldehyde **3.79** was achieved using Dess–Martin periodinane (DMP). Finally, a condensation reaction of 4–methoxy–1–cubanecarbaldehyde (**3.79**) and phthalide **3.81** using NaOMe in EtOAc gave the desired cubanisindione **3.80** in 33% yield.

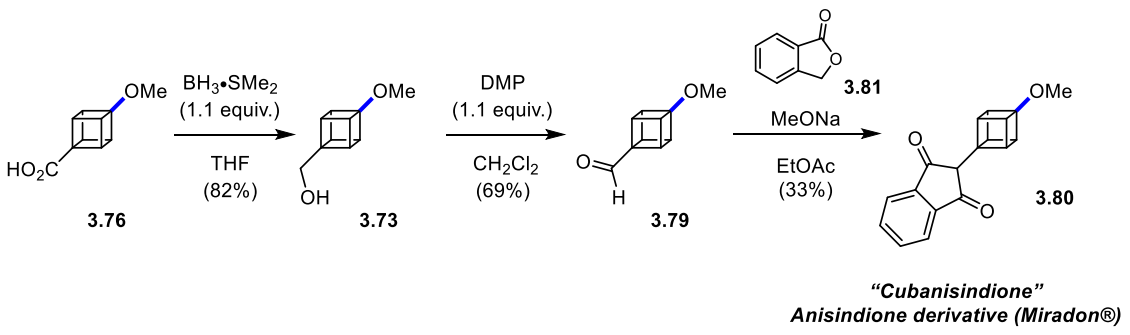

Scheme 38. Synthesis of Cubanisindione (Anisindione cubane derivative).[132,139]

3.2.7 The Hofer–Moest Mechanism

In the electrolysis at the Pt anode, unlike the C\PVDF anode, the addition of one equivalent of acetic acid was essential in order to achieve good yield of the methoxylated cubane **3.59**, leading to acidic Hofer–Moest reaction conditions. The formation of cross–Kolbe and hydrogenolysis products confirmed the two electron process of the Hofer–Moest *via* first the cubyl radical and then cubyl carbocation formation after further one electron oxidation (Scheme 39). However, intrigued by the need of acetic acid on Pt anode led us to perform cyclic voltammetry to see whether it has a role in the mechanism or not.

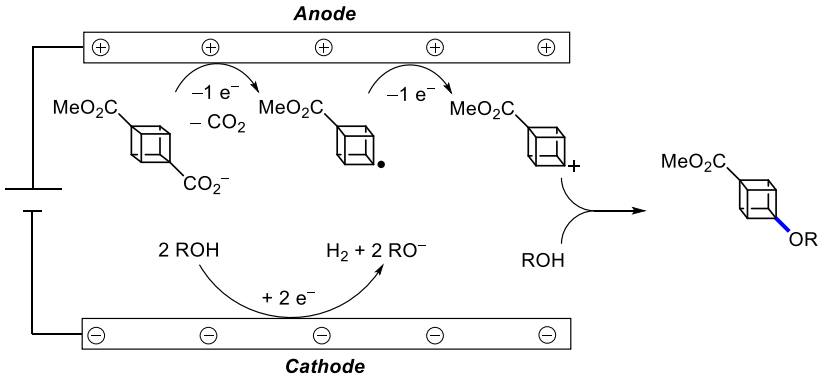

Scheme 39. Hofer–Moest mechanism applied to cubane substrates.

Cyclic voltammetry diagrams were recorded and as depicted in Figure 31 (top left, green curve), in the absence of base no oxidation peak could be observed at potentials prior to solvent decomposition, however, in the presence of half equivalent of triethylamine a clear oxidation peak at +1.63 V (Figure 31, top right, red curve) can be observed which confirmed the electroactive species to be the carboxylate anion. The addition of one equivalent of acetic acid did not change the peak (Figure 31, bottom left and right, blue line). We postulated that the presence of acetic acid modifies the properties of the surface, possibly by adsorbed methyl radicals.[140]

During a cyclic voltammetry experiment, the current passing through the electrode is limited by the diffusion of the species from the bulk solution to the electrode surface. Diffusion is influenced by the concentration gradient which is governed by the concentration of the species at the surface of the electrode. Consequently, a faster potential sweep during a cyclic voltammetry experiment will increase the concentration gradient between the bulk solution and electrode surface resulting in a higher measured current. The peak current increases by a factor equal to the square root of the change in scan rate. As depicted in Figure 32, (yellow line), when the scan rate was increased by a factor four (from 25 to 100 mV/s), the obtained peak current increases by a factor 2. Therefore, the electrochemical reaction is diffusion controlled and does not depend on the rate of subsequent chemical steps.

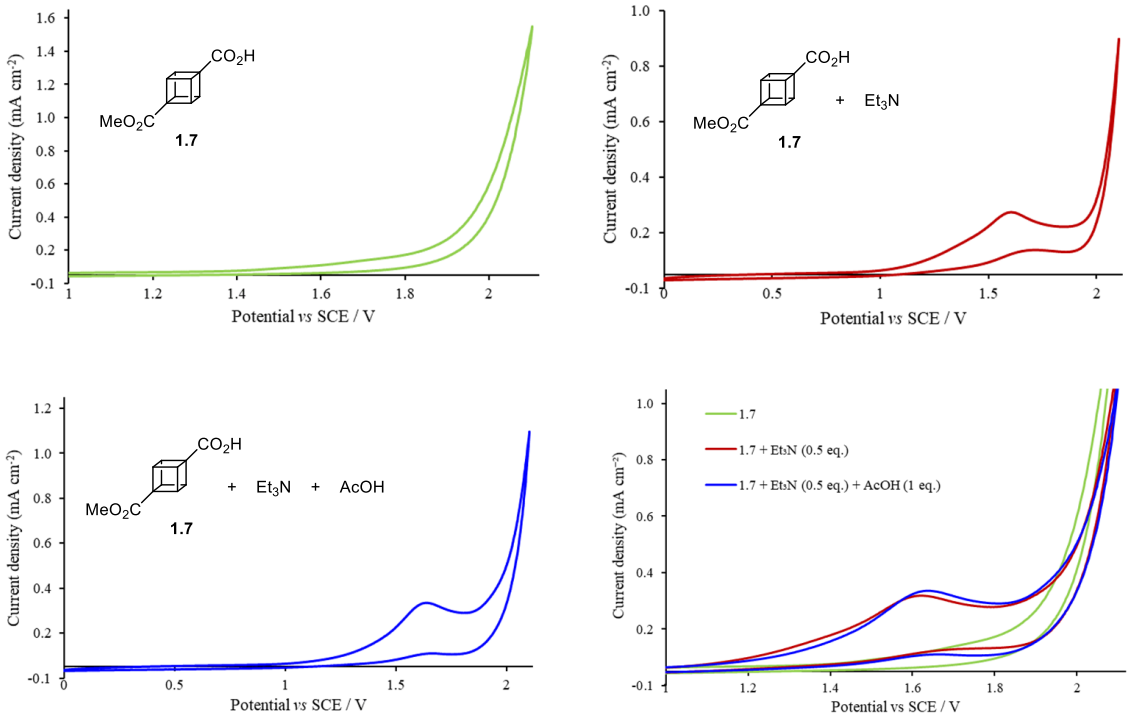

Figure 31. Cyclic voltammogram for (*Top left*) 5 mM cubane carboxylic acid in MeOH/0.1 M Et_4NBF_4. (*Top right*) 5 mM cubane carboxylic acid and 2.5 mM Et_3N in MeOH/0.1 M Et_4NBF_4. (*Bottom left*) 5 mM cubane carboxylic acid 2.5 mM Et_3N and 5 mM AcOH in MeOH/0.1 M Et_4NBF_4. (*Bottom right*) Overlapping of the CVs. Potential scan rate 25 mV s^{-1}.

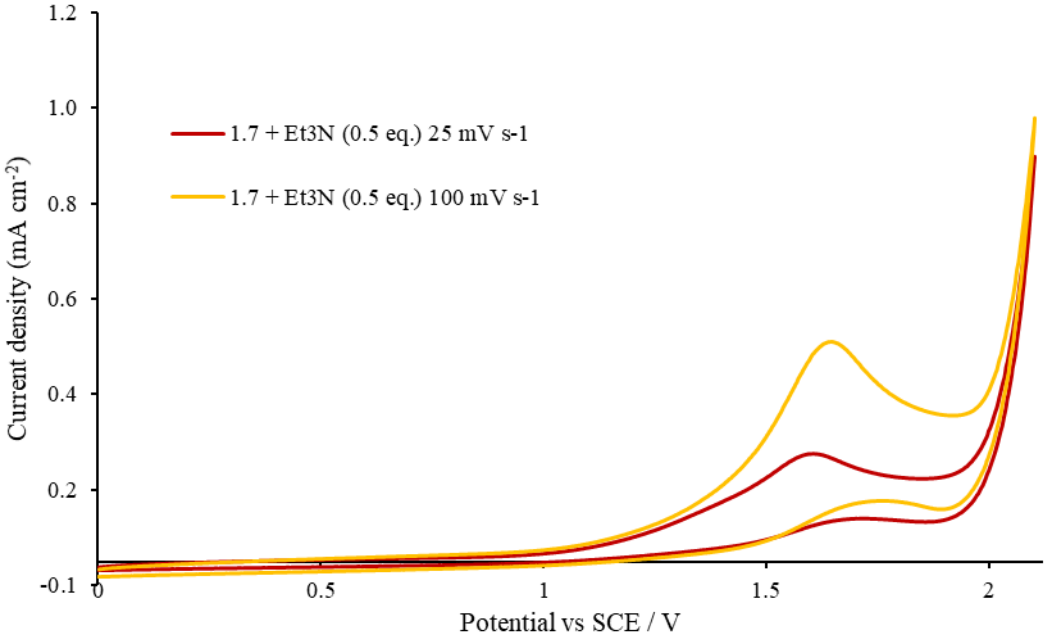

Figure 32. Cyclic voltammogram for 5 mM cubane carboxylic acid (1.7) and 2.5 mM Et_3N in MeOH/0.1 M Et_4NBF_4. Red line: Potential scan rate 25 mV s^{-1}; Orange line: Potential scan rate 100 mV s^{-1}.

3.3 Conclusion

Decarboxylation reactions represent a key synthetic pathway for the functionalisation of dimethyl 1,4–cubanedicarboxylate **1.35**, which is the only available cubane building block. However, most of the reported procedures rely on the use of activated esters, formed *in situ* or in a preceding step, known as reductive decarboxylation processes. In this chapter, we reported the first electrochemical cubane ring system functionalisation, through a Hofer–Moest oxidative decarboxylative ether formation. Successful investigation of the substrate scope involving potentially electrochemical oxidisable functionalities clearly indicated the mildness of the reaction conditions. The use of flow electrolysis facilitates laboratory scale–up, as shown by a gram–scale synthesis in a matter of hours in the same reactor and under the same conditions, nicely demonstrating the advantage this approach. As illustrated in Scheme 40, in contrast to the three synthetic steps reported previously, the developed electrochemical conditions enable to access **3.59** in one single step and avoiding the use of batch photoreactors with long electrolysis time (Scheme 40). A further straightforward 3–step process provided a cubanisidine biosiostere building block, and another example of a methoxycubane analogue of a drug is described. Organic electrosynthesis is considered as a sustainable methodology, since electrical current replaces potentially hazardous/toxic and costly chemical reagents, and any ensuing waste stream. No supporting electrolytes were required, facilitating purification. Hence, this first demonstration of an electrochemical reaction involving cubanes opens new window for its functionalisation and will be of great interest in medicinal and materials chemistry, two areas where cubane structure has attracted high interest, with great promise for further developments.

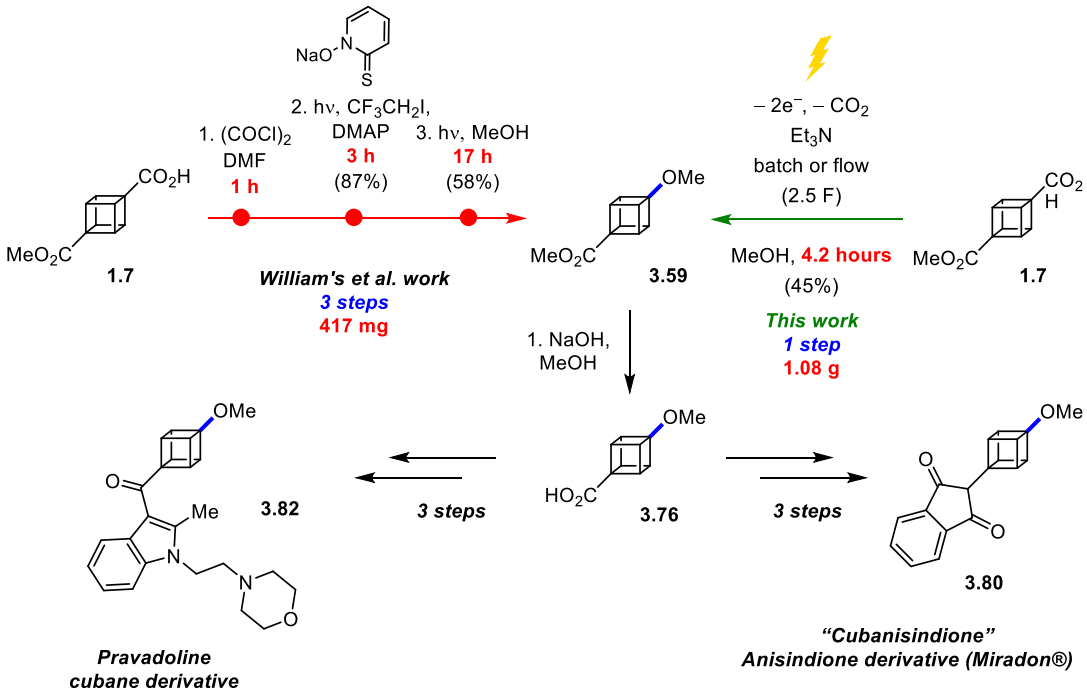

Scheme 40. Comparison of synthetic routes between William's synthesis of pravadoline analogue and this work.[132]

Chapter 4 Synthesis of 1,2,4–Tricarbonylated Cubanes

4.1 Introduction

4.1.1 Context

Most of the progress towards the functionalisation of cubanes has been made for the synthesis of *mono*– and *para*–substituted cubanes, starting from 1,4–cubane dicatboxylic acid and its derivatives. Nevertheless, as mentioned in Chapter 1, cubane present also close similarity in size to *ortho*– and *meta*–substituted benzene (Figure 33). Therefore, cubane could not only be considered for bioisosteric purposes but be more conveniently considered as a 3D scaffold with three of its substituents closely mimicking that of benzene, but offering an opportunity to introduce substituents perpendicular to the benzene plane. However, while several strategies has been reported, accessing *ortho*–functionalisation remains a challenging task.[35]

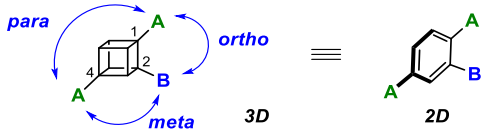

Figure 33. 1,2–, 1,3– and 1,4–substituted cubanes as *ortho–*, *meta–* and *para*–substituted benzene as a 3D molecular platform mimicking benzene core size–like.[35]

Three strategies have been reported and highlighted in Chapter 1 for the *ortho*–functionalisation of cubane, and consequently, were considered in this work. (1) Functionalisation of the cycloadduct prior to the [2+2] photocycloaddition.; (2) Generation of a cubyl anion through neighbouring group participation, namely, using *ortho*–metalation approach;[59] (3) Cubyl radical formation *via* hydrogen atom transfer.[63,64]

4.1.2 Hydrogen Abstraction of Cubane

4.1.2.1 Bond dissociation energy condiderations

Cleavage of the C–H bond of cubane is directly associated with the synthetic challenge of unactivated strong $C_{sp}{}^3$–H bond oxidation.[141] As depicted in Figure 34, the C–H bond dissociation enthalpy of cubane has a value of 104.7 kcal.mol^{-1}, and although the value has not been reported for dimethyl 1,4–cubanedicarboxylate (**1.35**), the presence of electron–withdrawing groups will make this C–H bond more electron deficient.[142,143,144] For instance, while the *tert*–butoxyl radical was shown to abstract a hydrogen from cubane or monosubstituted cubanes, no cubyl radical formation could be observed for **1.35**.[145] Moreover, regioselective hydrogen abstraction of monosubstituted cubane derivatives was shown to be particularly challenging due to the small BDEs differences between the

para–, *meta*– and *ortho*–hydrogens. In order to avoid *para*–H abstraction, Matsubara *et al.* reported the use of *para*–deuterated monocubanes due to the stronger C–D bond.[54]

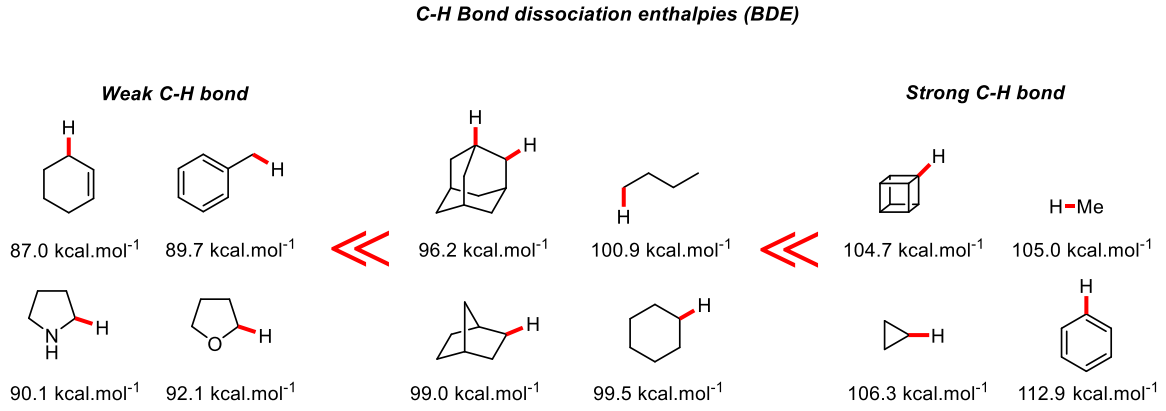

Figure 34. Representative BDE values of typical C−H bonds.[143]

4.1.2.2 Carboxylation *via* hydrogen abstraction

Carboxylic acid is a stable, non–toxic and one of the most versatile functional group for diversification in synthetic chemistry.[78] In the particular case of cubane, as highlighted in Chapter 1 and 3, direct or indirect decarboxylative pathways have proven to be powerful methods for its functionalisation.[42,44,46,139]

Nowadays, most of the reported C–H carboxylation procedures for C_{sp^3}–C_{sp^3/sp^2} bond formation rely on the use of transition metal complexes, photoredox catalysis processes, or both, usually, in presence of carbon dioxide. However, these procedures remain limited to allylic, benzylic, α–amino weak C–H bonds or organometallic aromatic chemistry.[146–154] Furthermore, the instability of cubane towards transition metals, which most of the reported C–H carboxylation procedures for C_{sp^3}–C_{sp^3/sp^2} bond formation rely, is a fundamental barrier.[155,52,132,156] An extensive investigation by Senge *et al.* for direct palladium–catalysed cross–coupling reactions from cubyl–halides has shown to be unsuccessful probably owing to the instability of the cubane core.[155] With the challenging cubyl radical formation in mind, Bashir–Hashemi's chlorine radical mediated cubane C–H chlorocarbonylation (cf chapter 1) remains of great interest despite the use of the toxic and corrosive oxalyl chloride in very large excess, and the use of a high–powered halogen lamp (≥ 275 W) operating at very high temperatures.[63,64] Recently, several milder conditions for the generation of chlorine radical have been reported for nickel mediated cross–coupling or Minisci–type reactions,[157,158] but large excesses of substrates (5 to 20 equiv.) are required, rendering these approaches unattractive with the synthesis of precious **1.35**. Therefore, after the previously discussed considerations, we proposed that an improved procedure for chlorocarbonylation of dimethyl 1,4–cubanedicarboxylate (**1.35**) would be highly desirable, and could enable further transformations.

4.2 Results and Discussion

4.2.1 Approach 1: cycloadduct functionalisation

Building our approach on the functionalisation of the cycloadduct prior to the [2+2] photocycloaddition, the lack of details in the experimental procedures did not enable us to initially reproduce the work of Lowe *et al*.[66] In order to avoid additional steps regarding the cubane synthesis as developed in Chapter 2, our investigations began with the non–protected cycloadduct dione **2.5** instead of the monoketal cycloadduct **1.47**. The methyl cuprate magnesium reagent was prepared and added according reported procedure and the formed enolate intermediate **4.1** was then trapped with trimethylsilyl chloride. Unlike the reported work, addition of trimethylsilyl chloride was required for the subsequent bromination step with *N*–bromosuccinimide. The tribrominated intermediate **4.2** was not purified and bromide elimination with pyridine in dimethylformamide led to the isolation of the corresponding methylated dione **1.51** in 6% overall yield.

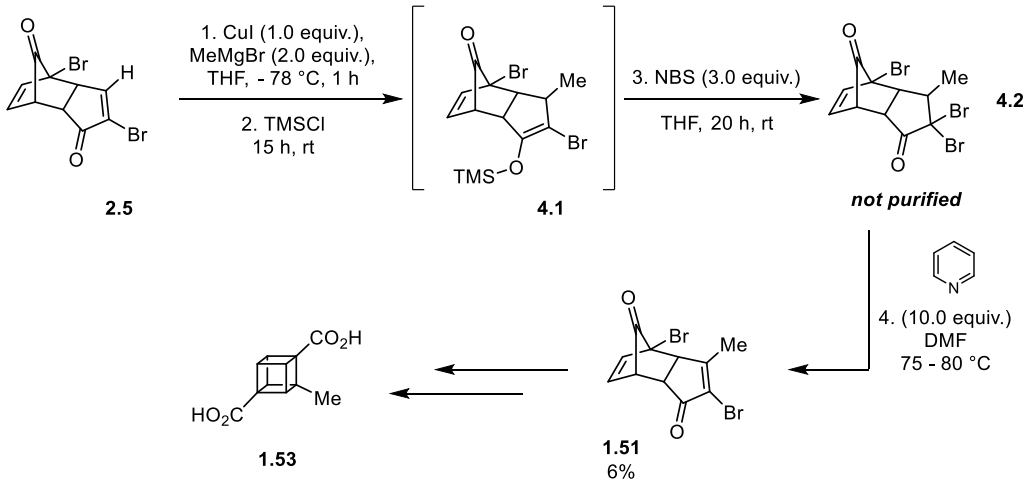

Scheme 41. 1,4–methyl cuprate addition on the corresponding dione 2.5.

Due to the obtained low yield, the reaction on the monoketal cycloadduct **1.47** (Scheme 42) was carried out following a literature report.[66] Starting from bisethylene ketal cycloadduct **2.11**, selective deprotection was achieved in acidic THF. 1,4–Conjugate addition of the formed methyl cuprate, followed by addition of trimethylsilyl chloride led to the isolation of the corresponding silyl enol ether **4.5**, and the resulting crude product was directly subjected to bromination. Tribrominated monoketal cycloadduct **1.49** was obtained in 33% yield after purification by column chromatography. Elimination reaction with pyridine followed by acetal hydrolysis led to the desired methylated dione **1.51** in 81% and 58% yield, respectively. Hence, starting from **2.11**, the methylated dione **1.51** was obtained through six chemical transformations in 15% overall yield. Next, **1.51** was subjected to the [2+2] photocycloaddition using the small–scale continuous–flow setup developed in this work (chapter 2), followed by the double Favorskii rearrangement. *Ortho*–methylated cubanedicarboxylic acid **1.53** could only be isolated on milligram–scale. Unlike **2.5**, methylated

dione **1.51** proved to be less soluble in methanol, and therefore, would presumably require re–optimisation of the photochemical step. Therefore, with the desire to access diverse trisubstituted cubane derivatives, it was concluded that this pathway was not flexible enough.

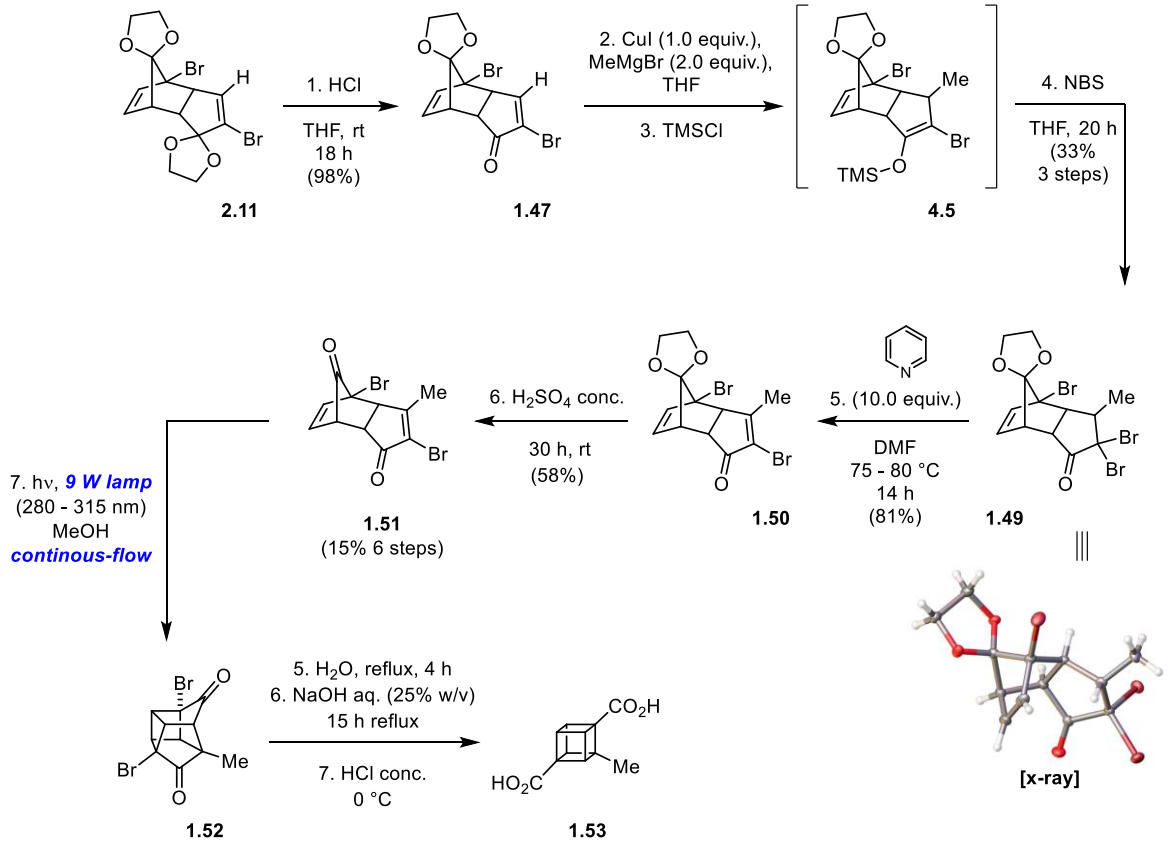

Scheme 42. Synthetic pathway for the synthesis of *ortho*–methylated dimethyl 1,4–cubanedicarboxylate 1.53.

4.2.2 Approach 2: directed metallation

Initially, this line of research was focused on using the reported *ortho*–lithiation strategy to achieve electrophilic cubane fluorination. Several attempts were carried out with the use of TMP_2Mg as magnesium amide base according the procedure reported by Eaton and Xiong and the use of *N*–fluorobenzenesulfonimide (NFSI) as electrophile.[59] While most of the starting material was recovered from the reaction, *ortho*–fluorinated diamide cubane **4.6** was confirmed by ^{19}F NMR and mass spectrometry (Scheme 43). However, we were not able to separate **4.6** from the starting material **1.23** and it was decided to use the mono–amide **4.7** to attempt the *ortho*–fluorination. However, no product **4.8** could be isolated.

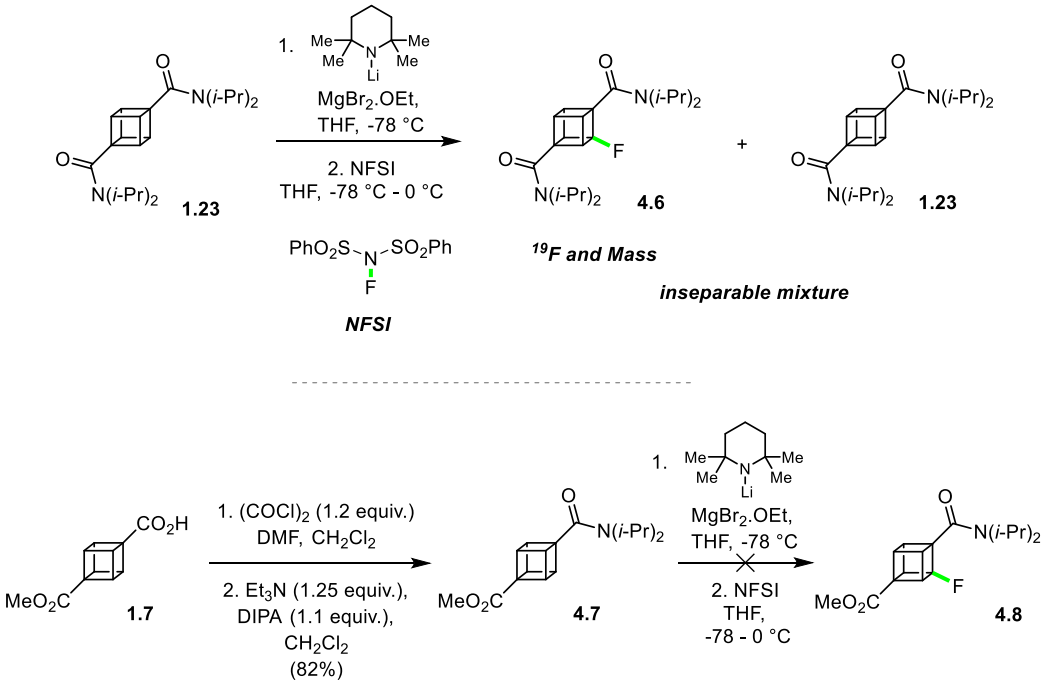

Scheme 43. *Ortho*–fluorination according the procedure reported by Eaton and Xiong.[59]

4.2.3 Approach 3: halogenation *via* hydrogen abstraction

In 2014, Britton *et al.* reported a UV–light–promoted C–H fluorination of strong unactivated aliphatic C–H bonds, up to 100 kcal.mol^{-1} , using the photocatalyst tetrabutylammonium decatungstate (TBADT), and NFSI as the fluorine source.[159] However, when this was attempted on **1.35**, no fluorinated dimethyl 1,4–cubanedicarboxylate **4.9** could be observed or isolated (Scheme 44). We assumed that the photoexcited catalyst TBADT was not capable to abstract a hydrogen from dimethyl 1,4–cubanedicarboxylate (**1.35**) under the reported conditions. In the search for thermodynamically favorable HAT, we found that Alexanian's *et al.* procedure's for aliphatic C–H chlorination led to *ortho*–chlorinated cubane **4.10** in 36% ^{1}H NMR yield *via* the formation of an amidyl radical under blue light irradiation.[160] However, at the same time, Matsubara *et al.*, reported the use of this strategy, by employing the corresponding bromoamide, for the synthesis of chiral cubanes,[54] and this line of research was thus terminated.

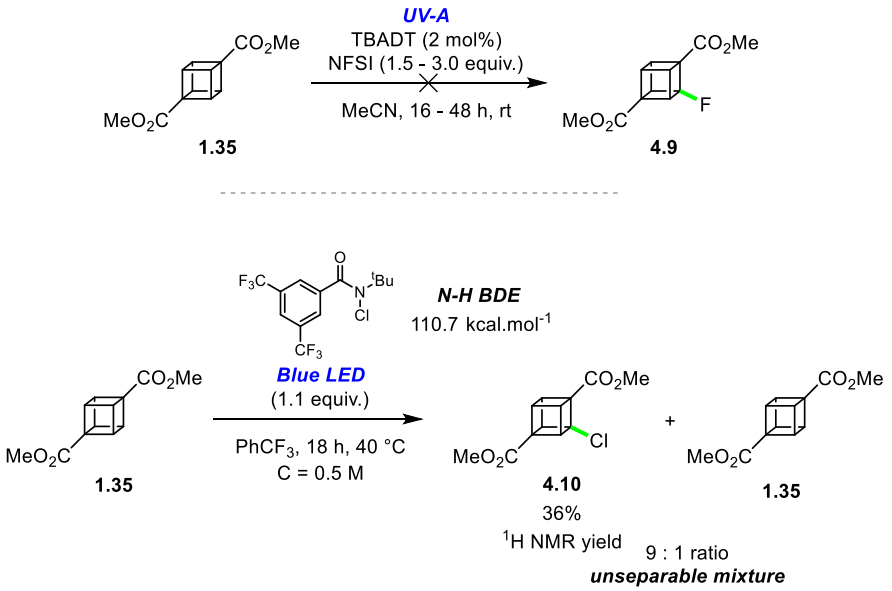

Scheme 44. Britton's *et al.* C–H fluorination and Alexanian's *et al.* C–H chlorination methods applied on 1.35.[159,160]

4.2.4 Approach 4: photochemical chlorocarbonylation hydrogen abstraction

4.2.4.1 Dissociation Mechanism of Oxalyl Chloride under Light Irradiation

For the development of safe, milder, practical and more efficient conditions to achieve powerful C–H chlorocarbonylation of dimethyl 1,4–cubanedicarboxylate (**1.35**) compared to Bashir–Hashemi's conditions, key considerations involved the excess of oxalyl chloride and the irradiation source. According the photodissociation wavelength of oxalyl chloride and the emission spectrum of halogen lamp (Scheme 45), we considered that a large part of the emitted light was lost, leading to our choice for UV–irradiation. In 1936, Krauskopf and Rollefson reported two different pathways according the emitted wavelength.[161] At low wavelengths (λ = 254 nm) the photodissociation proceed predominantly through the rupture of the carbon–to–carbon bond to form two molecules of acyl chloride radical whereas at high wavelength (λ = 365 nm) the predominant process involve the breaking of the carbon–to–chlorine bond to generate chlorine radical, carbon monoxide and an excited acyl chloride radical. Subsequently, this excited radical fragment can dissociate again to chlorine radical and carbon monoxide or lead to a stable radical COCl photoproduct. At high energetic wavelengths, the majority of the COCl* dissociates while at lower energetic wavelengths COCl* which may lead to an increase in the formation of a stable radical photoproduct.

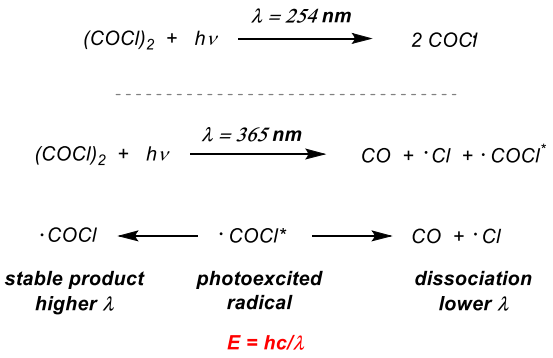

Scheme 45. Reported photodissociation mechanism of oxalyl chloride.[162,163]

4.2.4.2 Optimised Conditions for Chlorocarbonylation of Cubane diester

In the quest to develop the reaction in a solvent–based medium, dichloromethane was chosen as solvent, given the hydrocarbons and ethers, the only other solvents compatible with oxalyl chloride, will undergo efficient H–atom transfer (HAT) with the cubyl radical (ether α–C–H_{BDE} ≈ 92.1 kcal.mol^{-1}, hydrocarbon C–H_{BDE} ≤ 100 kcal.mol^{-1}). Then, we wished to use a microreactor as a safe and more efficient means for photochemical reactions, envisioning the possibility for a drastic reduction in lamp power. Moreover, the use of a microreactor seemed to be more appropriate regarding safety concerns with the generation of carbon monoxide. The home–made reactor setup using commercially available parts and a low powered 9 W bulb, as discussed in chapter 2, was used.

Our synthetic study began with UV–B irradiation of a 0.05 M solution of **1.35** in a continuous manner. However, the formation of carbon monoxide gas bubbles led to an uncontrolled flow rate, and consequently a low conversion towards the formation of chlorocarbonylated cubanes **4.11** (Table 9). The use of a back pressure regulator led to clogging and was therefore abandoned. Although the use of a microreactor remains strongly used in a continuous fashion, the need to adjust flow rates and wait for steady state before collection of each different variables adjustments, requires a large amount of compound compared to trial reactions in batch.[164] Therefore, in order to keep the inherent benefits of the photomicroreactor such as better light penetration, mixing, and heat transfer, it was decided to use the microreactor in a recycling mode, enabling the formed carbon monoxide to escape from the setup. In this case, an ice–water bath was used in order to keep the solution at room temperature during the reaction.

After some experimentation towards reducing the amount of oxalyl chloride, irradiation of dimethyl 1,4–cubanedicarboxylate (**1.35**) with twenty equivalents of oxalyl chloride for 3 hours under a recirculating flow rate of 0.2 mL.min^{-1}, followed by quenching with methanol, gave trimethyl 1,2,4–cubanetricarboxylate **4.12** in 23% yield along with unreacted **1.35** (Table 9, Entry 1). When the flow rate was increased to 3 mL.min^{-1}, the yield increased to 49% and increasing the irradiation time to 4 hours led to 62% yield and 7% of unreacted **1.35** (Table 9, Entry 2 and 3). With similar irradiation conditions, doubling the concentration of **1.35** does not improve the yield (Table 9, Entry 4).

Afterwards, the use of UV–C and UV–A lamps were investigated. The use of UV–C (λ = 100 – 280 nm) lamp decreased the yield to 32% (Table 9, Entry 5), in addition to reactor fouling. We explained this lower yield by the predominant rupture of the carbon–to–carbon bond followed by faster dissociation into 2 Cl and 2 CO photoproducts at lower wavelengths. Under similar conditions, replacing UV–B with UV–A also led to a lower yield (49%) for the same irradiation time. No product could be observed with the use of 40 W blue LED (λ = 450 nm) after 8 h irradiation (Table 9, Entry 7) reinforcing the inefficiency of halogen lamps initially reported. In regards to the large excess of oxalyl chloride used originally, doubling the concentration did not increase significantly the yield of **4.12** whereas decreasing two–fold still gave trimethyl 1,2,4–cubanetricarboxylate **4.12** in 55% yield (Table 9, Entry 8 and 9). Using the optimised conditions, replacing oxalyl chloride with methyl chlorooxoacetate, led to the desired product **4.12** formation in 8% yield (Table 9, Entry 10). Finally, as expected, a control experiment performed in absence of light gave no product (Table 9, Entry 11).

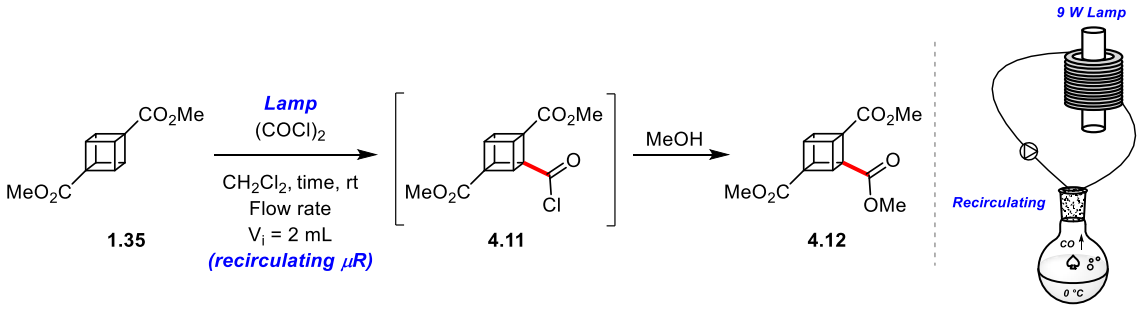

Table 9. Optimisation studies for *ortho*–chlorocarbonylation of dimethyl 1,4–cubanedicarboxylate (1.35).

Entry	Light	$(COCl)_2$ [equiv.]	Flow rate [mL.min^{-1}]	Time [h]	Yield [%][a]
1	UV–B	20	0.2	3	23[b]
2	UV–B	20	3	3	49[b]
3	UV–B	20	3	4	62[b]
4	UV–B	20	3	4	60[c]
5	UV–C	20	3	4	32[c],[d]
6	UV–A	20	3	4	49[b]
7	Blue LED	20	3	8	0[e]
8	UV–B	40	3	4	61
9	UV–B	10	3	4	55
10	UV–B	20[f]	3	4	8
11	No light	20	3	3	0

General Conditions: Optimised on 0.6 mmol of **1.35**. [a] ^{1}H NMR yield with 4–dimethyl terephthalate as internal standard. [b] c = 0.05 M, CH_2Cl_2 (10.95 mL), $(COCl)_2$ (1.05 mL). [c] c = 0.1 M, CH_2Cl_2 (4.95 mL), $(COCl)_2$ (1.05 mL). [d] Reactor fouling was observed (see Experimental section). [f] Methyl chlorooxoacetate instead.

4.2.4.3 Substrate Scope

Using the optimised conditions, the formed acyl chloride intermediate **4.11** was then trapped with various nucleophiles to demonstrate further *in situ* derivatisation while keeping the two original ester groups intact. Several 1,2,4–tricarbonyl cubane derivatives have been prepared (Scheme 46). Hydrolysis of **4.11** gave the crude carboxylic acid **4.13** in 56% yield. While upscaling can be challenging with the use of a recycling cell, doubling the amount of **1.35** and increasing the reaction time to 8 h led to isolation of **4.13** in 44% yield (Scheme 46). Attempting to trap the acyl chloride with more complex and bulkier alcohols at room temperature did not lead to isolation of the corresponding 1,2,4–triester cubanes, however, refluxing **4.11** in toluene in presence of one equivalent or slight excess of (–)–menthol and bile acid led to the corresponding desired product **4.14** and **4.15** in 30% and 37% yield respectively. The use of hydroxyphthalamide at room temperature enabled us to obtain the redox active ester **4.16** in low yield. In most cases, excess of triethylamine (5.0 equiv.) was added in order to avoid protonation and precipitation of the nucleophiles due to the formation of hydrochloric acid during the photochemical step. Changing alcohol for cyclohexyl mercaptan afforded **4.17** in 43% yield. Trapping the corresponding acyl chloride **4.11** with ammonium chloride in presence of triethylamine led to the isolation of the corresponding amide **4.18** in 37% yield. Primary amines (**4.19** to **4.24**) such as *para*–anisidine cubane isostere (**4.21**), electron poor (**4.22**) and rich (**4.23**) anilines and ampyrone (**4.24**) gave the corresponding amides in modest and good yields respectively, offering medicinally chemistry relevant motifs. Finally, secondary amides (**4.25** and **4.26**) with abundant drug motifs such as morpholine and piperidine were synthesised. Unfortunately, attempt to form carbonyl–carbon bond with Friedel–Craft acylation in presence of *N*–methyl–indole did not lead to the corresponding ketone **4.28**, probably due to the unlikely formation or stabilisation of the corresponding cubyl acylium ion.

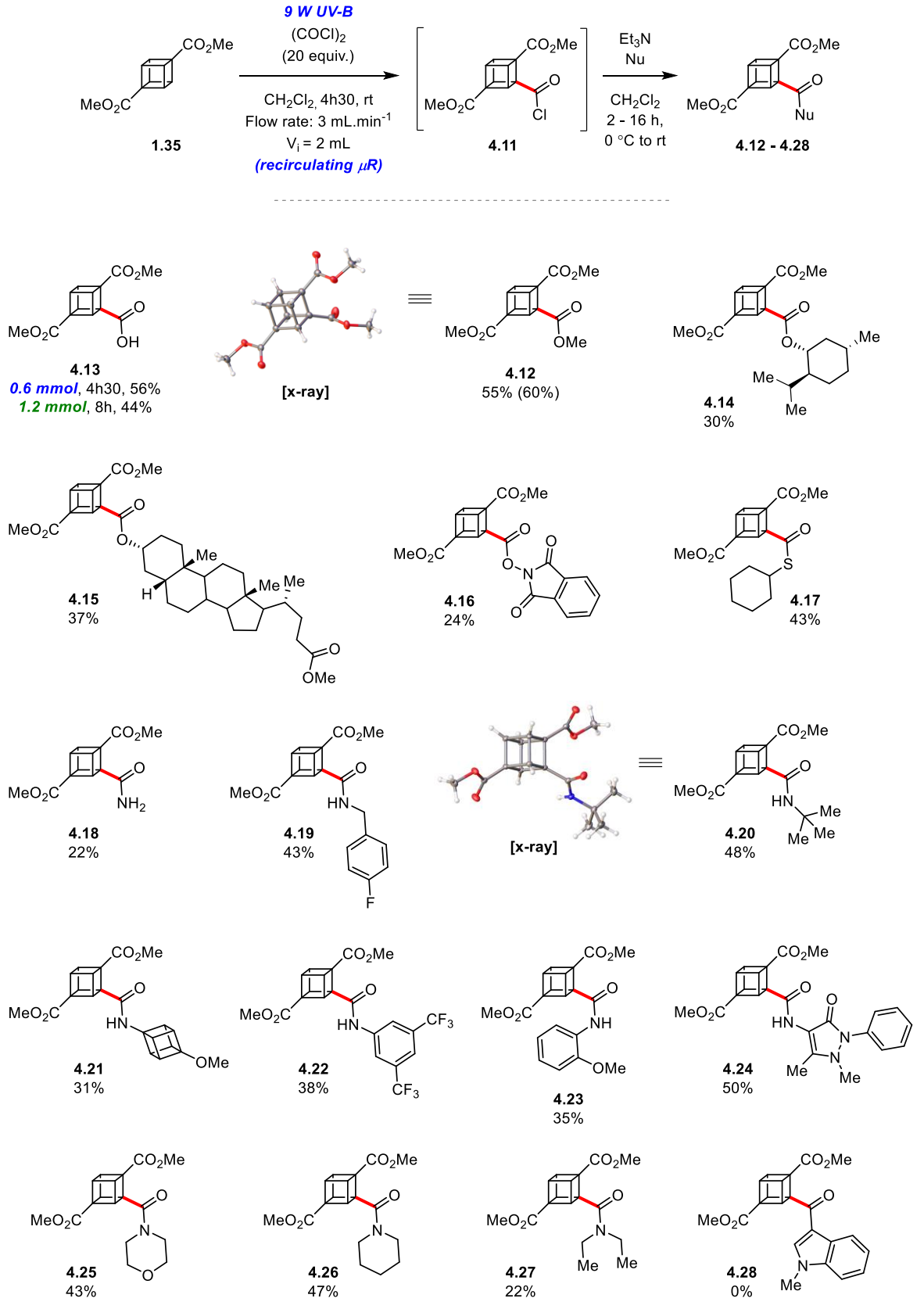

Scheme 46. ***In situ*** **derivatisation of the acyl chloride intermediate 4.13. Isolated yield based on 0.6 mmol of 1.35. 7 to 10% of 1.35 was recovered after the reaction.**

4.2.4.4 *Ortho*–Redox Active Ester Decarboxylation

With these 1,2,4–trisubstituted cubane derivatives in hand, further transformations were explored. Starting from the *ortho*–carboxylic acid **4.13**, the redox–active ester **4.16** was obtained in 92% yield (Scheme 47). This can now be used for a range of decarboxylative coupling methodologies to establish C_{cub}–C_{sp^3/sp^2} *ortho*–cubane functionalisation without the need to introduce directing amide groups to enable *ortho*–functionalisation as previously reported.[165] Applying the Senge nickel catalysed decarboxylative procedure[46] without further optimisation, *ortho*–phenyl cubane diester **4.29** was obtained in 32% yield from **4.16** in the presence of four equivalents of phenyl zincate chloride. Similarly, Giese–type reaction using benzyl acrylate as Michael acceptor gave **4.30** in 20% isolated yield.[45]

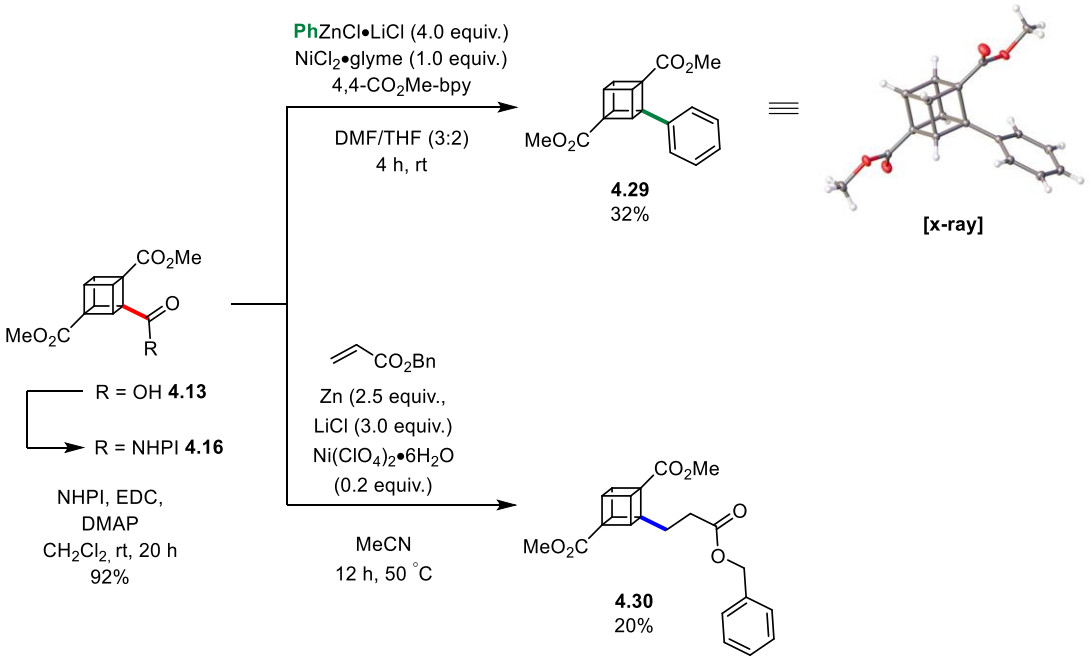

Scheme 47. Nickel catalysed *ortho*–functionalisation of RAE 1,2,4–cubane diester 4.16.[166]

4.2.4.5 Towards 1,2–cubane derivatives

The presence of the substituent at the 2–position leads to a differentiation of the two ester groups. Selective ester hydrolysis will allow fully differentiated functionalisation,[167] and can be used to further functionalise this position or, through decarboxylation, give access to 1,2– or 1,3–substituted cubane derivatives. Selective hydrolysis of the least hindered ester group was achieved: starting with **4.22**, saponification with one equivalent of sodium hydroxide led to the isolation of the corresponding carboxylic acid **4.31** in 84% yield in a 10:1 ratio (^{1}H NMR analysis) of the regiosiomers (Scheme 48). Saponification of **4.24** enabled isolation of **4.32** with complete regioselectivity (^{1}H NMR analysis) in 74% isolated yield.

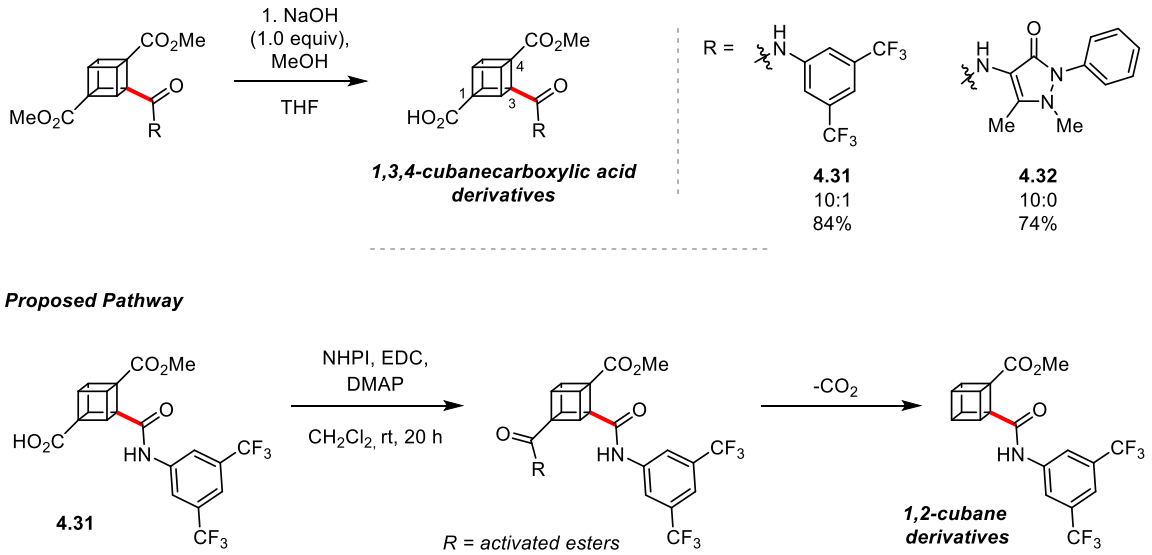

Scheme 48. Synthesis of 1,3,4–cubanecarboxylic acid derivatives and proposed pathway to access 1,2–cubane derivatives.

4.3 Conclusion

In conclusion, we have successfully developed a modified protocol for the radical–mediated C–H chlorocarbonylation of dimethyl 1,4–cubanedicarboxylate (**1.35**) using oxalyl chloride under light irradiation. Key improvements include the use of an adequate emission low–powered UV source, the use of a recirculating microreactor to enable continuous–flow conditions despite excessive gas formation, and the significant reduction in excess of oxalyl chloride by using a solvent, leading to a safe and accessible platform. This allows for convenient installation of the chlorocarbonyl group, and through its hydrolysis, of the versatile carboxylic acid group, both of which utility was exemplified by ester and amide formations and by *ortho*–arylation and alkylation via nickel catalysis, showing their potential for the synthesis of diverse 1,2,4–trisubstituted cubanes. Starting from dimethyl 1,4–cubanedicarboxylate (**1.35**), the optimised synthetic pathway enables access to new C_{cub}–C_{sp^3/sp^2} *ortho*–cubane diester derivatives in three steps, avoiding the introduction of amide groups to enable *ortho*–functionalisation as previously reported by Itami, Yagi *et al* (Scheme 49).[165] Finally, we proposed a synthetic strategy to access 1,2–cubane derivatives through regioselective saponification followed by decarboxylation. In addition, regioselective ester hydrolysis to access fully differentiated trisubstituted cubane derivatives is demonstrated, and by extension, for cubane–derived derivatives such as cyclooctatetraenes.[168]

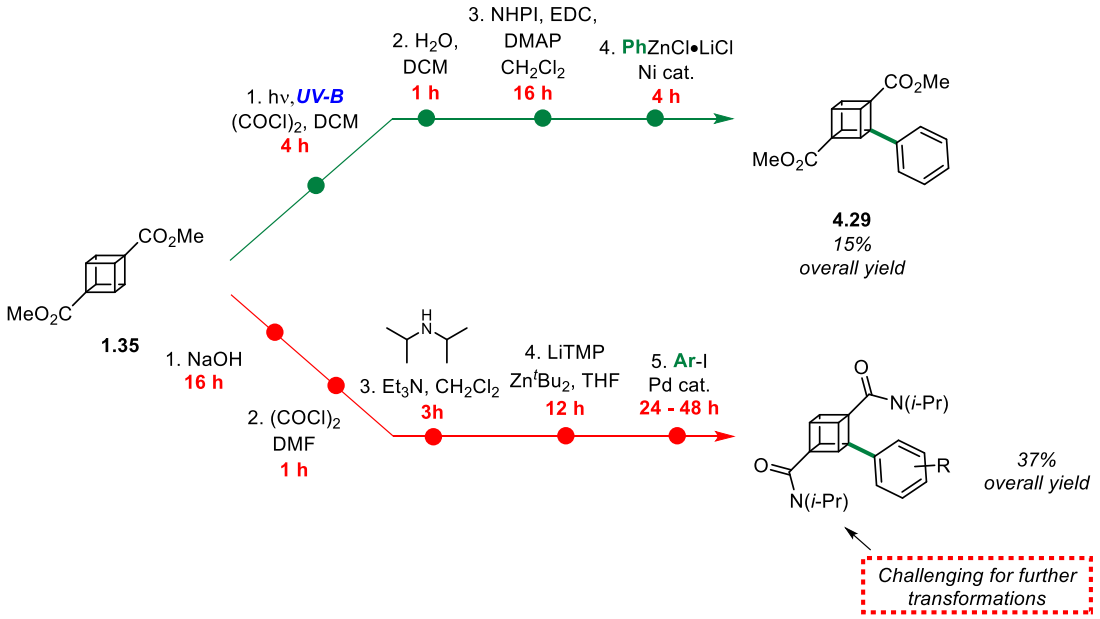

Scheme 49. Comparison of synthetic routes between this work and reported procedure for *ortho*–arylation of dimethyl 1,4–cubanedicarboxylate (1.35).[165]

Chapter 5 Experimental

5.1 General

Hydrogen (^{1}H) and carbon (^{13}C) were recorded on a Bruker® AVIIIHD 400 spectrometer (400/100 MHz). All chemical shifts are quoted on the δ scale in ppm. Assignments were made on the basis of chemical shifts. Coupling constants, and comparison with literature values where available. The NMR signals were designated as follows: s (singlet), d (doublet), t (triplet, q (quartet), quint (quintet), sept (septet), m (multiplet).

Mass spectra were carried out using electrospray ionisation on a directly injected WATERS quadrupole MSD using ESI+ or ESI- with MeOH/acetonitrile as solvent.

IR spectra were recorded on a Thermo Scientific™ Nicolet iS5 as a film and absorption peaks are given in cm^{-1} and the intensities were designated as follows: w (weak), m (medium), s (strong), br (broad).

Reagents (Sigma–Aldrich® or Acros Organics®) and solvents (Fisher Scientific®, Sigma–Aldrich®) provided from commercial sources were used and none further purifications were required. Silica gel (Merck silica gel 60, particle size 40–63 μm) was used for column chromatography and TLC were conducted on Merck 60 F_{254} silica gel precoated plates.

5.2 Continuous–Flow experiments

The microfluidic devices were constructed with Adtech Polymer Engineering® FEP tubing (0.8 mm ID x 1.6 mm OD). The connections were made with Upchurch Scientific® Super Flangeless™ nuts (natural PEEK, ¼–28 Flat-Bottom for 1/16 OD tubing), Upchurch Scientific® Super Flangeless™ ferrules (yellow ETFE, ¼–28 Flat–Bottom for 1/16 OD tubing). Upchurch Scientific® Luer Adapter (PEEK, 1/4–28 Female to Female) was used to connect syringes to the tubing. The feed solutions were conveyed to the microreactors using Aladdin Single–Syringe Pump and Ismatec® REGLO Digital Ms–2/6 peristaltic pump for large–scale reaction. Osram® (UVC 9W G23) and Phillips® UVB–Broadand (PL–S 9W/12/2P) and UVB–Narrowband (PL–L 36W/01/4P) lamps were used for the different experiments reported.

5.3 Chapter 2: Synthesis of Dimethyl 1,4–Cubanedicarboxylate

5.3.1 Synthetic Procedures

5.3.2 Synthesis of 1,4–dioxaspiro[4.4]nonane (2.17)

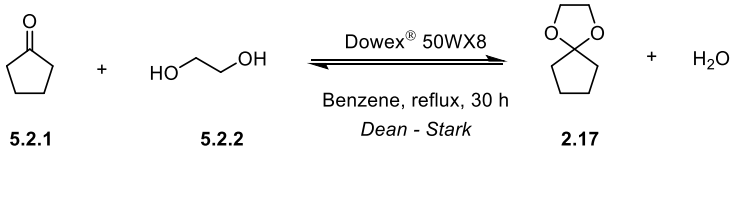

Following a procedure adapted from Tsanaktsidis and Bliese.[87] A solution cyclopentanone **5.2.1** (100 mL, 95.1 g, 1.13 mol, 1.0 equiv.) and ethylene glycol **5.2.2** (80 mL, 1.44 mol, 1.3 equiv.) in anhydrous benzene (200 mL) containing Dowex® 50WX8 50–100 (H) cation exchange resin (1.20 g, prewashed with anhydrous MeOH, followed by drying under vacuum) was heated at reflux under a Dean–Stark apparatus for 30 h. After cooling to room temperature, the resulting yellow mixture was washed with NaOH (4%) (2 × 100 mL) and brine (2 × 200 mL), dried over $MgSO_4$ and distilled under reduced pressure to afford 1,4–dioxaspiro[4.4]nonane **2.17** (112.6 g, 0.88 mol, 78%) as a colourless oil.

Formula $C_7H_{12}O_2$; **MW** 128.17 g.mol^{-1}; **^{1}H NMR** (400 MHz, $CDCl_3$) δ 3.90 (s, 4H), 1.81 – 1.74 (m, 4H), 1.71 – 1.65 (m, 4H) ppm; **^{13}C NMR** (101 MHz, $CDCl_3$) δ 118.5, 64.2, 35.9 (2C, CH_2), 23.5 (2C, CH_2) ppm. Data consistent with the literature.[169]

5.3.3 Synthesis of *Endo*–2,4–dibromodicyclopentadiene–1,8–dione bisethylene ketal (2.11)

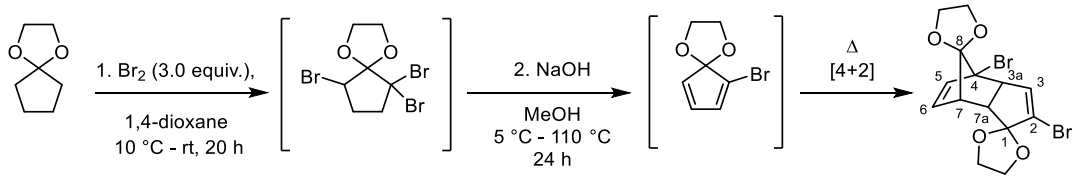

Following a procedure adapted from Tsanaktsidis and Bliese.[87] A solution of 1,4–dioxaspiro[4.4]nonane **2.17** (50.0 g, 390.0 mmol, 1.0 equiv.) in anhydrous 1,4–dioxane (310 mL) at 5 – 10 °C was purged with argon over 15 minutes. Molecular bromine (70 mL, 1.37 mol, 3.5 equiv.) was added dropwise (2 h), ensuring that the temperature was maintained between 10 – 15 °C, before being stirred at room temperature for 20 h. A NaOH (4%) trap was linked to the reaction flask to ensure the trapping of formed HBr. A solution of NaOH (121.4 g, 3.04 mol, 7.8 equiv.) in MeOH

(610 mL) was added dropwise via a dropping funnel over 2 h then the resulting brown mixture was heated at reflux for 24 h, before being cooled to room temperature and poured into a stirred ice–water bath (1.5 L). After filtration, the beige precipitate was washed with ice–cold H_2O (200 mL) and dried under high–vacuum for 6 h, to afford *endo*–2,4–dibromodicyclopentadiene–1,8–dione bisethylene ketal **2.11** (69.78 g, 171.8 mmol, 88%) as a pale beige solid.

Formula $C_{14}H_{14}O_4Br_2$; **MW** 406.07 g mol^{-1}; **mp** 180 – 181 °C (hexane/EtOAc) (Lit.[87] 172 – 174 °C); **^{1}H NMR** (400 MHz, $CDCl_3$) δ 6.19 (dd, *J* = 6.4, 3.7 Hz, 1H, H_6), 6.08 (d, *J* = 2.3 Hz, 1H, H_3), 5.84 (dd, *J* = 6.5, 0.7 Hz, 1H, H_5), 4.28 – 4.11 (4H, m, acetal), 4.04 – 3.87 (4H, m, acetal), 3.51 (dd, *J* = 7.4, 2.4 Hz, 1H, H_{3a}), 3.08 (1H, dd, J 7.4, 4.7 Hz, H_{7a}), 2.73 (1H, td, *J* = 4.7, 0.7 Hz, H_7) ppm; **^{13}C NMR** (101 MHz, $CDCl_3$) δ 134.5 (C_3H), 133.1 (C_5H), 132.6 (C_6H), 128.1 (C_1O), 126.1 (C_8O), 115.9 (C_2Br), 67.8 (C_4Br), 66.4 (acetal), 66.3 (acetal), 65.3 (acetal), 65.2 (acetal), 55.7 ($C_{3a}H$), 49.6 ($C_{7a}H$), 47.3 (C_7H) ppm; **IR** 2986 (w), 2890 (w), 1616 (w), 1471 (w), 1266 (m), 1142 (m), 1008 (s), 954 (s) 743 (s) cm^{-1}. ^{1}H NMR data consistent with the literature.[87]

Figure 35. Picture of cyclopentanone ethylene ketal (2.17) after the addition of bromine.

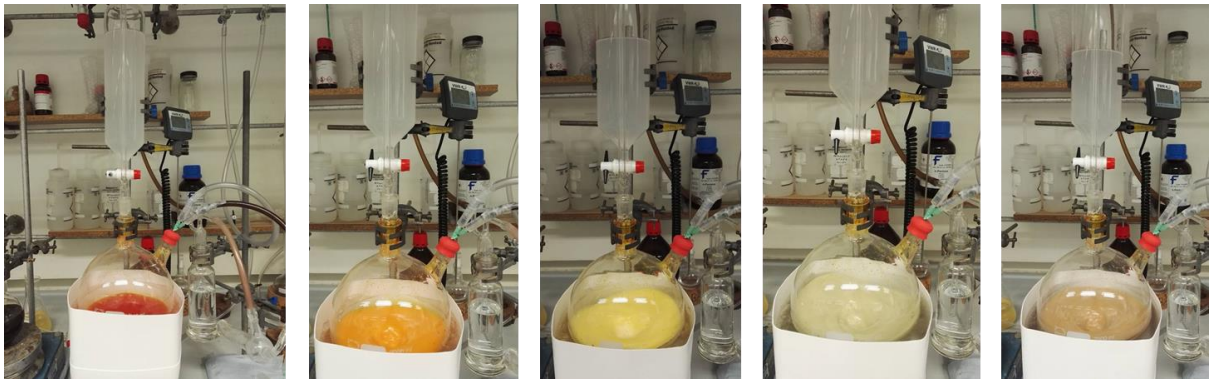

Figure 36. (*From left to right*) Change of colour with the addition of NaOH in methanol in the brominated cyclopentanone ethylene ketal.

Figure 37. (*Left*) Refluxed solution poured in an ice–water bath (*Right*) obtained *endo*–2,4–dibromodicylopentandien–1,8–one bisethylene ketal 2.11 after drying under high–vacuum.

5.3.4 Synthesis of *Endo*–2,4–dibromocyclopentadiene–1,8–dione (2.5)

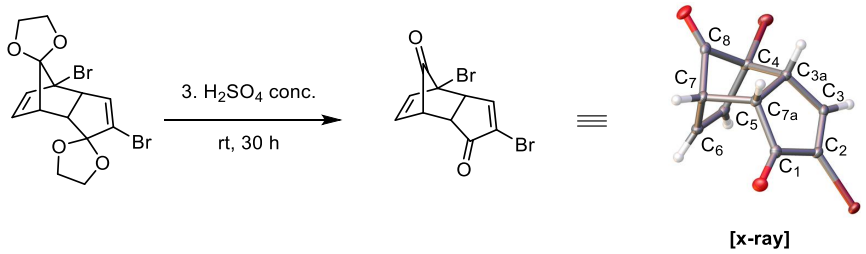

Following a procedure adapted from Tsanaktsidis and Bliese.[87] To a 500 mL flask, *endo*–2,4–dibromodicyclopentadiene–1,8–dione bisethylene ketal **2.11** (58.5 g, 0.14 mol, 1.0 equiv.) was dissolved portionwise in concentrated H_2SO_4 (>95%) (180 mL) at room temperature. After 30 h stirring at room temperature, the solution was slowly poured into a vigorously stirred ice–water bath (1 L), forming a beige precipitate. The resulting slurry was filtered under vacuum, washed with cold H_2O and dried under high–vacuum. The crude solid (47.2 g) was dissolved in EtOAc (472 mL) in a 2 L beaker with heating and stirring, then hexane (236 mL) was added. The pale beige precipitate formed was isolated by vacuum filtration, washed with ice–cold hexane/EtOAc (75 mL, 1:1), dried under vacuum and recrystallised from EtOAc/hexane to yield the title compound (28.15 g, 0.089 mol) as colourless crystals. Further evaporation of the filtrate gave a second crop (10.49 g, 0.033 mol) of colourless crystals to afford, overall, *endo*–2,4–dibromocyclopentadiene–1,8–dione **2.5** (38.64 g, 121.0 mmol, 84%).

Formula $C_{10}H_6O_2Br_2$; **MW** 317.96 g mol^{-1}; **mp** 164 – 165 °C as crystals (Lit.[87] 156–157 °C) ; **^{1}H NMR** (400 MHz, $CDCl_3$) δ 7.67 (d, *J* = 2.9 Hz, 1H, H_3), 6.36 (dd, *J* = 7.0, 3.9 Hz, 1H, H_6), 6.26 (dt, *J* = 6.8, 0.9 Hz, 1H, H_5), 3.59 (ddd, *J* = 4.8, 3.9, 0.9 Hz, 1H, H_7), 3.53 (1H, dd, *J* = 6.5, 2.9 Hz, H_{3a}), 3.21 (1H, dd, *J* = 6.4, 5.1 Hz, H_{7a}) ppm; **^{13}C NMR** (101 MHz, $CDCl_3$) δ 197.0 (C_1O), 192.4 (C_8O), 156.4 (C_3H), 134.1 (C_5H), 133.9 (C_6H), 129.8 (C_2Br), 60.3 (C_4Br), 49.0 ($C_{3a}H$), 47.3 (C_7H), 44.1 ($C_{7a}H$) ppm; **IR** 1789 (s), 1717 (s), 1580 (w), 1554 (w), 985 (m), 886 (m), 722 (s), 684 (s) cm^{-1}. Data consistent with the literature.[87]

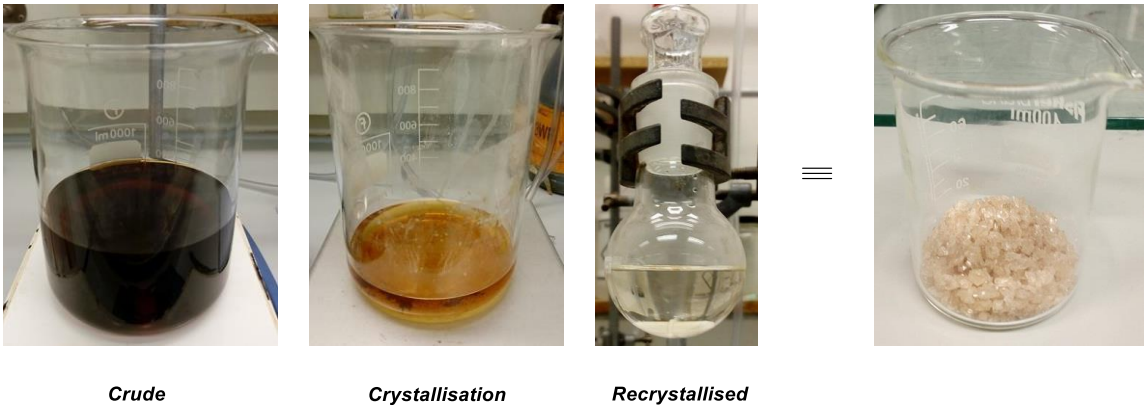

Figure 38. Recrystallisation of *endo*–2,4–dibromocyclopentadiene–1,8–dione (2.5).

5.3.5 Synthesis of Dimethyl 1,4–cubanedicarboxylate (1.35)

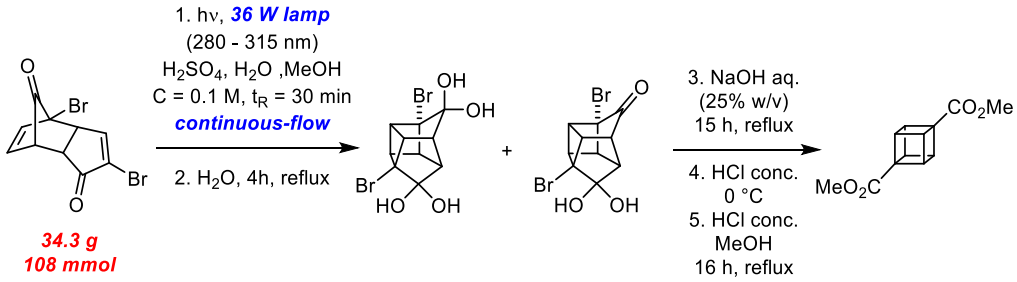

In a 2 L flask, *endo*–2,4–dibromocyclopentadiene–1,8–one **2.11** (34.31 g, 108.0 mmol, 1.0 equiv.) was dissolved in MeOH (907 mL), H_2O (163 mL) and H_2SO_4 (1.36 mL) then degassed with bubbling argon for 15 minutes. The resulting colourless solution was pumped (flow rate of 1.8 $mL.min^{-1}$) through the photoflow microreactor (V_i = 54 mL) using a peristaltic pump and a 36 W UV–B narrowband lamp. After reaching the steady–state (≈ 50 min), the product stream was collected until the solution had passed through the photoreactor. Pure methanol was then pumped through for 50 minutes. The resulting yellow solution was concentrated under vacuum then the obtained solid was heated at reflux in H_2O (312 mL) for 3.5 h to ensure full hydrolysis of any remaining dimethyl ketal. On cooling to room temperature, aq. NaOH (81.12 g, 26% w/v, 312 mL) was added portionwise to the mixture, and the dark brown solution stirred for 15 h at reflux. The solution was cooled to 0 °C, and concentrated HCl (~ 160 mL) was added dropwise until a pH ≈ 1 – 2 was reached. The brown precipitate was filtrated, and washed successively with ice–cold H_2O (200 mL) and ice–cold MeOH (15 mL). The crude solid was concentrated under high–vacuum for 6 h, then transferred to a 250 mL flask and heated under reduced pressure for several hours (60 °C) to afford 1,4–cubanedicarboxylic acid **1.1** (≈ 17.93 g) as a brown crude solid.

Afterwards, to 1,4–cubanedicarboxylic acid **1.1** (7.00 g) in anhydrous MeOH (200 mL) under argon in a 500 mL flask, was added concentrated HCl (2.0 mL, 66.0 mmol, 1.8 equiv.) dropwise. After 16 h at reflux under argon, the solvent was concentrated under vacuum and the obtained solid dissolved in CH_2Cl_2 (150 mL). The organic phase was washed with H_2O (7 × 100 mL), then the aqueous phases

were combined and extracted with CH_2Cl_2 (4 × 150 mL). The organic phases were combined, dried over $MgSO_4$, and concentrated under vacuum. The obtained black solid was dry–loaded and purified by flash column chromatography (8:2 hexane/EtOAc) to afford dimethyl 1,4–cubanedicarboxylate **1** (5.67 g, 25.7 mmol) as a white solid. This was subsequently repeated with 1,4–cubanedicarboxylic acid **1.1** (8.56 g) in anhydrous MeOH (245 mL) and concentrated HCl (2.45 mL, 0.081 mol, 1.8 equiv.), as above, to afford dimethyl 1,4–cubanedicarboxylate **1.35** (7.12 g, 32.3 mmol). Dimethyl 1,4–cubanedicarboxylate **1.35** (12.79 g, 58.1 mmol) was thus obtained in 54% overall yield from *endo*–2,4–dibromocyclopentadiene–1,8–one **2.5**.

1,4–Cubanedicarboxylic acid (1.1)

Formula $C_{10}H_8O_4$; **MW** 192.17 g mol^{-1}; **^{1}H NMR** (400 MHz, CD_3OD) δ 4.19 (s, 6H) ppm; **^{13}C NMR** (101 MHz, CD_3OD) δ 175.5 (2C, CO), 57.8 (2C, C cubyl), 48.3 (6C, CH cubyl) ppm. Data consistent with the literature.[87]

Dimethyl 1,4–cubanedicarboxylate (1.35)

Formula $C_{12}H_{12}O_4$; **MW** 220.22 g mol^{-1}; **R_f** 0.51 (8:2 hexane/EtOAc); **mp** 163 – 164 °C; **^{1}H NMR** (400 MHz, $CDCl_3$) δ 4.25 (s, 6H), 3.72 (s, 6H) ppm; **^{13}C NMR** (101 MHz, $CDCl_3$) δ 172.0 (2C, CO), 55.8 (2C, C cubyl), 51.6 (2C, CO_2CH_3), 47.1 (6C, CH cubyl) ppm; **IR** 3000 (s), 2955 (w), 1717 (s), 1440 (s), 1323 (s), 1206 (s), 1089 (s) cm^{-1}. Data consistent with the literature.[87]

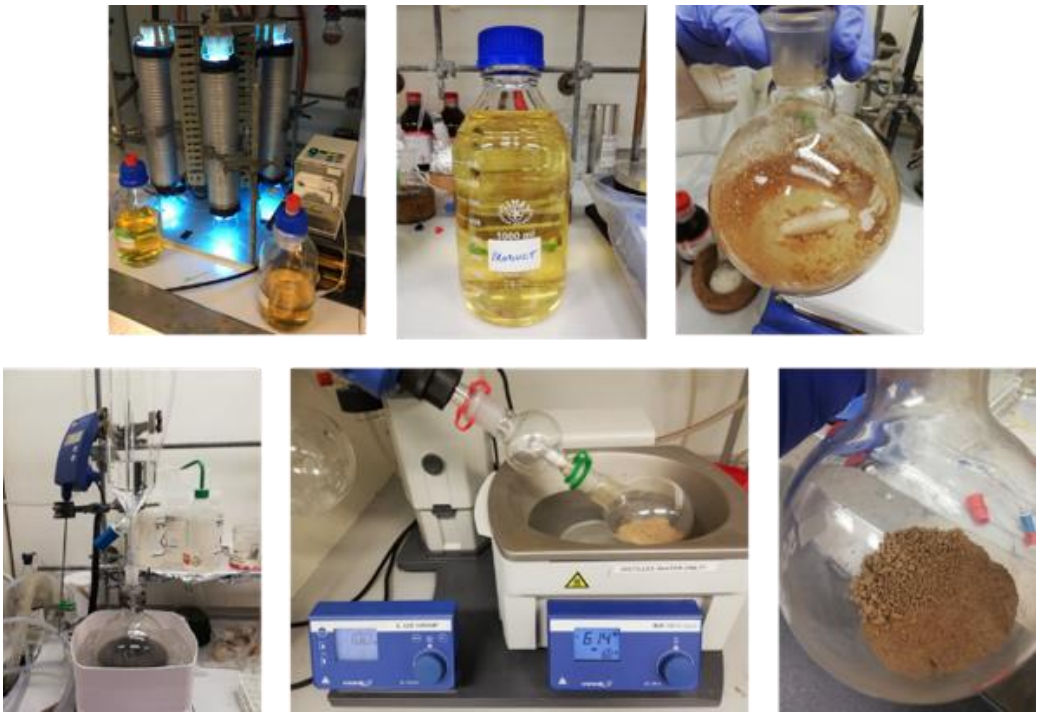

Figure 39. From collected [2+2] cycloadduct to 1,4–cubanedicarboxylic 1.1 : (*Middle top*) obtained solution after the photoreaction (*Top left*) [2+2]photocycloadduct 2.6a and 2.6b and after evaporation (*Top right*) Addition of HCl (*Middle bottom*) Drying of 1,4–cubanedicarboxylic acid (B*ottom right*) 1,4–cubanedicarboxylic acid 1.1.

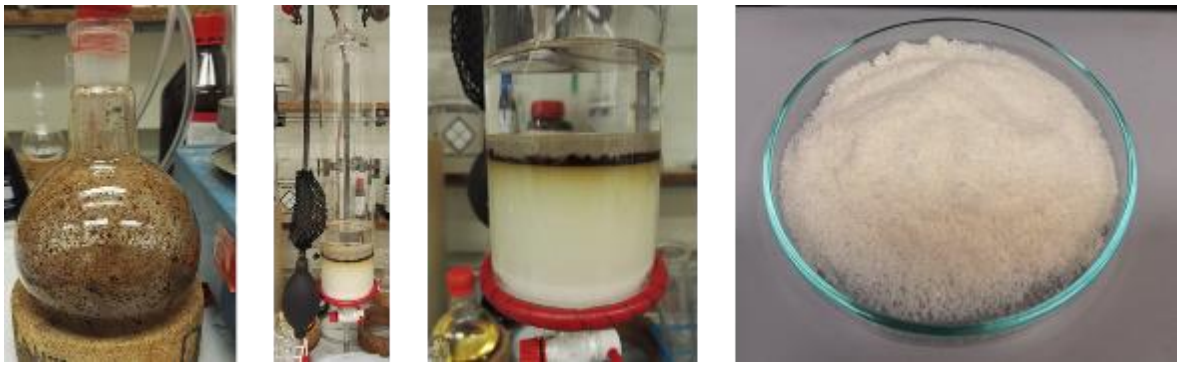

Figure 40. (*From left to right*) Obtained dimethyl 1,4–cubanedicarboxylate 1.35 after reaction + workup and dry–loaded compound on chromatography column and sample after purification.

5.4 Chapter 3: Electrochemistry

5.4.1 Synthetic Procedures

5.4.1.1 General procedure A: Electrolysis with platinum electrode

To a 10 mL volumetric flask, containing a solution of 4–methoxycarbonyl–1–cubanecarboxylic acid (**1.7**, 206 mg, 1.0 mmol, 1.0 equiv.) in the corresponding solvent, AcOH (60 µL, 1.0 mmol, 1.0 equiv.) and Et_3N (68 µL, 0.50 mmol, 0.50 equiv.) were added. The solution was stirred until homogenous and pumped through the Ammonite 8 reactor (internal volume = 1 mL) with a fixed flow rate of 0.2 mL min^{-1} and an applied current of 200 mA (which for these reactions lead to 6.2 F). After all the solution was passed through the reactor, the corresponding solvent was pumped through the reactor for 15 minutes. The solvent was removed under reduced pressure, and the crude reaction mixture was purified by column chromatography.

5.4.1.2 General procedure B: Electrolysis with Carbon/PVDF electrode

To a 10 mL volumetric flask, containing a solution of 4–methoxycarbonyl–1–cubanecarboxylic acid (**1.7**, 206 mg, 1.0 mmol, 1.0 equiv.) in the corresponding solvent, Et_3N (68 µL, 0.50 mmol, 0.50 equiv.) was added. The solution was stirred until homogenous and pumped through the Ammonite 8 reactor (internal volume = 1 mL) with a fixed flow rate of 0.5 mL min^{-1} and an applied current of 200 mA (which for these reactions lead to 2.5 F). After all the solution was passed through the reactor, the corresponding solvent was pumped through the reactor for 5 minutes. The solvent was removed under reduced pressure, and the crude reaction mixture was purified by column chromatography.

5.4.1.3 Gram–scale synthesis of methyl 4–methoxy–1–cubanecarboxylate (7)

To a 250 mL round-bottom flask, containing a solution of 4–methoxycarbonyl–1–cubanecarboxylic acid (**1.7**, 2.57 g, 12.5 mmol, 1.0 equiv.) in MeOH (125 mL) were added Et_3N (0.87 mL, 6.3 mmol, 0.50 equiv.). The solution was stirred until homogenous and pumped through the Ammonite 8 reactor with a flow rate of 0.5 mL min^{-1} (internal volume = 1 mL, theoretical residence time t_R = 2 min) with an applied current of 200 mA using a C/PVDF anode. After all the solution had passed through the reactor, pure methanol was passed through the reactor for 5 min. The solvent was removed under reduced pressure and purification was achieved via flash column chromatography (9:1 pentane/Et_2O) to afford methyl 4–methoxy–1–cubanecarboxylate (**7**, 1.08 g, 5.62 mmol, 45%) as an off–white solid and methyl cubanecarboxylate (**1.6**, 152 mg, 0.94 mmol, 8%) as a colourless solid.

NOTE: During the large-scale reaction, the voltage in the cell slowly but steadily increased with time due to a small deposit on the platinum electrode. When the voltage reached ≈ 10 V (usually between 2 – 4 V when the reaction starts), the starting material flask was switched with pure methanol

and passed through the reactor for 5 minutes and collected in the same collection flask as the product. The Ammonite 8 reactor was then disassembled, the platinum electrode was cleaned with a cotton wool and methanol to remove the deposit, and the cell was reassembled. The same above procedure was repeated until all the solution passed through the reactor.

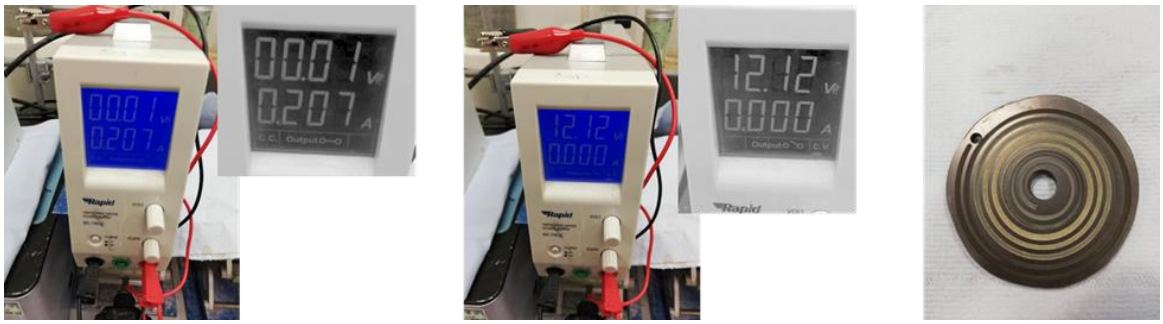

Figure 41. (*Left*) Selected current (200 mA). For the power supply used, the measured current ranged between 0.202 – 0.207 A. (*Middle*) Maximum selected voltage (12 V). (*Right*) Carbon/PVDF electrode after prolonged reaction.

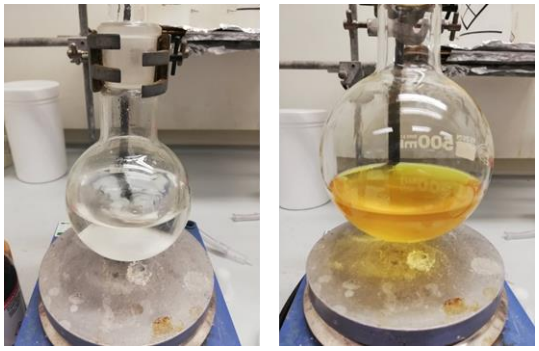

Figure 42. (*Left*) Solution of starting material 1.7. (*Right*) Solution obtained after reaction.

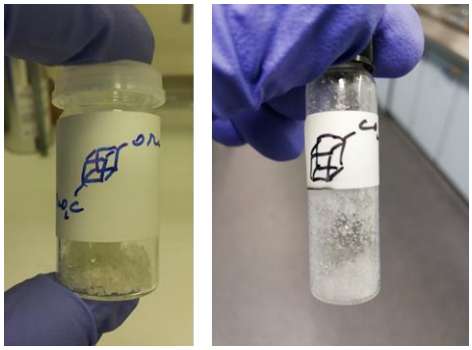

Figure 43. Obtained methyl 4–methoxy–1–cubane (1.7) and methyl cubanecarboxylate (1.6).

5.4.2 Flow Setup

5.4.2.1 Calculation for the current needed in the flow cell (I_{theo}) and charge applied (F)

The *theoretical current* (I_{theo}) needed for in a flow electrochemical process can be calculated using the following equation:

Faraday's law applied to flow conditions: $I_{theo} = n\ F\ C\ Q_v$

- I_{theo} = Theoretical current (A)
- n = number of electrons involved in the electrochemical process
- F = Faraday's constant (96 485 s A mol^{-1})
- C = Concentration (mol mL^{-1})
- Q_v = Flow rate (mL s^{-1})

The *current efficiency (CE)* of the electrochemical process can be calculated using the following equation:

Current efficiency: CE = $\frac{I_{theo}}{I_{cell}}$ × yield%

5.4.2.2 Platinum electrode

The Hofer–Moest reaction is to a 2-electron oxidation process (n = 2). The optimised conditions using a Pt electrode were identified as:

Concentration = 0.1 mol L^{-1} = 0.0001 mol mL^{-1}

Flow rate = 0.2 mL min^{-1} = 0.00333 mL s^{-1}

Therefore, with the equation shown above, the theoretical current (I_{theo}) for this transformation can be calculated:

I_{theo} = 0.064 A

But the applied cell current (I_{cell}) is 0.2 A, which means that a 3.1 fold excess of current is used. This is the stoichiometry of current required, and is represented by "*a*":

$I_{cell} = x\ F\ C\ Q_v$ Where: $x = n\ a$

$$x = \frac{0.2}{0.0001 \times 0.00333 \times 96485} = 6.2$$

"6.2 F (in Coulombs) is the charge applied to the electrochemical reaction with a Pt electrode"

Yield of **2** = 44%

$$CE = \frac{0.064}{0.2} \times 44\% = \mathbf{14\%}$$

5.4.2.3 C/PVDF electrode

Similarly, for the C/PVDF electrode:

Concentration = 0.1 mol L^{-1} = 0.0001 mol mL^{-1}

Flow rate = 0.5 mL min^{-1} = 0.00833 mL s^{-1}

I_{theo} = 0.16 A

I_{cell} = 0.2 A

Yield of **2** = 52%

x = 2.5 → *"2.5 F (Coulombs) is the charge applied to the electrochemical reaction with a C/PVDF electrode"*

CE = **42%**

5.4.3 Batch Setup

5.4.3.1 Calculation of the current needed in the batch cell (I_{theo}) and charge applied (F)

5.4.3.2 C/PVDF electrode

The *theoretical electrolysis time (t_{theo})* needed in a batch electrochemical process can be calculated using the following equation:

Faraday's law applied to batch conditions: $t_{theo} = \frac{n\,mF}{I}$

- t_{theo} = time of electrolysis (s)
- I = Current applied (A)
- *n* = number of electrons involved in the electrochemical process
- *m* = moles of substrate to be electrolysed (mol)
- *F* = Faraday's constant (96 485 s A mol^{-1})

The *current efficiency (CE)* of the electrochemical process for a batch-type reaction can be calculated using:

Current efficiency: CE = $\frac{t_{theo}}{t_{real}}$ × yield%

The Hofer–Moest reaction is to a 2-electron oxidation process (n = 2).

- *Surface area:* The surface area of the batch electrode used was 1.8 cm^2.
- *Current density:* The cell averaged current density used was the same as for the reaction in the Ammonite 8: 10 mA/cm^2. Therefore:
- *Current applied (I):* 10 mA/cm^2 x 1.8 cm^2 = 18 mA.
- *Moles of substrate (n):* 0.5 mmol (in 5 mL)

Therefore, with the equation shown above, the electrolysis time (t_{theo}) for this transformation can be calculated:

t_{theo} = 5400 s (90 min)

But the reaction required 180 min (10800 s) to achieve >95% conversion of starting material, which means that a 2 fold excess of current was used. This is the stoichiometry of current needed, and is represented by "*a*":

$$t = \frac{x\,m\,F}{I} \qquad \text{Where:} \qquad x = n\,a$$

$$x = \frac{0.018 \times 10800}{0.0005 \times 96485} = 4.0$$

"4.0 F (in Coulombs) is the charge applied to the batch electrochemical reaction with a C/PVDF electrode"

GC Yield of **7** = 50%

$$CE = \frac{5400}{10800} \times 50\% = \mathbf{25\%}$$

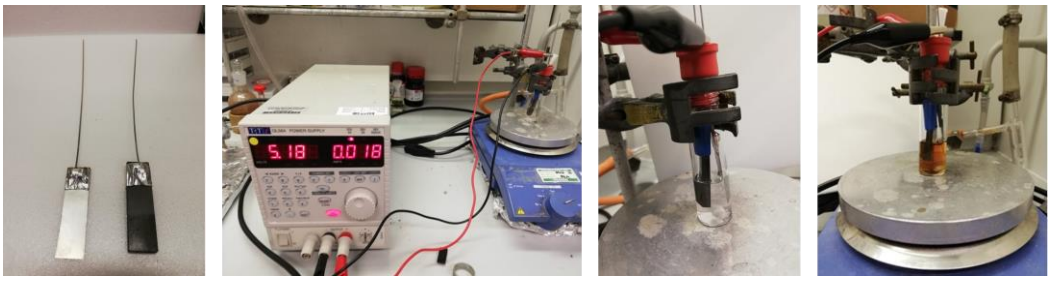

Figure S13. (*From left to right*): Steel and carbon/PVDF electrodes; Power supply (18 mA); Solution before electrolysis; Solution after 3 h of electrolysis.

5.4.3.3 Experimental procedure (batch electrolysis)

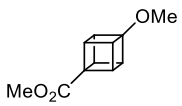

The acid **1.7** (103 mg, 0.500 mmol) and Et_3N (35 µL, 0.25 mmol) were dissolved in MeOH (5 mL) in a vial (see Figure S13). A C/PVDF anode and a stainless steel cathode (12 mm wide) were submerged in the solution, having a working surface of 1.8 cm^2. The solution was stirred and a constant current of 18 mA was applied. An aliquot was analysed by GC after 2 F of charge was passed (90 min), and the amount of product **3.59** was estimated to be 25% (50% starting material **1.7** remaining). The electrolysis was continued for another 90 minutes (4.0 F in total), and analysed by

GC. The amount of compound **3.59** was estimated to be 50% (GC yield) with full consumption of starting material. This is comparable to the GC yield obtained using the flow reactor conditions.

5.4.3.4 Methyl 4–methoxy–1–cubanecarboxylate (3.59)

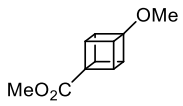

Prepared according to the **general procedure B**. The crude material was purified by flash column chromatography (9:1 pentane/Et_2O) to afford methyl 4–methoxy–1–cubanecarboxylate (**3.59**, 92 mg, 0.48 mmol, 48%) as an off–white solid. ^{1}H NMR data are consistent with the literature.[131]

Formula $C_{11}H_{12}O_3$; **MW** 192.21 g.mol^{-1}; **TLC** R_f 0.19 (9:1 pentane/Et_2O); **mp** 38 – 39 °C (Et_2O), [Lit.[3] 37 – 38 °C]; **^{1}H NMR** (400 MHz, $CDCl_3$) δ 4.18 (m, 3H), 4.00 (m, 3H), 3.71 (s, 3H), 3.34 (s, 3H) ppm; **^{13}C NMR** (101 MHz, $CDCl_3$) δ 172.8 (*C*OOMe), 91.4 (*C*–OMe), 56.7 (*C*–COOMe), 51.5 (2C, COO*CH*$_3$ + O*CH*$_3$), 50.5 (3C, CH cubyl), 42.5 (3C, CH cubyl) ppm; **IR** 2986 (w), 2832 (w), 1700 (s), 1436 (m), 1296 (s), 1210 (m), 1020 (m), 836 (s), 570 (s) cm^{-1}; **HRMS** (ESI) m/z for $[C_{11}H_{13}O_3]^+$ $[M+H]^+$ calcd: 193.0859 found: 193.0861.

5.4.3.5 Methyl cubanecarboxylate (1.6)

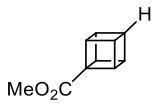

According the **general procedure B**, methyl cubanecarboxylate (**1.6**, 13 mg, 0.080 mmol, 8%) was isolated as a white solid. Data are consistent with the literature.[27]

Formula $C_{10}H_{10}O_2$; **MW** 162.19 g.mol^{-1}; **TLC** R_f 0.74 (9:1 pentane/Et_2O); **^{1}H NMR** (400 MHz, $CDCl_3$) δ 4.31 – 4.20 (m, 3H), 4.06 – 3.94 (m, 4H), 3.71 (s, 3H) ppm; **^{13}C NMR** (101 MHz, $CDCl_3$) δ 172.8 (CO), 55.6 (*C*–$COOCH_3$), 51.4 (COO*CH*$_3$), 49.5 (3C, CH cubyl), 47.8 (CH cubyl), 45.1 (3C, CH cubyl) ppm.

5.4.3.6 Synthesis of methyl 4–methoxy(*d*$_3$)–1–cubanecarboxylate (3.63)

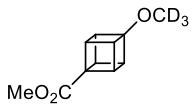

Prepared according to the **general procedure B**. The crude material was purified by flash column chromatography (9:1 pentane/Et_2O) to afford methyl 4–methoxy(*d*$_3$)–1–cubanecarboxylate (**3.63**, 79 mg, 0.40 mmol, 40%) as a white solid.

Formula $C_{11}H_9D_3O_3$; **MW** 195.23 g.mol^{-1}; **TLC** R_f 0.19 (9:1 pentane/Et_2O); **mp** 39 – 40 °C (hexane); **^{1}H NMR** (400 MHz, $CDCl_3$) δ 4.18 (m, 3H), 4.00 (m, 3H), 3.71 (s, 3H) ppm; **^{13}C NMR** (126 MHz, $CDCl_3$) δ 172.8 (*C*OOMe), 91.4 (*C*–OCD_3), 56.7 (*C*–COOMe), 51.5 (COO*CH_3* + O*CD_3*), 50.6 (3C, CH cubyl), 42.5 (3C, CH cubyl) ppm; **IR** 2988 (m), 2956 (w) 2847 (w), 1715 (s),1434 (m), 1304 (s br), 1207 (m), 1088 (m), 836 (s), 551 (s) cm^{-1}; **HRMS** (ESI) m/z for $[C_{11}H_{10}D_3O_3]^+$ $[M+H]^+$ calcd: 196.1048 found: 196.1046. $[M+Na]^+$ calcd: 218.0867 found: 218.0869.

5.4.3.7 Methyl 4–isopropoxy–1–cubanecarboxylate (3.64)

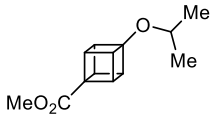

Prepared according to the **general procedure B** with C/PVDF anode. The crude material was purified by flash column chromatography (9:1 pentane/Et_2O) to afford methyl 4–isopropoxy–1–cubanecarboxylate (**3.64**, 19 mg, 0.086 mmol, 9%) as an off–white solid.

Formula: $C_{13}H_{16}O_3$; **MW** 220.27 g.mol^{-1}; **TLC** R_f 0.18 (9:1 pentane/Et_2O); **^{1}H NMR** (400 MHz, $CDCl_3$) δ 4.14 (m, 3H), 4.00 (m, 3H), 3.90 (spt, *J* = 6.2 Hz, 1H), 3.70 (s, 3H), 1.20 (d, *J* = 6.2 Hz, 6H) ppm; **^{13}C NMR** (101 MHz, $CDCl_3$) δ 172.9 (*C*OOMe), 90.1 (*C*–$OCH(CH_3)_2$), 68.4 (*CH*$(CH_3)_2$), 56.4 (*C*–COOMe), 52.4 (3C, CH cubyl), 51.5 (COO*CH_3*), 42.7 (3C, CH cubyl), 23.5 (2C, $CH(CH_3)_2$) ppm; **IR** 2978 (m), 1724 (s), 1296 (s), 1128 (m), 1088 (m) cm^{-1}; **HRMS** (ESI) m/z for $[C_{13}H_{17}O_3]^+$ $[M+H]^+$ calcd: 221.1172 found: 221.1174.

5.4.3.8 Methyl 4–ethoxy–1–cubanecarboxylate (3.65)

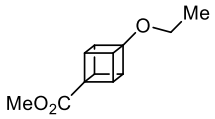

Prepared according to the **general procedure B** with C/PVDF anode. The crude material was purified by flash column chromatography (9:1 pentane/Et_2O) to afford methyl 4–ethoxy–1–cubanecarboxylate (**3.65**, 84 mg, 0.41 mmol, 41 %) as a yellowish–white solid.

Formula $C_{12}H_{14}O_3$; **MW** 206.24 g.mol^{-1}; **TLC** R_f 0.27 (9:1 pentane/Et_2O); **^{1}H NMR** (400 MHz, $CDCl_3$) δ 4.17 (m, 3H), 4.02 (m, 3H), 3.71 (s, 3H), 3.54 (q, *J* = 7.1 Hz, 2H), 1.27 (t, *J* =7.0 Hz, 3H) ppm; **^{13}C NMR** (101 MHz, $CDCl_3$) δ 172.9 (*C*OOMe), 90.6 (*C*–OCH_2CH_3), 59.9 (*C*H_2CH_3), 56.6 (*C*–COOMe), 51.5 (COO*CH_3*), 51.2 (3C, CH cubyl), 42.6 (3C, CH cubyl), 15.4 (CH_2*C*H_3) ppm; **IR** 2974 (m), 2873 (w), 1722 (s), 1303 (s), 1124 (s), 1045 (s) cm^{-1}; **HRMS** (ESI) m/z for $[C_{12}H_{15}O_3]^+$ $[M+H]^+$ calcd: 207.1016 found: 207.1016.

5.4.3.9 Methyl 4–trifluoroethoxy–1–cubanecarboxylate (3.66)

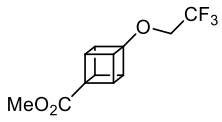

Prepared according to the **general procedure A**. The crude material was purified by flash column chromatography (hexane/Et_2O gradient from 10:1 to 9:1) to afford methyl 4–trifluoroethoxy–1–cubanecarboxylate (**3.66**, 62 mg, 0.24 mmol, 24%) as a yellow solid.

NOTE: purification of fluorinated alkoxy–cubanes required repeated column chromatography.

Formula $C_{12}H_{11}F_3O_3$; **MW** 260.21 g.mol^{-1}; **TLC** R_f 0.14 (9:1 hexane/Et_2O); **^{1}H NMR** (400 MHz, $CDCl_3$) δ 4.21 (m, 3H), 4.04 (m, 3H), 3.86 (q, *J* = 8.7 Hz, 2H), 3.71 ppm (s, 3H) ppm; **^{19}F NMR** (376 MHz, CDl_3) δ –74.41 (t, *J* = 8.7 Hz, CF_3) ppm; **^{13}C NMR** (101 MHz, $CDCl_3$) δ 172.4 (*C*OOMe), 123.6 (q, *J* = 278.0 Hz, CF_3), 91.4 (*C*–OCH_2CF_3), 62.7 (q, *J* = 34.5 Hz, CH_2), 56.6 (*C*–COOMe), 51.6 (COO*CH*$_3$) 51.0 (3C, CH cubyl), 42.5 (3C, CH cubyl) ppm; **IR** 2988 (w), 2957 (w), 1712 (s), 1437 (m), 1263 (s), 1162 (s), 961 (s), 837 (s), 691 (s) cm^{-1}; **HRMS** (ESI) m/z for $[C_{12}H_{11}F_3O_3Na]^+$ $[M+Na]^+$ calcd: 283.0552 found: 283.0558.

5.4.3.10 Methyl 4–(1,1,1,3,3,3–hexafluoroisopropoxy)–1–cubanecarboxylate (3.67)

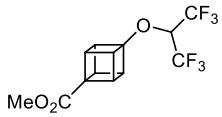

Prepared according to the **general procedure A**. The crude material was purified by flash column chromatography (hexane/Et_2O gradient from 10:1 to 9:1) to afford methyl 4–(1,1,1,3,3,3–hexafluoroisopropoxy)–1–cubanecarboxylate (**3.67**, 89 mg, 0.27 mmol, 27%) as a white solid.

NOTE: purification of fluorinated alkoxy–cubanes required repeated column chromatography.

Formula $C_{13}H_{10}F_6O_3$; **MW** 328.21 g.mol^{-1}; **TLC** R_f 0.22 (9:1 hexane/Et_2O); **mp** 103 – 105 °C (HFIP); **^{1}H NMR** (400 MHz, $CDCl_3$) δ 4.25 (m, 3H), 4.19 (spt, *J* = 6.0 Hz, 1H), 4.07 (m, 3H), 3.72 (s, 3H) ppm; **^{19}F NMR** (376 MHz, $CDCl_3$) δ –73.74 (6F, d, *J* = 5.2 Hz, 2 CF_3) ppm; **^{13}C NMR** (126 MHz, $CDCl_3$) δ 172.1 (*C*OOMe), 121.0 (q, *J* = 283.2 Hz, CF_3), 121.0 (q, *J* = 282.9 Hz, CF_3), 93.1 (C–O), 71.6 (spt, *J* = 33.1 Hz, *CH*$(CF_3)_2$), 56.6 (*C*–COOMe), 51.7 (3C, CH cubyl), 51.6 (COO*CH*$_3$), 42.4 (3C, CH cubyl) ppm; **IR** 2995 (w), 2949 (w), 1716 (s), 1377 (s), 1266 (s), 1191 (m), 1087 (m), 878 (s), 686 (s) cm^{-1}; **HRMS** (ESI) m/z for $[C_{13}H_{11}F_6O_3]^+$ $[M+H]^+$ calcd: 283.0607 found: 283.0605.

5.4.3.11 Synthesis of (4–methoxycubyl)(piperidin–1–yl)methanone (3.68)

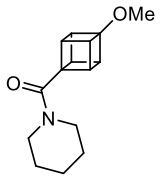

Prepared according to the **general procedure B** with C/PVDF anode. The crude material was purified by flash column chromatography (6:4 hexane/EtOAc) to afford (4–methoxycubyl)(piperidin–1–yl)methanone (**3.68**, 139 mg, 0.57 mmol, 57%) as an off–white solid.

Formula $C_{15}H_{19}NO_2$; **MW** 245.32 g.mol^{-1}; **TLC** R_f 0.13 (6:4 hexane/EtOAc); **^{1}H NMR** (400 MHz, $CDCl_3$) δ 4.16 (m, 3H), 3.96 (m, 3H), 3.56 – 3.46 (m, 2H), 3.33 (s, 3H), 3.24 – 3.13 (m, 2H), 1.70 – 1.60 (m, 2H), 1.60 – 1.48 (m, 4H) ppm; **^{13}C NMR** (101 MHz, $CDCl_3$) δ 169.9 (CON), 90.6 (*C*–OMe), 59.2 (*C*–CON), 51.4 (OCH_3), 49.9 (3C, CH cubyl), 45.7 (CH_2), 42.7 (CH_2), 42.5 (3C, CH cubyl), 26.8 (CH_2), 25.4 (CH_2), 24.6 (CH_2) ppm; **IR** 2977 (w), 2936 (br), 1611 (s), 1441 (s), 1289 (s), 1016 (m), 728 (m) cm-1; **HRMS** (ESI) m/z for $[C_{15}H_{20}NO_2]^+$ $[M+H]^+$ calcd: 246.1489 found: 246.1489; for $[C_{15}H_{19}NNaO_2]^+$ $[M+Na]^+$ calcd: 268.1308 found: 268.1307.

5.4.3.12 Synthesis of *N,N*–diethyl–4–methoxycubane–1–carboxamide (3.69)

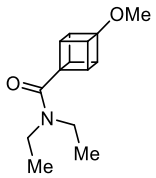

Prepared according to the **general procedure B** with C/PVDF anode. The crude material was purified by flash column chromatography (6:4 hexane/EtOAc) to afford *N,N*–diethyl–4–methoxycubane–1–carboxamide (**3.69**, 138 mg, 0.59 mmol, 59%) as a colourless oil.

Formula $C_{14}H_{19}NO_2$; **MW** 233.31 g.mol^{-1}; **TLC** R_f 0.42 (6:4 hexane/EtOAc); **^{1}H NMR** (400 MHz, $CDCl_3$) δ 4.15 (m, 3H), 3.97 (m, 3H), 3.35 (q, *J* = 7.1 Hz, 2H), 3.33 (s, 3H), 3.14 (q, *J* = 7.1 Hz, 2H), 1.19 (t, *J* = 7.1 Hz, 3H), 1.11 (t, *J* = 7.1 Hz, 3H) ppm; **^{13}C NMR** (101 MHz, $CDCl_3$) δ 170.9 (CON), 90.7 (*C*–OMe), 59.5 (*C*–CON), 51.4 (OCH_3), 49.8 (3C, CH cubyl), 42.7 (3C, CH cubyl), 40.6 (CH_2CH_3), 39.1 (CH_2CH_3), 14.6 (CH_2CH_3), 12.8 (CH_2CH_3) ppm; **IR** 2979 (s), 2831 (w), 1622 (s), 1442 (w), 1313 (s), 1294 (w), 1018 (m) cm^{-1}; **HRMS** (ESI) m/z for $[C_{14}H_{20}NO_2]^+$ $[M+H]^+$calcd: 234.1489 found: 234.1485; for $[C_{14}H_{19}NNaO_2]^+$ $[M+Na]^+$calcd: 256.1308 found: 256.1303.

5.4.3.13 Synthesis of *N*,*N*–diisopropyl–4–methoxycubane–1–carboxamide (3.70)

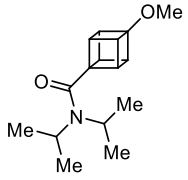

Prepared according to the **general procedure B** with C/PVDF anode and 4–*N*,*N*–diisopropylcarbamoyl–1–cubanecarboxylic acid (**5.3.15**, 254 mg, 0.90 mmol, 1.00 equiv.), Et_3N (62 µL, 0.45, 0.5 equiv.) in MeOH (9 mL). The crude material was purified by flash column chromatography (6:4 hexane/EtOAc) to afford *N*,*N*–diisopropyl–4–methoxycubane–1–carboxamide (**3.70**, 144 mg, 0.55 mmol, 60%) as a beige solid.

Formula $C_{16}H_{23}NO_2$; **MW** 261.37 g.mol^{-1}; **TLC** R_f 0.13 (7:3 hexane/EtOAc); **^{1}H NMR** (400 MHz, $CDCl_3$) δ 4.13 (m, 3H), 3.93 (m, 3H), 3.52 (spt, *J* = 6.7 Hz, 1H), 3.33 (s 1H), 3.29 (spt, *J* = 6.6 Hz, 1H), 1.41 (d, *J* = 6.8 Hz, 6H), 1.20 (d, *J* = 6.6 Hz, 6H) ppm; **^{13}C NMR** (101 MHz, $CDCl_3$) δ 170.8 (CON), 90.6 (*C*–OMe), 60.4 (*C*–CON), 51.4 (OCH_3), 49.7 (3C, CH cubyl), 48.1 (*CH*(CH_3)$_2$), 45.8 (*CH*(CH_3)$_2$), 42.4 (3C, CH cubyl), 21.0 (2C, CH(*CH*$_3$)$_2$), 20.5 (2C, CH(*CH*$_3$)$_2$) ppm; **IR** 2974 (m), 2932 (m), 2834 (w) 1618 (s), 1442 (s), 1308 (s), 1010, (s), 730 (m), 622 (m) cm^{-1}; **HRMS** (ESI) m/z for $[C_{16}H_{24}NO_2]^+$ $[M+H]^+$ calcd: 262.1802 found: 262.1806; for $[C_{16}H_{23}NNaO_2]^+$ $[M+Na]^+$ calcd: 284.1621 found: 284.1621.

5.4.3.14 Synthesis of (4-methoxycubyl)(morpholino)methanone (3.71)

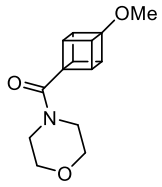

Prepared according to the **general procedure B** with C/PVDF anode and 4–morpholinocarbonyl–1–cubanecarboxylic acid (**5.3.16**, 210 mg, 0.80 mmol, 1.00 equiv.), Et_3N (56 µL, 0.40 mmol, 0.50 equiv.) in MeOH (8 mL). The crude material was purified by flash column chromatography (95:5 chloroform/methanol) to afford (4–methoxycubyl)(morpholino)methanone (**3.71**, 95 mg, 0.38 mmol, 48%) as a yellow solid.

Formula $C_{14}H_{17}NO_3$; **MW** 247.29 g.mol^{-1}; **^{1}H NMR** (400 MHz, $CDCl_3$) δ 4.18 (m, 3H), 3.99 (m, 3H), 3.70 – 3.65 (m, 5H), 3.63 – 3.56 (m, 2H), 3.34 (s, 3H), 3.30 – 3.24 (m, 2H) ppm; **^{13}C NMR** (101 MHz, $CDCl_3$) δ 170.3 (CON), 90.5 (*C*–OMe), 66.9 (2C, OCH_2), 58.8 (*C*–CON), 51.5 (OCH_3), 50.0 (3C, CH cubyl), 45.2 (NCH_2), 42.4 (3C, CH cubyl), 41.9 (NCH_2) ppm; **IR** 2989 (w), 2917 (w), 1610 (s), 1430 (m), 1112 (s), 1004 (s) cm^{-1}; **HRMS** (ESI) m/z for $[C_{14}H_{18}O_3]^+$ $[M+H]^+$ calcd: 248.1281 found: 248.1285.

5.4.3.15 Synthesis of 4-methoxy-1-cubanebenzylether (3.72)

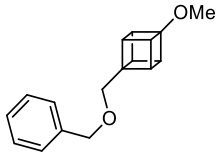

Prepared according to the **general procedure B** with C/PVDF anode and 4–benzyloxy–1–cubanecarboxylic acid **xx** (90 mg, 0.33 mmol, 1.00 equiv.), Et_3N (23 µL, 0.17 mmol, 0.50 equiv.) in MeOH (3.3 mL). The crude material was purified by flash column chromatography (9:1 hexane/EtOAc), followed by prep TLC (9:1 hexane/EtOAc) to afford 4–methoxy–1–cubanebenzylether (**3.72**, 17 mg, 0.067 mmol, 20%) as a white solid.

Formula $C_{17}H_{18}O_2$; **MW** 254.33 g.mol^{-1}; **TLC** R_f 0.33 (9:1 hexane/EtOAc); **^{1}H NMR** (400 MHz, $CDCl_3$) δ 7.39 – 7.28 (m, 5H), 4.57 (s, 2H), 4.09 (m, 3H), 3.65 (m, 3H), 3.61 (s, 2H), 3.34 (s, 3H) ppm; **^{13}C NMR** (101 MHz, $CDCl_3$) δ 138.7 (Ar), 128.3 (2C, Ar), 127.6 (2C, Ar), 127.5 (Ar), 92.1 (*C*–OMe), 73.1 (Ar–*CH*$_2$), 70.9 (C_{cubyl}–*CH*$_2$), 58.5 (*C*$_{cubyl}$–CH_2), 51.2 (OCH_3), 49.9 (3C, CH cubyl), 40.5 (3C, CH cubyl) ppm; **IR** 2978 (s), 2828 (m), 1451 (w), 1292 (s), 1071 (s), 1019 (s), 734 (m), 697 (s) cm^{-1}; **HRMS** (ESI) m/z for $[C_{17}H_{18}NaO_2]^+$ $[M+Na]^+$ calcd: 277.1199 found: 277.1197.

5.4.3.16 Synthesis of 4–methoxy–1–cubylmethanol (3.73)

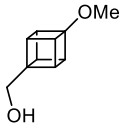

NOTE: 4–Hydroxymethyl–1–cubanecarboxylic acid is not soluble in methanol at a concentration of 0.1 M, therefore, 0.05 M concentration was used with a reduced current of 100 mA (instead of 200 mA) at the same flow rate to keep the charge constant (2.5 F).

Prepared according to the **general procedure B** with C/PVDF anode and 4–hydroxymethyl–1–cubanecarboxylic acid (**5.3.9**, 99 mg, 0.56 mmol, 1.00 equiv.), and Et_3N (39 µL, 0.28 mmol, 0.50 equiv.) in MeOH (11 mL). The crude material was purified by flash column chromatography (6:4 pentane/Et_2O) to afford 4–methoxy–1–cubylmethanol (**3.73**, 42 mg, 0.26 mmol, 46%) as a white solid.

Formula $C_{10}H_{12}O_2$; **MW** 164.20 g.mol^{-1}; **TLC** R_f 0.18 (6:4 pentane/Et_2O); **^{1}H NMR** (400 MHz, $CDCl_3$) δ 4.10 (m, 3H), 3.79 (br s, 2H), 3.64 (m, 3H), 3.34 (s, 3H) ppm; **^{13}C NMR** (101 MHz, $CDCl_3$) δ 92.2 (*C*–Me), 63.9 (CH_2), 59.7 (*C*–CH_2), 51.2 (OCH_3), 49.7 (3C, CH cubyl), 39.8 (3C, CH cubyl) ppm; **IR** 3443 (br) 2974 (w), 2960 (w), 2844 (w), 1455 (w), 1285 (s), 1006 (s) cm^{-1}; **LRMS** (EI) m/z 163.9 for $C_{10}H_{12}O_2$ $[M–H]^–$.

5.4.3.17 Synthesis of *tert–butyl* 4–methoxy–1–cubanecarboxylate (3.74)

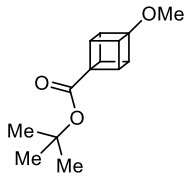

Prepared according to the **general procedure B** with C/PVDF anode and 4–*tert–but*oxycarbonyl–1–cubanecarboxylic acid (**5.3.10**, 111 mg, 0.45 mmol, 1.0 equiv.), and Et_3N (31 µL, 0.23 mmol, 0.5 equiv.) in MeOH (4.5 mL). The crude material was purified by flash column chromatography (95:5 hexane/EtOAc) to afford *tert*–butyl 4–methoxy–1–cubanecarboxylate (**3.74**, 46 mg, 0.20 mmol, 44%) as a white solid.

Formula $C_{14}H_{18}O_3$; **MW** 234.30 g.mol^{-1}; **^{1}H NMR** (400 MHz, $CDCl_3$) δ 4.14 (m, 3H), 3.92 (m, 3H), 3.33 (s, 3H), 1.46 (s, 9H) ppm; **^{13}C NMR** (101 MHz, $CDCl_3$) δ 172.1 (*C*OO*t*Bu), 91.4 (*C*–OMe), 80.1 (O*C*(CH_3)$_3$), 57.8 (*C*–COO*t*Bu), 51.4 (O*C*H_3), 50.3 (3C, CH cubyl), 42.4 (3C, CH cubyl), 28.1 (3C, OC(*C*H_3)$_3$) ppm; **IR** 2981 (s), 2932 (w), 1709 (s), 1304 (s), 1121 (s), 1018 (m), 837 (m), 568 (w) cm^{-1}; **HRMS** (ESI) m/z for $[C_{14}H_{18}NaO_3]^+$ [M+Na]$^+$ calcd: 257.1148 found: 257.1151.

5.4.3.18 Synthesis of 4–methoxy–1–cubanecarboxylic acid (3.76)

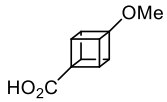

To a 25 mL flask, containing a solution of methyl 4–methoxy–1–cubanecarboxylate (**3.59**, 192 mg, 1 mmol, 1.0 equiv.) in THF (10 mL) was added NaOH (400 mg, 10.0 mmol, 10.0 equiv.) portionwise. After 16 h at room temperature, solvent was evaporated and the obtained solid was redissolved in 10 mL of water and washed with CH_2Cl_2 (3 × 5 mL). The aqueous phase was acidified with concentrated HCl (pH ≈ 1–2), and extracted with CH_2Cl_2 (4 × 5 mL). The combined organic extract was dried over $MgSO_4$ and concentrated under reduced pressure to afford 4–methoxy 1–cubanecarboxylic acid (**3.76**, 167 mg, 0.94 mmol, 94%) as a white powder.

Formula $C_{10}H_{10}O_3$; **MW** 178.19 g.mol^{-1}; **^{1}H NMR** (400 MHz, $CDCl_3$) δ 4.21 (m, 3H), 4.05 (m, 3H), 3.35 (s, 3H) ppm; **^{13}C NMR** (101 MHz, $CDCl_3$) δ 177.5 (COOH), 91.4 (*C*–OMe), 56.3 (*C*–COOH), 51.6 (OCH_3), 50.6 (3C, CH cubyl), 42.5 (3C, CH cubyl) ppm; **IR** 2988 (w), 2980 (w), 2835 (w), 2848 (w), 2589 (w), 1667 (s), 1424 (m), 1294 (s), 1122 (m), 1010 (m) cm^{-1}; **HRMS** (ESI) m/z for $[C_{10}H_9O_3]^-$ [M–H]$^-$ calcd: 177.0557 found: 177.0561.

5.4.3.19 Synthesis of *tert*–butyl 4–Methoxy–1–cubylcarbamate (3.75)

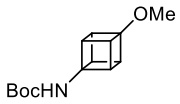

To a 50 mL flask, containing a solution of 4–methoxy–1–cubanecarboxylic acid (**3.76**, 500 mg, 2.81 mmol, 1.0 equiv.) in anhydrous *tert*-BuOH (10 mL) were added Et_3N (1.56 mL, 11.2 mmol, 4.0 equiv.) and diphenylphosphoryl azide (DPPA) (0.890 mL, 4.21 mmol, 1.5 equiv.). The resulting solution was heated under reflux for 14 h, then cooled to rt, and the solvent was removed under reduced pressure. The resulting brown oil was dissolved in EtOAc (25 mL) and washed with brine (3 × 10 mL). The combined organic phase was dried over $MgSO_4$ and concentrated under reduced pressure. Purification by flash column chromatography (8:2 hexane/EtOAc) afforded *tert*–butyl 4–(ethoxy–1–cubylcarbamate (**3.75**, 483 mg, 1.94 mmol, 69%) as a white powder.

Formula $C_{14}H_{19}NO_3$; **MW** 249.31 g.mol^{-1}; **TLC** R_f 0.34 (8:2 hexane /Et_2O); **^{1}H NMR** (400 MHz, $CDCl_3$) δ 5.09 (br s, 1H), 4.03 (br s, 3H), 3.81 (br s, 3H), 3.33 (s, 3H), 1.46 (s, 9H) ppm; **^{13}C NMR** (126 MHz, $CDCl_3$) δ 153.8 (NH*C*OOC$(CH_3)_3$), 92.0 (*C*–OMe), 79.8 (*C*–NHBoc), 67.3 (*C*$(CH_3)_3$), 51.3 (OCH_3), 47.8 (3C, CH cubyl), 45.5 (3C, CH cubyl), 28.3 (3C, C(*CH_3*)$_3$) ppm; **IR** 3288 (m), 2991 (w), 2931 (w), 1675 (s), 1448 (w), 1521 (s), 1277 (s), 1166 (s), 1012 (s), 630 (m) cm^{-1}; **HRMS** (ESI+) m/z for $[C_{14}H_{20}O_3]^+$ $[M+H]^+$ calcd: 250.1438 found: 250.1440.

5.4.3.20 Synthesis of 4–methoxy–1–cubanamine hydrochloride (3.77)

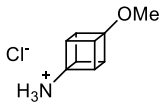

To a solution of *tert*–butyl 4–(methoxy)–1–cubylcarbamate (**23**, 670 mg, 2.69 mmol, 1.00 equiv.) in methanol (20 mL) at 0 °C was added a solution of HCl (6.75 mL of 4 N in 1,4–dioxane, 27.0 mmol, 10.0 equiv.) dropwise. The resulting solution was stirred for 7 h at rt. The solvent was concentrated under reduced pressure and the resulting solid was washed with Et_2O/acetone (4:1, 20 mL) to afford 4–methoxy–1–cubanamine hydrochloride (**3.77**, 456 mg, 2.46 mmol, 91%) as an off–white solid.

Formula $C_9H_{12}NOCl$; **MW** 185.65 g.mol^{-1}; **^{1}H NMR** (400 MHz, D_2O) δ 4.19 (m, 3H), 4.00 (m, 3H), 3.37 (s, 3H) ppm; **^{13}C NMR** (101 MHz, D_2O) δ 91.6 (*C*–OMe), 65.4 (*C*–NH_3Cl), 51.4 (CH_3), 48.1 (3C, CH cubyl), 43.1 (3C, CH cubyl) ppm; **IR** 3487 (w), 2905 (br), 1330 (s), 1318 (w), 1014 (s) cm^{-1}.

5.4.3.21 Synthesis of 4–methoxy–1–cubancarbaldehyde (3.79)

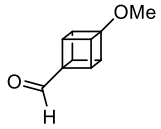

To a solution of 4–methoxy–1–cubylmethanol (**3.73**, 100 mg, 0.610 mmol, 1.0 equiv.) in CH_2Cl_2 (7 mL) was added Dess–Martin periodinane (0.284 g, 0.67 mmol, 1.1 equiv.) portionwise. The solution was stirred for 1 h, diluted with Et_2O (1.5 mL), poured into a saturated solution of $NaHCO_3$ containing sodium thiosulfate (0.611 g, 3.88 mmol, 6.4 equiv.), and stirred vigorously for 10 min. The phases were separated and the organic phase was washed with H_2O (3 × 2 mL), dried over $MgSO_4$ and concentrated under reduced pressure. Purification by flash column chromatography (8:2 pentane/Et_2O) afforded 4–methoxy–1–cubacarbaldehyde (**3.79**, 69 mg, 0.42 mmol, 69%) as a white powder.

Formula $C_{10}H_{10}O_2$; **MW** 162.19 g.mol^{-1}; **TLC** R_f 0.39 (8:2 pentane/Et_2O); **^{1}H NMR** (400 MHz, $CDCl_3$) δ 9.78 (1H, s), 4.20 (m, 3H), 4.13 (m, 3H), 3.35 (s, 3H) ppm; **^{13}C NMR** (126 MHz, $CDCl_3$) δ 198.4 (CHO), 91.4 (*C*–OMe), 63.6 (*C*–CHO), 51.5 (CH_3), 50.7 (3C, CH cubyl), 41.3 (3C, CH cubyl) ppm; **IR** 2995 (w), 2829 (w), 1681 (s), 1455 (m), 1283 (s), 1120 (m), 1013 (s) cm^{-1}; **HRMS** (ESI) m/z for $[C_{10}H_{11}O_2]^+$ $[M+H]^+$ calcd: 163.0754 found: 163.0755.

5.4.3.22 Synthesis of Cubanisindione (3.80)

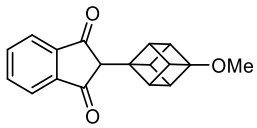

To a solution of 4–methoxy–1–cubancarbaldehyde **3.79** (114.0 mg, 0.703 mmol, 1.0 equiv.) and phthalide (**3.81**, 95 mg, 0.71 mmol, 1.0 equiv.) in EtOAc (2 mL) under N_2 atmosphere, was added a solution of NaOMe in MeOH (0.640 mL of 25 wt%, 2.82 mmol, 4.00 equiv.). The resulting solution was stirred at 40 °C for 3 h, then cooled to rt and concentrated under reduced pressure. The resulting red oil was dissolved in water (10 mL) and the aqueous solution was acidified with HCl (2 N) (pH ≈ 3). The aqueous phase was extracted with $CHCl_3$ (3 × 10 mL), dried over $MgSO_4$, and the solvent was removed under reduced pressure. Purification by flash chromatography (8:2 hexane/EtOAc), and recrystallisation from Et_2O, afforded cubanisindione (**3.80**, 65.0 mg, 0.24 mmol, 33%) as an off–white powder.

Formula $C_{18}H_{14}O_3$; **MW** 278.31 g.mol^{-1}; **TLC** R_f 0.21 (8:2 hexane/EtOAc); **^{1}H NMR** (400 MHz, $CDCl_3$) δ 7.97 (dd, *J* = 5.7, 3.1 Hz, 2H), 7.85 (dd, *J* = 5.6, 3.1 Hz, 2H), 4.10 (m, 3H), 3.84 (m, 3H), 3.31 (s, 3H), 3.29 (s, 1H) ppm; **^{13}C NMR** (101 MHz, $CDCl_3$) δ 198.9 (2C, CO), 142.6 (2C, C_{Ar}), 135.7 (2C, CH_{Ar}), 123.1 (2C, CH_{Ar}), 92.1 (*C*–OMe), 57.5 (*C*CHCO), 55.3 (C*CH*CO), 51.3 (OCH_3),

50.5 (3C, CH cubyl), 41.8 (3C, CH cubyl) ppm; **IR** 2985 (w), 2929 (w), 1706 (s), 1321 (m), 1253 (s) cm^{-1}; **HRMS** (ESI) *m/z* for $[C_{18}H_{14}NaO_3]^+$ $[M+Na]^+$ calcd: 301.0835 found: 301.0840.

5.4.3.23 Synthesis of 4–methoxy–1–cubylmethanol (3.76)

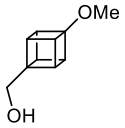

To a 50 mL flame-dried flask, methyl 4–methoxy–1–cubanecarboxylic acid (**3.76**, 500 mg, 2.81 mmol, 1.00 equiv.) was dissolved in anhydrous THF (15 mL) and cooled to 0 °C using an ice–bath. Afterwards, a solution of BH_3•SMe_2 (5 M in Et_2O, 0.6 mL, 3.0 mmol, 1.1 equiv.) was added dropwise and stirred for 2 h at rt. The reaction mixture was quenched carefully with H_2O (2 mL) and diluted with Et_2O (14 mL). The organic phase was washed with H_2O (2 × 14 mL) and brine (14 mL), dried over $MgSO_4$ and concentrated under reduced pressure. Purification was achieved *via* flash column chromatography (6:4 pentane/Et_2O) to afford 4–methyl–1–cubylmethanol (**3.73**, 380 mg, 2.31 mmol, 82%) as a white powder. See above for characterisation data.

5.4.3.24 Synthesis of 1–*tert*–butyl 4–methyl cubanedicarboxylate (5.3.1)

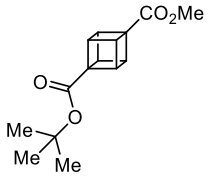

Following a procedure adapted from Ma *et al*.[170] To a solution of 4–methoxycarboxyl–1–cubanecarboxylic acid (**1.7**, 412 mg, 1.99 mmol, 1.0 equiv.) in anhydrous DMF (3 mL) and anhydrous *tert*–butanol (1.9 mL, 20.0 mmol, 10.0 equiv.) were added *N*–(3–dimethylaminopropyl)–*N′*–ethylcarbodiimide (EDC) (575 mg, 2.99 mmol, 1.5 equiv.), 4–dimethylaminopyridine (DMAP) (244 mg. 1.99mmol, 1.00 equiv.) and the mixture was stirred for 20 h at rt. Then, the resulting mixture was diluted with EtOAc (10 mL) and the organic phase was washed with aqueous HCl (4 mL of 1N), saturated $NaHCO_3$ (4 mL), H_2O (5 × 10 mL), dried over $MgSO_4$ and concentrated under reduced pressure to afford 1–*tert*–butyl 4–methyl cubanedicarboxylate (**5.3.1**, 219 mg, 0.835 mmol, 42%) as a white powder. The *tert*–butyl ester **5.3.1** was used in the next step without further purification.

Formula $C_{15}H_{18}O_4$; **MW** 262.31 $g.mol^{-1}$; **^{1}H NMR** (400 MHz, $CDCl_3$) δ 4.23 – 4.14 (m, 6H), 3.72 (s, 3H), 1.47 (s, 9H) ppm; **^{13}C NMR** (101 MHz, $CDCl_3$) δ 172.2 (*C*OOMe), 171.2 (*C*O*t*Bu), 80.4 (O*C*$(CH_3)_3$), 56.9 (*C*–COO*t*Bu), 55.8 (*C*–COOMe), 51.6 (COO*C*H_3), 47.0 (3C, CH cubyl), 46.9 (3C, CH cubyl), 28.1 (3C, OC(*C*H_3)$_3$) ppm; **IR** 2985 (s), 2952 (w), 1707 (s), 1321 (s), 1228 (s), 1086 (s), 862 (m), 731 (w) cm^{-1}; **HRMS** (ESI) *m/z* for $[C_{15}H_{18}NaO_4]^+$ $[M+Na]^+$ calcd: 285.1097 found: 285.1104.

5.4.3.25 Synthesis of methyl 4–hydroxymethyl–1–cubanecarboxylate (5.3.2)

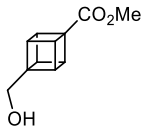

Following a procedure adapted from Burton *et al.*[27] To a 25 mL flame–dried flask, 4–methoxycarboxyl–1–cubanecarboxylic acid (**1.7**, 412 mg, 1.99 mmol, 1.0 equiv.) was dissolved in anhydrous THF (12 mL) and cooled to 0 °C using an ice-water bath. BH_3•SMe_2 solution (0.60 mL of 5 M in Et_2O, 3.0 mmol, 1.5 equiv.) was added dropwise, and the resulting solution was stirred for 2 h at rt. The reaction mixture was quenched by careful addition of H_2O (2 mL) and diluted with Et_2O (12 mL). The organic phase was washed with H_2O (2 × 5 mL), brine (5 mL), dried over $MgSO_4$ and concentrated under reduced pressure. Purification by flash column chromatography (1:1 hexane/EtOAc) afforded methyl 4–hydroxymethyl–1–cubanecarboxylate (**5.3.2**, 336 mg, 1.75 mmol, 88%) as a white powder. Data are consistent with the literature.[27]

Formula $C_{11}H_{12}O_3$; **MW** 192.21 g.mol^{-1}; **TLC** R_f 0.24 (1:1 hexane/EtOAc); **^{1}H NMR** (400 MHz, $CDCl_3$) δ 4.11 – 4.19 (m, 3H), 3.85 – 3.93 (m, 3H), 3.78 (s, 2H), 3.71 (s, 3H), 1.39 (br s, 1H) ppm; **^{13}C NMR** (101 MHz, $CDCl_3$) δ 172.6 (*C*OOMe), 63.3 (CH_2), 58.8 (*C*–CH_2), 56.4 (*C*–COOMe), 51.5 (COO*C*H_3), 46.3 (3C, CH cubyl) 44.4 (3C, CH cubyl) ppm; **IR** 3288 (br), 2984 (w), 2859 (w), 1716 (s), 1440 (s), 1304 (s), 1198 (s), 1091 (s), 1027 (s), 999 (s) cm^{-1}.

5.4.3.26 Synthesis of methyl 4–benzyloxymethyl–1–cubanecarboxylate (5.3.3)

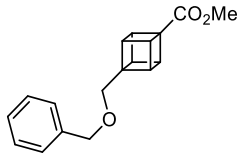

To a solution of methyl 4–hydroxymethyl–1–cubanecarboxylate (**5.3.2**, 300 mg, 1.56 mmol, 1.0 equiv.) in anhydrous THF (5 mL) were added benzyl bromide (0.280 mL, 2.34 mmol, 1.5 equiv.) sodium hydride (125 mg of 60% in mineral oil, 3.12 mmol, 2.0 equiv.). The mixture was stirred for 18 h under argon atmosphere, then carefully quenched with saturated $NaHCO_3$ (2 mL) and diluted with H_2O (5 mL). The organic phase was extracted with Et_2O (3 × 5 mL), dried over $MgSO_4$ and concentrated under reduced pressure. Purification by flash column chromatography (7:3 hexane/EtOAc) afforded methyl 4–benzyloxymethyl–1–cubanecarboxylate (**5.3.3**, 127 mg, 0.45 mmol, 29%) as a white powder.

Formula $C_{18}H_{18}O_3$; **MW** 282.34 g.mol^{-1}; **TLC** R_f 0.38 (7:3 hexane/EtOAc); **^{1}H NMR** (400 MHz, $CDCl_3$) δ 7.28 – 7.39 (m, 5H), 4.56 (s, 2H), 4.15 (m, 3H), 3.89 (m, 3H), 3.71 (s, 3H), 3.60 (s, 2H) ppm; **^{13}C NMR** (101 MHz, $CDCl_3$) δ 172.7 (*C*OOMe), 138.5 (Ar), 128.4 (2C, Ar), 127.6 (2C, Ar) 127.6 (Ar), 73.2 (Ar–*C*H_2), 70.4 (C_{cubyl}–*C*H_2), 57.6 (*C*$_{cubyl}$–CH_2), 56.2 (*C*–COOMe), 51.5 (COO*C*H_3),

46.6 (3C, CH cubyl), 45.2 (3C, CH cubyl) ppm; **IR** 2973 (m), 2854 (m), 1715 (s), 1305 (m), 1207 (s), 1068 (s), 748 (m), 594 (m) cm^{-1}; **HRMS** (ESI) *m*/*z* for $[C_{16}H_{18}NaO_3]^+$ $[M+Na]^+$ calcd: 305.1148 found: 305.1148.

5.4.3.27 Synthesis of methyl 4–((*tert*–butoxycarbonyl)amino)–1–cubanecarboxylate (5.3.4)

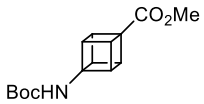

Following a procedure adapted from Nicolaou *et al*.[171] To a solution of 4–methoxycarboxyl–1–cubanecarboxylic acid (**1.7**, 500 mg, 2.42 mmol, 1.0 equiv.) in anhydrous *tert*–BuOH (15 mL) under an argon atmosphere, were added Et_3N (1.34 mL, 9.66 mmol, 4.0 equiv.) and diphenylphosphoryl azide (DPPA, 0.77 mL, 3.6 mmol, 1.5 equiv.). The mixture was heated under reflux for 12 h, then the solvent was removed under reduced pressure and the resulting crude material was disolved in EtOAc (20 mL). The solution was washed with brine (3 × 10 mL), dried over $MgSO_4$ and concentrated under reduced pressure. Purification by flash column chromatography (1:0 to 4:1 hexane/EtOAc) methyl 4–((*tert*–butoxycarbonyl)amino)–1–cubanecarboxylate (**5.3.4**, 322 mg, 1.16 mmol, 48%) as a white powder. Data are consistent with the literature.[171]

Formula $C_{15}H_{19}NO_4$; **MW** 277.32 $g.mol^{-1}$; **^{1}H NMR** (500 MHz, $CDCl_3$) δ 5.09 (br s, 1H), 4.10 (br s, 6H), 3.71 (s, 3H), 1.46 (s, 9H) ppm; **^{13}C NMR** (126 MHz, $CDCl_3$) δ 172.7 (*C*OOMe), 153.9 (NH*C*OOtBu), 79.9 (O*C*$(CH_3)_3$), 66.3 (*C*–NHBoc), 56.0 (*C*–COOMe), 51.5 (COO*C*H_3), 50.2 (3C, CH cubyl), 44.5 (3C, CH cubyl), 28.3 (3C, C(CH_3)$_3$) ppm; **IR** 3395 (s), 2983 (w), 2951 (w), 1724 (s), 1689 (s), 1496 (s), 1313 (s), 1201 (s), 1087 (s) cm^{-1}.

5.4.4 General procedure C for the synthesis of amides

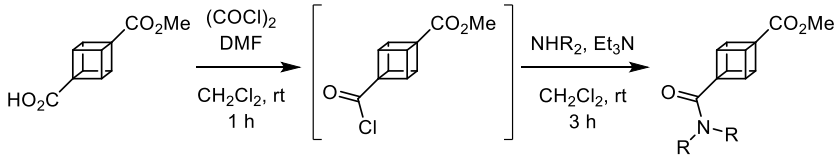

To a 25 mL flame-dried flask, containing a solution of 4–methoxycarbonyl–1–cubanecarboxylic acid (**1.7**, 412 mg, 1.99 mmol, 1.0 equiv.) in anhydrous CH_2Cl_2 (10 mL) were added oxalyl chloride (0.26 mL, 3.0 mmol, 1.5 equiv.) and 2 drops of anhydrous DMF. The solution was stirred for 1 h at rt. Then, the solution was concentrated under reduced pressure and the crude acyl chloride was dissolved in anhydrous CH_2Cl_2 (5 mL) and cooled to 0 °C. A solution of the corresponding amine (1.2 equiv.) and Et_3N (0.33 mL, 2.4 mmol, 1.2 equiv.) in anhydrous CH_2Cl_2 (2 mL) was transferred dropwise to the acyl chloride solution, and the resulting solution was stirred under argon for 3 h. The reaction mixture was quenched carefully with HCl (5 mL of 1N) and the aqueous phase was extracted

with CH_2Cl_2 (3 × 5 mL), dried over $MgSO_4$ and concentrated under reduced pressure. The crude mixture was purified by column chromatography if required or used without further purification.

5.4.4.1 Synthesis of methyl 4–(piperidine–1–carbonyl)–1–cubanecarboxylate (5.3.5)

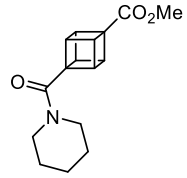

Prepared according to the **general procedure C** with piperidine. The crude material was purified by flash column chromatography (8:2 hexane/EtOAc) to afford methyl 4–(piperidine–1–carbonyl)–1–cubanecarboxylate (**5.3.5**, 476 mg, 1.74 mmol, 87%) as a white solid.

Formula $C_{16}H_{19}NO_3$; **MW** 273.33 g.mol^{-1}; **^{1}H NMR** (400 MHz, $CDCl_3$) δ 4.27 – 4.15 (m, 6H), 3.71 (s, 3H), 3.59 – 3.47 (m, 2H), 3.24 – 3.12 (m, 2H), 1.71 – 1.61 (m, 2H), 1.60 – 1.48 (m, 4H) ppm; **^{13}C NMR** (101 MHz, $CDCl_3$) δ 172.2 (*C*OOMe), 169.1 (CON), 58.3 (*C*–CON), 54.7 (*C*–COOMe), 51.6 (COO*CH*$_3$), 47.0 (3C, CH cubyl), 46.4 (3C, CH cubyl), 45.9 (CH_2), 42.7 (CH_2), 26.7 (CH_2), 25.4 (CH_2), 24.6 (CH_2) ppm; **IR** 2991 (m), 2936 (m), 2853 (m), 1724 (s), 1615 (s), 1435 (s), 1224 (s), 1087 (s), 729 (s) cm^{-1}; **HRMS** (ESI) m/z for $[C_{16}H_{20}NO_3]^+$ $[M+H]^+$ calcd: 274.1438 found: 274.1435; for $[C_{16}H_{19}NNaO_3]^+$ $[M+Na]^+$ calcd: 296.1257 found: 296.1255.

5.4.4.2 Synthesis of methyl 4–(diethylcarbamoyl)–1–cubanecarboxylate (5.3.6)

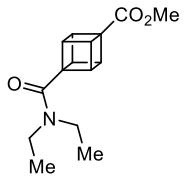

Prepared according to the **general procedure C** with diethylamine. The crude material was purified by flash column chromatography (8:2 hexane/EtOAc) to afford methyl 4–(diethylcarbamoyl)–1–cubanecarboxylate (**5.3.6**, 471 mg, 1.802 mmol, 90%) as a white solid.

Formula $C_{15}H_{19}NO_3$; **MW** 261.32 g.mol^{-1}; **TLC** R_f (8:2 hexane/EtOAc); **^{1}H NMR** (400 MHz, $CDCl_3$) δ 4.23 – 4.20 (m, 6H), 3.71 (s, 3H), 3.35 (q, *J* = 7.1 Hz, 2H), 3.13 (q, *J* = 7.1 Hz, 2H), 1.19 (t, *J* = 7.1 Hz, 3H), 1.12 (t, *J* = 7.1 Hz, 3H) ppm; **^{13}C NMR** (101 MHz, $CDCl_3$) δ 172.2 (*C*OOMe), 170.1 (CON), 58.5 (*C*–CON), 54.8 (C–COOMe), 51.6 (COO*CH*$_3$), 47.2 (3C, CH cubyl), 46.4 (3C, CH cubyl), 40.8 (N*CH*$_2$CH$_3$), 39.2 (N*CH*$_2$CH$_3$), 14.6 (NCH$_2$*CH*$_3$), 12.8 (NCH$_2$*CH*$_3$) ppm; **IR** 2972 (m), 2934 (w), 1716 (s), 1614 (s), 1434 (m), 1323 (s), 1211 (s), 1087 (s), 842 (w), cm^{-1}; **HRMS** (ESI) m/z for $[C_{15}H_{20}NO_3]^+$ $[M+H]^+$ calcd: 262.1438 found: 262.1436; for $[C_{15}H_{19}NNaO_3]^+$ $[M+Na]^+$ calcd: 284.1257 found: 284.1256.

5.4.4.3 Synthesis of methyl 4–(*N*,*N*–diisopropylcarbamoyl)–1–cubanecarboxylate (5.3.7)

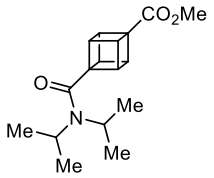

Prepared according to the **general procedure C** with diisopropylamine, but adapted to a larger scale using 4–methoxycarbonyl–1–cubanecarboxylic acid (**1.7**, 500 mg, 2.42 mmol). The crude material was purified by flash column chromatography (8:2 hexane/EtOAc) to afford methyl 4–(*N*,*N*–diisopropylaminocarbonyl)–1–cubanecarboxylate (**5.3.7**, 567 mg, 1.96 mmol, 81%) as a white solid. Data are consistent with the literature.[60]

Formula $C_{17}H_{23}NO_3$; **MW** 289.38 g.mol^{-1}; **TLC** R_f 0.4 (8:2 hexane/EtOAc); **^{1}H NMR** (400 MHz, $CDCl_3$) δ 4.26 – 4.14 (m, 6H), 3.72 (s, 3H), 3.48 (spt, *J* = 6.8 Hz, 1H), 3.32 (spt, *J* = 6.8 Hz, 1H), 1.43 (d, *J* = 6.7 Hz, 6H), 1.22 (d, *J* = 6.6 Hz, 6H) ppm; **^{13}C NMR** (101 MHz, $CDCl_3$) δ 172.2 (*C*OOMe), 170.1 (CON), 59.4 (*C*–CON(*i*Pr)$_2$), 54.7 (*C*–COOMe), 51.6 (COO*CH$_3$*) 48.4 (*CH*(CH_3)$_2$), 47.0 (3C, CH cubyl), 46.2 (3C, CH cubyl), 45.90 (CH), 21.0 (2C, CH(*CH$_3$*)$_2$), 20.5 (2C, CH(*CH$_3$*)$_2$) ppm.

5.4.4.4 Synthesis of methyl 4–(morpholine–4–carbonyl)–1–cubanecarboxylate (5.3.8)

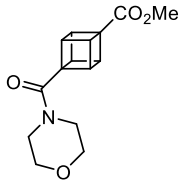

Prepared according to the **general procedure C** with morpholine. No further purification was carried out. Methyl 4–(morpholine–4–carbonyl)–1–cubanecarboxylate (**5.3.8**, 532 mg, 1.93 mmol, 97%) as a white solid.

Formula $C_{15}H_{17}NO_4$; **MW** 275.30 g.mol^{-1}; **^{1}H NMR** (400 MHz, $CDCl_3$) δ 4.26 – 4.18 (m, 6H), 3.71 (s, 3H), 3.69 – 3.64 (m, 4H), 3.62 – 3.57 (m, 2H), 3.28 – 3.22 (m, 2H) ppm; **^{13}C NMR** (101 MHz, $CDCl_3$) δ 171.9 (*C*OOMe), 169.5 (CON), 66.8 (O*CH$_2$*), 66.8 (O*CH$_2$*), 57.8 (*C*–CON), 54.7 (*C*–COOMe), 51.6 (COO*CH$_3$*), 46.9 (3C, CH cubyl), 46.5 (3C, CH cubyl), 45.4 (N*CH$_2$*), 41.9 (N*CH$_2$*) ppm; **IR** 2954 (m), 2851 (m), 1713 (s), 1621 (s), 1424 (s), 1227 (s), 1111 (s), 1027 (s), 849 (s), 588 (s) cm^{-1}; **HRMS** (ESI) m/z for $[C_{15}H_{18}NO_4]^+$ [M+H]$^+$ calcd: 276.1230 found: 276.1225.

5.4.5 General procedure D for the synthesis of cubanecarboxylic acids

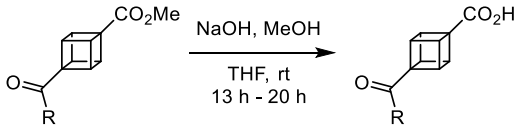

To a solution of the corresponding cubanecarboxylate ester in THF and powdered NaOH (between 1.0 – 30.0 equiv.) was added portionwise. After 12 h, the solvent was evaporated and the obtained solid was dissolved in the minimum amount of water and washed with CH_2Cl_2. The aqueous phase was acidified with concentrated HCl (pH ≈ 1 – 2) and extracted with CH_2Cl_2. The combined organic phase was dried over $MgSO_4$ and concentrated under reduced pressure to afford the cubanecarboxylic acid as a white powder. No further purification was carried out.

5.4.5.1 Synthesis of 4–*tert*–butoxycarbonyl–1–cubanecarboxylic acid (5.3.9)

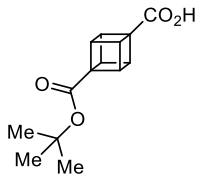

Prepared according to the **general procedure D** from *tert*–butyl 4–methyl–1–cubanedicarboxylate (**5.3.1**, 207 mg, 0.79 mmol, 1.0 equiv.) THF (8 mL) and NaOH (32 mg, 0.79 mmol, 1.0 equiv.). After extraction with CH_2Cl_2, the solution was dried over $MgSO_4$ and concentrated under reduced pressure to afford 4–*tert*–butoxycarbonyl–1–cubanecarboxylic acid (**5.3.9**, 121 mg, 0.49 mmol, 62%) as a white solid.

Formula $C_{14}H_{17}NO_3$; **MW** 247.28 g.mol^{-1}; **^{1}H NMR** (400 MHz, $CDCl_3$) δ 4.25 (m, 3H), 4.20 (m, 3H), 1.47 (s, 9H) ppm; **^{13}C NMR** (101 MHz, $CDCl_3$) δ 177.4 (*C*OOH), 171.1 (*C*OO*t*Bu), 80.6 (O*C*(CH$_3$)$_3$), 56.9 (*C*–COO*t*Bu), 55.5 (*C*–COOH), 47.1 (3C, CH cubyl), 46.8 (3C, CH cubyl), 28.1 (3C, OC(*CH$_3$*)$_3$) ppm; **IR** 2990 (br), 2929 (w), 2607 (w), 1717 (s), 1675 (s), 1321 (s), 1160 (s), 1086 (s), 843 (s) cm^{-1}; **HRMS** (ESI) m/z for $[C_{14}H_{16}O_4]^-$ [M–H]$^-$ calcd: 247.0976 found: 247.0971.

5.4.5.2 Synthesis of 4–hydroxymethyl–1–cubanecarboxylic acid (5.3.10)

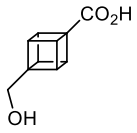

Prepared according to the **general procedure D** from methyl 4–hydroxymethyl–1–cubanecarboxylate (**5.3.2**, 200 mg, 1.04 mmol, 1.0 equiv.), THF (10 mL) and NaOH (416 mg, 10.4 mmol, 10.0 equiv.). Extraction with EtOAc, drying over $MgSO_4$ and concentration under reduced

pressure, afforded 4–hydroxymethyl–1–cubanecarboxylic acid (**5.3.10**, 110 mg, 0.62 mmol, 62%) as a white solid.

Formula $C_{10}H_{10}O_3$; **MW** 178.19 g.mol^{-1}; **^{1}H NMR** (400 MHz, CD_3OD) δ 4.09 (m, 3H), 3.86 (m, 3H), 3.67 (s, 2H) ppm; **^{13}C NMR** (101 MHz, CD_3OD) δ 176.4 (COOH), 63.6 (CH_2), 60.6 (*C*–CH_2), 58.3 (*C*–COOH), 47.6 (3C, CH cubyl), 45.8 (3C, CH cubyl) ppm; **IR** 3247 (br), 2991 (br), 2860 (w), 1655 (s), 1375 (s), 994 (s), 703 (w) cm^{-1}.

5.4.5.3 Synthesis of 4–benzyloxymethyl–1–cubanecarboxylic acid (5.3.11)

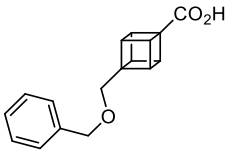

Prepared according to the **general procedure D** using methyl 4–benzyloxymethyl–1–cubanecarboxylate **(5.3.3**, 114 mg, 0.40 mmol, 1.0 equiv.) THF (10 mL) and NaOH (488 mg, 12.2 mmol, 30.0 equiv.). Extraction with CH_2Cl_2, drying over $MgSO_4$ and concentration under reduced pressure afforded 4–benzyloxymethyl–1–cubanecarboxylic acid (**5.3.11**, 101 mg, 0.38 mmol, 95%) as a white solid.

Formula $C_{17}H_{16}O_3$; **MW** 268.31 g.mol^{-1}; **^{1}H NMR** (400 MHz, $CDCl_3$) δ 7.39 – 7.27 (m, 5H), 4.57 (s, 2H), 4.19 (m, 3H), 3.90 (m, 3H), 3.61 (s, 2H) ppm; **^{13}C NMR** (101 MHz, $CDCl_3$) δ 177.7 (COOH), 138.5 (*Ar*–CH_2), 128.4 (2C, Ar), 127.6 (3C, Ar), 73.2 (Ar–*CH_2*), 70.2 (C_{cubyl}–*CH_2*), 57.6 (*C_{cubyl}*–CH_2), 55.9 (*C*–$COOCH_3$), 46.6 (3C, CH cubyl), 45.2 (3C, CH cubyl) ppm; **IR** 2987 (br), 2852 (br), 1681 (s), 1307 (m), 1205 (m), 1069 (s), 697 (s) cm^{-1}; **HRMS** (ESI) m/z for $[C_{17}H_{15}O_3]^-$ $[M–H]^-$ calcd: 267.1027 found: 267.1018.

5.4.5.4 Synthesis of 4–((*tert*–butoxycarbonyl)amino)–1–cubanecarboxylic acid (5.3.12)

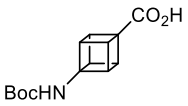

Prepared according to the **general procedure D** using methyl 4–((*tert*–butoxycarbonyl)amino)–1–cubanecarboxylate **(5.3.4**, 289 mg, 1.04 mmol, 1.0 equiv.) THF (10 mL) and NaOH (416 mg, 10.4 mmol, 10 equiv.). Extraction with CH_2Cl_2, drying over $MgSO_4$ and concentration under reduced pressure afforded 4–((*tert*–butoxycarbonyl)amino)–1–cubanecarboxylic acid (**5.3.12**, 230 mg, 0.87 mmol, 84%) as a white solid.

Formula $C_{14}H_{17}NO_4$; **MW** 263.29 g.mol^{-1}; **^{1}H NMR** (500 MHz, CD_3OD) δ 4.03 (br s, 6H), 1.45 (s, 9H) ppm; **^{13}C NMR** (126 MHz, CD_3OD) δ 176.4 (COOH), 156.7 (NH*C*O*O*tBu), 80.9 (*C*–NHBoc), 67.9 (O*C*$(CH_3)_3$), 57.9 (*C*–COOH), 51.2 (3C, CH cubyl), 45.9 (3C, CH cubyl), 28.8 (3C, C(*CH_3*)$_3$)

ppm; **IR** 2978 (m), 2936 (br), 2859 (m), 1608 (s), 1441 (s), 1290 (s), 1025 (s), 841 (m), 568 (m) cm^{-1}; **HRMS** (ESI) m/z for $[C_{14}H_{16}NO_4]^-$ $[M–H]^-$ calcd: 262.1085 found: 262.1078.

5.4.5.5 Synthesis of 4–(piperidine–1–carbonyl)–1–cubanecarboxylic acid (5.3.13)

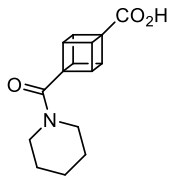

Prepared according to the **general procedure D** using methyl 4–(piperidine–1-carbonyl)–1–cubanecarboxylate (**5.3.5** ,407 mg, 1.49 mmol, 1.0 equiv.) THF (10 mL) and NaOH (600 g, 15.0 mmol, 10.0 equiv.). Extraction with CH_2Cl_2, drying over $MgSO_4$ and concentration under reduced pressure afforded 4–(piperidine–1–carbonyl)–1–cubanecarboxylic acid (**5.3.13**, 346 mg, 1.33 mmol, 89%) as a white solid.

Formula $C_{15}H_{17}NO_3$; **MW** 259.31 $g.mol^{-1}$; **^{1}H NMR** (400 MHz, $CDCl_3$) δ 4.31 – 4.18 (m, 6H) 3.60 – 3.48 (m, 2H) 3.24 – 3.13 (m, 2H) 1.72 – 1.62 (m, 2H) 1.62 – 1.50 (m, 4H) ppm; **^{13}C NMR** (101 MHz, $CDCl_3$) δ 176.6 (COOH), 169.3 (CON), 58.2 (*C*–CON), 54.5 (*C*–COOH), 47.1 (3C, CH cubyl), 46.5 (3C, CH cubyl), 46.0 (NCH_2), 42.9 (NCH_2), 26.7 (CH_2), 25.4 (CH_2), 24.6 (CH_2) ppm; **IR** 2933 (w), 2851 (w), 1704 (s), 1568 (s), 1470 (m), 1290 (m), 1200 (s), 855 (m) cm^{-1}; **HRMS** (ESI) m/z for $[C_{15}H_{18}NO_3]^+$ $[M+H]^+$ calcd: 260.1281 found: 260.1275.

5.4.5.6 Synthesis of 4–(*N*,*N*–diethylcarbamoyl)–1–cubanecarboxylic acid (5.3.14)

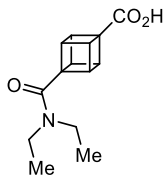

Prepared according to the **general procedure D** using methyl 4–(*N*,*N*–diethylcarbamoyl)–1–cubanecarboxylate (**5.3.6**, 385 mg, 1.47 mmol, 1.0 equiv.) THF (10 mL) and NaOH (600 mg, 15.0 mmol, 10.0 equiv.). Extraction with CH_2Cl_2, drying over $MgSO_4$ and concentration under reduced pressure afforded 4–(*N*,*N*–diethylcarbamoyl)–1–cubanecarboxylic acid (**5.3.14**, 346 mg, 1.40 mmol, 95%) as a white solid.

Formula $C_{14}H_{17}NO_3$; **MW** 247.29 $g.mol^{-1}$; **^{1}H NMR** (400 MHz, $CDCl_3$) δ 4.25 (6H, br s), 3.37 (2H, q, *J* = 6.5 Hz), 3.15 (2H, q, *J* = 7.0 Hz), 1.21 (3H, t, *J* = 6.8 Hz), 1.13 (3H, t, *J* = 6.8 Hz) ppm; **^{13}C NMR** (101 MHz, $CDCl_3$) δ 176.6 (COOH), 170.4 (CON), 58.5 (*C*–$CONEt_2$), 54.7 (*C*–COOH), 47.3 (3C, CH cubyl), 46.4 (3C, CH cubyl), 40.9 (NCH_2CH_3), 39.3 (NCH_2CH_3), 14.6 (NCH_2CH_3), 12.8 (NCH_2CH_3) ppm; **IR** 2987 (br), 2944 (w), 1714 (s), 1591 (s), 1196 (m), 1080 (m), 846 (m), 700 (s), 660 (w) cm^{-1}; **HRMS** (ESI) *m/z* 246.9 for $[C_{15}H_{16}NO_3]^-$ $[M–H]^-$ calcd: 246.1136 found: 246.1131.

5.4.5.7 Synthesis of 4–(*N*,*N*–diisopropylcarbamoyl)–1–cubanecarboxylic acid (5.3.15)

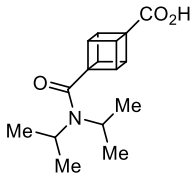

Prepared according to the **general procedure D** using methyl 4–(*N*,*N*–diisopropylcarbamoyl)–1–cubanecarboxylate (**5.3.7**, 340 mg, 1.17 mmol, 1.0 equiv.), THF (10 mL) and NaOH (1.44 g, 36.0 mmol, 30.0 equiv.). Extraction with CH_2Cl_2, drying over $MgSO_4$ and concentration under reduced pressure afforded 4–(*N*,*N*–diisopropylcarbamoyl)–1–cubanecarboxylic acid (**5.3.15**, 320 mg, 1.16 mmol, 97%) as a white solid.

Formula $C_{16}H_{21}NO_3$; **MW** 275.35 g.mol^{-1}; **^{1}H NMR** (400 MHz, $CDCl_3$) δ 4.27 – 4.15 (m, 6H), 3.48 (1H, spt, *J* = 6.7 Hz), 3.32 (1H, spt, *J* = 6.7 Hz), 1.43 (6H, d, *J* = 6.7 Hz), 1.22 (6H, d, *J* = 6.7 Hz) ppm; **^{13}C NMR** (101 MHz, $CDCl_3$) δ 176.7 (COOH), 170.2 (CON), 59.4 (*C*–CON(*i*Pr)$_2$), 54.6 (*C*–COOH), 48.5 (*CH*$(CH_3)_2$), 47.0 (3C, CH cubyl), 46.3 (3C, CH cubyl), 46.0 (*CH*$(CH_3)_2$), 21.0 (2C, CH(*CH*$_3$)$_2$), 20.5 (2C, CH(*CH*$_3$)$_2$) ppm; **IR** 2971 (br), 2931 (w), 1712 (s), 1578 (s), 1445 (m), 1213 (s), 1036 (m), 729 (s) cm^{-1}; **HRMS** (ESI) m/z for $[C_{16}H_{22}NO_3]^+$ $[M+H]^+$ calcd: 276.1594 found: 276.1593.

5.4.5.8 Synthesis of 4–(morpholine–4–carbonyl)–1–cubanecarboxylic acid (5.3.16)

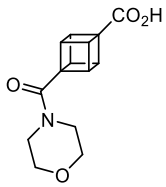

Prepared according to the **general procedure D** using methyl 4–(morpholine–4–carbonyl)–1–cubanecarboxylate (**5.3.8**, 350 mg, 1.27 mmol, 1.0 equiv.), THF (12 mL) and NaOH (520 mg, 13.0 mmol, 10.0 equiv.). Extraction with EtOAc, drying over $MgSO_4$ and concentration under reduced pressure afforded 4–(morpholine–4–carbonyl)–1–cubanecarboxylic acid (**5.3.16**, 230 mg, 0.88 mmol, 69%) as a white solid.

Formula $C_{14}H_{15}NO_4$; **MW** 261.28 g.mol^{-1}; **^{1}H NMR** (400 MHz, $CDCl_3$) δ 4.34 – 4.16 (m, 6H), 3.73 – 3.66 (m, 4H), 3.65 – 3.55 (m, 2H), 3.31 – 3.19 ppm (m, 2H) ppm; **^{13}C NMR** (101 MHz, $CDCl_3$) δ 175.9 (COOH), 169.5 (CON) 66.9 (OCH_2), 66.8 (OCH_2), 57.9 (*C*–CON, 54.4 (*C*–COOH), 47.0 (3C, CH cubyl), 46.5 (3C, CH cubyl), 45.4 (NCH_2), 42.0 (NCH_2) ppm; **IR** 3144 (w), 2995 (m), 2918 (m), 1712 (s), 1626 (s), 1428 (s), 1104 (m), 846 (m) cm^{-1}; **HRMS** (ESI) m/z for $[C_{14}H_{14}NO_4]^-$ $[M–H]^-$ calcd: 260.0928 found 260.0922.

5.5 Chapter 4: Synthesis of 1,2,4–Tricarbonylated Cubanes

5.5.1 Synthetic procedures

5.5.2 General procedure

To a 25 mL round–bottom flask, containing a solution of dimethyl 1,4–cubanedicarboxylate **1.35** (132.13 mg, 0.6 mmol, 1.0 equiv.) in anhydrous dichloromethane (5.0 mL) were added oxalyl chloride (1.05 mL, 12.0 mmol, 20.0 equiv.). The resulting solution was pumped through the microflow photoreactor (internal volume = 2 mL) with a flow rate of 3 mL.min^{-1} and irradiated for 4h30. During the reaction time, the solution was cooled down with an ice–bath. Afterwards, the pumped solution was switched for anhydrous dichloromethane and 2 mL was pumped through the reactor and collected in the same flask as the product. The obtained solution was concentrated under reduced pressure to remove the excess of oxalyl chloride. The corresponding acyl chloride was dissolved in anhydrous CH_2Cl_2 (2 mL) (or others and the corresponding nucleophilic solvent), cooled down to 0 ˚C, Et_3N anhydrous (0.42 mL, 3.0 mmol, 5.0 equiv.) and the corresponding nucleophile was added. The resulting solution was stirred at room temperature for the indicated time. Afterwards, the reaction mixture was quenched with saturated NH_4Cl solution (10 mL) or H_2O (10 mL), the aqueous phase was extracted with CH_2Cl_2 (3 × 5 mL), dried over $MgSO_4$ and concentrated under reduced pressure. The crude reaction mixture was purified by column chromatography accordingly.

Note: 90 – 93 % conversion is achieved during the reaction, 7 – 10 % of dimethyl 1,4–cubanedicarboxylate **1.35** can be recovered.

5.5.3 Pictures of the setup and experimental details

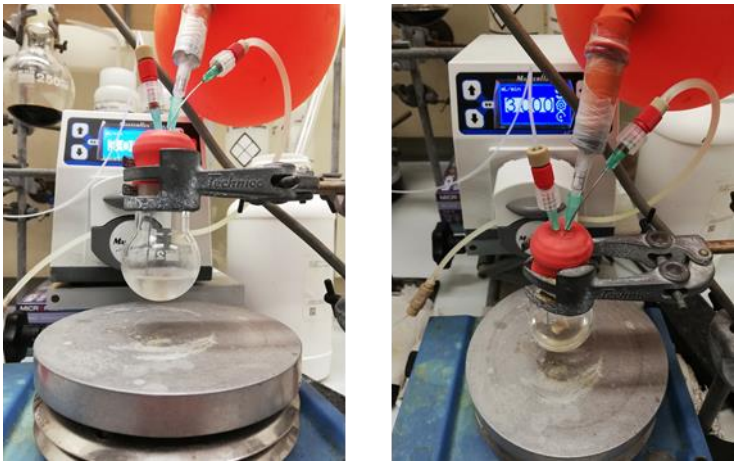

Figure S5. Pictures of the prepared solution before reaction.

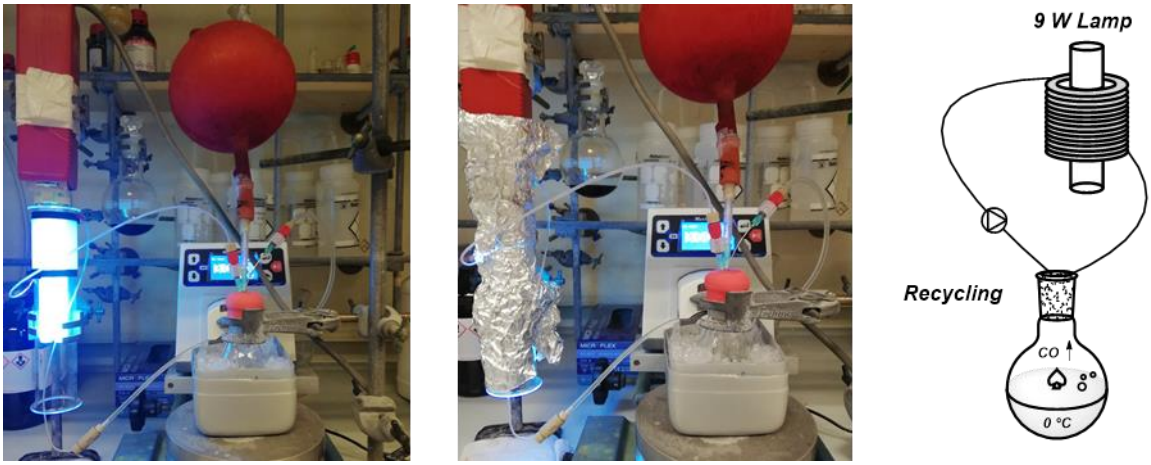

Figure S6. (*Left*) Picture of the recycling photochemical reactor. (*Middle*) Picture of the setup during the reaction. (*Right*) Schematic representation of the setup.

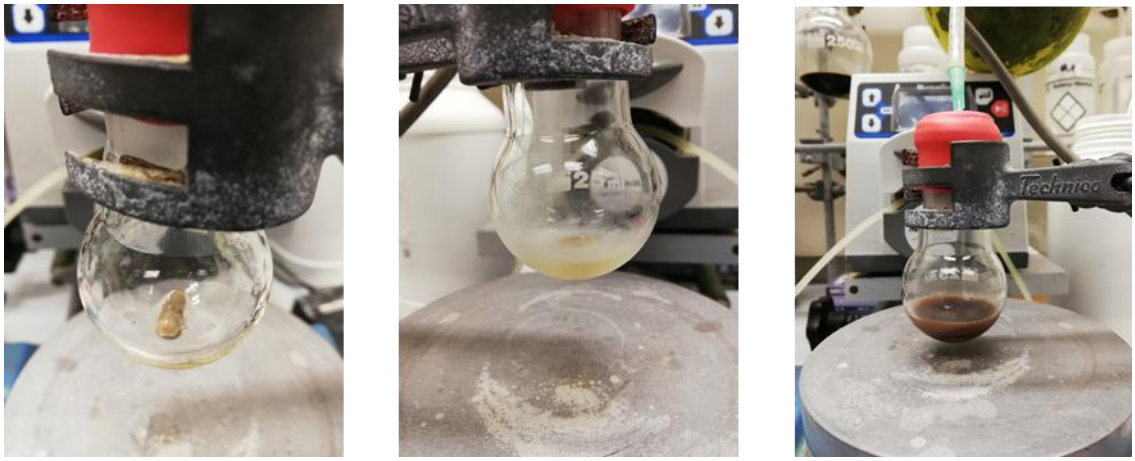

Figure S7. (*Left*) Obtained crude residue after concentrated under reduced pressure. (*Middle*) Residue dissolved in CH_2Cl_2 anhydrous and cooled down to 0 ˚C. (*Right*) After addition of Et_3N.

5.5.4 Trimethyl 1,2,4–cubanetricarboxylate (4.12)

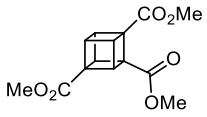

Prepared according to the **general procedure**. The obtained crude residue was dissolved in anhydrous methanol (2 mL). The resulting yellow mixture was stirred for 4 h at room temperature. Methanol was removed under reduced pressure and the crude reaction mixture dissolved in CH_2Cl_2 (5 mL), washed with H_2O (2 mL), dried over $MgSO_4$ and concentrated under reduced pressure. Purification by flash column chromatography (8:2 hexane/EtOAc) afforded trimethyl 1,2,4–cubanetricarboxylate (**4.12**, 92 mg, 0.33 mmol, 55%) as a white solid.

Formula $C_{14}H_{14}O_6$; **MW** 278.26 g.mol^{-1}; **TLC** R_f 0.14 (8:2 hexane/EtOAc); **mp** 80 – 82 ˚C ($CHCl_3$/MeOH); **^{1}H NMR** (400 MHz, $CDCl_3$) δ 4.52 – 4.41 (m, 2H), 4.27 – 4.22 (m, 2H), 4.22 – 4.17 (m, 1H), 3.73 (s, 3H), 3.72 (s, 3H), 3.72 (s, 3H) ppm; **^{13}C{^{1}H} NMR** (101 MHz, $CDCl_3$) δ 170.8 (*C*OOMe), 169.6 (*C*OOMe), 169.2 (*C*OOMe), 57.9 (C cubyl), 55.3 (*C* cubyl), 53.5 (*C* cubyl), 51.9 (COO*CH*$_3$), 51.9 (COO*CH*$_3$), 51.8 (COO*CH*$_3$), 49.2 (2C, CH cubyl), 47.5 (1C, CH cubyl), 45.2 (2C, CH cubyl) ppm; **IR** 3006 (w), 2955 (w), 1709 (s), 1446 (s), 1322 (s), 1214 (s), 1092 (m) cm^{-1}; **HRMS** (ESI) m/z for $C_{14}H_{14}NaO_6$ $[M+Na]^+$ calcd.: 301.0683 found: 301.0685.

5.5.5 2,4–Dimethoxycarbonyl 1–cubanecarboxylic acid (4.13)

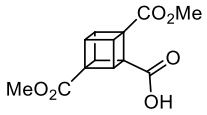

Prepared according to the **general procedure**. The obtained crude residue was dissolved in CH_2Cl_2 (2 mL) and H_2O (0.5 mL). The resulting mixture was stirred for 2 h. The resulting crude mixture was separated and the aqueous layer was extracted with chloroform. The combined organic layers were extracted with $NaHCO_3$ (5% w/v, 3 × 20 mL). The combined aqueous layers were brought to pH ≈ 1 with concentrated HCl, extracted with chloroform, dried over $MgSO_4$ and concentrated under reduced pressure to afford the crude 2,4–dimethoxycarbonyl 1–cubanecarboxylic acid (**4.13**, 89 mg, 0.34 mmol, 56 %).

Formula $C_{13}H_{12}O_6$; **MW** 264.23 g.mol^{-1}; **^{1}H NMR** (400 MHz, $CDCl_3$) δ 4.55 – 4.48 (m, 2H), 4.30 – 4.29 (m, 1H), 4.30 – 4.25 (m, 2H), 4.25 – 4.19 (m, 1H), 3.76 (s, 3H), 3.74 (s, 3H) ppm; **^{13}C{^{1}H} NMR** (101 MHz, $CDCl_3$) δ 173.2 (*C*OOH), 170.7 (*C*OOMe), 170.4 (*C*OOMe), 57.9 (C cubyl), 54.9 (C cubyl), 53.6 (C cubyl), 52.2 (COO*CH*$_3$), 51.9 (COO*CH*$_3$), 49.4 (2C, CH cubyl), 47.6 (1C, CH cubyl), 45.4 (2C, CH cubyl) ppm; **IR** 3514 (br w), 3005 (w), 2954 (w), 1715 (br s), 1436 (s), 1325 (s), 1215 (s), 1092 (m) cm^{-1}; **HRMS** (ESI) m/z for $C_{13}H_{12}NaO_6$ $[M+Na]^+$ calcd.: 287.0526 found: 287.0533.

5.5.6 Dimethyl 2–((1R,2S,5R)–2–isopropyl–5–methylcyclohexyl)–1,4–cubanetricarboxylate (4.14)

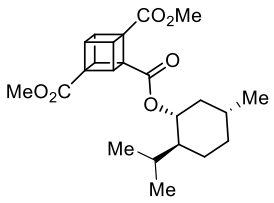

Prepared according to the **general procedure**. The obtained crude residue was dissolved in toluene (3 mL) and Et_3N (0.42 mL, 3.0 mmol, 5.0 equiv.), (–)menthol (112.5 mg, 0.9 mmol, 1.2 equiv.) were added at 0 ˚C. The resulting brown solution was stirred at 100 ˚C for 3 h, followed by overnight at 50 ˚C. The reaction mixture was quenched with saturated NH_4Cl solution (10 mL), the aqueous phase was extracted with CH_2Cl_2 (3 × 5 mL), dried over $MgSO_4$ and concentrated under reduced pressure. Purification by flash column chromatography (8:2 hexane/EtOAc) afforded dimethyl 2–((1R,2S,5R)–2–isopropyl–5–methylcyclohexyl)–1,4–cubanetricarboxylate (**4.14**, 71 mg, 0.18 mmol, 30 %) as a yellow oil.

Formula $C_{23}H_{30}O_6$; **MW** 402.49 g.mol^{-1}; **TLC** R_f 0.27 (8:2 hexane/EtOAc); **^{1}H NMR** (400 MHz, $CDCl_3$) δ 4.76 – 4.66 (m, 1H), 4.43 (m, 2H), 4.27 – 4.20 (m, 2H), 4.20 – 4.14 (m, 1H), 3.72 (s, 3H), 3.70 (s, 3H), 1.93 – 2.03 (m, 1H), 1.82 (dtd, *J* = 13.9, 7.0, 2.7 Hz, 1H), 1.73 – 1.63 (m, 2H), 1.56 – 1.43 (m, 1H), 1.42 – 1.31 (m, 1H), 1.13 – 0.92 (m, 2H), 0.89 (dd, *J* = 6.7, 3.9 Hz, 7H), 0.76 (d, *J* = 7.0 Hz, 3H) ppm; **^{13}C{^{1}H} NMR** (101 MHz, $CDCl_3$) δ 170.9, 169.6, 168.3, 74.7 (O*CH*), 57.9 (C cubyl), 55.6 (C cubyl), 53.5 (C cubyl), 51.8 (COO*CH$_3$*), 51.7 (COO*CH$_3$*), 49.1 (1C, CH cubyl), 49.0 (1C, CH cubyl), 47.6 (CH), 46.7 (CH), 45.1 (1C, CH cubyl), 44.9 (1C, CH cubyl), 40.8 (CH_2), 34.1 (CH_2), 31.3 (CH), 26.0 (CH), 23.4 (CH_2), 22.0 (CH_3), 20.8 (CH_3), 16.3 (CH_3) ppm; **IR** 3003 (w), 2952 (m), 2870 (w), 1717 (s), 13252 (s), 1212 (s), 1090 (s) cm^{-1}; **HRMS** (ESI) m/z for $C_{23}H_{30}NaO_6$ $[M+Na]^+$ calcd.: 425.1935 found: 425.1942.

5.5.7 Dimethyl 2–((methyl 3α–hydroxy–5β–cholan–24-oate)carbonyl)–1,4–cubanedicarboxylate (4.15)

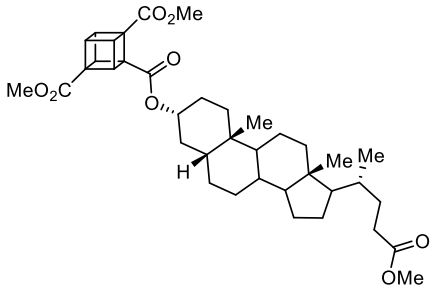

Prepared according to the **general procedure**. The obtained crude residue was dissolved in toluene (3 mL) and Et_3N (0.42 mL, 3.0 mmol, 5.0 equiv.), Methyl 3α–hydroxy–5β–cholan–24–oate (234 mg,

0.6 mmol, 1.0 equiv.) were added added at 0 ˚C. The resulting brown solution was stirred at 100 ˚C for 4 h, followed by overnight at 50 ˚C. The reaction mixture was quenched with saturated NH_4Cl solution (10 mL), the aqueous phase was extracted with CH_2Cl_2 (3 × 5 mL), dried over $MgSO_4$ and concentrated under reduced pressure. Purification by flash column chromatography (8:2 hexane/EtOAc) afforded dimethyl 2–((methyl 3α–hydroxy–5β–cholan–24-oate)carbonyl)–1,4–cubanedicarboxylate (**4.15**, 138 mg, 0.22 mmol, 37 %) as a white solid foam.

Formula $C_{38}H_{52}O_8$; **MW** 636.83 g.mol^{-1}; **TLC** R_f 0.16 (8:2 hexane/EtOAc); **^{1}H NMR** (400 MHz, $CDCl_3$) δ 4.77 (tt, *J* = 11.3, 4.7 Hz, H–3β, 1H), 4.48 – 4.43 (m, 2H), 4.28 – 4.22 (m, 2H), 4.22 – 4.17 (m, 1H), 3.73 (s, 3H), 3.72 (s, 3H), 3.67 (s, 3H), 2.36 (ddd, *J* = 15.4, 10.3, 5.3 Hz, H–23, 1H), 2.22 (ddd, *J* = 16.0, 9.8, 6.6 Hz, H–23', 1H), 0.93 (s, H–19, 3H), 0.92 (d, *J* = 6.4 Hz, H–21, 3H), 0.65 (s, H–18, 3H) ppm; **^{13}C{^{1}H} NMR** δ (101 MHz, $CDCl_3$) δ 174.8 (C–24), 171.0 (*C*OOMe), 169.7 (*C*OOMe), 168.4 (*C*OOMe), 74.8 (C–3), 57.9 (1C, C cubyl), 56.5 (CH), 56.0 (CH), 55.5 (1C, C cubyl), 53.4 (1C, C cubyl), 51.8 (COO*CH*$_3$), 51.7 (COO*CH*$_3$), 51.5 (COO*CH*$_3$), 49.1 (2C, CH cubyl), 47.6 (1C, CH cubyl), 45.1 (2C, CH cubyl), 42.7 (C–13), 41.9 (CH), 40.4 (CH), 40.1 (CH_2), 35.8 (CH), 35.4 (CH), 35.0 (CH_2), 34.6 (C–10), 32.2 (CH_2), 31.1 (C–23), 31.0 (C–22), 28.2 (CH_2), 27.0 (CH_2), 26.6 (CH_2), 26.3 (CH_2), 24.2 (CH_2), 23.3 (C–19), 20.8 (CH_2), 18.3 (C–21), 12.0 (C–18) ppm; **IR** 2936 (m), 2865 (w), 1726 (br s), 1207 (s), 1166 (m) 1090 (m) cm^{-1}; **HRMS** (ESI) m/z for $C_{38}H_{52}NaO_8$ $[M+Na]^+$ calcd.: 659.3554 found: 659.3556.

5.5.8 Dimethyl 2–(*N*–hydroxyphthalamide)–1,4–cubanedicarboxylate (4.16)

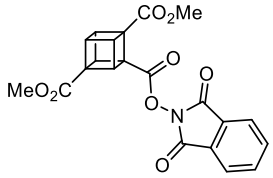

Prepared according to the **general procedure**. The obtained crude residue was dissolved in CH_2Cl_2 anhydrous (2 mL) and Et_3N (0.42 mL, 3.0 mmol, 5.0 equiv.), A solution of *N*–hydroxyphthalamide (147 mg, 0.9 mmol, 1.5 equiv.), Et_3N (0.9 mmol, 1.0 equiv.) in CH_2Cl_2 anhydrous (1 mL) were added at 0 ˚C. The resulting brown solution was stirred for 16 h at room temperature. The reaction mixture was quenched with saturated NH_4Cl solution (10 mL), the aqueous phase was extracted with CH_2Cl_2 (3 × 5 mL), dried over $MgSO_4$ and concentrated under reduced pressure. Purification by flash column chromatography (6:4 hexane/acetone) afforded dimethyl 2–(*N*–hydroxyphthalamide)–1,4–cubanedicarboxylate (**4.16**, 59 mg, 0.23 mmol, 24%) as an off–white foam.

Note: The redox–active ester decomposes on silica during column chromatography which explains the low yield obtained.

Formula $C_{21}H_{15}NO_8$; **MW** 409.35 g.mol^{-1}; **TLC** R_f 0.13 (6:4 hexane/acetone); **^{1}H NMR** (400 MHz, $CDCl_3$) δ 7.89 (dd, *J* = 5.6, 3.0 Hz, 2H), 7.82 – 7.78 (dd, *J* = 5.6, 3.0 Hz, 2H), 4.72 – 4.69 (m, 2H), 4.37 (t, *J* = 4.9 Hz, 2H), 4.25 (tt, *J* = 5.0, 2.4 Hz, 1H), 3.84 (s, 3H), 3.77 (s, 3H) ppm; **^{13}C{^{1}H} NMR** δ (101 MHz, $CDCl_3$) δ 170.2 (CO), 168.7 (CO), 164.5 (CO), 161.5 (2C, CON), 134.7 (2C, CH_{Ar}), 128.9 (2C, C_{Ar}), 123.9 (2C, CH_{Ar}), 58.6 (C cubyl), 54.2 (C cubyl), 52.8 (C cubyl), 52.3 (COO*CH*$_3$), 52.0 (COO*CH*$_3$), 49.4 (2C, CH cubyl), 47.6 (1C, CH cubyl), 45.6 (2C, CH cubyl) ppm; **IR** 3009 (w), 2954 (m), 1780 (w), 1744 (w), 1330 (m), 1218 (m) cm^{-1}; **HRMS** No HRMS could be obtained due to instability of the material under ESI and CI tested conditions.[46]

5.5.9 Dimethyl (2–(cyclohexylthio)carbonyl)–1,4–cubanetricarboxylate (4.17)

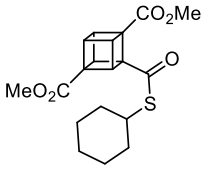

Prepared according to the **general procedure**. The obtained crude residue was dissolved in CH_2Cl_2 (2 mL) and Et_3N (0.42 mL, 3.0 mmol, 5.0 equiv.), cyclohexanethiol (0.15 mL, 1.2 mmol, 2.0 equiv.) were added at 0 °C. The resulting brown solution was stirred for 16 h. The reaction mixture was quenched with saturated NH_4Cl solution (10 mL), the aqueous phase was extracted with CH_2Cl_2 (3 × 5 mL), dried over $MgSO_4$ and concentrated under reduced pressure. Purification by flash column chromatography (8:2 hexane/EtOAc) afforded dimethyl 2–((cyclohexylthio)carbonyl)–1,4–cubanetricarboxylate (**4.17**, 95 mg, 0.26 mmol, 43%) as an off–white solid.

Formula $C_{19}H_{22}O_5S$; **MW** 362.44 g.mol^{-1}; **TLC** R_f 0.50 (6:4 Hexane/EtOAc); **^{1}H NMR** (400 MHz, $CDCl_3$) δ 4.55 – 4.47 (m, 2H), 4.25 – 4.21 (m, 2H), 4.21 – 4.17 (m, 1H), 3.74 (s, 3H), 3.72 (s, 3H), 3.63 – 3.54 (m, 1H), 1.76 – 1.65 (m, 2H), 1.63 – 1.53 (m, 1H), 1.50 – 1.37 (m, 4H), 1.35 – 1.21 (m, 2H) ppm; **^{13}C{^{1}H} NMR** (101 MHz, $CDCl_3$) δ 194.4 (*C*OS), 170.7 (*C*OOMe), 169.3 (*C*OOMe), 61.8 (C cubyl), 59.5 (C cubyl), 53.4 (C cubyl), 51.9 (COO*CH*$_3$), 51.8 (COO*CH*$_3$), 50.5 (2C, CH cubyl), 47.6 (1C, CH cubyl), 44.8 (2C, CH cubyl), 42.1 (*CH*S), 33.0 (3C, CH_2), 25.9 (1C, CH_2), 25.5 (1C, CH_2) ppm; **IR** 3001 (w), 2930 (m), 2853 (w), 1524 (s), 1435 (m), 1213 (s), 1090 (m) cm^{-1}; **HRMS** (ESI) m/z for $C_{19}H_{22}NaO_5S$ $[M+Na]^+$ calcd.: 385.1080 found: 385.1084.

5.5.10 Dimethyl 2–carbamoyl–1,4–cubanedicarboxylate (4.18)

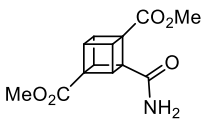

Prepared according to the **general procedure**. The obtained crude residue was dissolved in CH_2Cl_2 (2 mL) and Et_3N (0.42 mL, 3.0 mmol, 5.0 equiv.), NH_4OH solution (30 μL, 0.6 mmol, 1.0 equiv.,

35%) were added at 0 °C. The resulting brown solution was stirred for 2 h. The reaction mixture was quenched with saturated NH_4Cl solution (10 mL), the aqueous phase was extracted with CH_2Cl_2 (3 × 5 mL), dried over $MgSO_4$ and concentrated under reduced pressure. Purification by flash column chromatography (6:4 to 0:10 hexane/acetone) afforded dimethyl 2–carbamoyl–1,4–cubanedicarboxylate (**4.18**, 35 mg, 0.13 mmol, 22%) as a white solid.

Formula $C_{13}H_{13}NO_5$; **MW** 263.25 g.mol^{-1}; **TLC** R_f 0.16 (6:4 hexane/acetone); **^{1}H NMR** (400 MHz, $CDCl_3$) δ 7.08 (br s, 1H), 5.92 (br s, 1H), 4.47 – 4.42 (m, 2H), 4.25 – 4.18 (m, 3H), 3.75 (s, 3H), 3.71 (s, 3H) ppm; **^{13}C{^{1}H} NMR** (101 MHz, $CDCl_3$) δ 171.3 (COOMe), 171.2 (CONH2) 170.8 (COOMe) , 58.1 (C cubyl), 56.6 (C cubyl), 53.4 (C cubyl), 52.1 (COOCH3), 51.8 (COOCH3),, 49.6 (2C, CH cubyl), 47.6 (1C, CH cubyl), 45.2 (2C, CH cubyl) ppm; **IR** 3008 (w), 2953 (w), 1714 (s), 1662 (s), 1216 (s), 906.38 (s) cm^{-1}; **HRMS** (ESI) m/z for $C_{13}H_{13}NNaO_5$ $[M+Na]^+$ calcd.: 286.0686 found: 286.0685.

5.5.11 Dimethyl 2–(4–fluorobenzylcarbamoyl)–1,4–cubanedicarboxylate (4.19)

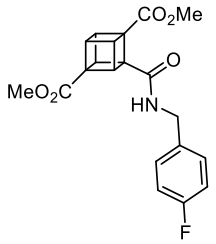

Prepared according to the **general procedure**. The obtained crude residue was dissolved in CH_2Cl_2 (2 mL) and Et_3N (0.42 mL, 3.0 mmol, 5.0 equiv.), 4–fluorobenzylamine (0.34 mL, 3.0 mmol, 5.0 equiv.) were added at 0 °C. The resulting brown solution was stirred for 16 h at room temperature. The reaction mixture was quenched with saturated NH_4Cl solution (10 mL), the aqueous phase was extracted with CH_2Cl_2 (3 × 5 mL), dried over $MgSO_4$ and concentrated under reduced pressure. Purification by flash column chromatography (8:2 hexane/EtOAc) afforded dimethyl 2–(diethylcarbamoyl)–1,4–cubanedicarboxylate (**4.19**, 95 mg, 0.26 mmol, 43%) as a beige solid.

Formula $C_{20}H_{18}FNO_5$; **MW** 371.36 g.mol^{-1}; **TLC** R_f 0.34 (5:5 hexane/acetone); **^{1}H NMR** (400 MHz, $CDCl_3$) δ 4.49 – 4.45 (m, 2H), 4.27 – 4.16 (m, 3H), 3.72 (s, 6H), 3.36 (q, J = 7.1 Hz, 2H), 3.11 (q, J = 7.1 Hz, 2H), 1.17 (t, J = 7.0 Hz, 3H), 1.10 (t, J = 7.2 Hz, 3H) ppm; **^{13}C{^{1}H} NMR** (101 MHz, $CDCl_3$) δ 171.5 (*C*OOMe), 170.8 (*C*OOMe), 168.7 (*C*ON), 162.1 (d, $J_{C\text{-}F}$ = 245.75 Hz, CF), 134.0 (d, $J_{C\text{-}F}$ = 2.93 Hz, CF), 129.5 (d, $J_{C\text{-}F}$ J = 8.07 Hz, CF), 115.4 (d, $J_{C\text{-}F}$ = 21.27 Hz, CF), 58.1 (C cubyl), 56.8 (C cubyl), 53.4 (C cubyl), 52.1 (COO*CH$_3$*), 51.8 (COO*CH$_3$*), 49.6 (2C, CH cubyl), 47.5 (2C, CH cubyl), 45.2 (1C, CH cubyl), 42.5 (CH_2) ppm; **^{19}F NMR** (376 MHz, CDl_3) δ – 115.45 (s, C-F); **IR** 3225 (w), 3067 (w), 2925 (w), 1711 (s), 1628 (s), 1511 (s), 1323 (s), 1209 (s) cm^{-1}; **HRMS** (ESI) m/z for $C_{20}H_{19}FNO_5$ $[M+H]^+$ calcd.: 372.1242 found: 372.1244.

5.5.12 Dimethyl 2–(*tert*–butylcarbamoyl)–1,4–cubanedicarboxylate (4.20)

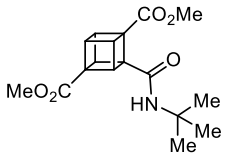

Prepared according to the **general procedure**. The obtained crude residue was dissolved in CH_2Cl_2 (2 mL) and Et_3N (0.42 mL, 3.0 mmol, 5.0 equiv.), *tert*–butylamine anhydrous (0.13 mL, 1.2 mmol, 2.0 equiv.) were added at 0 °C. The resulting brown solution was stirred for 16 h at room temperature. The reaction mixture was quenched with saturated NH_4Cl solution (10 mL), the aqueous phase was extracted with CH_2Cl_2 (3 × 5 mL), dried over $MgSO_4$ and concentrated under reduced pressure. Purification by flash column chromatography (8:2 hexane/acetone) afforded dimethyl 2–(*tert*–butylcarbamoyl)–1,4–cubanedicarboxylate (**4.20**, 90 mg, 0.28 mmol, 47%) as a white solid.

Formula $C_{17}H_{21}NO_5$; **MW** 319.36 g.mol^{-1}; **TLC** R_f 0.74 (5:5 hexane/acetone); **mp** 171 – 172 ˚C (CH_2Cl_2); **^{1}H NMR** (400 MHz, $CDCl_3$) δ 6.91 (br s, 1H), 4.44 – 4.36 (m, 2H), 4.22 – 4.14 (m, 3H), 3.75 (s, 3H), 3.71 (s, 3H), 1.36 (s, 9H) ppm; **^{13}C{^{1}H} NMR** (101 MHz, $CDCl_3$) δ 171.5 (*C*OOMe), 171.0 (*C*OOMe), 168.1 (*C*ON), 58.3 (C cubyl), 57.5 (C cubyl), 53.2 (C cubyl), 52.0 (COO*CH*$_3$), 51.8 (COO*CH*$_3$), 51.1 (*C*(CH_3)$_3$), 49.6 (2C, CH cubyl), 47.5 (1C, CH cubyl), 45.0 (2C, CH cubyl), 28.7 (3 x CH_3) ppm; **IR** 3394 (m), 2951 (m), 2845 (w) 1716 (s), 1645 (s), 1514 (s), 1325 (s), 1208 (s), 1020 (s) cm^{-1}; **HRMS** (ESI) m/z for $C_{17}H_{22}NO_5$ $[M+H]^+$ calcd.: 320.1492 found: 320.14.89, $C_{17}H_{21}NNaO_5$ $[M+Na]^+$ calcd.: 342.1312 found: 342.1312.

5.5.13 Dimethyl 2–(4–methoxy–1–cubanamine)carbonyl)–1,4–cubanedicarboxylate (4.21)

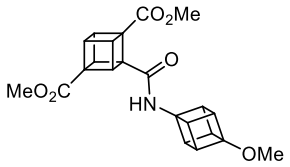

Prepared according to the **general procedure**. The obtained crude residue was dissolved in CH_2Cl_2 (2 mL) and Et_3N (0.42 mL, 3.0 mmol, 5.0 equiv.), 4–methoxy–1–cubanamine hydrochloride (111.4 mg, 0.6 mmol, 1.0 equiv.) were added at 0 °C. The resulting brown solution was stirred for 16 h at room temperature. The reaction mixture was quenched with saturated NH_4Cl solution (10 mL), the aqueous phase was extracted with CH_2Cl_2 (3 × 5 mL), dried over $MgSO_4$ and concentrated under reduced pressure. Purification by flash column chromatography (8:2 to 6:5 hexane/acetone) afforded dimethyl 2–(4–methoxy–1–cubanamine)carbonyl)–1,4–cubanedicarboxylate (**4.21**, 73 mg, 0.18 mmol, 31 %) as a white foam.

Formula $C_{22}H_{21}NO_6$; **MW** 395.41 g.mol^{-1}; **TLC** R_f 0.13 (6:4 hexane/acetone); **^{1}H NMR** (400 MHz, $CDCl_3$) δ 7.96 (s, 1H), 4.48 – 4.42 (m, 2H), 4.26 – 4.17 (m, 3H), 4.13 – 4.05 (m, 3H), 3.96 – 3.88

(m, 3H), 3.77 (s, 3H), 3.71 (s, 3H), 3.33 (s, 3H) ppm; **^{13}C{^{1}H} NMR** δ (101 MHz, $CDCl_3$) δ 171.9 (*C*OOMe), 170.8 (*C*OOMe), 168.2 (*C*ONH), 91.9 (*C*–OMe), 67.3 (*C*–NH_2CO), 58.2 (C cubyl), 56.6 (C cubyl), 53.4 (C cubyl), 52.2 (COO*CH*$_3$), 51.8 (COO*CH*$_3$), 51.4 (O*CH*$_3$), 49.8 (2C, CH cubyl), 48.4 (3C, CH cubyl), 47.6 (1C, CH cubyl), 45.5 (3C, CH cubyl), 45.4 (2C, CH cubyl) ppm; **IR** 3275 (m), 2991 (m), 2976 (m), 1720 (s), 1619 (s), 1517 (s), 1302 (s), 1088 (s) cm^{-1}; **HRMS** (ESI) m/z for $C_{22}H_{22}NO_6$ $[M+H]^+$ calcd.: 396.1442 found: 396.1439.

5.5.14 Dimethyl 2–((3,5–bis(trifluoromethyl)arylcarbamoyl)–1,4–cubanedicarboxylate (4.22)

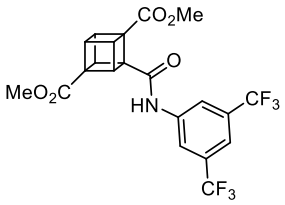

Prepared according to the **general procedure**. The obtained crude residue was dissolved in CH_2Cl_2 (2 mL) and Et_3N (0.42 mL, 3.0 mmol, 5.0 equiv.), 3,5–bis(trifluoromethyl)aniline (0.19 mL, 1.2 mmol, 2.0 equiv.) were added at 0 °C. The resulting brown solution was stirred for 16 h at room temperature. The reaction mixture was quenched with saturated NH_4Cl solution (10 mL), the aqueous phase was extracted with CH_2Cl_2 (3 × 5 mL), dried over $MgSO_4$ and concentrated under reduced pressure. Purification by flash column chromatography (9:1 to 8:2 hexane/EtOAc) afforded dimethyl 2–((3,5–bis(trifluoromethyl)arylcarbamoyl)–1,4–cubanedicarboxylate (**4.22**, 109 mg, 0.23 mmol, 38%) as an off–white solid.

Formula $C_{21}H_{15}F_6NO_5$; **MW** 475.34 g.mol^{-1}; **TLC** R_f 0.35 (6:4 hexane/EtOAc); **^{1}H NMR** (400 MHz, $CDCl_3$) δ 10.52 (br s, 1H), 8.16 (s, 2H), 7.60 (s, 1H), 4.57 (m, 2H), 4.35 – 4.27 (m, 3H), 3.88 (s, 3H), 3.76 (s, 3H) ppm; **^{13}C{^{1}H} NMR** (101 MHz, $CDCl_3$) δ 173.2 (*C*OOMe), 170.5 (*C*OOMe), 168.1 (*C*ON), 139.6 (C_{Ar}–NHCO), 132.2 (2C, q, $J_{C\text{-}F}$ = 33.3 Hz, CH–CF_3), 121.8 (q, $J_{C\text{-}F}$ = 272.9 Hz, 2CF_3), 119.2 (d, $J_{C\text{-}F}$ = 3.7 Hz, CH_{Ar}), 117.3 (m, CH_{Ar}), 58.5 (C cubyl), 57.2 (C cubyl), 53.7 (C cubyl), 52.8 (COO*CH*$_3$), 52.0 (COO*CH*$_3$), 50.2 (2C, CH cubyl), 47.7 (1C, CH cubyl), 45.8 (2C, CH cubyl) ppm; **IR** 3082 (w), 3020 (w) 1673 (s), 1381 (s), 1581 (s), 1274 (s), 1120 (s) cm^{-1}; **HRMS** (ESI) m/z for $C_{21}H_{16}F_6NO_5$ $[M+H]^+$ calcd.: 476.0927 found: 476.0924.

5.5.15 Dimethyl 2–((*ortho*–methoxy)arylcarbamoyl))–1,4–cubanedicarboxylate (4.23)

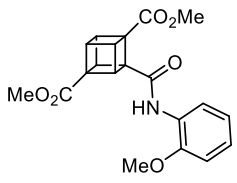

Prepared according to the **general procedure**. The obtained crude residue was dissolved in CH_2Cl_2 (2 mL) and Et_3N (0.42 mL, 3.0 mmol, 5.0 equiv.), *ortho*–anisidine (0.34 mL, 3.0 mmol, 5.0 equiv.) were added at 0 °C. The resulting brown solution was stirred for 16 h at room temperature. The reaction mixture was quenched with saturated NH_4Cl solution (10 mL), the aqueous phase was extracted with CH_2Cl_2 (3 × 5 mL), dried over $MgSO_4$ and concentrated under reduced pressure. Purification by flash column chromatography (9:1 to 7:3 hexane/EtOAc gradient) afforded dimethyl 2–((*ortho*–methoxy)arylcarbamoyl))–1,4–cubanedicarboxylate (**4.23**, 79 mg, 0.21 mmol, 35%) as a brown gummy solid.

Formula $C_{20}H_{19}NO_6$; **MW** 369.37 g.mol^{-1}; **TLC** R_f 0.32 (acetone); **^{1}H NMR** (400 MHz, $CDCl_3$) δ 8.79 (br s, 1H), 8.40 (dd, *J* = 7.9, 1.1 Hz, 1H), 7.05 (td, *J* = 7.7, 1.5 Hz, 1H), 6.95 (td, *J* = 7.7, 1.3 Hz, 1H), 6.89 (dd, *J* = 8.1, 1.2 Hz, 1H), 4.53 (m, 2H), 4.30 – 4.21 (m, 3H), 3.91 (s, 3H), 3.77 (s, 3H), 3.74 (s, 3H) ppm; **^{13}C{^{1}H} NMR** (101 MHz, $CDCl_3$) δ 170.8 (*C*OOMe), 170.6 (*C*OOMe), 166.7 (*C*ON), 148.4 (C_{Ar}–OMe), 127.5 (CH_{Ar}), 124.0 (CH_{Ar}), 121.1 (CH_{Ar}), 120.3 (CH_{Ar}), 110.2 (CH_{Ar}), 58.6 (C cubyl), 57.8 (C cubyl, 55.8 (C_{Ar}–OCH_3), 53.3 (C cubyl, 52.1 (COOCH_3), 51.8 (COOCH_3), 49.7 (2C, CH cubyl), 47.6 (1C, CH cubyl), 45.0 (2C, CH cubyl) ppm; **IR** 3004 (w), 2951 (w), 1720 (s), 1526 (s), 1460 (m), 1435 (w), 1327 (s), 1219 (s) cm^{-1}; **HRMS** (ESI) m/z for $C_{20}H_{20}NO_6$ $[M+H]^+$ calcd.: 370.1285 found: 370.1282 for $C_{20}H_{19}NNaO_6$ $[M+Na]^+$ calcd.: 392.1105 found: 394.1105.

5.5.16 Dimethyl 2–((4–aminoantipyrine)carbonyl)–1,4–cubanedicarboxylate (4.24)

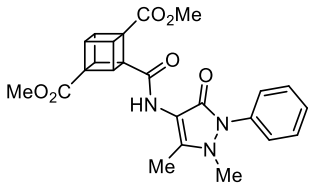

Prepared according to the **general procedure**. The obtained crude residue was dissolved in CH_2Cl_2 (2 mL) and Et_3N (0.42 mL, 3.0 mmol, 5.0 equiv.), 4–aminoantipyrine (243.9 mg, 1.2 mmol, 2.0 equiv.) were added at 0 °C. The resulting brown solution was stirred for 16 h at room temperature. The reaction mixture was quenched with saturated NH_4Cl solution (10 mL), the aqueous phase was extracted with CH_2Cl_2 (3 × 5 mL), dried over $MgSO_4$ and concentrated under reduced pressure. Purification by flash column chromatography (8:2 hexane/acetone) afforded dimethyl 2–((4–aminoantipyrine)carbonyl)–1,4–cubanedicarboxylate (**4.24**, 134 mg, 0.30 mmol, 50 %) as an orange foam.

Formula $C_{24}H_{23}N_3O_6$; **MW** 449.46 g.mol^{-1}; **TLC** R_f 0.41 (8:2 hexane/acetone); **^{1}H NMR** (400 MHz, $CDCl_3$) δ 8.46 (br s, 1H), 7.49 – 7.43 (m, 2H), 7.42 – 7.38 (m, 2H), 7.32 –7.27 (m, 1H), 4.54 – 4.50 (m, 2H), 4.29 (m, 1H), 4.29 – 4.20 (m, 2H), 3.78 (s, 3H), 3.73 (s, 3H), 3.07 (s, 3H), 2.29 (s, 3H) ppm; **^{13}C{^{1}H} NMR** (101 MHz, $CDCl_3$) δ 170.9 (*C*OOMe), 170.8 (*C*OOMe), 167.5 (*C*ON), 161.5 (*C*ON), 149.3 (*C*–Me), 134.8 (C_{Ar}), 129.2 (2C, CH_{Ar}), 126.7 (1C, CH_{Ar}), 124.0 (2C, CH_{Ar}), 108.4 (*C*–NH),

58.5 (C cubyl), 57.1 (C cubyl), 53.4 (C cubyl), 52.3 (COO*CH*$_3$), 51.8 (COO*CH*$_3$), 49.8 (2C, CH cubyl), 47.6 (1C, CH cubyl), 45.3 (2C, CH cubyl), 36.3 (CH_3), 12.6 (CH_3) ppm; **IR** 3170 (w), 3004 (m), 2951 (w), 1723 (s), 1652 (s), 1324 (s), 1218 (s) 1092 (m) cm^{-1}; **HRMS** (ESI) m/z for $C_{24}H_{24}N_3O_6$ $[M+H]^+$ calcd.: 450.1660 found: 450.1668.

5.5.17 Dimethyl 2–(morpholine–4–carbonyl)–1,4–cubanedicarboxylate (4.25)

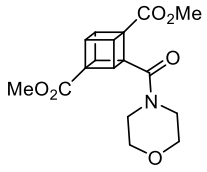

Prepared according to the **general procedure**. The obtained crude residue was dissolved in CH_2Cl_2 (2 mL) and Et_3N (0.42 mL, 3.0 mmol, 5.0 equiv.), morpholine (0.11 mL, 1.2 mmol, 2.0 equiv.) were added at 0 °C. The resulting brown solution was stirred for 16 h at room temperature. The reaction mixture was quenched with saturated NH_4Cl solution (10 mL), the aqueous phase was extracted with CH_2Cl_2 (3 × 5 mL), dried over $MgSO_4$ and concentrated under reduced pressure. Purification by flash column chromatography (8:2 hexane/EtOAc followed by a gradient 8:2 to 6:4 hexane/acetone) afforded dimethyl 2–(morpholine–4–carbonyl)–1,4–cubanedicarboxylate (**4.25**, 86 mg, 0.26 mmol, 43%) as an off–white solid.

Formula $C_{17}H_{19}NO_6$; **MW** 333.34 g.mol^{-1}; **TLC** R_f 0.19 (8:2 hexane/EtOAc); **^{1}H NMR** (400 MHz, $CDCl_3$) δ 4.54 – 4.42 (m, 2H), 4.28 – 4.23 (m, 2H), 4.23 – 4.18 (m, 1H), 3.75 (s, 3H), 3.72 (s, 3H), 3.69 – 3.62 (m, 4H), 3.62 – 3.57 (m, 2H), 3.33 – 3.21 (m, 2H) ppm; **^{13}C{^{1}H} NMR** (101 MHz, $CDCl_3$) δ 171.0 (*C*OOMe), 170.2 (*C*OOMe), 166.7 (*C*ON), 66.8 (O*CH*$_2$), 66.6 (O*CH*$_2$), 57.8 (2C, C cubyl), 53.0 (1C, C cubyl), 51.9 (COO*CH*$_3$), 51.9 (COO*CH*$_3$), 49.8 (2C, CH cubyl), 46.5 (1C, CH cubyl), 45.6 (N*CH*$_2$), 44.7 (2C, CH cubyl), 42.0 (N*CH*$_2$) ppm; **IR** 2999 (w), 2953 (w), 2855 (w), 1716 (s), 1630 (s), 1434 (s) 1216 (S), 1112 (m) cm^{-1}; **HRMS** (ESI) m/z for $C_{17}H_{20}NO_6$ $[M+H]^+$ calcd.: 334.1285 found: 334.1283 $C_{17}H_{19}NNaO_6$ $[M+Na]^+$ calcd.: 356.1105 found: 356.1105.

5.5.18 Dimethyl 2–(piperidine–1–carbonyl)–1,4–cubanedicarboxylate (4.26)

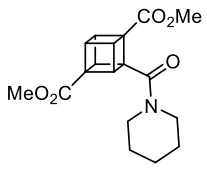

Prepared according to the **general procedure**. The obtained crude residue was dissolved in CH_2Cl_2 (2 mL) and Et_3N (0.42 mL, 3.0 mmol, 5.0 equiv.), piperidine (0.30 mL, 3.0 mmol, 5.0 equiv.) were added at 0 °C. The resulting brown solution was stirred for 16 h at room temperature. The reaction mixture was quenched with saturated NH_4Cl solution (10 mL), the aqueous phase was extracted with

CH_2Cl_2 (3 × 5 mL), dried over $MgSO_4$ and concentrated under reduced pressure. Purification by flash column chromatography (8:2 hexane/EtOAc) afforded dimethyl 2–(piperidine–1–carbonyl)–1,4–cubanedicarboxylate (**4.26**, 93 mg, 0.28 mmol, 47%) as a white solid.

Formula $C_{18}H_{21}NO_5$; **MW** 331.37 g.mol^{-1}; **TLC** R_f 0.74 (5:5 hexane/acetone); **^{1}H NMR** (400 MHz, $CDCl_3$) δ 4.48 – 4.44 (m, 2H), 4.25 – 4.21 (m, 2H), 4.21 – 4.15 (m, 1H), 3.73 (s, 3H), 3.71 (s, 3H), 3.55 – 3.48 (m, 2H), 3.19 – 3.12 (m, 2H), 1.67 – 1.58 (m, 3H), 1.57 – 1.49 (m, 3H) ppm; **^{13}C{^{1}H} NMR** (101 MHz, $CDCl_3$) δ 171.1 (*C*OOMe), 170.4 (*C*OOMe), 166.2 (*C*ON), 58.3 (C cubyl), 57.7 (C cubyl), 52.9 (C cubyl), 51.8 (COO*CH*$_3$), 51.8 (COO*CH*$_3$), 50.0 (2C, CH cubyl), 46.4 (1C, CH cubyl), 46.2 (NCH_2), 44.5 (2C, CH cubyl), 42.8 (NCH_2), 26.4 (CH_2), 25.4 (CH_2), 24.4 (CH_2) ppm; **IR** 3003. (w), 2952 (m), 2870 (w), 1717 (s), 13252 (s), 1212 (s), 1090 (s) cm^{-1}; **HRMS** (ESI) m/z for $C_{18}H_{22}NO_5$ $[M+H]^+$ calcd.: 332.1492 found: 332.1488.

5.5.19 Dimethyl 2–(diethylcarbamoyl) 1,4–cubanedicarboxylate (4.27)

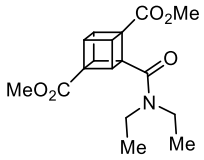

Prepared according to the **general procedure**. The obtained crude residue was dissolved in CH_2Cl_2 (2 mL) and Et_3N (0.42 mL, 3.0 mmol, 5.0 equiv.), diethylamine (0.31 mL, 3.0 mmol, 5.0 equiv.) were added at 0 °C. The resulting brown solution was stirred for 16 h at room temperature. The reaction mixture was quenched with saturated NH_4Cl solution (10 mL), the aqueous phase was extracted with CH_2Cl_2 (3 × 5 mL), dried over $MgSO_4$ and concentrated under reduced pressure. Purification by flash column chromatography (8:2 to 5:5 hexane/EtOAc) followed by HPLC (8:2 hexane/acetone) afforded dimethyl 2–(diethylcarbamoyl)–1,4–cubanedicarboxylate (**4.27**, 43 mg, 0.13 mmol, 22%) as a yellow oil.

Formula $C_{17}H_{21}NO_5$; **MW** 319.36 g.mol^{-1}; **TLC** R_f 0.13 (8:2 hexane/acetone); **^{1}H NMR** (400 MHz, $CDCl_3$) δ 4.49 – 4.45 (m, 2H), 4.27 – 4.16 (m, 3H), 3.72 (s, 6H), 3.36 (q, *J* = 7.1 Hz, 2H), 3.11 (q, *J* = 7.1 Hz, 2H), 1.17 (t, *J* = 7.0 Hz, 3H), 1.10 (t, *J* = 7.2 Hz, 3H) ppm; **^{13}C{^{1}H} NMR** (101 MHz, $CDCl_3$) δ 171.2 (*C*OOMe), 170.4 (*C*OOMe), 167.2 (*C*ON), 58.4 (C cubyl), 57.8 (C cubyl), 52.8 (C cubyl), 51.8 (COO*CH*$_3$), 51.7 (COO*CH*$_3$), 50.1 (2C, CH cubyl), 46.6 (1C, CH cubyl), 44.5 (2C, CH cubyl), 40.8 (CH_2), 38.9 (CH_2), 14.3 (CH_3), 12.5 (CH_3) ppm; **IR** 2997 (w), 2938 (w), 1714 (s), 1621 (s), 1427 (m), 1319 (m), 1210 (s), 1090 (s) cm^{-1}; **HRMS** (ESI) m/z for $C_{17}H_{22}NO_5$ $[M+H]^+$ calcd.: 320.1492 found: 320.1489.

5.5.20 Synthesis of redox–active ester (4.16)

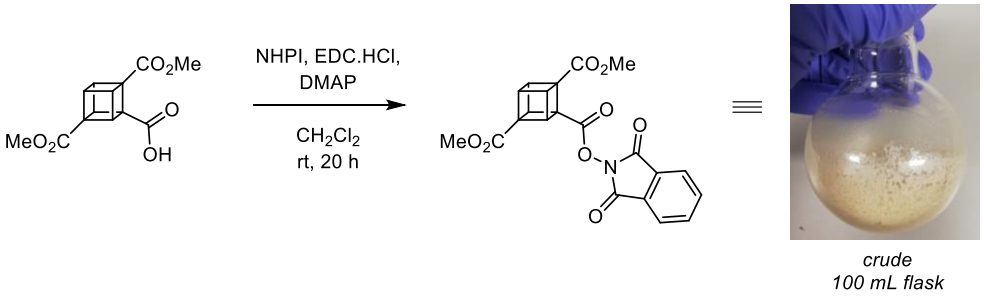

Following a procedure adapted from G. Doyle *et al.*[1] To a 25 mL flask containing the crude acid (**4.13**, 117 mg, 0.44 mmol, 1.0 equiv.), *N*–hydroxyphthalimide (72.0 mg, 0.44 mmol, 1.0 equiv.), 4–dimethylaminopyridine (DMAP) (5.0 mg, 0.044 mmol, 0.1 equiv.) and *N*–(3–dimethylaminopropyl)–*N'*–ethylcarbodiimide hydrochloride (EDC.HCl) (94 mg, 0.49 mmol, 1.1 equiv.) were added and dissolved CH_2Cl_2 anhydrous (5.7 mL) under argon. The reaction mixture was stirred for 20 h at room temperature. Afterwards, the reaction mixture was quenched with water (10 mL) and extracted with CH_2Cl_2 (3 × 10 mL). The organic layers were washed with $NaHCO_3$ sat. (10 mL) and then water (10 mL), dried over $MgSO_4$, filtrated, passed through a plug of celite and concentrated under reduced pressure to afford 2–(*N*–hydroxyphthalamide)–1,4–cubanedicarboxylate (**4.16**, 165 mg, 0.40 mmol, 92%) as a beige/white foam.

Note: If the foam does not form after concentration under reduced pressure with CH_2Cl_2, add Et_2O and evaporate (repeat this procedure several times). The obtained redox–active ester **4.16** decomposes on silica, therefore, no purification was carried out. For this reason, EDC.HCl has to be used instead of *N*,*N'*–diisopropylcarbodiimide **(**DIC) or *N*,*N'*–dicyclohexylcarbodiimide (DCC) which cannot be removed during aqueous workup or through a plug of celite.

5.5.21 Synthesis of dimethyl 2–(phenyl)–1,4–cubanedicarboxylate (20)

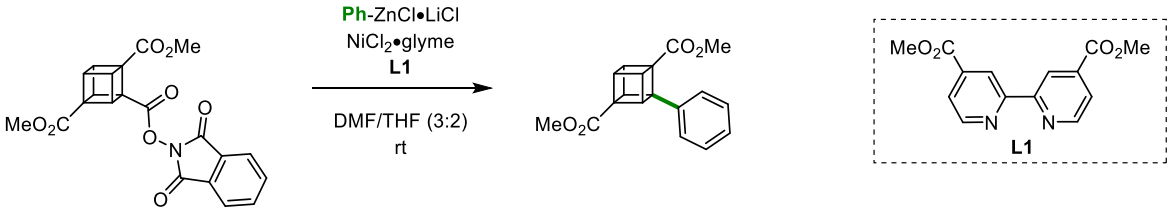

Synthesis of L1

Following a procedure adapted from Sugimoto *et al.*[172] To a 100 mL flask containing 2'–bipyridine–4,4'–dicarboxylic acid (1.08 g, 4.41 mmoles) in methanol (30 mL), H_2SO_4 concentrated (2 mL) was added slowly and the resulting heterogenous solution was refluxed for 17 h (DrySyn® heating mantle). The homogeneous (pink) solution was cooled down and poured in distilled water (100 mL).

The pH value of the slurry was adjusted to 12 with NaOH acqueous (25% w/v). The product was then extracted with chloroform (3 x 50 mL), dried over MgSO4 and evaporated to afford 4,4'–dimethoxycarbonyl–2,2'–bipyridine (**L1**, 1.12 g, 4.11 mmol, 93%) as a white solid. Data consistent with the literature.[172]

Following a procedure adapted from Senge *et al.*[2] To a flame–dried schlenk flask, a stir bar, LiCl (212 mg, 5.0 mmol) and magnesium turnings (120 mg, 5.0 mmol) were heated under vacuum. After cooling–down to room temperature, an iodine crystal was added, the flask was filled with argon and anhydrous THF (1 mL) was added. Afterwards, bromobenzene (0.42 mL, 4.0 mmol) dissolved in anhydrous THF (3 mL) was added slowly until slight clouding and warming of the solution indicate the start of the Grignard formation. It was assumed that the Grignard was completely formed after 1–2 h stirring. In another flask, $ZnCl_2$ (545.1 mg, 4.0 mmol) was heated under vacuum and after cooling–down at room temperature, dissolved in anhydrous THF (4 mL, c = 1 M). Finally, the Grignard was added to the $ZnCl_2$ solution and stirred for 20 minutes (at least) before use.

To a microwave vial, the redox–active ester cubane (81.9 mg, 0.2 mmol, 1.0 equiv.), $NiCl_2$–glyme (44 mg, 0.2 mmol, 1.0 equiv.) and ligand **L1** (108 mg, 0.4 mmol, 2.0 equiv.). The flask was evacuated and backfilled with argon (repeated 3 times). Finally, the solids were dissolved in DMF (2.28 ml) and stirred under argon for 5 minutes. Then PhZnCl*LiCl solution (1.6 ml, 0.05 M, 0.8 mmol, 4.0 equiv.) was added in one portion and the mixture was stirred for 4 h at room temperature. The reaction mixture was quenched with HCl (40 ml, 1 M) and ethyl acetate (50 ml). The organic phase was washed with water (20 mL) and brine (20 mL), dried over $MgSO_4$ and concentrated under vacuum. Purification by flash column chromatography (9:1 hexane/EtOAc) followed by HPLC (9:1 hexane/EtOAc) afforded dimethyl 2–(phenyl)–1,4–cubanedicarboxylate (**4.29**, 18.9 mg, 0.064 mmol, 32%) as a white solid.

Note: Hydrogen abstraction by the formed cubyl radical leads to dimethyl 1,4–cubanedicarboxylate **1.35** which in this case is observed as byproduct. Separation of **1.35** and the product **4.29** has proven to be challenging. For this reason larger–scale than 0.1 mmol is preferable.

Formula $C_{18}H_{16}O_4$; **MW** 296.32 g.mol^{-1}; **TLC** R_f 0.5 (6:4 hexane/EtOAc); **^{1}H NMR** (400 MHz, $CDCl_3$) δ 7.39 – 7.33 (m, 2H), 7.29 – 7.18 (m, 4H), 4.51 – 4.45 (m, 2H), 4.32 – 4.24 (m, 4H), 3.71 (s, 3H), 3.51 (s, 3H) ppm; **^{13}C{^{1}H} NMR** δ (101 MHz, $CDCl_3$) δ 171.7 (*C*OOMe), 170.2 (*C*OOMe), 137.7 (C_{Ar}), 128.4 (2C, CH_{Ar}), 127.0 (C_{Ar}), 125.4 (2C, CH_{Ar}), 60.6 (C cubyl), 60.5 (C cubyl), 52.7 (C cubyl), 51.7 (COO*CH*$_3$), 51.3 (COO*CH*$_3$), 50.6 (2C, CH cubyl), 47.8 (1C, CH cubyl), 43.7 (2C, CH cubyl) ppm; **IR** 2294 (w), 2949 (w), 1708 (s), 1318 (s), 1210 (s), 1081 (s), 699 (s) cm^{-1}; **HRMS** (ESI) m/z for $C_{18}H_{17}O_4$ $[M+H]^+$ calcd.: 297.1121 found: 297.1117.

5.5.22 Procedure for the Ni–catalyzed Giese Conjugate Addition

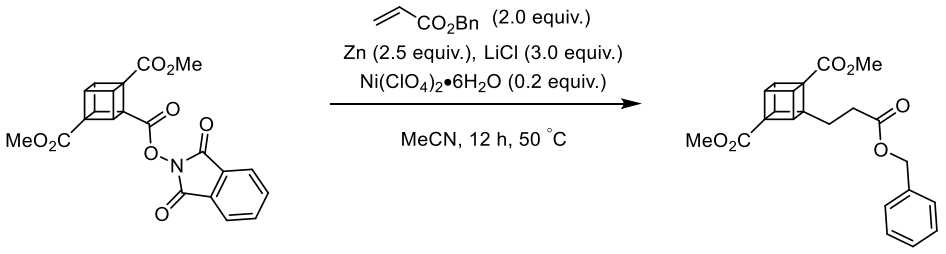

Following a procedure adapted from Baran *et al.*[3] In a flame–dried test tube, LiCl (51.0 mg, 1.20 mmol, 3.0 equiv.) was added and heated under reduced pressure, afterwards, Zn (65.0 mg, 1.00 mmol, 2.5 equiv.), $Ni(ClO_4).6H_2O$ (29 mg, 0.08 mmol 0.2 equiv.) and the NHPI ester (**4.16**, 165 mg, 0.40 mmol, 1.0 equiv.). A stir bar was added and the test tube was evacuated and back filled with argon. Afterwards, acrylonitrile (0.12 mL, 0.800 mmol, 2.0 equiv.) was added followed by MeCN anhydrous (2.0 mL, c = 0.2 M) and the green–black mixture was stirred for 18 h at 50 °C. The resulting black–grey mixture was quenched with water (2 mL) followed by NH_4Cl sat. (2 mL), extracted with EtOAc, dried over $MgSO_4$ and concentrated under reduced pressure. Purification by flash column chromatography (8:2 hexane/EtOAc) afforded dimethyl 2–(ethylbenzoate)–1,4–cubanedicarboxylate (**4.30**, 30.1 mg, 0.08 mmol, 20%) as a white solid.

Formula $C_{22}H_{22}O_6$; **MW** 382.41 g.mol^{-1}; **TLC** R_f 0.33 (7:3 hexane/EtOAc); **^{1}H NMR** (400 MHz, $CDCl_3$) δ 7.29 – 7.41 (m, 5H), 5.12 (s, 2H), 4.18 – 4.24 (m, 1H), 4.07 – 4.13 (m, 2H), 4.00 (dd, *J* = 4.8, 2.4 Hz, 2H), 3.70 (s, 3H), 3.69 (s, 3H), 2.33 – 2.40 (m, 2H), 2.13 – 2.06 (m, 2H) ppm; **^{13}C{^{1}H} NMR** δ (101 MHz, $CDCl_3$) δ 173.0 (COOBn), 171.7 (COOMe), 171.1 (COOMe), 135.9 (C_{Ar}), 128.5 (2C, CH_{Ar}), 128.2 (3C, CH_{Ar}), 66.4 (CH_2Ph), 58.4 (C cubyl), 56.8 (C cubyl), 52.6 (C cubyl), 51.6 (COO*CH*$_3$), 51.5 (COO*CH*$_3$), 48.2 (2C, CH cubyl), 47.7 (CH cubyl), 43.9 (2C, C cubyl), 28.5 (CH_2), 25.3 (CH_2) ppm; **IR** 3995 (w), 2360 (m), 1723 (s), 1212 (m) cm^{-1}; **HRMS** (ESI) m/z for for $C_{22}H_{22}NaO_6$ $[M+Na]^+$ calcd.: 405.1309, found 405.1315.

5.5.23 4–Methoxycarbonyl 3–(3,5–bis(trifluoromethyl)arylcarbamoyl)–1–cubanecarboxylic acid (4.31)

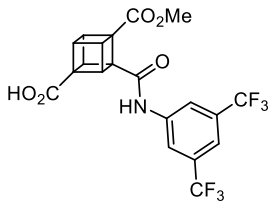

To a 5 mL round–bottom flask, dimethyl 2–((3,5–bis(trifluoromethyl)arylcarbamoyl)–1,4–cubanedicarboxylate (**4.22**, 50.2 mg, 0.106 mmol, 1.0 equiv.) was dissolved in THF (1 mL) and a solution of NaOH (4.2 mg, 0.106 mmol, 1.0 equiv.) in methanol (0.5 mL) was added. The resulting solution was stirred for 16 h at room temperature. The solvent was evaporated and the obtained solid

was dissolved in the minimum amount of water and washed with chloroform (5 mL). The aqueous phase was acidified with concentrated HCl until pH ≈ 1 – 2 was reached and extracted with chloroform. The combined organic phases were dried over $MgSO_4$ and concentrated under reduced pressure to afford 4–methoxycarbonyl 3–(3,5–bis(trifluoromethyl)arylcarbamoyl) 1–cubanecarboxylic acid (**4.31**, 41.0 mg, 0.089 mmol, 84%) as an off–white solid. No further purification was carried out.

Formula $C_{20}H_{13}F_6NO_5$; **MW** 461.32 g.mol^{-1}; **^{1}H NMR** (400 MHz, CD_3OD) δ 8.26 (s, 2H), 7.67 – 7.64 (m, 1H), 4.85 (s, 6H), 4.55 – 4.51 (m, 2H), 4.27 – 4.23 (m, 2H), 4.22 – 4.18 (m, 1H), 3.74 (s, 3H) ppm; **^{13}C{^{1}H} NMR** δ (101 MHz, CD_3OD) δ δ 173.9 (CO), 172.9 (CO), 170.8 (CO), 142.0 (C_{Ar}–NHCO), 133.4 (2C, q, $J_{C\text{-}F}$ = 33.3 Hz, *C*–CF_3), 120.9 (q, $J_{C\text{-}F}$ = 272.2 Hz, CF_3), 123.7 d, $J_{C\text{-}F}$ = 2.9 Hz, CH_{Ar}), 117.9 (m, CH_{Ar}), 60.7 (C cubyl), 59.0 (C cubyl), 54.9 (C cubyl), 52.5 (COO*C*H_3), 50.8 (2C, CH cubyl), 46.8 (2C, CH cubyl) ppm; **^{19}F NMR** (376 MHz, CD_3OD) δ – 64.87 (s, 2 × CF_3) ppm; **HRMS** (ESI) m/z for $C_{20}H_{12}F_6NO_5$ $[M–H]^-$ calcd.: 460.0625 found: 460.0633.

5.5.24 4–Methoxycarbonyl 3–(4–aminoantipyrine)carbonyl–1–cubanecarboxylic acid (4.32)

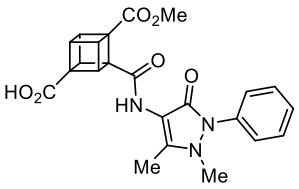

To a 5 mL round–bottom flask, dimethyl 2–((4–aminoantipyrine)carbonyl)–1,4–cubanedicarboxylate (**4.24**, 30.5 mg, 0.068 mmol, 1.0 equiv.) was dissolved in THF (0.6 mL) and a solution of NaOH (2.7 mg, 0.068 mmol, 1.0 equiv.) in methanol (0.3 mL) was added. The resulting solution was stirred for 16 h at room temperature. The solvent was evaporated and the obtained solid was dissolved in the minimum amount of water and washed with chloroform (5 mL). The aqueous phase was acidified with concentrated HCl until pH ≈ 1 – 2 was reached and extracted with chloroform. The combined organic phases were dried over $MgSO_4$ and concentrated under reduced pressure to afford 4–methoxycarbonyl 3–(4–aminoantipyrine)carbonyl 1–cubanecarboxylic acid (**4.32**, 22.0 mg, 0.052 mmol, 74%) as a beige solid. No further purification was carried out.

Formula $C_{23}H_{21}N_3O_6$; **MW** 435.44 g.mol^{-1}; **^{1}H NMR** (400 MHz, CD_3OD) δ 7.48 – 7.36 (m, 3H), 4.58 – 4.50 (m, 2H), 4.25 – 4.22 (m, 2H), 4.21 – 4.16 (m, 1H), 3.72 (s, 3H), 3.21 (s, 3H), 2.25 (s, 3H) ppm; **^{13}C{^{1}H} NMR** δ (101 MHz, CD_3OD) δ 173.5 (CO), 172.9 (CO), 172.2 (CO), 163.6 (*C*ON), 152.9 (*C*–Me), 135.4 (C_{Ar}), 130.7 (2C, CH_{Ar}), 129.7 (2C, CH_{Ar}), 127.5 (2C, CH_{Ar}), 106.0 (*C*–NH), 60.5 (C cubyl), 58.6 (C cubyl), 55.0 (C cubyl), 52.4 (COO*C*H_3), 50.7 (2C, CH cubyl), 49.0 (1C, CH cubyl), 46.7 (2C, CH cubyl), 35.4 (CH_3), 11.0 (CH_3) ppm; **IR** 2918 (w), 2850 (w), 1717 (s), 1652

(s), 1303 (s) ,1215 (s), 1019 (m) cm^{-1}; **HRMS** (ESI) m/z for $C_{23}H_{20}N_3O_6$ $[M–H]^–$ calcd.: 434.1358 found: 434.1350.

5.6 X–Ray Crystallographic Data

All crystal structures have been determined by Mark E. Light.

5.6.1 *Endo*–2,4–dibromocyclopentadiene–1,8–dione [CCDC: 1894382] (2.5)

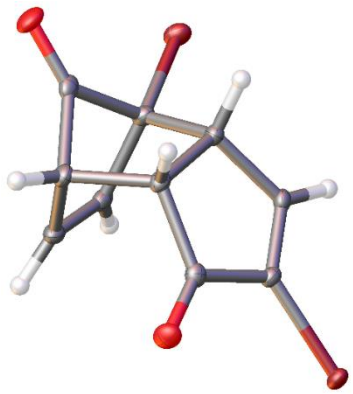

Figure 44. Structure of 2.5 with thermal ellipsoids drawn at the 50% probability level.

Experimental. Single clear colourless fragment-shaped crystals of **DC_8346_009** were recrystallised from a mixture of hexane and EtOAc by slow evaporation. A suitable crystal 0.47×0.20×0.05 mm^3 was selected and mounted on a MITIGEN holder silicon oil on a Rigaku AFC12 FRE-HF diffractometer. The crystal was kept at a steady T = 100(2) K during data collection. The structure was solved with the **ShelXT**[173] structure solution program using the Intrinsic Phasing solution method and by using **Olex2**[174] as the graphical interface. The model was refined with version 2016/6 of **ShelXL**[175] using Least Squares minimisation.

Table 10. Crystal data of 2.5.

Formula	$C_{10}H_6Br_2O_2$
$D_{calc.}$/ g cm^{-3}	2.207
μ/mm^{-1}	8.436
Formula Weight	317.97
Colour	clear colourless
Shape	fragment
Size/mm^3	0.47×0.20×0.05
T/K	100(2)
Crystal System	monoclinic
Space Group	$P2_1/c$
a/Å	7.7120(2)
b/Å	6.4673(2)
c/Å	19.3311(6)
α/°	90
β/°	96.995(3)
μ/°	90
V/$Å^3$	956.98(5)
Z	4
Z'	1
Wavelength/Å	0.71073
Radiation type	MoK_α
Θ_{min}/°	3.196
Θ_{max}/°	28.495
Measured Refl.	23163
Independent Refl.	2429
Reflections with I > 2(I)	2289
R_{int}	0.0632
Parameters	127
Restraints	0
Largest Peak	0.588
Deepest Hole	-0.585
GooF	1.116
wR_2 (all data)	0.0545
wR_2	0.0534
R_1 (all data)	0.0281
R_1	0.0256

5.6.2 Methyl 4–methoxy–1–cubanecarboxylate [CCDC: 1905443 2019sot0002_K1_100K] (3.59)

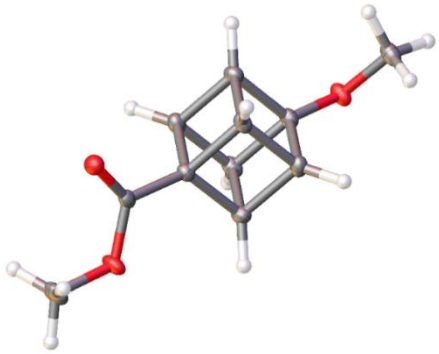

Figure 45. Structure of 3.59 with thermal ellipsoids drawn at the 50% probability level.

Experimental. Single clear colourless prism-shaped crystals of **DC_8620_53** crystallised from Et_2O by slow evaporation. A suitable crystal 0.25×0.20×0.10 mm^3 was selected and mounted on a MITIGEN holder silicon oil on a Rigaku AFC12 FRE-HF diffractometer. The crystal was kept at a steady T = 100(2) K during data collection. The structure was solved with the **ShelXT**[173] structure solution program using the Intrinsic Phasing solution method and by using **Olex2**[174] as the graphical interface. The model was refined with version 2016/6 of **ShelXL**[175] using Least Squares minimisation.

Table 11. Crystal data of 3.59.

Formula	$C_{11}H_{12}O_3$
$D_{calc.}$/ g cm^{-3}	1.392
μ/mm^{-1}	0.101
Formula Weight	192.21
Colour	clear colourless
Shape	prism
Size/mm^3	0.25×0.20×0.10
T/K	100(2)
Crystal System	monoclinic
Space Group	$P2_1/c$
a/Å	7.2351(2)
b/Å	8.0399(2)
c/Å	31.7327(5)
α/°	90
β/°	96.243(2)
γ/°	90
V/$Å^3$	1834.93(7)
Z	8
Z'	2
Wavelength/Å	0.71073
Radiation type	MoK_α
Θ_{min}/°	2.982
Θ_{max}/°	28.499
Measured Refl.	40539
Independent Refl.	4658
Reflections with I > 2(I)	4415
R_{int}	0.0480
Parameters	257
Restraints	0
Largest Peak	0.404
Deepest Hole	–0.224
GooF	1.276
wR_2 (all data)	0.1408
wR_2	0.1379
R_1 (all data)	0.0707
R_1	0.0655

5.6.3 Methyl 4–(1,1,1,3,3,3–hexafluoroisopropoxy)–1–cubanecarboxylate [CCDC: 1889723 2018sot0040_K1_100K] (3.67)

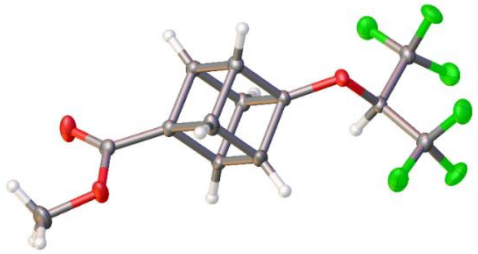

Figure 46. Structure of 3.67 with thermal ellipsoids drawn at the 50% probability level.

Experimental. Single clear colourless prism-shaped crystals of **DC_8507_67** crystallised from HFIP by slow evaporation. A suitable crystal 0.46×0.28×0.10 mm^3 was selected and mounted on a MITIGEN holder silicon oil on a Rigaku AFC12 FRE-HF diffractometer. The crystal was kept at a steady T = 100(2) K during data collection. The structure was solved with the **ShelXT**[173] structure solution program using the Intrinsic Phasing solution method and by using **Olex2**[174] as the graphical interface. The model was refined with version 2016/6 of **ShelXL**[175] using Least Squares minimisation.

Table 12. Crystal data of 3.67.

Formula	$C_{13}H_{10}F_6O_3$
$D_{calc.}$/ g cm^{-3}	1.738
μ/mm^{-1}	0.179
Formula Weight	328.21
Colour	clear colourless
Shape	prism
Size/mm^3	0.46×0.28×0.10
T/K	100(2)
Crystal System	monoclinic
Space Group	$P2_1/n$
a/Å	11.2408(3)
b/Å	9.7652(2)
c/Å	12.5959(3)
α/°	90
β/°	114.902(3)
γ/°	90
V/$Å^3$	1254.09(6)
Z	4
Z'	1
Wavelength/Å	0.71073
Radiation type	MoK_α
Θ_{min}/°	2.888
Θ_{max}/°	28.500
Measured Refl.	18889
Independent Refl.	3169
Reflections with I > 2(I)	2860
R_{int}	0.0488
Parameters	200
Restraints	0
Largest Peak	0.375
Deepest Hole	–0.272
GooF	1.075
wR_2 (all data)	0.1007
wR_2	0.0969
R_1 (all data)	0.0471
R_1	0.0416

5.6.4 Methyl 4–ethoxy–1–cubanecarboxylate [CCDC: 1919701 2019sot0009_K1_100K] (3.65)

Figure 47. Structure of 3.65 with thermal ellipsoids drawn at the 50% probability level.

Experimental. Single clear colourless plate-shaped crystals of **DC_8620_76** crystallised from hexane by slow evaporation. A suitable crystal 0.40×0.21×0.08 mm^3 was selected and mounted on a MITIGEN holder with silicon oil on a Rigaku AFC12 FRE-HF diffractometer. The crystal was kept at a steady T = 100(2) K during data collection. The structure was solved with the **ShelXT**[173] structure solution program using the Intrinsic Phasing solution method and by using **Olex2**[174] as the graphical interface. The model was refined with version 2016/6 of **ShelXL**[175] using Least Squares minimisation.

Table 13. Crystal data of 3.65.

Formula	$C_{12}H_{14}O_3$
$D_{calc.}$/ g cm^{-3}	1.334
μ/mm^{-1}	0.095
Formula Weight	206.23
Colour	clear colourless
Shape	plate
Size/mm^3	0.40×0.21×0.08
T/K	100(2)
Crystal System	monoclinic
Space Group	$P2_1/n$
a/Å	5.7615(2)
b/Å	28.2305(8)
c/Å	6.3185(2)
α/°	90
β/°	92.235(3)
γ/°	90
V/$Å^3$	1026.92(6)
Z	4
Z'	1
Wavelength/Å	0.71073
Radiation type	MoK_α
Θ_{min}/°	3.306
Θ_{max}/°	28.493
Measured Refl.	15175
Independent Refl.	2609
Reflections with I > 2(I)	2434
R_{int}	0.0513
Parameters	138
Restraints	0
Largest Peak	0.439
Deepest Hole	–0.264
GooF	1.251
wR_2 (all data)	0.1566
wR_2	0.1531
R_1 (all data)	0.0907
R_1	0.0823

5.6.5 Methyl 4–methoxy(d_3)–1–cubanecarboxylate [CCDC: 19199782019sot0008_R1_100K] (3.63)

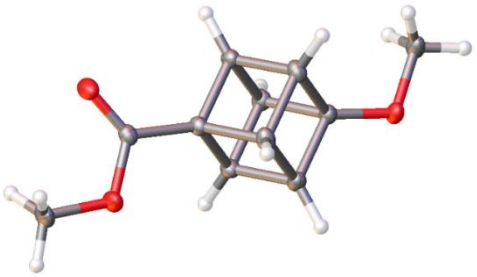

Figure 48. Structure of 3.63 with thermal ellipsoids drawn at the 50% probability level.

Experimental. Single clear colourless prism-shaped crystals of **DC_8620_78** crystallised from hexane by slow evaporation. A suitable crystal 0.25×0.15×0.10 mm^3 was selected and mounted on a MITIGEN holder with silicon oil on a Rigaku AFC12 FRE-VHF diffractometer. The crystal was kept at a steady T = 100(2) K during data collection. The structure was solved with the **ShelXS**[176] structure solution program using the Direct Methods solution method and by using **Olex2**[174] as the graphical interface. The model was refined with version 2016/6 of **ShelXL**[175] using Least Squares minimisation.

Table 14. Crystal data of 3.63.

Formula	$C_{11}H_9D_3O_3$
$D_{calc.}$/ g cm^{-3}	1.417
μ/mm^{-1}	0.101
Formula Weight	195.22
Colour	clear colourless
Shape	prism
Size/mm^3	0.25×0.15×0.10
T/K	100(2)
Crystal System	monoclinic
Space Group	$P2_1/c$
a/Å	7.2266(2)
b/Å	8.0387(2)
c/Å	31.6932(6)
α/°	90
β/°	96.282(2)
γ/°	90
V/Å^3	1830.08(8)
Z	8
Z'	2
Wavelength/Å	0.71073
Radiation type	MoK_α
Θ_{min}/°	1.939
Θ_{max}/°	31.816
Measured Refl.	48674
Independent Refl.	5842
Reflections with I > 2(I)	5373
R_{int}	0.0889
Parameters	258
Restraints	0
Largest Peak	0.313
Deepest Hole	–0.313
GooF	1.097
wR_2 (all data)	0.1383
wR_2	0.1364
R_1 (all data)	0.0514
R_1	0.0485

5.6.6 4-methoxycubyl)(piperidin–1–yl)methanone (3.68)

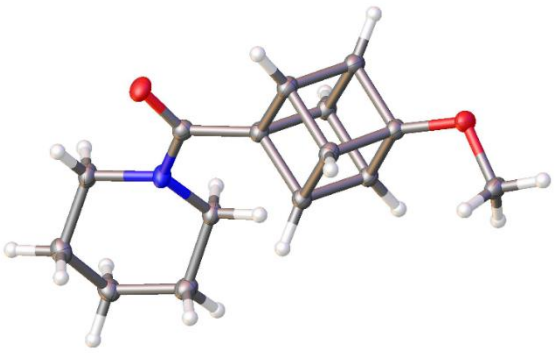

Figure 49. Structure of 3.68 with thermal ellipsoids drawn at the 50% probability level.

Experimental. Single clear colourless prism-shaped crystals of **2019sot0026_K1_100K** were recrystallised from a mixture of chloroform and hexane by slow evaporation. A suitable crystal 0.50×0.23×0.11 mm^3 was selected and mounted on a MITIGEN holder with silicon oil on a Rigaku AFC12 FRE-HF diffractometer. The crystal was kept at a steady T = 100(2) K during data collection. The structure was solved with the **ShelXT**[173] structure solution program using the Intrinsic Phasing solution method and by using **Olex2**[174] as the graphical interface. The model was refined with version 2016/6 of **ShelXL**[175] using Least Squares minimisation.

Table 15. Crystal data of 3.68.

Formula	$C_{15}H_{19}NO_2$
$D_{calc.}$/ g cm^{-3}	1.343
μ/mm^{-1}	0.089
Formula Weight	245.31
Colour	clear colourless
Shape	prism
Size/mm^3	0.50×0.23×0.11
T/K	100(2)
Crystal System	monoclinic
Space Group	$P2_1/c$
a/Å	16.0713(3)
b/Å	7.62370(10)
c/Å	19.8566(3)
α/°	90
β/°	93.939(2)
γ/°	90
V/$Å^3$	2427.14(7)
Z	8
Z'	2
Wavelength/Å	0.71073
Radiation type	MoKα
Θ_{min}/°	2.863
Θ_{max}/°	28.497
Measured Refl.	62922
Independent Refl.	6147
Reflections with I > 2(I)	5670
R_{int}	0.0373
Parameters	327
Restraints	0
Largest Peak	0.414
Deepest Hole	-0.234
GooF	1.097
wR_2 (all data)	0.1367
wR_2	0.1328
R_1 (all data)	0.0558
R_1	0.0514

5.6.7 Trimethyl–1,2,4–cubanetricarboxylate [CCDC: 1977608] (4.12)

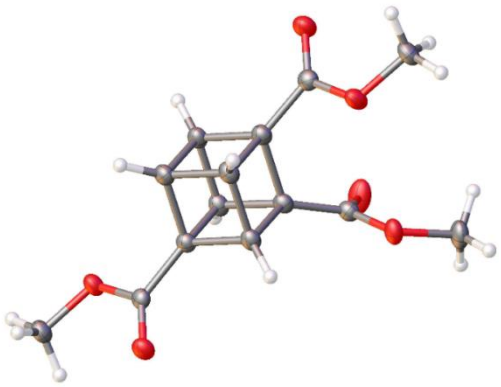

Figure 50. Structure of 4.12 with thermal ellipsoids drawn at the 50% probability level.

Experimental. Single clear colourless plate-shaped crystals of **DC_8835_53** were recrystallised from a mixture of CHCl3 and methanol by slow evaporation. A suitable crystal 0.35×0.06×0.02 mm^3 was selected and mounted on a MITIGEN holder with silicon oil on a Rigaku AFC12 FRE-HF diffractometer. The crystal was kept at a steady T = 100(2) K during data collection. The structure was solved with the **ShelXT**[173] structure solution program using the Intrinsic Phasing solution method and by using **Olex2**[174] as the graphical interface. The model was refined with version 2016/6 of **ShelXL**[175] using Least Squares minimisation. Code: 2019sot0028_K1_100K.

Table 16. Crystal data of 4.12.

Formula	$C_{14}H_{14}O_6$
$D_{calc.}$/ g cm^{-3}	1.475
μ/mm^{-1}	0.116
Formula Weight	278.25
Colour	clear colourless
Shape	plate
Size/mm^3	0.35×0.06×0.02
T/K	100(2)
Crystal System	triclinic
Space Group	P-1
a/Å	6.0744(4)
b/Å	7.0437(4)
c/Å	14.9245(9)
α/°	91.359(5)
β/°	101.082(6)
γ/°	90.857(5)
V/$Å^3$	626.36(7)
Z	2
Z'	1
Wavelength/Å	0.71073
Radiation type	MoK_α
Θ_{min}/°	2.893
Θ_{max}/°	28.493
Measured Refl.	9481
Independent Refl.	3086
Reflections with I >2	2429
2(I)	
R_{int}	0.0398
Parameters	184
Restraints	0
Largest Peak	0.453
Deepest Hole	-0.309
GooF	1.117
wR_2 (all data)	0.1631
wR_2	0.1493
R_1 (all data)	0.0881
R_1	0.0664

5.6.8 Dimethyl–2–(*tert*-Butylcarbamoyl)–1,4–cubanedicarboxylate [CCDC: 1986355] (4.20)

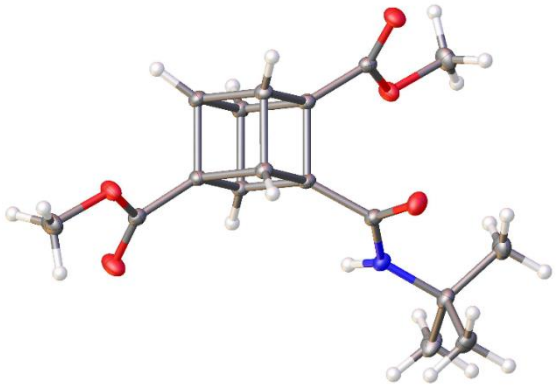

Figure 51. Structure of 4.20 with thermal ellipsoids drawn at the 50% probability level.

Experimental. Single clear colourless plate-shaped crystals of **DC_9040_** were recrystallised from DCM by slow evaporation. A suitable crystal 0.50×0.33×0.03 mm^3 was selected and mounted on a MITIGEN holder with silicon oil on a Rigaku AFC12 FRE-HF diffractometer. The crystal was kept at a steady T = 100(2) K during data collection. The structure was solved with the **ShelXT**[173] structure solution program using the Intrinsic Phasing solution method and by using **Olex2**[174] as the graphical interface. The model was refined with version 2016/6 of **ShelXL**[175] using Least Squares minimisation. Code: 2020sot0005_K1_100K

Table 17. Crystal data of 4.20.

Formula	$C_{17}H_{21}NO_5$
$D_{calc.}$/ g cm^{-3}	1.377
μ/mm^{-1}	0.101
Formula Weight	319.35
Colour	clear colourless
Shape	plate
Size/mm^3	0.50×0.33×0.03
T/K	100(2)
Crystal System	triclinic
Flack Parameter	0.2(2)
Hooft Parameter	0.23(18)
Space Group	$P1$
a/Å	5.96360(10)
b/Å	6.93180(10)
c/Å	10.2011(2)
α/°	99.157(2)
β/°	97.994(2)
γ/°	109.110(2)
V/$Å^3$	385.032(13)
Z	1
Z'	1
Wavelength/Å	0.71073
Radiation type	MoK_α
Θ_{min}/°	3.187
Θ_{max}/°	32.239
Measured Refl.	24276
Independent Refl.	5106
Reflections with I >2(I)	5061
R_{int}	0.0297
Parameters	217
Restraints	3
Largest Peak	0.422
Deepest Hole	-0.249
GooF	1.036
wR_2 (all data)	0.0900
wR_2	0.0898
R_1 (all data)	0.0338
R_1	0.0335

5.6.9 Dimethyl 2–(phenyl)–1,4–cubanedicarboxylate [CCDC: 2057837] (4.29)

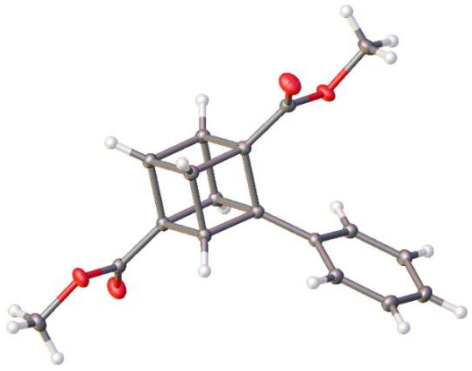

Figure 52. Structure of 4.29 with thermal ellipsoids drawn at the 50% probability level.

Experimental. Single clear colourless prism crystals of **DC_9040_78** recrystallised from a mixture of hexane and EtOAc by slow evaporation. A suitable crystal with dimensions 0.21 × 0.05 × 0.04 mm3 was selected and mounted on a MITIGEN holder in perfluoroether oil on a Rigaku AFC12 FRE-VHF diffractometer. The crystal was kept at a steady T = 100(2) K during data collection. The structure was solved with the **ShelXT**[173] solution program using dual methods and by using **Olex2**[174] as the graphical interface. The model was refined with **ShelXL**[175] using full matrix least squares minimisation on F^2. Code: 2020sot0036_R1_100K.

Table 18. Crystal data of 4.29.

Formula	$C_{18}H_{16}O_4$
$D_{calc.}$/ g cm^{-3}	1.429
μ/mm^{-1}	0.101
Formula Weight	296.31
Colour	clear colourless
Shape	prism
Size/mm^3	0.21×0.05×0.04
T/K	100(2)
Crystal System	triclinic
Space Group	P-1
a/Å	5.88770(10)
b/Å	7.21410(10)
c/Å	17.5076(3)
a/°	96.614(2)
b/°	96.525(2)
g/°	109.116(2)
V/Å^3	688.81(2)
Z	2
Z'	1
Wavelength/Å	0.71073
Radiation type	Mo K_α
Θ_{min}/°	2.373
Θ_{max}/°	32.599
Measured Refl's.	37759
Indep't Refl's	4500
Refl's I≥2 s(I)	3939
R_{int}	0.0306
Parameters	201
Restraints	0
Largest Peak	0.491
Deepest Hole	-0.325
GooF	1.086
wR_2 (all data)	0.1191
wR_2	0.1156
R_1 (all data)	0.0455
R_1	0.0400

Appendix A Synthesis of Dimethyl Cubane Dicarboxylate

A.1 Characterisation of the dione 2.6

The dione **2.6** is not stable and after 4 months at room temperature in a closed vial the mixture of hydrates was re–obtained. Repeated azeotropic distillation in toluene on the rotavap can be carried out in order to obtain the dione **2.6**.

Procedure: Add toluene in a mixture of hydrates and evaporate slowly under vacuum at 60 ˚C. Repeat this procedure several times. Afterwards, chloroform is added (most of the solid should dissolved as the dione **2.6** is soluble in chloroform and evaporate). This last sequence is repeated 2–3 times and the sample is left under high–vacuum for 1 h.

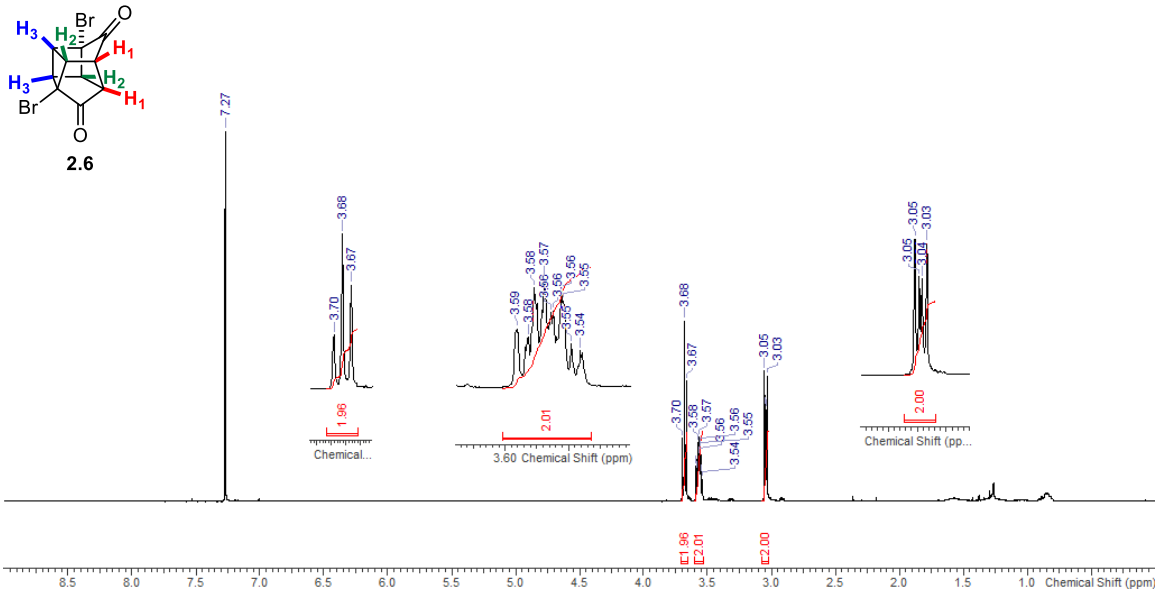

Figure 53. ^{1}H NMR of 2.6 (400 MHz, $CDCl_3$). Reprinted with permission from ref [83]. Copyright 2021 Georg Thieme Verlag KG.

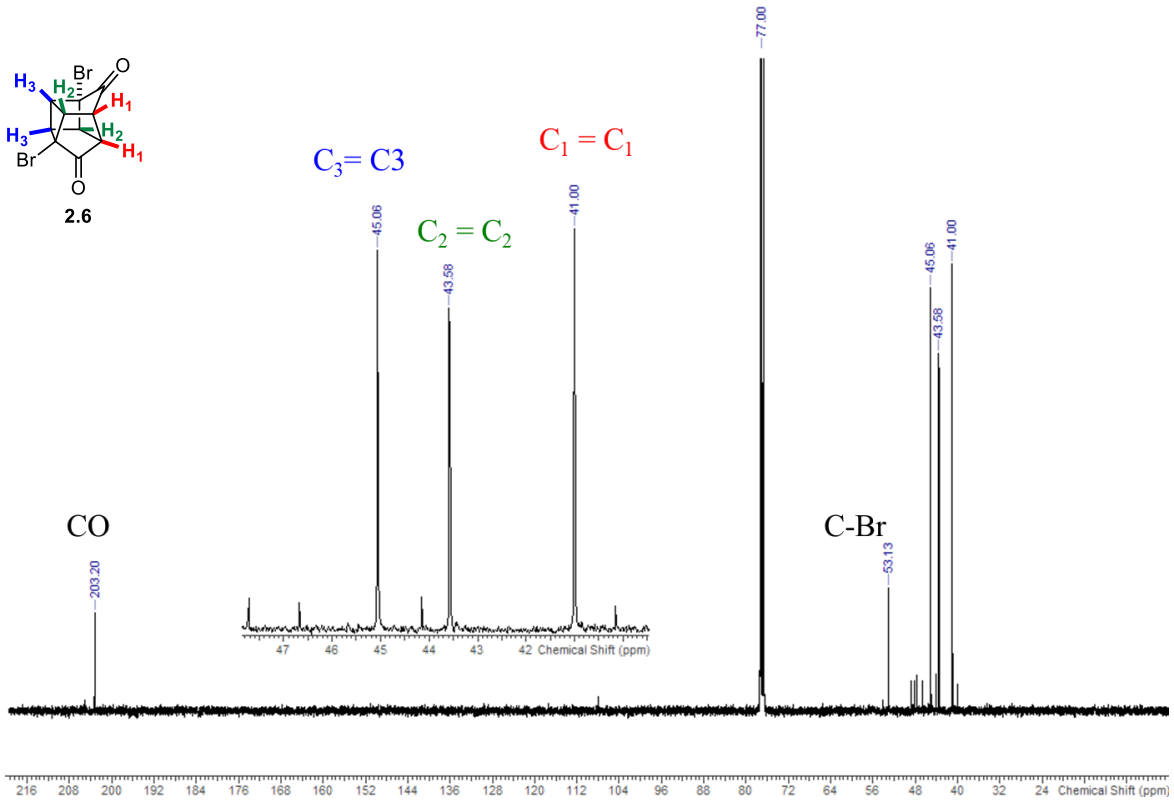

Figure 54. ^{13}C NMR of 2.6 (101 MHz, $CDCl_3$). Reprinted with permission from ref.[83] Copyright 2021 Georg Thieme Verlag KG.

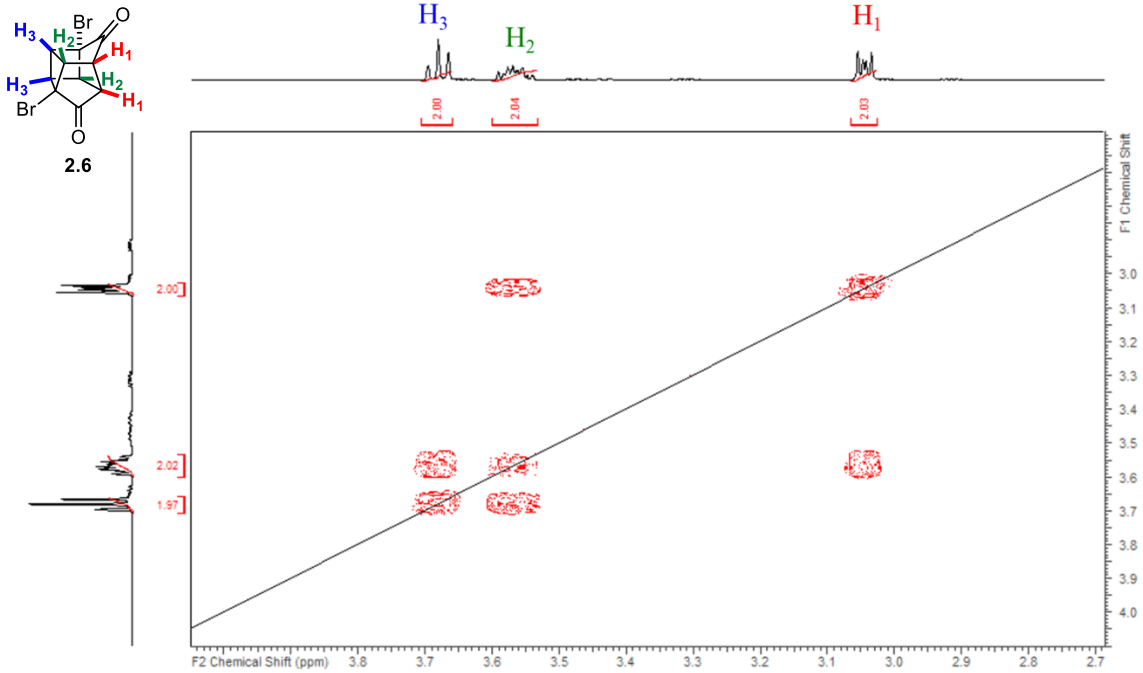

Figure 55. ^{1}H COSY NMR of 2.6 (400 MHz, $CDCl_3$). Reprinted with permission from ref.[83] Copyright 2021 Georg Thieme Verlag KG.

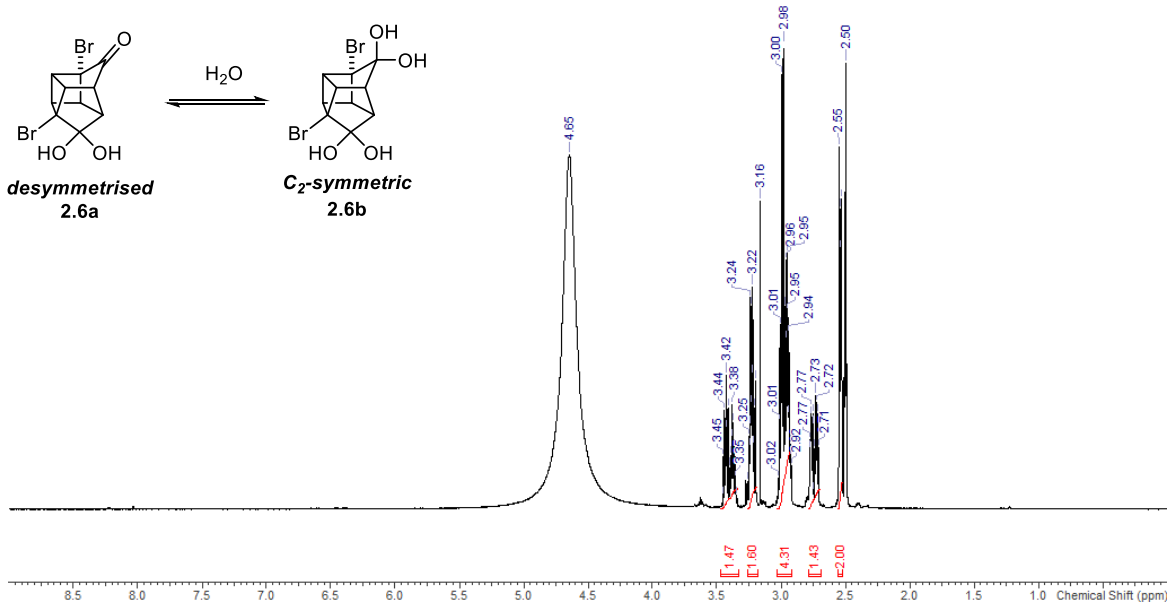

Figure 56. ^{1}H NMR of 2.6a and 2.6b (400 MHz, DMSO–d_6). Reprinted with permission from ref. [83] Copyright 2021 Georg Thieme Verlag KG.

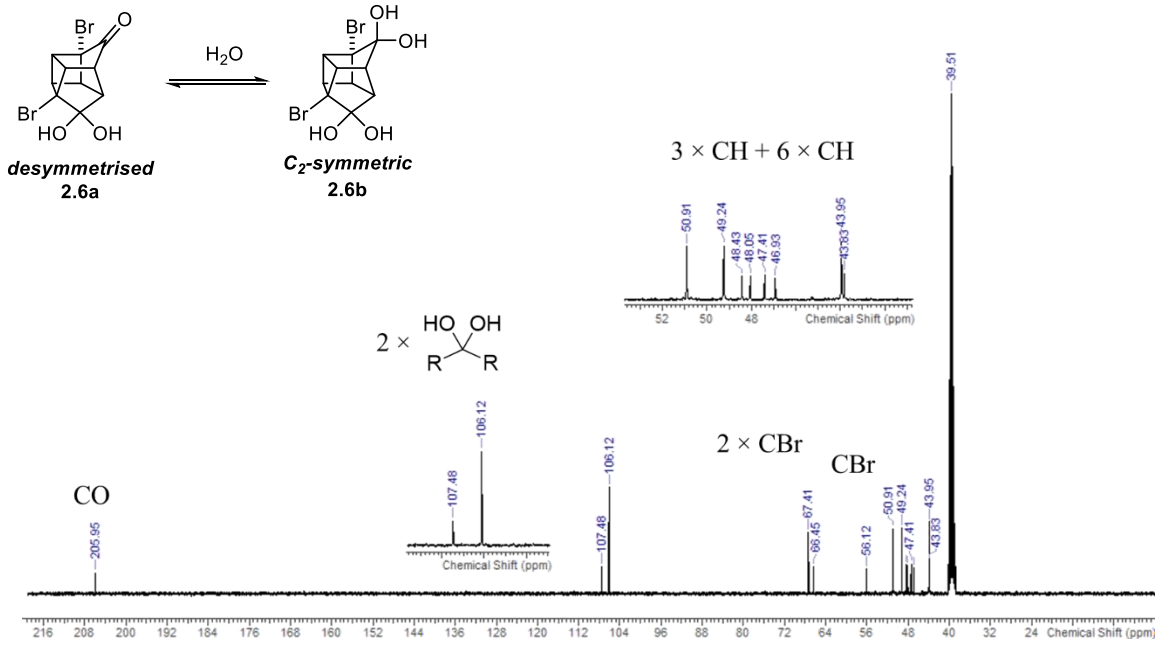

Figure 57. ^{13}C NMR of 2.6a and 2.6b (101 MHz, DMSO–d_6). Reprinted with permission from ref.[83] Copyright 2021 Georg Thieme Verlag KG.

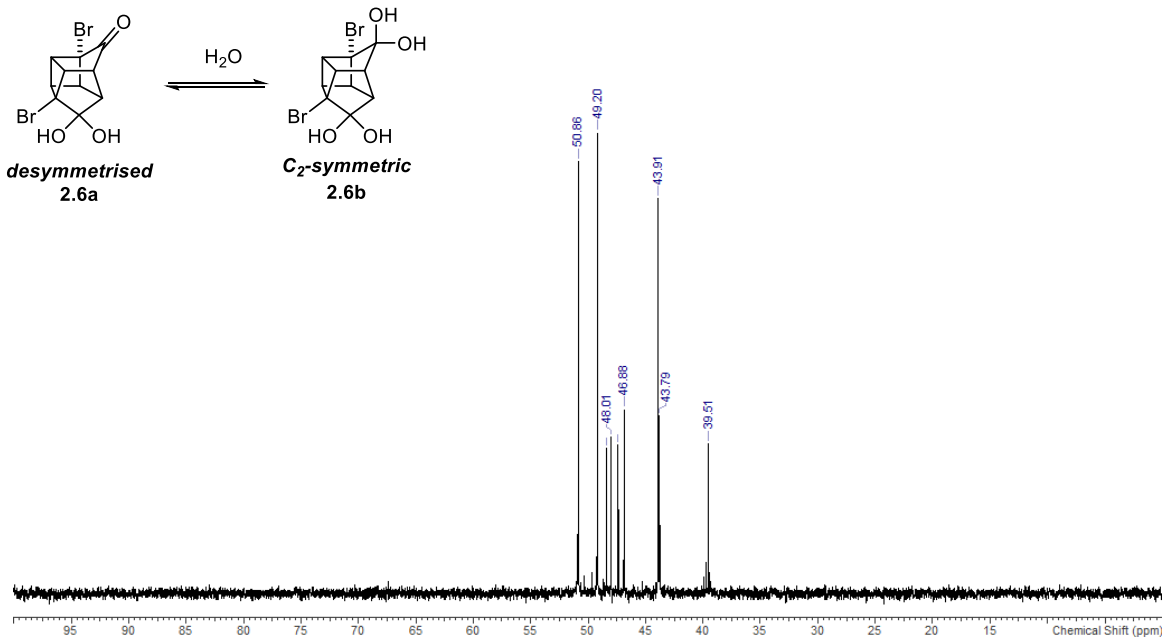

Figure 58. ^{13}C NMR DEPT 45 of 2.6a amd 2.6b (101 MHz, DMSO–d_6).

A.2 Conversion calculated towards 2.6 according the residence time

The [2+2]cycloadduct correspond to a mixture of hydrates, and according ^{1}H COSY NMR, we concluded the observation of two equilibrated species, **2.6a** and **2.6b** an unsymmetric and symmetric molecule respectively. The conversion was calculated by using the sum of the integral values of both "observed" products, compared to the respective integral value of the characteristic olefinic proton of the dione **2.5.**

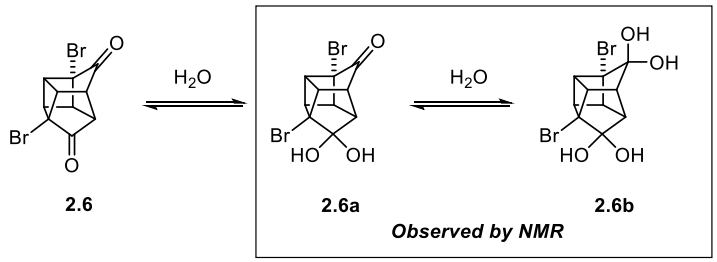

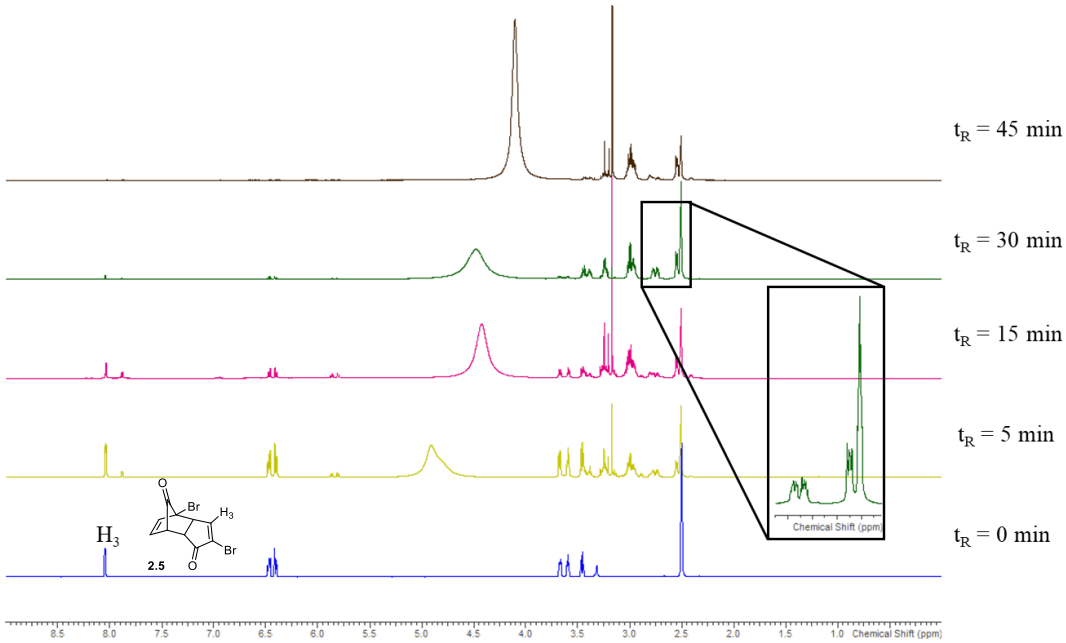

Figure 59. ^{1}H NMR collected according the residence time using 9 W UV–B broadband lamp.

Formula:

$$Conversion\ \% = \frac{I\left(\frac{2.54\ ppm}{2}\right) + I\left(\frac{2.75\ ppm}{2}\right)}{I\left(\frac{8.03\ ppm}{1}\right) + I\left(\frac{2.54\ ppm}{2}\right) + I\left(\frac{2.75\ ppm}{2}\right)} * 100$$

Theoretical productivity calculations for the photochemical reactors:

$$P_{theo} = \left(\frac{Flow\ rate\ \times\ Concentration}{1000}\right) \times MW\ \times 60 \times Conversion$$

Concentration = 0.1 M

Molecular Weight = 317.96 g.mol^{-1}

Conversion = 99%

A.3 UV–Spectra

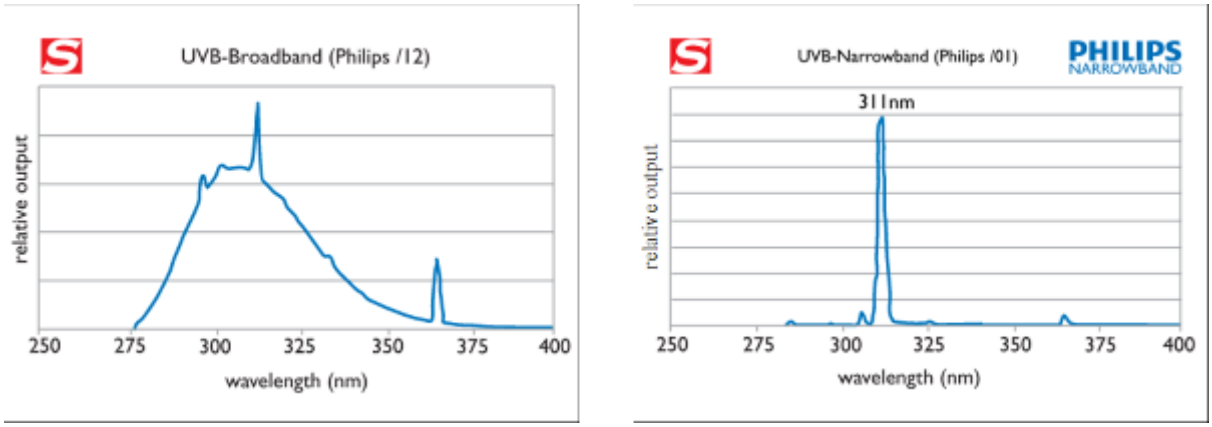

Figure 60. UV–spectra of UV–B broadband and narrowband lamps. Reprinted with permission from ref.[83] Copyright 2021 Georg Thieme Verlag KG.

Bibliography

(1) Lamberth, C.; Jeanmart, S.; Luksch, T.; Plant, A. Current Challenges and Trends in the Discovery of Agrochemicals. *Science* **2013**, *341*, 742–746.

(2) Khanna, I. Drug Discovery in Pharmaceutical Industry: Productivity Challenges and Trends. *Drug Discov. Today* **2012**, *17*, 1088–1102.

(3) Suryanarayana Birudukota, N. V.; Franke, R.; Hofer, B. An Approach to "Escape from Flatland": Chemo-Enzymatic Synthesis and Biological Profiling of a Library of Bridged Bicyclic Compounds. *Org. Biomol. Chem.* **2016**, *14*, 3821–3837.

(4) Brown, D. G.; Boström, J. Analysis of Past and Present Synthetic Methodologies on Medicinal Chemistry: Where Have All the New Reactions Gone? *J. Med. Chem.* **2016**, *59*, 4443–4458.

(5) Lovering, F.; Bikker, J.; Humblet, C. Escape from Flatland: Increasing Saturation as an Approach to Improving Clinical Success. *J. Med. Chem.* **2009**, *52*, 6752–6756.

(6) Hung, A. W.; Ramek, A.; Wang, Y.; Kaya, T.; Wilson, J. A.; Clemons, P. A.; Young, D. W. Route to Three-Dimensional Fragments Using Diversity-Oriented Synthesis. *Proc. Natl. Acad. Sci. U. S. A.* **2011**, *108*, 6799–6804.

(7) Lovering, F. Escape from Flatland 2: Complexity and Promiscuity. *Med. Chem. Commun.* **2013**, *4*, 515–519.

(8) Morrison, C. N.; Prosser, K. E.; Stokes, R. W.; Cordes, A.; Metzler-Nolte, N.; Cohen, S. M. Expanding Medicinal Chemistry into 3D Space: Metallofragments as 3D Scaffolds for Fragment-Based Drug Discovery. *Chem. Sci.* **2020**, *11*, 1216–1225.

(9) Auberson, Y. P.; Brocklehurst, C.; Furegati, M.; Fessard, T. C.; Koch, G.; Decker, A.; La Vecchia, L.; Briard, E. Improving Nonspecific Binding and Solubility: Bicycloalkyl Groups and Cubanes as Para-Phenyl Bioisosteres. *ChemMedChem* **2017**, *12*, 590–598.

(10) Langmuir, I. Isomorphism, Isosterism and Covalence. *J. Am. Chem. Soc.* **1919**, *41*, 1543–1559.

(11) Patani, G. A.; LaVoie, E. J. Bioisosterism: A Rational Approach in Drug Design. *Chem. Rev.* **1996**, *96*, 3147–3176.

(12) Meanwell, N. A. Synopsis of Some Recent Tactical Application of Bioisosteres. *J. Med. Chem.* **2011**, *54*, 2529–2591.

(13) Meanwell, N. A. The Influence of Bioisosteres in Drug Design: Tactical Applications to Address Developability Problems. In *Tactics in Contemporary Drug Design*; Springer: Berlin, Heidelberg, 2013; pp 283–381.

(14) Thornber, C. W. Isosterism and Molecular Modification in Drug Design. *Chem. Soc. Rev.* **1979**, *8*, 563–580.

(15) Brown, N. Bioisosterism in Medicinal Chemistry. In *Bioisosteres in Medicinal Chemistry*; Wiley-VCH Verlag GmbH & Co. KGaA: Weinheim, Germany, 2012; Vol. 54, pp 1–14.

(16) Huchet, Q. A.; Kuhn, B.; Wagner, B.; Kratochwil, N. A.; Fischer, H.; Kansy, M.; Zimmerli, D.; Carreira, E. M.; Müller, K. Fluorination Patterning: A Study of Structural Motifs That Impact Physicochemical Properties of Relevance to Drug Discovery. *J. Med. Chem.* **2015**, *58*, 9041–9060.

(17) Zhou, Y.; Wang, J.; Gu, Z.; Wang, S.; Zhu, W.; Acenã, J. L.; Soloshonok, V. A.; Izawa, K.; Liu, H. Next Generation of Fluorine-Containing Pharmaceuticals, Compounds Currently in Phase II-III Clinical Trials of Major Pharmaceutical Companies: New Structural Trends and Therapeutic Areas. *Chem. Rev.* **2016**, *116*, 422–518.

(18) Meanwell, N. A. Fluorine and Fluorinated Motifs in the Design and Application of Bioisosteres for Drug Design. *J. Med. Chem.* **2018**, *61*, 5822–5880.

(19) Lipinski, C. A. Bioisosterism in Drug Design. In *Annual Reports in Medicinal Chemistry*; 1986; Vol. 21, pp 283–291.

(20) Lima, L.; Barreiro, E. Bioisosterism: A Useful Strategy for Molecular Modification and Drug Design. *Curr. Med. Chem.* **2012**, *12*, 23–49.

(21) Mykhailiuk, P. K. Saturated Bioisosteres of Benzene: Where to Go Next? *Org. Biomol. Chem.* **2019**, *17*, 2839–2849.

(22) Tse, E.; Houston, S.; Williams, C.; Savage, G. P.; Rendina, L.; Hallyburton, I.; Anderson, M.; Sharma, R.; Walker, G.; Obach, R. S.; Todd, M. Non-Classical Phenyl Bioisosteres as Effective Replacements in a Series of Novel Open Source Antimalarials. *J. Med. Chem.* **2020**.

(23) Qiao, J. X.; Cheney, D. L.; Alexander, R. S.; Smallwood, A. M.; King, S. R.; He, K.; Rendina, A. R.; Luettgen, J. M.; Knabb, R. M.; Wexler, R. R.; Lam, P. Y. S. Achieving Structural Diversity Using the Perpendicular Conformation of Alpha-Substituted Phenylcyclopropanes to Mimic the Bioactive Conformation of Ortho-Substituted Biphenyl P4 Moieties: Discovery of Novel, Highly Potent Inhibitors of Factor Xa. *Bioorg. Med. Chem. Lett.* **2008**, *18*, 4118–4123.

(24) Stepan, A. F.; Subramanyam, C.; Efremov, I. V; Dutra, J. K.; O'Sullivan, T. J.; DiRico, K. J.; McDonald, W. S.; Won, A.; Dorff, P. H.; Nolan, C. E.; Becker, S. L.; Pustilnik, L. R.; Riddell, D. R.; Kauffman, G. W.; Kormos, B. L.; Zhang, L.; Lu, Y.; Capetta, S. H.; Green, M. E.; Karki, K.; Sibley, E.; Atchison, K. P.; Hallgren, A. J.; Oborski, C. E.; Robshaw, A. E.; Sneed, B.; O'Donnell, C. J. Application of the Bicyclo[1.1.1]Pentane Motif as a Nonclassical Phenyl Ring Bioisostere in the Design of a Potent and Orally Active γ-Secretase Inhibitor. *J. Med. Chem.* **2012**, *55*, 3414–3424.

(25) Aguilar, A.; Lu, J.; Liu, L.; Du, D.; Bernard, D.; McEachern, D.; Przybranowski, S.; Li, X.; Luo, R.; Wen, B.; Sun, D.; Wang, H.; Wen, J.; Wang, G.; Zhai, Y.; Guo, M.; Yang, D.; Wang, S. Discovery of 4-((3′ R ,4′ S ,5′ R)-6″-Chloro-4′-(3-Chloro-2-Fluorophenyl)-1′-Ethyl-2″-Oxodispiro[Cyclohexane-1,2′-Pyrrolidine-3′,3″-Indoline]-5′-Carboxamido)Bicyclo[2.2.2]Octane-1-Carboxylic Acid (AA-115/APG-115): A Potent and Orally Active Murine Double. *J. Med. Chem.* **2017**, *60*, 2819–2839.

(26) Eaton, P. E. Cubanes: Starting Materials for the Chemistry of the 1990s and the New Century. *Angew. Chem. Int. Ed.* **1992**, *31*, 1421–1436.

(27) Wlochal, J.; Davies, R. D. M.; Burton, J. Cubanes in Medicinal Chemistry: Synthesis of Functionalized Building Blocks. *Org. Lett.* **2014**, *16*, 4094–4097.

(28) Chalmers, B. A.; Xing, H.; Houston, S.; Clark, C.; Ghassabian, S.; Kuo, A.; Cao, B.; Reitsma, A.; Murray, C.-E. P.; Stok, J. E.; Boyle, G. M.; Pierce, C. J.; Littler, S. W.; Winkler, D. A.; Bernhardt, P. V.; Pasay, C.; De Voss, J. J.; McCarthy, J.; Parsons, P. G.; Walter, G. H.; Smith, M. T.; Cooper, H. M.; Nilsson, S. K.; Tsanaktsidis, J.; Savage, G. P.; Williams, C. M. Validating Eaton's Hypothesis: Cubane as a Benzene Bioisostere. *Angew. Chem. Int. Ed.* **2016**, *55*, 3580–3585.

(29) Nicolaou, K. C.; Vourloumis, D.; Totokotsopoulos, S.; Papakyriakou, A.; Karsunky, H.; Fernando, H.; Gavrilyuk, J.; Webb, D.; Stepan, A. F. Synthesis and Biopharmaceutical Evaluation of Imatinib Analogues Featuring Unusual Structural Motifs. *ChemMedChem* **2016**, *11*, 31–37.

(30) Joubert, J.; Geldenhuys, W. J.; VanderSchyf, C. J.; Oliver, D. W.; Kruger, H. G.; Govender, T.; Malan, S. F. Polycyclic Cage Structures as Lipophilic Scaffolds for Neuroactive Drugs. *ChemMedChem* **2012**, *7*, 375–384.

(31) Wilkinson, S. M.; Gunosewoyo, H.; Barron, M. L.; Boucher, A.; McDonnell, M.; Turner, P.; Morrison, D. E.; Bennett, M. R.; McGregor, I. S.; Rendina, L. M.; Kassiou, M. The First Cns-Active Carborane: A Novel P2x7 Receptor Antagonist with Antidepressant Activity. *ACS Chem. Neurosci.* **2014**, *5*, 335–339.

(32) Danon, J. J.; Reekie, T. A.; Kassiou, M. Challenges and Opportunities in Central Nervous System Drug Discovery. *Trends Chem.* **2019**, *1*, 612–624.

(33) Cheung, Y. W.; Röthlisberger, P.; Mechaly, A. E.; Weber, P.; Levi-Acobas, F.; Lo, Y.; Wong, A. W. C.; Kinghorn, A. B.; Haouz, A.; Paul Savage, G.; Hollenstein, M.; Tanner, J. A. Evolution of Abiotic Cubane Chemistries in a Nucleic Acid Aptamer Allows Selective Recognition of a Malaria Biomarker. *Proc. Natl. Acad. Sci. U. S. A.* **2020**, *117*, 16790–16798.

(34) Reekie, T. A.; Williams, C. M.; Rendina, L. M.; Kassiou, M. Cubanes in Medicinal Chemistry. *J. Med. Chem.* **2019**, *62*, 1078–1095.

(35) Mykhailiuk, P. K. Saturated Bioisosteres of Benzene: Where to Go Next? *Org. Biomol. Chem.* **2019**, *17*, 2839–2849.

(36) Biegasiewicz, K. F.; Griffiths, J. R.; Savage, G. P.; Tsanaktsidis, J.; Priefer, R. Cubane: 50 Years Later. *Chem. Rev.* **2015**, *115*, 6719–6745.

(37) Eaton, P. E.; Cole, T. W. Cubane. *J. Am. Chem. Soc.* **1964**, *86*, 3157–3158.

(38) Della, E. W.; Tsanaktsidis, J. Decarboxylation of Bridgehead Carboxylic Acids by the Barton Procedure. *Aust. J. Chem.* **1985**, *39*, 2061–2066.

(39) Publication, A. Reductive Radical Decarboxylation of Aliphatic Carboxylic Acids. *Org. Synth.* **2012**, *89*, 471.

(40) Moriarty, R. M.; Khosrowshahi, J. S.; Miller, R. S.; Flippen-Andersen, J.; Gilardi, R. Free-Radical Arylation of Cubane Using Cubyl Lead Acylates. *J. Am. Chem. Soc.* **1989**, *111*, 8943–8944.

(41) Kochi, J. K. A New Method for Halodecarboxylation of Acids Using Lead(IV) Acetate. *J. Am. Chem. Soc.* **1965**, *87*, 2500–2502.

(42) Gianatassio, R.; Kawamura, S.; Eprile, C. L.; Foo, K.; Ge, J.; Burns, A. C.; Collins, M. R.; Baran, P. S. Simple Sulfinate Synthesis Enables C-H Trifluoromethylcyclopropanation. *Angew. Chem. Int. Ed.* **2014**, *53*, 9851–9855.

(43) Cornella, J.; Edwards, J. T.; Qin, T.; Kawamura, S.; Wang, J.; Pan, C.-M.; Gianatassio, R.; Schmidt, M.; Eastgate, M. D.; Baran, P. S. Practical Ni-Catalyzed Aryl–Alkyl Cross-Coupling of Secondary Redox-Active Esters. *J. Am. Chem. Soc.* **2016**, *138*, 2174–2177.

(44) Toriyama, F.; Cornella, J.; Wimmer, L.; Chen, T. G.; Dixon, D. D.; Creech, G.; Baran, P. S. Redox-Active Esters in Fe-Catalyzed C-C Coupling. *J. Am. Chem. Soc.* **2016**, *138*, 11132–11135.

(45) Qin, T.; Malins, L. R.; Edwards, J. T.; Merchant, R. R.; Novak, A. J. E.; Zhong, J. Z.; Mills, R. B.; Yan, M.; Yuan, C.; Eastgate, M. D.; Baran, P. S. Nickel-Catalyzed Barton Decarboxylation and Giese Reactions: A Practical Take on Classic Transforms. *Angew. Chem. Int. Ed.* **2017**, *56*, 260–265.

(46) Bernhard, S. S. R.; Locke, G. M.; Plunkett, S.; Meindl, A.; Flanagan, K. J.; Senge, M. O. Cubane Cross-Coupling and Cubane–Porphyrin Arrays. *Chem. Eur. J.* **2018**, *24*, 1026–1030.

(47) Li, C.; Wang, J.; Barton, L. M.; Yu, S.; Tian, M.; Peters, D. S.; Kumar, M.; Yu, A. W.; Johnson, K. A.; Chatterjee, A. K.; Yan, M.; Baran, P. S. Decarboxylative Borylation. *Science* **2017**, *356*.

(48) Fawcett, A.; Pradeilles, J.; Wang, Y.; Mutsuga, T.; Myers, E. L.; Aggarwal, V. K. Photoinduced Decarboxylative Borylation of Carboxylic Acids. *Science* **2017**, *357*, 283–286.

(49) Eaton, P. E.; Maggini, M. Cubene (1, 2-Dehydrocubane). *J. Am. Chem. Soc.* **1988**, *110*, 7230–7232.

(50) Eaton, P. E.; Tsanaktsidis, J. The Reactions of 1,4-Dihalocubanes with Organolithiums. The Case for 1,4-Cubadiyl. *J. Am. Chem. Soc.* **1990**, *112*, 876–878.

(51) Eaton, P. E.; Pramod, K.; Emrick, T.; Gilardi, R. Building with Cubane-1,4-Diyl. Synthesis of Aryl-Substituted Cubanes, p- [n]Cubyls, and Cubane-Separated Bis(Arenes). *J. Am. Chem. Soc.* **1999**, *121*, 4111–4123.

(52) Plunkett, S.; Flanagan, K. J.; Twamley, B.; Senge, M. O. Highly Strained Tertiary Sp^3 Scaffolds: Synthesis of Functionalized Cubanes and Exploration of Their Reactivity under Pd(II) Catalysis. *Organometallics* **2015**, *34*, 1408–1414.

(53) Kato, Y.; Williams, C. M.; Uchiyama, M.; Matsubara, S. A Protocol for an Iodine-Metal Exchange Reaction on Cubane Using Lithium Organozincates. *Org. Lett.* **2019**, *21*, 473–475.

(54) Yoshino, N.; Kato, Y.; Mabit, T.; Nagata, Y.; Williams, C. M.; Harada, M.; Muranaka, A.; Uchiyama, M.; Matsubara, S. Cubane Chirality via Substitution of a "Hidden" Regular Tetrahedron. *Org. Lett.* **2020**, *22*, 4083–4087.

(55) Beak, P.; Snieckus, V. Directed Lithiation of Aromatic Tertiary Amides: An Evolving Synthetic Methodology for Polysubstituted Aromatics. *Acc. Chem. Res.* **1982**, *15*, 306–312.

(56) Eaton, P. E.; Castaldi, G. Systematic Substitution on the Cubane Nucleus. Amide Activation for Metalation of "Saturated" Systems. *J. Am. Chem. Soc.* **1985**, *107*, 724–726.

(57) Bashir-Hashemi, A. New Developments in Cubane Chemistry: Phenylcubanes. *J. Am. Chem.*

Soc. **1988**, *110*, 7234–7235.

(58) Eaton, P. E.; Cunkle, G. T.; Marchioro, G.; Martin, R. M. Reverse Transmetalation: A Strategy for Obtaining Certain Otherwise Difficultly Accessible Organometallics. *J. Am. Chem. Soc.* **1987**, *109*, 948–949.

(59) Eaton, P. E.; Lee, C. H.; Xiong, Y. Magnesium Amide Bases and Amido-Grignards. 1. Ortho Magnesiation. *J. Am. Chem. Soc.* **1989**, *111*, 8016–8018.

(60) Eaton, P. E.; Xiong, Y.; Zhou, J. P. Systematic Substitution on the Cubane Nucleus: Steric and Electronic Effects. *J. Org. Chem.* **1992**, *57*, 4277–4281.

(61) Hayata, Y. NII-Electronic Library Service. *Chem. Pharm. Bull.* **1993**, *41*, 1760–1768.

(62) Eaton, P. E.; Xiong, Y.; Gilardi, R. Systematic Substitution on the Cubane Nucleus. Synthesis and Properties of 1,3,5-Trinitrocubane and 1,3,5,7-Tetranitrocubane. *J. Am. Chem. Soc.* **1993**, *115*, 10195–10202.

(63) Bashir-Hashemi, A. Photochemical Carboxylation of Cubanes. *Angew. Chem. Int. Ed.* **1993**, *32*, 612–613.

(64) Bashir-Hashemi, A.; Li, J.; Gelber, N.; Ammon, H. Photochemical Functionalization of Cubanes. *J. Org. Chem.* **1995**, *60*, 698–702.

(65) Kharasch, M. S.; Brown, H. C. The Photochemical Reactions of Oxalyl Chloride and Phosgene with Cyclohexane. *J. Am. Chem. Soc.* **1940**, *62*, 454–454.

(66) Lowe, D.; Moorhouse, C.; Walter, J.; Tsanaktsidis, J. A New Approach to Alkylated Cubanes: The Synthesis of Dimethyl 2-Methylcubane-1,4-Dicarboxylate. *Aust. J. Chem.* **1994**, *47*, 1647–1650.

(67) Gutmann, B.; Cantillo, D.; Kappe, C. O. Continuous-Flow Technology - A Tool for the Safe Manufacturing of Active Pharmaceutical Ingredients. *Angew. Chem. Int. Ed.* **2015**, *54*, 6688–6728.

(68) Jiménez-González, C.; Poechlauer, P.; Broxterman, Q. B.; Yang, B. S.; Am Ende, D.; Baird, J.; Bertsch, C.; Hannah, R. E.; Dell'Orco, P.; Noorman, H.; Yee, S.; Reintjens, R.; Wells, A.; Massonneau, V.; Manley, J. Key Green Engineering Research Areas for Sustainable Manufacturing: A Perspective from Pharmaceutical and Fine Chemicals Manufacturers. *Org. Process Res. Dev.* **2011**, *15*, 900–911.

(69) Newman, S. G.; Jensen, K. F. The Role of Flow in Green Chemistry and Engineering. *Green Chem.* **2013**, *15*, 1456–1472.

(70) Plutschack, M. B.; Pieber, B.; Gilmore, K.; Seeberger, P. H. The Hitchhiker's Guide to Flow Chemistry. *Chem. Rev.* **2017**, *117*, 11796–11893.

(71) Su, Y.; Straathof, N. J. W.; Hessel, V.; Noël, T. Photochemical Transformations Accelerated in Continuous-Flow Reactors: Basic Concepts and Applications. *Chem. Eur. J.* **2014**, *20*, 10562–10589.

(72) Knowles, J. P.; Elliott, L. D.; Booker-Milburn, K. I. Flow Photochemistry: Old Light through New Windows. *Beilstein J. Org. Chem.* **2012**, *8*, 2025–2052.

(73) Cambié, D.; Bottecchia, C.; Straathof, N. J. W.; Hessel, V.; Noël, T. Applications of Continuous-Flow Photochemistry in Organic Synthesis, Material Science, and Water Treatment. *Chem. Rev.* **2016**, *116*, 10276–10341.

(74) Elliott, L. D.; Knowles, J. P.; Koovits, P. J.; Maskill, K. G.; Ralph, M. J.; Lejeune, G.; Edwards, L. J.; Robinson, R. I.; Clemens, I. R.; Cox, B.; Pascoe, D. D.; Koch, G.; Eberle, M.; Berry, M. B.; Booker-Milburn, K. I. Batch versus Flow Photochemistry: A Revealing Comparison of Yield and Productivity. *Chem. Eur. J.* **2014**, *20*, 15226–15232.

(75) Yan, M.; Kawamata, Y.; Baran, P. S. Synthetic Organic Electrochemical Methods Since 2000: On the Verge of a Renaissance. *Chem. Rev.* **2017**, *117*, 13230–13319.

(76) Green, R. A.; Brown, R. C. D.; Pletcher, D. Electrosynthesis in Extended Channel Length Microfluidic Electrolysis Cells. *J. Flow Chem.* **2016**, *6*, 191–197.

(77) Pletcher, D.; Green, R. A.; Brown, R. C. D. Flow Electrolysis Cells for the Synthetic Organic Chemistry Laboratory. *Chem. Rev.* **2018**, *118*, 4573–4591.

(78) Patra, T.; Maiti, D. Decarboxylation as the Key Step in C−C Bond-Forming Reactions. *Chem. Eur. J.* **2017**, *23*, 7382–7401.

(79) Weltner, W. "Acetylenic" Strained Hydrocarbons. *J. Am. Chem. Soc.* **1953**, *75*, 4224–4231.

(80) Freedman, H. . Tetraphenylcyclobutadiene Derivatives. IV.1 "Octaphenylcubane"; A Dimer of Tetraphenylcyclobutadiene. *J. Am. Chem. Soc.* **1962**, *84*, 2837–2838.

(81) Throndsen, H.P., Wheatley, P.J., Zeiss, H. Reduction of Cyclohexanones to Axial Alcohols via Iridium-Containing Catalysis. *Proc. Chem. Soc.* **1964**, 357–358.

(82) Eaton, P. E.; Cole, T. W. The Cubane System. *J. Am. Chem. Soc.* **1964**, *86*, 962–964.

(83) Collin, D. E.; Jackman, E. H.; Jouandon, N.; Sun, W.; Light, M. E.; Harrowven, D. C.; Linclau, B. Decagram Synthesis of Dimethyl 1,4-Cubanedicarboxylate Using Continuous-

Flow Photochemistry. *Synthesis* **2021**, *53*, 1307–1314.

(84) Chapman, N. B.; Key, J. M.; Toyne, K. J. The Preparation and Properties of Cage Polycyclic Systems. I. Pentacyclo[5.3.0.02,5.03,9.04,8]Decane and Pentacyclo[4.3.0.02,5.03,8.04,7]Nonane Derivatives. *J. Org. Chem.* **1970**, *35*, 3860–3867.

(85) DePuy, C. H.; Ponder, B. W.; Fitzpatrick, J. D. Cyclopentadienone Ethylene Ketal 1. *J. Org. Chem.* **1964**, *29*, 3508–3510.

(86) Lüh, T. Y.; Stock, L. M. On the Preparation of 1,4-Dicarboxycubane. *J. Org. Chem.* **1972**, *37*, 338–339.

(87) Bliese, M.; Tsanaktsidis, J. Dimethyl Cubane-1,4-Dicarboxylate: A Practical Laboratory Scale Synthesis. *Aust. J. Chem.* **1997**, *50*, 189–192.

(88) Falkiner, M. J.; Littler, S. W.; McRae, K. J.; Savage, G. P.; Tsanaktsidis, J. Pilot-Scale Production of Dimethyl 1,4-Cubanedicarboxylate. *Org. Process Res. Dev.* **2013**, *17*, 1503–1509.

(89) Barborak, J. C.; Watts, L.; Pettit, R. A Convenient Synthesis of the Cubane System. *J. Am. Chem. Soc.* **1966**, *88*, 1328–1329.

(90) Pelosi, L. F.; Miller, W. T. Syntheses from Perfluoro-2-Butyne. 2. Perfluorooctamethylcubane, Perfluorooctamethylcuneane, and Perfluorooctamethylcyclooctatetraene. *J. Am. Chem. Soc.* **1976**, *98*, 4311–4312.

(91) Gleiter, R.; Karcher, M. Synthesis and Properties of a Bridgedsyn-Tricyclo[4.2.0.02,5]Octa-3,7-Diene: Formation of Propella[34]Prismane. *Angew. Chem. Int. Ed.* **1988**, *27*, 840–841.

(92) Gleiter, R.; Brand, S. Generation of Octamethylcuneane and Octamethylcubane from Syn-Octamethyltricyclo[4.2.0.02,5]Octa-3,7-Diene. *Tetrahedron Letters* **1994**, *35*, 4969–4972.

(93) De Meijere, A.; Redlich, S.; Frank, D.; Magull, J.; Hofmeister, A.; Menzel, H.; König, B.; Svoboda, J. Octacyclopropylcubane and Some of Its Isomers. *Angew. Chem. Int. Ed.* **2007**, *46*, 4575–4576.

(94) Harrowven, D. C.; Mohamed, M.; Gonçalves, T. P.; Whitby, R. J.; Bolien, D.; Sneddon, H. F. An Efficient Flow-Photochemical Synthesis of 5H-Furanones Leads to an Understanding of Torquoselectivity in Cyclobutenone Rearrangements. *Angew. Chem. Int. Ed.* **2012**, *51*, 4405–4408.

(95) Bényei, G. Y.; Jalsovszky, I.; Slugovc, C.; Trimmel, G.; Pelzl, G.; Vajda, A.; Éber, N.; Fodor-Csorba, K. Structure and Properties of New Liquid Crystalline Cubane-1,4-Dicarboxylic Acid

Derivatives. *Liq. Cryst.* **2005**, *32*, 197–205.

(96) Dunn, G. L.; DiPasquo, V. J.; Hoover, J. R. E. Synthesis of Pentacyclo[4.3.0.03′5.03′8.04′7]None and Some 4-Substituted Derivatives. *Tetrahedron Letters* **1966**, *7*, 3737–3742.

(97) Stedman, R. J.; Davis, L. D. Nuclear Magnetic Resonance Spectra of Cage Ketones and Ketals. *Tetrahedron Letters* **1968**, *9*, 1871–1874.

(98) Pletcher, D. Electrolysis Cells for Laboratory Organic Synthesis. *Curr. Opin. Electrochem.* **2020**, *24*, 1–5.

(99) Lund, H. A Century of Organic Electrochemistry. *J. Electrochem. Soc.* **2002**, *149*, S21.

(100) Faraday, M. Siebente Reihe von Experimental-Untersuchungen Über Elektricität. *Ann. Phys.* **1834**, *109*, 481–520.

(101) Kolbe, H. Untersuchungen Über Die Elektrolyse Organischer Verbindungen. *Ann. der Chemie und Pharm.* **1849**, *69*, 257–294.

(102) Schäfer, H.-J. Recent Contributions of Kolbe Electrolysis to Organic Synthesis. In *Electrochemistry IV*; Springer-Verlag: Berlin/Heidelberg, 2005; pp 91–151.

(103) Tafel, J.; Hahl, H. Vollständige Reduktion Des Benzylacetessigesters. *Berichte der Dtsch. Chem. Gesellschaft* **1907**, *40*, 3312–3318.

(104) Pletcher, D.; Walsh, F. C. *Industrial Electrochemistry*; Springer Netherlands: Dordrecht, 1993; Vol. 35.

(105) Fuchigami, T.; Inagi, S. Electrochemical Fluorination for Preparation of Alkyl Fluorides. In *Fluorination*; Springer Singapore, 2020; pp 107–128.

(106) Shono, T.; Hamaguchi, H.; Matsumura, Y. Electroorganic Chemistry. XX. Anodic Oxidation of Carbamates. *J. Am. Chem. Soc.* **1975**, *97*, 4264–4268.

(107) Kuleshova, J.; Hill-Cousins, J. T.; Birkin, P. R.; Brown, R. C. D.; Pletcher, D.; Underwood, T. J. The Methoxylation of N-Formylpyrrolidine in a Microfluidic Electrolysis Cell for Routine Synthesis. *Electrochim. Acta* **2012**, *69*, 197–202.

(108) Kuleshova, J.; Hill-Cousins, J. T.; Birkin, P. R.; Brown, R. C. D.; Pletcher, D.; Underwood, T. J. A Simple and Inexpensive Microfluidic Electrolysis Cell. *Electrochim. Acta* **2011**, *56*, 4322–4326.

(109) Frankowski, K. J.; Liu, R.; Milligan, G. L.; Moeller, K. D.; Aubé, J. Practical Electrochemical

Anodic Oxidation of Polycyclic Lactams for Late Stage Functionalization. *Angew. Chem. Int. Ed.* **2015**, *54*, 10555–10558.

(110) Suga, S.; Okajima, M.; Fujiwara, K.; Yoshida, J. "Cation Flow" Method: A New Approach to Conventional and Combinatorial Organic Syntheses Using Electrochemical Microflow Systems. *J. Am. Chem. Soc.* **2001**, *123*, 7941–7942.

(111) Yoshida, J.; Suga, S. Basic Concepts of "Cation Pool" and "Cation Flow" Methods and Their Applications in Conventional and Combinatorial Organic Synthesis. *Chem. Eur. J.* **2002**, *8*, 2650.

(112) Yoshida, J. I.; Shimizu, A.; Hayashi, R. Electrogenerated Cationic Reactive Intermediates: The Pool Method and Further Advances. *Chem. Rev.* **2018**, *118*, 4702–4730.

(113) Green, R. A.; Jolley, K. E.; Al-Hadedi, A. A. M.; Pletcher, D.; Harrowven, D. C.; De Frutos, O.; Mateos, C.; Klauber, D. J.; Rincón, J. A.; Brown, R. C. D. Electrochemical Deprotection of Para-Methoxybenzyl Ethers in a Flow Electrolysis Cell. *Org. Lett.* **2017**, *19*, 2050–2053.

(114) Gütz, C.; Bänziger, M.; Bucher, C.; Galvão, T. R.; Waldvogel, S. R. Development and Scale-Up of the Electrochemical Dehalogenation for the Synthesis of a Key Intermediate for NS5A Inhibitors. *Org. Process Res. Dev.* **2015**, *19*, 1428–1433.

(115) Waters, J. A. Anodic Decarboxylation of Carboxylic Acids. *J. Org. Chem.* **1964**, *29*, 428–430.

(116) Gassman, P. G.; Fox, B. L. Electrolytic Decarboxylation of Quinuclidine-2-Carboxylic Acid. *J. Org. Chem.* **1967**, *32*, 480–482.

(117) Kitagawa, I.; Yoshikawa, M.; Kamigauchi, T.; Shirakawa, K.; Ikeda, Y. Chemical Transformation of Uronic Acids Leading to Aminocyclitols. III. Syntheses of Aminocyclitols and Aminocyclitol-Oligoglycosides from Uronic Acids and Glucuronide-Saponins by Means of Electrolytic Decarboxylation. *Chem. Pharm. Bull.* **1981**, *29*, 2571–2581.

(118) Stapley, J. A.; BeMiller, J. N. The Hofer-Moest Decarboxylation of d-Glucuronic Acid and d-Glucuronosides. *Carbohydr. Res.* **2007**, *342*, 610–613.

(119) Renaud, P.; Seebach, D. Electrochemical Decarboxylation of Hydroxyproline: A Simple Three-Step Conversion of (2 S ,4 R)-4-Hydroxyproline to (R)-γ-Amino-β-Hydroxybutanoic Acid (GABOB). *Synthesis* **1986**, *1986*, 424–426.

(120) Kienzler, T.; Strazewski, P.; Tamm, C. Synthesis of 1-Aminocyclopropanol by Anodic Oxidation. *Synlett* **1991**, *1991*, 737–738.

(121) Corey, E. J.; bauld, N. L.; Casanova, J.; Kaiser, E. T. Generation of Cationic Carbon by Anodic Oxidation of Carboxylic Acids. *J. Am. Chem. Soc.* **1960**, *82*, 2645–2646.

(122) Shono, T.; Hayashi, J.; Omoto, H.; Matsumura, Y. The Migratory Aptitude in the Anodic Oxidation of β-Hydroxycarboxylic Acids, and a New Synthesis of Di-Muscone. *Tetrahedron Letters* **1977**, *18*, 2667–2670.

(123) Xiang, J.; Shang, M.; Kawamata, Y.; Lundberg, H.; Reisberg, S. H.; Chen, M.; Mykhailiuk, P.; Beutner, G.; Collins, M. R.; Davies, A.; Del Bel, M.; Gallego, G. M.; Spangler, J. E.; Starr, J.; Yang, S.; Blackmond, D. G.; Baran, P. S. Hindered Dialkyl Ether Synthesis with Electrogenerated Carbocations. *Nature* **2019**, *573*, 398–402.

(124) Gianatassio, R.; Lopchuk, J. M.; Wang, J.; Pan, C.-M.; Malins, L. R.; Prieto, L.; Brandt, T. A.; Collins, M. R.; Gallego, G. M.; Sach, N. W.; Spangler, J. E.; Zhu, H.; Zhu, J.; Baran, P. S. Strain-Release Amination. *Science* **2016**, *351*, 241–246.

(125) Staveness, D.; Sodano, T. M.; Li, K.; Burnham, E. A.; Jackson, K. D.; Stephenson, C. R. J. Providing a New Aniline Bioisostere through the Photochemical Production of 1-Aminonorbornanes. *Chem* **2019**, *5*, 215–226.

(126) Roughley, S. D.; Jordan, A. M. The Medicinal Chemist's Toolbox: An Analysis of Reactions Used in the Pursuit of Drug Candidates. *J. Med. Chem.* **2011**, *54*, 3451–3479.

(127) Magnus, P.; Freund, W. A.; Moorhead, E. J.; Rainey, T. Formal Synthesis of (±)-Methyl Rocaglate Using an Unprecedented Acetyl Bromide Mediated Nazarov Reaction. *J. Am. Chem. Soc.* **2012**, *134*, 6140–6142.

(128) Sodano, T. M.; Combee, L. A.; Stephenson, C. R. J. Recent Advances and Outlook for the Isosteric Replacement of Anilines. *ACS Med. Chem. Lett.* **2020**, *11*, 1785–1788.

(129) Zhang, D.; Ogan, M.; Gedamke, R.; Roongta, V.; Dai, R.; Zhu, M.; Kent Rinehart, J.; Klunk, L.; Mitroka, J. Protein Covalent Binding of MaxiPost through a Cytochrome P450-Mediated Ortho-Quinone Methide Intermediate in Rats. *Drug Metab. Dispos.* **2003**, *31*, 837–845.

(130) Reddy, D. S.; Sollott, G. P.; Eaton, P. E. Photolysis of Cubyl Iodides: Access to the Cubyl Cation. *J. Org. Chem.* **1989**, *54*, 722–723.

(131) Irngartinger, H.; Strack, S.; Gredel, F.; Dreuw, A.; Della, E. W. The Cubane Cage – A Sensitive Probe for Assessing Substituent Effects on a Four-Membered Ring, Part II. *Eur. J. Org. Chem.* **1999**, No. 5, 1253–1257.

(132) Xing, H.; Houston, S. D.; Chen, X.; Ghassabian, S.; Fahrenhorst-Jones, T.; Kuo, A.; Murray, C. P.; Conn, K.; Jaeschke, K. N.; Jin, D.; Pasay, C.; Bernhardt, P. V.; Burns, J. M.;

Tsanaktsidis, J.; Savage, G. P.; Boyle, G. M.; De Voss, J. J.; McCarthy, J.; Walter, G. H.; Burne, T. H. J.; Smith, M. T.; Tie, J.; Williams, C. M. Cyclooctatetraene: A Bioactive Cubane Paradigm Complement. *Chem. Eur. J.* **2019**, *25*, 2729–2734.

(133) Moriarty, R. M.; Tuladhar, S. M.; Penmasta, R.; Awasthi, A. K. Solvolyses of Cubyl Triflates. The Cubyl Cation. *J. Am. Chem. Soc.* **1990**, *112*, 3228–3230.

(134) Eaton, P. E.; Nordari, N.; Tsanaktsidis, J.; Upadhyaya, S. P. Barton Decarboxylation of Cubane-1,4-Dicarboxylic Acid: Optimized Procedures for Cubanecarboxylic Acid and Cubane. *Synthesis* **1995**, *1995*, 501–502.

(135) Pirali, T.; Serafini, M.; Cargnin, S.; Genazzani, A. A. Applications of Deuterium in Medicinal Chemistry. *J. Med. Chem.* **2019**, *62*, 5276–5297.

(136) Schulz, L.; Enders, M.; Elsler, B.; Schollmeyer, D.; Dyballa, K. M.; Franke, R.; Waldvogel, S. R. Reagent- and Metal-Free Anodic C−C Cross-Coupling of Aniline Derivatives. *Angew. Chem. Int. Ed.* **2017**, *56*, 4877–4881.

(137) Kabeshov, M. A.; Musio, B.; Murray, P. R. D.; Browne, D. L.; Ley, S. V. Expedient Preparation of Nazlinine and a Small Library of Indole Alkaloids Using Flow Electrochemistry as an Enabling Technology. *Org. Lett.* **2014**, *16*, 4618–4621.

(138) Lee, M.; Kwon, J.; Kim, S. N.; Kim, J. E.; Koh, W. S.; Kim, E. J.; Chung, M. K.; Han, S. S.; Song, C. W. CDNA Microarray Gene Expression Profiling of Hydroxyurea, Paclitaxel, and p-Anisidine, Genotoxic Compounds with Differing Tumorigenicity Results. *Environ. Mol. Mutagen.* **2003**, *42*, 91–97.

(139) Collin, D. E.; Folgueiras-Amador, A. A.; Pletcher, D.; Light, M. E.; Linclau, B.; Brown, R. C. D. Cubane Electrochemistry: Direct Conversion of Cubane Carboxylic Acids to Alkoxy Cubanes Using the Hofer–Moest Reaction under Flow Conditions. *Chem. Eur. J.* **2020**, *26*, 374–378.

(140) Conway, B. E.; Liu, T. C. Potential Relaxation and Interfacial Capacitance Behaviour of the Kolbe Coupling Reaction at Pt. *J. Electroanal. Chem.* **1988**, *242*, 317–322.

(141) White, M. C. Adding Aliphatic C-H Bond Oxidations to Synthesis. *Science* **2012**, *335*, 807–809.

(142) Newhouse, T.; Baran, P. S. If C-H Bonds Could Talk: Selective C-H Bond Oxidation. *Angew. Chem. Int. Ed.* **2011**, *50*, 3362–3374.

(143) Xue, X.-S.; Ji, P.; Zhou, B.; Cheng, J.-P. The Essential Role of Bond Energetics in C–H Activation/Functionalization. *Chem. Rev.* **2017**, *117*, 8622–8648.

(144) Agapito, F.; Santos, R. C.; Borges Dos Santos, R. M.; Martinho Simões, J. A. The Thermochemistry of Cubane 50 Years after Its Synthesis: A High-Level Theoretical Study of Cubane and Its Derivatives. *J. Phys. Chem. A* **2015**, *119*, 2998–3007.

(145) Della, E. W.; Head, N. J.; Mallon, P.; Walton, J. C. Homolytic Reactions of Cubanes. Generation and Characterization of Cubyl and Cubylcarbinyl Radicals. *J. Am. Chem. Soc.* **1992**, *114*, 10730–10738.

(146) Suga, T.; Mizuno, H.; Takaya, J.; Iwasawa, N. Direct Carboxylation of Simple Arenes with CO2 through a Rhodium-Catalyzed C–H Bond Activation. *Chem. Commun.* **2014**, *50*, 14360–14363.

(147) Masuda, Y.; Ishida, N.; Murakami, M. Light-Driven Carboxylation of o-Alkylphenyl Ketones with CO2. *J. Am. Chem. Soc.* **2015**, *137*, 14063–14066.

(148) Ishida, N.; Masuda, Y.; Uemoto, S.; Murakami, M. A Light/Ketone/Copper System for Carboxylation of Allylic C-H Bonds of Alkenes with CO2. *Chem. Eur. J.* **2016**, *22*, 6524–6527.

(149) Seo, H.; Katcher, M. H.; Jamison, T. F. Photoredox Activation of Carbon Dioxide for Amino Acid Synthesis in Continuous Flow. *Nat. Chem.* **2017**, *9*, 453–456.

(150) Ueno, A.; Takimoto, M.; Hou, Z. Synthesis of 2-Aryloxy Butenoates by Copper-Catalysed Allylic C-H Carboxylation of Allyl Aryl Ethers with Carbon Dioxide. *Org. Biomol. Chem.* **2017**, *15*, 2370–2375.

(151) Gui, Y. Y.; Zhou, W. J.; Ye, J. H.; Yu, D. G. Photochemical Carboxylation of Activated C(Sp3)−H Bonds with CO2. *ChemSusChem* **2017**, *10*, 1337–1340.

(152) Michigami, K.; Mita, T.; Sato, Y. Cobalt-Catalyzed Allylic C(Sp3)-H Carboxylation with CO2. *J. Am. Chem. Soc.* **2017**, *139*, 6094–6097.

(153) Meng, Q. Y.; Schirmer, T. E.; Berger, A. L.; Donabauer, K.; König, B. Photocarboxylation of Benzylic C-H Bonds. *J. Am. Chem. Soc.* **2019**, *141*, 11393–11397.

(154) Ishida, N.; Masuda, Y.; Imamura, Y.; Yamazaki, K.; Murakami, M. Carboxylation of Benzylic and Aliphatic C-H Bonds with CO2 Induced by Light/Ketone/Nickel. *J. Am. Chem. Soc.* **2020**, *141*, 19611–19615.

(155) Cassar, L.; Eaton, P. E.; Halpern, J. Silver(I)- and PaIIadium(II)-Catalyzed Jsomerizations of Cubane. Synthesis and Characterization of Cuneane. *J. Am. Chem. Soc.* **1970**, *92*, 6366–6368.

(156) Houston, S. D.; Xing, H.; Bernhardt, P. V.; Vanden Berg, T. J.; Tsanaktsidis, J.; Savage, G.

P.; Williams, C. M. Cyclooctatetraenes through Valence Isomerization of Cubanes: Scope and Limitations. *Chem. Eur. J.* **2019**, *25*, 2735–2739.

(157) Shields, B. J.; Doyle, A. G. Direct C(Sp3)-H Cross Coupling Enabled by Catalytic Generation of Chlorine Radicals. *J. Am. Chem. Soc.* **2016**, *138*, 12719–12722.

(158) Xu, P.; Chen, P.; Xu, H. Scalable Photoelectrochemical Dehydrogenative Cross-Coupling of Heteroarenes with Aliphatic C−H Bonds. *Angew. Chem. Int. Ed.* **2020**, *59*, 14275–14280.

(159) Halperin, S. D.; Fan, H.; Chang, S.; Martin, R. E.; Britton, R. A Convenient Photocatalytic Fluorination of Unactivated C-H Bonds. *Angew. Chem. Int. Ed.* **2014**, *53*, 4690–4693.

(160) Quinn, R. K.; Könst, Z. A.; Michalak, S. E.; Schmidt, Y.; Szklarski, A. R.; Flores, A. R.; Nam, S.; Horne, D. A.; Vanderwal, C. D.; Alexanian, E. J. Site-Selective Aliphatic C-H Chlorination Using N-Chloroamides Enables a Synthesis of Chlorolissoclimide. *J. Am. Chem. Soc.* **2016**, *138*, 696–702.

(161) Krauskoff, K. B.; Rollefson, G. K. The Photochemical Decomposition of Oxalyl Chloride Vapor. *J. Am. Chem. Soc.* **1936**, *58*, 443–448.

(162) Baklanov, A. V.; Krasnoperov, L. N. Oxalyl Chloride - A Clean Source of Chlorine Atoms for Kinetic Studies. *J. Phys. Chem. A* **2001**, *105*, 97–103.

(163) Ghosh, B.; Papanastasiou, D. K.; Burkholder, J. B. Oxalyl Chloride, ClC(O)C(O)Cl: UV/Vis Spectrum and Cl Atom Photolysis Quantum Yields at 193, 248, and 351 Nm. *J. Chem. Phys.* **2012**, *137*, 164315.

(164) Sullivan, R. J.; Newman, S. G. Reaction Cycling for Kinetic Analysis in Flow. *J. Org. Chem.* **2020**, *85*, 5464–5474.

(165) Okude, R.; Mori, G.; Yagi, A.; Itami, K. Programmable Synthesis of Multiply Arylated Cubanes through C–H Metalation and Arylation. *Chem. Sci.* **2020**, *11*, 7672–7675.

(166) Collin, D. E.; Kovacic, K.; Light, M. E.; Linclau, B. Synthesis of Ortho -Functionalized 1,4-Cubanedicarboxylate Derivatives through Photochemical Chlorocarbonylation. *Org. Lett.* **2021**, *23*, 5164–5169.

(167) Castaldi, G.; Colombo, R.; Allegrini, P. A Convenient Synthetic Route to 1,2,4-Tri and 1,3-Disubstituted Cubanes. *Tetrahedron Letters* **1991**, *32*, 2173–2176.

(168) Houston, S. D.; Fahrenhorst-Jones, T.; Xing, H.; Chalmers, B. A.; Sykes, M. L.; Stok, J. E.; Farfan Soto, C.; Burns, J. M.; Bernhardt, P. V.; De Voss, J. J.; Boyle, G. M.; Smith, M. T.; Tsanaktsidis, J.; Savage, G. P.; Avery, V. M.; Williams, C. M. The Cubane Paradigm in

Bioactive Molecule Discovery: Further Scope, Limitations and the Cyclooctatetraene Complement. *Org. Biomol. Chem.* **2019**, *17*, 6790–6798.

(169) Ingalsbe, M. L.; St. Denis, J. D.; Gleason, J. L.; Savage, G. P.; Priefer, R. Synthesis of a Novel Chiral Cubane-Based Schiff Base Ligand and Its Application in Asymmetric Nitro-Aldol (Henry) Reactions. *Synthesis* **2010**, No. 1, 98–102.

(170) Ma, X.; Sloman, D. L.; Han, Y.; Bennett, D. J. A Selective Synthesis of 2,2-Difluorobicyclo[1.1.1]Pentane Analogues: "BCP-F 2 ." *Org. Lett.* **2019**, *21*, 7199–7203.

(171) Nicolaou, K. C.; Vourloumis, D.; Totokotsopoulos, S.; Papakyriakou, A.; Karsunky, H.; Fernando, H.; Gavrilyuk, J.; Webb, D.; Stepan, A. F. Synthesis and Biopharmaceutical Evaluation of Imatinib Analogues Featuring Unusual Structural Motifs. *ChemMedChem* **2016**, *11*, 31–37.

(172) Miyoshi, D.; Karimata, H.; Wang, Z.-M.; Koumoto, K.; Sugimoto, N. Artificial G-Wire Switch with 2,2'-Bipyridine Units Responsive to Divalent Metal Ions. *J. Am. Chem. Soc.* **2007**, *129*, 5919–5925.

(173) Sheldrick, G. M. SHELXT – Integrated Space-Group and Crystal-Structure Determination. *Acta Crystallogr. Sect. A Found. Adv.* **2015**, *71*, 3–8.

(174) Dolomanov, O. V.; Bourhis, L. J.; Gildea, R. J.; Howard, J. A. K.; Puschmann, H. OLEX2 : A Complete Structure Solution, Refinement and Analysis Program. *J. Appl. Crystallogr.* **2009**, *42*, 339–341.

(175) Sheldrick, G. M. Crystal Structure Refinement with SHELXL. *Acta Crystallogr. Sect. C Struct. Chem.* **2015**, *71*, 3–8.

(176) Sheldrick, G. M. A Short History of SHELX. *Acta Crystallogr. Sect. A Found. Crystallogr.* **2008**, *64*, 112–122.